Department für Biotechnologie

Institut für angewandte Mikrobiologie
Vorstand: Ao.Univ.Prof. Dipl.-Ing.Dr. Florian Rüker

Betreuer: Assoc. Prof. Dipl.-Ing. Dr. Johannes Grillari

The Impact Of Extracellular Vesicles On *In Vitro* Bone Formation

Dissertation
zur Erlangung des Doktorgrads
an der Universität für Bodenkultur

Eingereicht von
Dipl.-Ing. Weilner Sylvia

Wien, Juli 2014

1 Contents

2 Danksagung

Denken und danken sind verwandte Wörter; wir danken dem Leben, in dem wir es bedenken (Thomas Mann). Nachdem ich mir ganz nach Thomas Mann über die letzten 3.5 Jahre viele Gedanken gemacht habe, ist es wohl nun an der Zeit den Menschen die zum Gelingen dieser Arbeit beigetragen haben zu danken.

Zu Beginn möchte ich meinem Betreuer Prof. Johannes (Giovanni) Grillari und der Firma Evercyte danken. Danke Giovanni, dass du mir die Möglichkeit gegeben hast in deiner Gruppe/Firma meine Dissertation machen zu dürfen, für deine verständnisvolle, menschliche und offene Weise eine Gruppe zu leiten, für meinen „Kopf“ und damit die Freiheit die du mir gelassen hast um eigenen Ideen nachzugehen aber auch um Fehler zu machen und hoffentlich daraus zu lernen. Lieber Giovanni, vielen Dank, dass du immer für mich Zeit gefunden hast wenn es notwendig war, für unsere vielen inspirierenden Gesprächen und dein Vertrauen. In all den Jahren unsere Zusammenarbeit habe ich niemals unkonstruktive Kritik sondern immer nur mögliche Lösungsansätze von dir gehört. Deine Art einer jeden Situation etwas Positives abzugewinnen und deine ansteckende Begeisterung für die Wissenschaft sind unglaublich motivierend. Ich bin mir nicht sicher, ob ich ohne die Diplomarbeit in deiner Gruppe überhaupt jemals ein Doktorat angedacht hätte aber ich weiß, dass die letzten 3.5 Jahre in beruflicher und persönlicher Hinsicht sehr lehrreich waren und ich diese Zeit nicht missen möchte.

Ein herzliches Dankeschön möchte ich auch meinen Mitbetreuern Prof. Heinz Redl und Prof. Peter Pietschmann aussprechen. Lieber Heinz, vielen Dank für unsere zahlreichen gemeinsamen Besprechungen, für dein offenes Ohr wann immer ich dich darum gebeten haben, dafür dass ich mich an deinem Institut immer willkommen gefühlt habe, für all die Möglichkeiten die du mir/uns gegeben hast um Ideen umzusetzen, dafür dass du deine Erfahrungen und dein Wissen mit mir geteilt hast, für deine Bemühungen Forscher zueinander zu führen damit wir gegenseitig voneinander lernen können bzw. uns das Forscherleben gegenseitig erleichtern, für deine andere Sicht auf manche Dinge wodurch sich immer wieder spannende Ideen und nicht zuletzt das Thema meiner Dissertation ergeben haben.

Lieber Peter, ich weiß noch wie ich aus meiner “in vitro“ – 2D Welt kommend zum ersten Mal in deinem Büro gesessen haben. Ich möchte mich bei dir für deine Unterstützung und die Zeit bedanken, die du dir genommen hast um meine Daten zu

beurteilen und um meine zu Beginn sicher sehr “naiven“ Fragen zu beantworten aber vor allem für deine vielen Ratschläge die *in vivo* Versuche betreffend wodurch du mich beim Sprung aus meiner 2D Zellkultur in die 3D *in vivo* Welt unglaublich unterstützt hast. Ich habe nicht zuletzt durch deine großartige Vorlesung einen tollen Einblick erhalten wie unglaublich komplex der Mensch und im Speziellen der Knochen ist, was die Sichtweise auf meine Arbeit stark beeinflusst hat.
Ich denke, dass ich mich sehr glücklich schätzen kann ein Betreuerteam mit euch an meiner Seite gehabt zu haben und hoffe mich auch in Zukunft an euch wenden zu dürfen.

Weiters möchte ich mich bei meinen Kollegen auf der BOKU bedanken. Bei Lisa, die den Grundstein für meine Arbeit gelegt hat und bei Matthias, von dem ich schon so viel während meiner Diplomarbeit lernen konnte und der mir auch während meiner Dissertation zur Seite gestanden hat - ohne deine Erfahrung und deine bereitwillige Weise dein Wissen mit anderen zu teilen wäre die Arbeit so viel schwieriger geworden. Du bist eine Bereicherung für jedes Labor und soweit ich es beurteilen kann, eine große Unterstützung für jeden Studenten. Grazie Rossella, Gracias Rita! Natürlich könnte ich euch beiden für die gute Zusammenarbeit im Labor danken was auch zweifellos der Wahrheit entsprechen würde. Allerdings möchte ich mich vor allem für unsere vielen Gespräche, für eure einfühlsamen Worte und dafür dass ihr mir in schwierigen Zeiten Halt gegeben habt bedanken. Obwohl sich beruflich unsere Wege getrennt haben hoffe ich dass wir auch weiterhin den privaten Kontakt halten können.
Ganz herzlich möchte ich mich auch beim Rest der Gruppe, meinen Dissertations-Mitstreitern Markus, Hanna, Hammeed, Eva, Luci, Ingo und Lukas bedanken. Nicht nur für die so oft geleistete Hilfe im Labor sondern ganz speziell für das tolle Arbeitsklima, für die netten Gespräche und Diskussionen zwischendurch und für euer offenes Ohr. Danke Eva für das viele gemeinsame Lachen und das “Dach über´n Kopf“. Danke Ingo für die vielen “interessanten“ Diskussionen die ich mit dir führen durfte. Danke Luci für deine dich sorgende Art. Vielen Dank Lukas für dein Bemühen meinen Koffeinspielgel zu „maintainen“, für die gemeinsamen Pausen, für das gemeinsame Lachen aber vor allem auch für die Zeit ersthafte Gespräche zu führen. Deine “nüchtern“/professionelle Weise manche Dinge zu sehen waren nicht nur einmal eine gute Ergänzung zu meiner Sichtweise und haben mir das Leben erleichtert.

Danke an Matthias, Regina und die Mädls von Evercyte – Susanne, Agatha und Patricia. Durch euer Organisationstalent hält ihr das Labor am Laufen und ermöglicht erst ein effizientes Arbeiten – vielen Dank dafür.

Ein ganz besonderes Dankeschön möchte ich den Bakkalaureats- und Masterstudenten Florian, Michael, Verena, Melanie und Anja aussprechen, die mit mir an diesem Projekt gearbeitet haben. Ich hatte großes Glück so tolle Studenten an meiner Seite zu haben, die mit so viel Engagement diese Arbeit vorangetrieben haben.

Besonders hervorheben möchte ich natürlich auch die Gruppe aus dem Ludwig Boltzmann Institut. Vielen Dank an die Knochengruppe – an Thomas, James, und Sylvia bei eurer Umsetzung die *in vivo* Versuche betreffend. Danke an Patrick für die schnelle Analyse der Knochen, an Paul für deine Hilfe mit dem Skalpell aber auch an Susi und Florian für eure Unterstützung die Stammzellen betreffend.

Auch möchte ich mich bei meinen Freunden bedanken. Danke, dass ihr immer für den notwendigen Ausgleich zur Arbeit gesorgt habt und ich so viele unterhaltsame und schöne Stunden mit euch verbringen durfte wonach das Arbeiten immer wieder leichter fiel.

Danke auch an die Feuerwehr und vor allem an Herbert und Horst. Danke für euer Verständnis, dass ich in den letzten Monaten nicht so mithelfen und präsent sein konnte wie es meine Funktion von mir verlangen würde.

Zu guter Letzt möchte ich meiner Familie für ihre bedingungslose Unterstützung und ihr Vertrauen danken. Wenn ich an die vergangen Jahre zurück denke und mir bewusst mache was ich euch alles zu verdanken habe, fürchte ich, dass ich es trotz aller Bemühungen nicht schaffen werde meine Gefühle und meine Dankbarkeit richtig in Worte zu fassen

Danke mein Bruderherz, für die vielen netten Stunden und Gespräche die wir miteinander hatten und für deine Meinung, die du mir immer ehrlich gesagt hast. Es gibt nur wenige Menschen in meinem Leben die mir so nahe stehen wie du es tust - ich habe dich lieb!

Ein riiiiieeeeesen großes Dankeschön möchte ich meinen Eltern sagen. Vielen Danke für euer Vertrauen, eure Geduld und dass ihr nicht in Pension gegangen seit bevor ich meine Studienzeit abgeschlossen habe ☺ Ich möchte mich bei euch für eure Unterstützung bedanken, dafür dass ihr mich von meiner Kindheit an immer gefördert habt, mir ein Studium ermöglicht habt und mir das Gefühl vermittelt habt in meinem Leben alles erreichen zu können. Mit Eltern wie ihr es seit und der Sicherheit, dass ihr

hinter mir steht, war es nicht schwer selbstbewusst und furchtlos die Welt um mich zu erkunden um letztendlich meinen eigenen Weg zu finden.

Mit dem Ausspruch: „Die Bitte ist immer heiß, der Dank kalt“ möchte ich nun auch dieses Kapitel schließen und hoffe, dass ich mit diesen Zeilen all jenen Menschen an die ich in den vergangenen Jahren so brennend heiß meine Bitten gestellt habe zumindest lauwarm danken konnte.

3 Abstract

Adult stem cells are part of the repair system that counteracts damage to cells and tissues. The functionality of stem cells declines with age and is therefore thought to contribute to age associated accumulation of damaged cells and age related diseases. One tissue that is noticeable affected by this decline is the human skeleton. In particular the number of bone forming osteoblasts deriving from mesenchymal stem cells (MSCs) was found to decrease with age. While much is known about intrinsic factors which influence the osteogenic differentiation capacity of adult stem cells hardly any extrinsic factors are known that impact on the commitment of MSCs to osteoblasts. Here we focused on age associated extracellular effector molecules which are able to influence the osteogenic differentiation process of MSCs. While searching for factors we found extracellular vesicles (EVs) and showed that plasma derived EVs of young individuals boost *in vitro* bone formation of MSCs while EVs isolated from elderly fail to induce osteogenic differentiation. In order to elucidate the underlying molecular mechanism we found that the cargo of these vesicles changes with the donor age. In particular two factors within these vesicles which are differentially secreted with age and impact on osteogenesis were identified. On the one hand we demonstrate that Galectin-3 enhances osteogenesis *in vitro* and to be decreasingly secreted by vesicles derived from elderly donors. On the other hand microRNA-31-5p was shown to inhibit osteogenesis and to be enriched within EVs of elderly donors. In summary we identified new factors that impact on the regenerative power of MSCs which might contribute to improve the therapeutic outcome of future MSC based therapies especially in the case of elderly hosts.

4 Zusammenfassung

Adulte Stammzellen (SZ) stellen einen wichtigen Teil des körpereigenen Reparatursystems dar und tragen dazu bei zellulären sowie organischen Schäden entgegenzuwirken. Der Ersatz beschädigter Zellen durch die Aktivität adulter Stammzellen nimmt mit dem Alter jedoch ab wodurch die Funktionalität von Organen negativ beeinträchtigt wird. Ein Organ, welches von dem Aktivitätsverlust adulter Stammzellen betroffen ist, ist der Knochen. Mit steigendem Alter nimmt die Knochenstärke ab. Dies ist unter anderem auf eine Reduktion der osteogenen Differenzierungskapazität von mesenchymalen Stammzellen (MSZ) zurückzuführen. Während bereits einiges über zelleigene Faktoren bekannt ist, die zu diesem Aktivitätsverlust in MSZ beitragen, ist der Einfluss des Milieus auf ihre Regenerationskapazität kaum erforscht. Auf der Suche nach extrazellulären Faktoren, welche auf das osteogene Differenzierungsverhalten von MSZ Einfluss nehmen, wurden in dieser Arbeit zirkulierende Vesikel entdeckt. Es konnte gezeigt werden, dass extrazelluläre Vesikel aus dem Plasma junger Spender die *in vitro* Knochenbildung beschleunigen während Vesikel von älteren Spendern diese hemmen. Nach genauerer Untersuchung des Inhalts dieser Vesikel konnten zwei Faktoren identifiziert werden welche den beobachteten Effekt auch zellbiologisch erklären. Einerseits wurde nachgewiesen, dass pro-osteogenes Galectin-3 in den Vesikeln älterer Spender fehlt. Andererseits wurde entdeckt, dass anti-osteogene microRNA-31 in den Vesikeln älterer Spender angereichert ist. Zusammengefasst konnte in dieser Arbeit gezeigt werden, dass extrazelluläre Vesikel in Abhängigkeit vom Spenderalter die osteogene Differenzierungskapazität von MSZ unterschiedlich beeinflussen und dass dieser Unterschied auf die veränderte Beladung dieser Vesikel zurückzuführen ist. Diese Ergebnisse können dazu beitragen den therapeutischen Effekt zukünftiger auf MSZ basierender Therapien in älteren Patienten zu verbessern.

5 Introduction

“It's paradoxical that the idea of living a long life appeals to everyone, but the idea of getting old doesn't appeal to anyone.” This statement made by the US journalist Andy Rooney excellently reflects the mixed feelings prompted on the subject of aging. Great medical progress has been made in the past decades so that people are living longer than ever before. This increase in life expectancy resulted in a change of health issues seniors are nowadays confronted with. While in the US more than 50% died of infectious diseases in 1900 (Mackenbach & Looman 2013), the majority nowadays dies on typical age associated diseases like cancer or cardiovascular diseases (Mackenbach & Looman 2013). Since the functionality of our bodies and minds constantly declines as we age gaining insights into the mechanisms of aging and age associate diseases will help to establish strategies and medical therapies for physical, medical and social well-being in older age.

The attempt to understand the biological principles of the aging process led to multiple theories which can be assigned in two main categories: The programmed or the damage theory (Jin 2010). The programmed theory assumes that aging is a natural inherent process influenced and driven by a change in gene expression (Davidovic et al. 2010) which results in typical age associated hormonal changes (Heemst 2010) or a degeneration of the immune system (Cornelius 1972). Interestingly studies on homozygote twins indicate that approximately 25% of the aging process are genetically determined (Lykken et al. 1993; Herskind et al. 1996; Ljungquist et al. 1998). Follower of the damage theory support the opinion that aging is caused by an accumulation of environmentally triggered damage to cells and tissues (Jin 2010). However aging proved to be a much more complex process and none of the proposed theories were fully satisfactory. The combination of both suggests that the efficiency to repair environmentally caused damage to cells and organs is genetically programmed is most likely to drive the aging process (Jin 2010).

5.1 Molecular mechanism of cellular and organismal aging

In 1965 Leonard Hayflick and colleagues described for the first time that human diploid cell strains stop to proliferate *in vitro* after a certain number of population doublings (Hayflick 1965). This *in vitro* phenomenon was referred to as “senescence” and intensively studied over the past decades. The irreversible growth arrest can be

triggered by a wide range of causes such as critically short telomeres or other stressors, for example DNA damage, oncogenic signals (Serrano et al. 1997) or chromatin perturbations (Campisi & d'Adda di Fagagna 2007). However, no matter how cellular senescence was triggered only two molecular pathways were identified so far to mediate the irreversible growth arrest by the activation of the cell cycle inhibitor p16INK4a or p21 (Westin et al. 2011; Yang et al. 2008; Campisi & d'Adda di Fagagna 2007). The observation that damaged or dangerous cells that are at risk to undergo malignant transformations enter senescence and are thereby growth arrested (Serrano et al. 1997), struck on the idea that cellular senescence is a potent tumour protection mechanism (Braig et al. 2005; Collado et al. 2005; Courtois-Cox et al. 2006; Feldser & Greider 2007; Ventura et al. 2007).

The hypothesis that senescence also occurs *in vivo* and that senescent cells contribute to the organismal aging process was confirmed by several studies which report on an accumulation of senescent cells with age in rodents (Lazzerini Denchi et al. 2005), non-human primates (Herbig et al. 2006; Jeyapalan et al. 2007) and humans (Dimri et al. 1995) as well as a delayed onset of age associated diseases due to the removal of senescent cells (Baker et al. 2011). Supportingly the activation of telomerase, which protects against telomere dysfunction and therefore against replicatively triggered senescence, resulted in an extended life expectancy (Bernardes de Jesus et al. 2012) and protected against tissue degeneration in mice (Jaskelioff et al. 2011).

In addition several studies demonstrated that cells isolated from elderly donors exhibited a lower population doubling level before entering senescence than cells deriving from young individuals (Martin et al. 1970; Schneider & Mitsui 1976; Bierman 1978; Bruce et al. 1986).Taken together these studies confirm that cellular senescence reflects the organismal aging process. Therefore senescent cells are widely used as *in vitro* aging model.

But how might senescent cells contribute to aging or even age associated diseases? On the one hand the defining feature of these cells, the irreversible growth arrest, causes a reduction of functional cells *in vivo* and might thereby contribute to this effect. However, the cell cycle block is not the only phenotype these cells differ from early quiescent passage cells. Cellular senescent cells were shown to be more resistant to apoptosis (Hampel et al. 2005), which might explain the observed long-term persistence of these cells *in vivo* (Dimri et al. 1995), and to exhibit an altered intracellular protein (Stein et al. 1994), mRNA (Park et al. 2001), microRNA (Hackl et al. 2010) expression as well as

secretory profile (Coppé et al. 2010). In particular the senescence associated secretory phenotype (SASP) might contribute to cell non-autonomous effects on the microenvironment of senescent cells (Coppé et al. 2008). The composition of released molecules was shown to depend on the cell type and the kind of senescence inducing stress (Rodier & Campisi 2011). However, some core factors were identified whose enhanced secretion was characteristic for almost all senescent cells. This group of extensively released soluble factors consists for example of cytokines like interleukin-6 (IL-6) (Coppé et al. 2008), chemokines such as chemokine (C-X-C motif) ligands (CXCLs) (Sarkar et al. 2004) and chemokine (C-C motif) ligands (CCLs) (Davalos et al. 2010), insulin-like growth factor binding proteins (IGFBPs) (Coppé et al. 2008) and a wide range of extracellular proteases like matrix metalloproteinases (MMPs) (Liu & Hornsby 2007). By now several studies demonstrated that the altered secretion profile of senescent cells reinforces the senescent phenotype in an autocrine manner (Coppé et al. 2010). However other studies suggest paracrine functions on their microenvironment for instance the promotion of angiogenesis or cell proliferation of leukocytes, mammary and prostate epithelial cells as well as of keratinocytes (Coppé et al. 2010). Moreover the secretory phenotype of senescent cells was also reported to enhance cell invasion, migration as well as metastasis and to impact on cell differentiation of epithelial and endothelial cells (Rodier & Campisi 2011). In summary the described effects of SASP on neighbouring cells suggest that effector molecules released by senescent cells contribute to tumour progression and to the activation of the immune system, both considered as typical hallmarks of aging and age-related diseases.

5.2 Stem cells and aging

Adult stem cells are important to maintain and repair tissues and organs (Conboy & Rando 2005). They are multipotent cells, which have the ability to self-renew (Sacchetti et al. 2007), producing two identical daughter cells through symmetrical cell division in order to maintain the stem cell pool. Additionally they have the ability to divide asymmetrically resulting in two non-identical daughter cells (Sacchetti et al. 2007), whereas one cell retains the stem cell phenotype and the other differentiates into a specialized cell type in order to replace specialized cells for maintaining tissue homeostasis or for repair in the case of injury throughout an organisms life.

The decision whether an adult stem cell remains quiescent or re-enters the cell cycle in order to divide in a symmetrical or asymmetrical way depends on intrinsic factors, the microenvironment, the extracellular matrix and extrinsic stimuli (Scadden 2006). In principle two different populations of adult stem cells are distinguished in humans. One population was discovered and characterised in 1961 and is called hematopoietic stem cells (HSCs) (Till & McCulloch 1961). By now these cells were successfully isolated from the bone marrow, the peripheral blood or the umbilical vein blood and were demonstrated to give rise to blood forming (erythrocytes and platelets) as well as immune cells, in particular also to bone resorbing osteoclasts (Teitelbaum 2000). The second group of adult stem cells consists of mesenchymal stem cells. In 1974 Friedenstein and colleagues describet at first a fraction of multipotent stromal cells isolated from the bone marrow which exhibited the ability to differentiate into cells of mesodermal origin such as bone forming osteoblasts, cartilage producing chondroblasts or adipocytes (Friedenstein et al. 1974). Meanwhile MSCs have not only been shown to be located in the bone marrow but have also been isolated from several other tissues and organs such as the blood, synovial fluid, amniotic fluid, trabecular bone, cartilage, muscle tendons, adipose tissue, periosteum, spleen, placenta, amnion, umbilical cord, thymus, dermis, lung, liver, pancreas, skin, synovial membrane and teeth (da Silva Meirelles et al. 2006). The International Society for Cellular Therapy defined in 2006 three minimal criteria isolated human MSCs have to fulfil *in vitro* (Dominici et al. 2006): (I) Plastic adherence under standard cultivation conditions (Dominici et al. 2006). (II) Positive for CD73 (ecto-5´-nucleotidase), CD90 (THY1) and CD105 (Endoglin) surface receptors as well as negative for CD34 (marker for myeloid B and T-cell progenitors as well as endothelial cells), CD45 (marker for pan-leukocyte), CD11b and CD14 (marker for monocytes), CD19 and CD79a (marker for B-cells) as well as HLA-DR (MHC class II cell surface receptor) (Dominici et al. 2006). (III) Multipotency which involves the ability to differentiate at least into the osteogenic, chondrogenic and the adipogenic mesenchymal lineage (Dominici et al. 2006). However, in recent years MSCs have also been shown to differentiate not only in the three above mentioned cell types but also into other cells of mesodermal origin (myocyte, endothelium, cardiomyocytes) (Uccelli et al. 2008) and to transdifferentiate into non-mesodermal cells such as neurons (Kopen et al. 1999) and epithelial cells which are assigned to the ectoderm as well endodermal cells like hepatic (Petersen et al. 1999), pancreatic, respiratory and intestinal epithelial cells (Uccelli et al. 2008) (Figure 1).

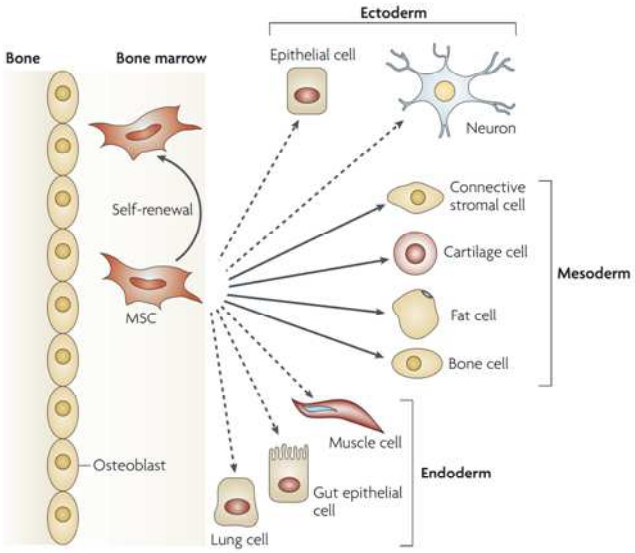

Figure 1: Cell fate of MSCs upon activation

This figure was adapted from A. Uccelli et al. (Uccelli et al. 2008) and shows the ability of MSCs to self-renew or to differentiation into various cell types of mesodermal (myocyte, chondrocyte, adipocyte, osteocyte), ectodermal (epithelial cell, neuron) or endodermal (intestinal and respiratory epithelial cell) origin.

5.3 The skeleton system

The human skeleton consists of 220 bones. Generally 5 different types of bone are distinguished according to their shape: (I) Long bones like the femur, (II) short bones such as the ankle bones, (III) flat bones as for instance the cranial bones, (IV) sesamoid bones e.g. patella and (V) the irregular bones exemplified by facial bones. Besides the skeletons mechanical functions such as locomotion, support and the protection of inner organs it has an important role as site of haematopoiesis and mineral balance homeostasis (Boskey & Coleman 2010). 99% of calcium, 85% of phosphate and 50% of magnesium were shown to be stored in the skeleton indicating its importance of the skeleton in maintaining mineral levels (Marcus et al. 2010). In particular tight regulation of Ca^{2+} blood levels is essential to ensure the function of muscles and nerves (Török 2007). Consequently decreased calcium levels lead to the secretion of parathyroid hormone (PTH) by the parathyroid gland (Sahota et al. 2004). This hormone acts on the skeleton by activating osteoclasts which results in the resorption of bone and consequently a release of stored Ca^{2+} (Sahota et al. 2004). Additionally PTH stimulates the kidney to produce active 1.25 $(OH)_2$ vitamin D which in turn facilitates the

expression of transient receptor potential (TRP) channels in the intestine (Bouillon & Suda 2014) in order to enhance active Ca^{2+} absorption (Sahota et al. 2004).

The adult skeleton consists of (I) an inorganic matrix, for the most part impure hydroxyapatite $Ca_{10}(PO_4)_6(OH)_2$ (Boskey 2007), (II) an organic phase (Marcus et al. 2010), which is to 98% made of type I collagen (Marcus et al. 2010) but also contains proteoglycans, glycoproteins and serum proteins, (III) cells, (IV) lipids and (V) water (Boskey & Coleman 2010). The combination of organic and inorganic matrices confers flexibility and strength. Accordingly cortical and trabecular bones can be distinguished by their porosity. Cortical bone makes up 80% of total bone mass and represents the dense outer shell of the bone. 90% of cortical bone is calcified and it has a low metabolic rate (Marcus et al. 2010). The porosity of cortical bone is approximately 5-20% (Marcus et al. 2010). The inner part of the bone is formed by a highly porous sponge-like structure called trabecular bone which is filled with bone marrow (Marcus et al. 2010). The porosity is between 40%, in young individuals and 95% in patients suffering from osteoporosis (Marcus et al. 2010). The trabecular porosity is an important parameter for stiffness and strength of trabecular bone (Marcus et al. 2010). In addition to trabecular porosity, the trabecular architecture expressed in parameters such as the trabecular number, separation and thickness gives some indication of bone stiffness and strength (Marcus et al. 2010). 80% of bone remodelling occurs in the trabecular bone whereby it is more subjected to changes in bone turnover (Marcus et al. 2010). Several years ago bone was considered as static system. By now it is known to be a highly dynamic, vascularized and metabolic active tissue which is constantly remodelled by cells in order to repair fractures, response and to adapt to factors like mechanical loading but also to replace old bone and to maintain calcium homeostasis throughout an organisms life (Marcus et al. 2010). In particular 25% of trabecular and 2,5% of cortical bone are replaced within one year. Bone is constantly remodelled by the coordinated action of bone resorbing multinucleated osteoclasts and bone matrix forming osteoblasts (Marcus et al. 2010). However, approximately 90% of cells within the bone are neither osteoclasts nor osteoblasts but osteocytes (Marcus et al. 2010). Osteocytes originate from bone matrix encapsulated osteoblasts. These cells exhibit dendrite like cytoplasmatic processes, thereby forming a complex network which allows the contact to other osteocytes and to the bone surface lining cells, which mainly consist of inactive quiescent and active osteoblasts (Aarden et al. 1994). These connection is facilitated by channels in the bone calles canaliculi (Aarden et al. 1994). Osteocytes were shown to

play an important role as mechanosensors, in orchestrating bone remodelling and in regulating mineral homeostasis as well as matrix mineralization (Adachi et al. 2009; Weinstein et al. 1998; Bonewald 2013; Galli et al. 2010). However, from the late second to the third decade of life bone mass starts to decline (Bonjour et al. 1994) resulting in a reduction of cortical and trabecular bone strength with age (Marcus et al. 2010). Similar to other tissues a sufficient number of adult stem cells is essential to enable bone function since hematopoietic stem cells give rise to osteoclasts while mature osteoblasts and osteocytes originate from MSCs (Kassem & Marie 2011). Since osteoclasts, osteoblasts, osteocytes and consequently also their precursor cells are necessary to remodel bone age related changes of these cells are briefly outlined in the next chapters.

5.3.1.1 Bone cells of the mesenchymal lineage

Osteoblasts are bone forming cells. Consequently a reduction of osteoblasts or functional decline of their precursor cells, the mesenchymal stem cells, might shift the balance between bone resorption and formation resulting in bone loss. Several studies were performed investigating the number of MSCs with some observing no differences in the number of MSCs after skeletal maturation between young and elderly individulas (Stenderup et al. 2001) and others demonstrating a reduction of MSCs with age (Kuznetsov et al. 2009; Nishida et al. 1999). This controversal data might be explained by the differences in stem cell isolation methods but also by the differences in mean age of the compared groups. In general a strong decline in the number of MSC was observed after the termination of skeletal growth (Kassem & Marie 2011). This suggests that the age related decline in bone mass is not due to a reduced number of osteoprogenitor cells but rather due to a reduced expansion or commitment of MSCs into the osteogenic lineage (Kassem & Marie 2011). Although the number of isolated MSCs did not differ significantly in young and elderly individuals after completion of skeletal growth, MSCs isolated from elderly were shown to enter senescence at an earlier *in vitro* population doubling number compared to those of young donors (Stenderup et al. 2003) indicating that senescence might also affect the proliferation and differentiation capacity of MSCs *in vivo*. Supportingly the share of senescent MSCs isolated from elderly was shown to be higher compared to MSCs isolated from young donors (Stenderup et al. 2003; S Zhou et al. 2008). This hypothesis is supported by the observation that human telomerase reverse transcriptase (hTERT) overexpressing MSCs are able to undergo more population doublings and exhibit an enhanced

osteogenic differentiation potential *in vitro* (Simonsen et al. 2002) and *in vivo* (Shi et al. 2002) compared to normal MSCs. In contrast to MSCs a reduced number of mature osteoblasts was observed with age (Almeida et al. 2007) indicating that the function or the osteogenic commitment of MSCs is impaired with age. In particular Roholl and colleagues demonstrated that the number of pre-osteoblasts, pre-osteoclasts and osteoclasts does not change with age per unit bone length in elderly rats but they observed a strong decline of mature osteoblasts (Roholl et al. 1994) supporting the theory that impaired osteogenesis contributes to age related bone loss

In addition to the reduction of bone located osteoblasts circulating osteoblasts were identified in the peripheral blood of post-menopausal women expressing not only inflammatory but also osteoclastogenesis promoting factors like receptor activator of nuclear factor κB ligand (RANKL) and intercellular adhesion molecule 1 (ICAM-1) (Undale et al. 2010; Eghbali-Fatourechi et al. 2007).

When osteoblasts get embedded in their own synthesized mineralized bone matrix they differentiate into osteocytes within 3 days (Bonewald 2013). Although the majority of osteoblasts becomes apoptotic and only 10 - 20% of osteoblasts differentiate into osteocytes, osteocytes represent 90% of all bone cells (Boskey & Coleman 2010). Compared to osteoclasts and osteoblasts which are only active for days or weeks, osteocytes are considered as long-living bone cells which reside within the bone tissue for several years (Manolagas & Parfitt 2010). The viability of osteocytes has been demonstrated to decrease from 99% at birth to only 25% at an age of 80 which might addionally contribute to a reduction in bone formation (Tomkinson et al. 1997).

Besides the observation that osteocytes die by apoptosis it was also demonstrated that the percentage of senescent osteocytes increases with age (Tomkinson et al. 1997).

5.3.1.2 Bone cells of the hematopoietic lineage

In 1992 osteoclasts were isolated for the first time (van der Plas & Nijweide 1992). Upon activation these cells excavate bone by tightly attaching to the bone surface and releasing hydroxychlorid acid in order to resolve inorganic bone components and enzymes like cathepsin K to degrade the organic matrix (Teitelbaum 2000). Not only osteogenic differentiation seems to be impaired with age but the differentiation into osteoclasts was shown to be enhanced with age (Cao et al. 2005). Additionally decline of bone density with age might be explained by the observation of Henriksen and

colleagues who demonstrated, that the activity of osteoclasts is higher when resorbing old compared to newly synthesized bones (Henriksen et al. 2007).

In summary the combination of an age-related reduction in proliferation and differentiation of osteoprogenitor cells leading to a decreased number of bone forming mature osteoblasts and bone remodelling orchestrating osteocytes as well as an enhanced activity of osteoclasts might be the decisive factor for changes in bones strength and quality with age.

5.3.2 Mechanisms of osteogenic differentiation

Bones are constantly remodelled and maintained by the coordinated activity of bone forming osteoblasts and bone excavating osteoclasts (Kozhevnikova et al. 2008). In order to maintain bone mass and consequently its mechanical properties the amount of bone resorbed by osteoclasts equals to the newly synthesized bone. Although much is known about the differentiation of HSC via monocytes to osteoclasts (Ash et al. 1980), the mechanism and factors influencing osteogenic differentiation are still incompletely understood. In principle the osteogenic differentiation process of MSCs into osteoblasts is influenced by three types of factors. Firstly transcription factors which have the ability to influence the transcription of genes in a positive or negative way by binding to the gene regulatory elements of the DNA. (Kozhevnikova et al. 2008) One of the most important transcription factors in regard to bone formation is runt related transcription factor-2 (Runx-2) which exclusively acts in the osteogenic differentiation process after birth (Komori 2005; Karsenty & Wagner 2002). Secondly mRNA-binding protein factors such as microRNAs which bind to the mRNA of a relevant gene thereby suppressing or activating its translation (Kozhevnikova et al. 2008). And thirdly signalling proteins which act via a signalling cascade and affect the transcription of genes relevant for osteogenesis by targeting transcription factors like Runx-2 or changing the chromatin structure (Kozhevnikova et al. 2008). Subsequently a short summary of the wingless-type MMTV integration site family (Wnt) pathway which was shown to be very important in bone formation is given.

5.3.2.1 Wnt signalling pathway

The Wnt protein family consist of 19 secreted lipid-modified Wnt proteins in humans which could theoretically bind to 10 different Frizzled (Fzd) seven-pass transmembrane receptors (van Amerongen et al. 2008) in order to activate an intracellular signalling

cascade. Wnt proteins bind to two types of receptors. On the one hand to the cysteine rich domain of Frizzled receptors and on the other hand to the co-receptor lipoprotein receptor-related protein 5 (LRP5) or LRP6 (Verkaar & Zaman 2010). The intracellular effect of extracellular Wnt binding to the cell depends on the type of Wnt ligand and the set of receptors which is present on the cellular surface (van Amerongen et al. 2008). In principle three different signalling pathways which are induced upon Wnt binding are distinguished: (I) The Wnt-β-Catenin dependent signalling pathway (Gordon & Nusse 2006), (II) the still poorly understood Wnt-β-Catenin independent signalling pathway (E. H. Lee et al. 2008) and (III) the Wnt-Ca^{2+}dependent pathway, which leads to the release of intracellular Ca^{2+} due to heterotrimeric G-protein activation (Kohn & Moon n.d.).

The Wnt-β-Catenin dependent signalling pathway is best understood and of particular importance in regard to osteogenesis since loss of function of β-Catenin in mice results in severe skeletal malformations (Otto et al. 1997) and knock out in mesenchymal stem cells leads to increased chondrogenesis and an inhibition of osteogenesis (Kobayashi et al. 2000). On the other hand gain of function of β-Catenin in MSCs results in a commitment towards osteogenic differentiation and an inhibition of chondrogenesis and adipogenesis (Chen et al. 2007; Baron & Rawadi 2007). Upon binding of some Wnts to Frizzled receptors such as Wnt10b (Bennett et al. 2007; Bennett et al. 2005; Stevens et al. 2010), β-Catenin is no longer phosphorylated and can therefore escape its degradation by the destruction complex consisting of glycogen synthase kinase 3 β (GSK-3β), axin and adenomatous polyposis coli (APC) (Gordon & Nusse 2006). As a consequence β-Catenin is stabilized, accumulates and translocates into the nucleus where it associates with and thereby activates the transcription factors nuclear T cell factor (TCF) and Lymphoid enhancer factor (LEF) resulting in the expression of osteogenesis relevant genes such as the master regulator Runx-2 (Gordon & Nusse 2006). Interestingly the expression of Runx-2 alone is not sufficient to regulate osteogenesis. In order to induce the expression of genes necessary for osteocalcin production, a typical marker for mature osteoblasts, Runx-2 has to interact with Smad1, Smad5 and Smad8 in the nucleus (Hanai et al. 1999; Lee et al. 2000). Upon binding of extracellular bone morphogenic protein 2 (BMP2) to its receptor, Smad1, 5 and 8 become phosphorylated, associate with Smad4, translocate into the nucleus and are thereby able to interact with Runx-2 (Hanai et al. 1999; Lee et al. 2000). The Wnt signalling pathway is graphically outlined in Figure 2.

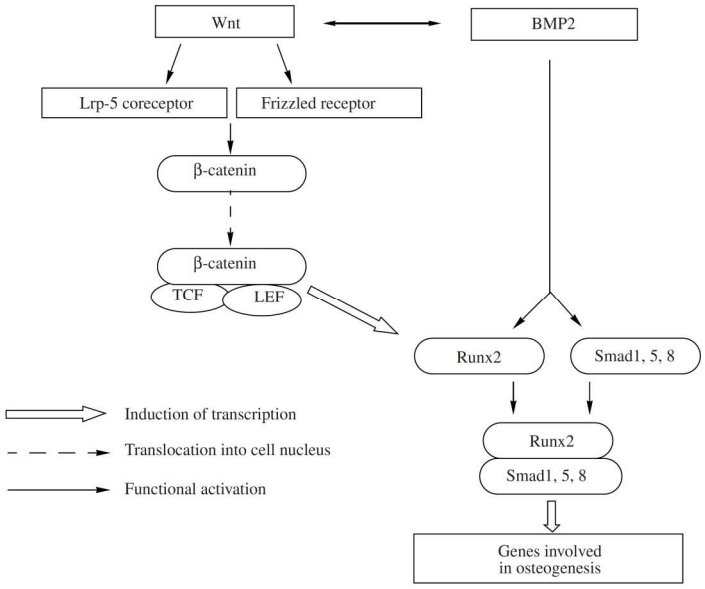

Figure 2: The Wnt-β-Catenin dependent signalling pathway

This figure was adapted from M.N. Kozhevnikova et al. and shows the proteins involved to induce the expression of osteogenesis relevant genes (Kozhevnikova et al. 2008). Upon Wnt binding to Fzd and Lrp receptor, β-Catenin is stabilized, translocates in the nucleus and associates with TCF and LEF. Subsequently osteogenesis relevant genes such as Runx-2 are expressed. However, in order to differentiate into mature osteoblasts the transcription factor Runx-2 has to interact with Smad1, 5 and 8. Upon BMP2 binding Smad1, 5 and 8 are phosphorylated, translocate into the nucleus and initiate the expression genes important for mature osteoblasts by associating with Runx-2.

5.3.3 Osteoporosis

Osteoporosis means porous bones and is generally characterised by a decrease in bone strength which affects the whole skeleton and subsequently leads to an increased fracture risk where fractures already occur in the case of low-impact trauma (Panel 2001). Bone strength is not determined by a single parameter but it is a rather complex function of several parameters such as bone geometry, microarchitecture of the cortical and trabecular bone as well as the degree of bone mineralization and the extent of collagen I crosslinks which provides information about bone density and bone quality (Marcus et al. 2010). When suffering from osteoporosis the hip, the spine and the wrist are especially prone to fracture (Marcus et al. 2010). Therefore forearm, vertebral and hip fractures caused by low impact traumas in the elderly are considered as the typical osteoporotic fracture (Marcus et al. 2010). In principle two types of primary osteoporosis are distinguished: Type I is caused by hormonal changes in women after menopause which typically results in a loss of trabecular bone due to a deficiency in estrogen (Marcus et al. 2010) while osteoporosis type II concerns men as well as women and is considered as an age-associated disease (Marcus et al. 2010). There are various

causes leading to type II osteoporosis as for example an impaired bone remodelling process (Marcus et al. 2010) but all of them have in common that typically not only trabecular but also cortical bone is lost in humans (Marcus et al. 2010). Over all the age related loss of bone mass in men was shown to proceed gradually throughout the life after skeletal maturation while in women bone loss seems to additionally accelerate shortly after menopause (Marcus et al. 2010). Typical factors influencing the peak bone mass and subsequently also the risk of suffering from osteoporosis in older age were shown to be genetical as well as environmental (Marcus et al. 2010). In particular environmental factors increasing the risk for osteoporosis are a low body mass index (BMI), low Ca^{2+} intake, smoking, high alcohol intake, glucocorticoid treatment and prolonged immobility (Marcus et al. 2010).

Epidemiologically 75 million people were suffering from osteoporosis in Europe, USA and Japan in 2003 and the number of patients is constantly increasing due to democratic shifts (Anon 1997). According to current estimations by the Wold Health Organization (WHO) approximately 30% of all European women older than 50 years are suffering from osteoporosis nowadays (Melton et al. 1992). Additional studies revealed that 8.9 million people suffer from a fracture due to osteoporosis each year (Johnell & Kanis 2006). Elderly women spend more time in the hospital because of an osteoporotic fracture than for many other diseases (Kanis et al. 1997) and the risk to suffer from osteoporosis is higher than to suffer from breast cancer in women (van Staa et al. 2001). Due to this data WHO classed Osteoporosis as a priority health issue (Marcus et al. 2010). Since osteoporosis is an asymptomatic disease assessing the fracture risk before clinically recognizing fractures, is still one of the main challenges (Kanis 2002). A woman is considered as suffering from osteoporosis when her bone mineral density (BMD) is at least 2,5 standard deviations lower compared to the average density of the young healthy female population (Kanis et al. 1997). According to WHO guidelines BMD is measured by dual-energy X-ray absorptiometry (DXA) at the hip or spine in order to estimate the fracture risk (Marcus et al. 2010). A study of Kanis and colleagues revealed, that the share of women exhibiting a osteoporotic BMD constantly increases with age, starting with 0,6% in 50 year old women it constitutes up to 47,5% in women older than 80 years (Kanis et al. 1997). Although BMD was proven to correlate with fracture risk it is not sensitive enough to solely predict the fracture risk of an individual (Siris et al. 2004; Sornay-Rendu et al. 2005; Pasco et al. 2006). For example BMD clearly correlates with the BMI but patients suffering from type II diabetes usually exhibit

a high BMI and a normal BMD but are more prone to fracture (Oei et al. 2013). Consequently markers for a better fracture risk assessment are of utmost need.

5.4 Extracellular vesicles

Extracellular vesicles (EVs) are small vesicles released by probably all but certainly many cells types *in vitro* (Fais et al. 2013). The history of extracellular vesicles goes back to the 1980s when vesicles blebbing from the plasma membrane of a tumour cell line were discovered for the first time (Trams et al. 1981). A few years later a different type of vesicles was reported which does not originate by pinching off from the plasma membrane but from the endosomal compartment in reticulocytes (Pan & Johnstone 1983). Depending on their biogenesis and the cellular state three different types of EVs are distinguished nowadays (Mathivanan, Ji, et al. 2010). (I) EVs called “shedding microvesicles” also referred to as “ectosomes” which directly shed from the cellular plasma membrane (Mathivanan, Ji, et al. 2010), generally thought to be 100 – 1000 nm in diameter (Mathivanan, Ji, et al. 2010). However, Booth and colleagues observed in 2006 also smaller vesicles of 30 – 100nm in size directly blebbing from the plasma membrane of T-cells indicating that the vesicular diameter is unsuitable to distinguish between different subsets of EVs (Booth et al. 2006). In contrast to the cellular plasma membrane they are originating from these vesicles expose phosphatidylserine on their surface (Mathivanan, Ji, et al. 2010; Weilner et al. 2012).

Regarding the subcellular localization of biogenesis (II) apoptotic bodies might be considered as closely related to ecotosomes since they bleb from the plasma membrane as well (van Niel et al. 2006). However, apoptotic bodies are exclusively released by cells in the late stage of apoptosis, but also present phosphatidylserine on their surface, are of irregular shape and are larger than 50nm in diameter (Mathivanan, Ji, et al. 2010). In contrast to other types of extracellular vesicles they can contain DNA (Mathivanan, Ji, et al. 2010).

The last type of EVs are (III) exosomes which originate by inward budding of the late endosomal compartments thereby forming multivesicular bodies (MVBs) (van Niel et al. 2006; Simpson et al. 2008). These MVBs can either fuse with lysosomes, resulting in the degradation of its content, or with the plasma membrane (Simpson et al. 2009). Upon fusion of MVBs with the plasma membrane intraluminal vesicles are released as exosomes. Exosomes are 30 – 120nm in diameter (Simpson et al. 2008). By now there

are no markers available in order to distinguish the different types of vesicles. For that reason the collective term extracellular vesicles is used subsequently.

The cargo selection of extracellular vesicles is strongly regulated and does not only depend on the producer cell type but also on the environmental trigger to release vesicles and probably also on the subcellular localisation they originate from (Kowal et al. 2014). The membrane of extracellular vesicles is enriched in cholesterol, sphingolipids and saturated fatty acids (Fais et al. 2013). In addition they contain proteins which are specific for the donor cell but also more general proteins like heat shock protein 70kDa (HSP70) or CD63 which can be found in almost all extracellular vesicles from different cell types (Fais et al. 2013). RNAs, mainly consisting of mRNAs and small non coding RNAs, represent the genetic component of extracellular vesicles (Nolte'T Hoen et al. 2012). Interestingly it has been found that the cellular composition of RNAs does not necessarily reflect the vesicular content since some microRNAs are specifically enriched or excluded within extracellular vesicles (Kogure et al. 2011). The presence of microRNAs within extracellular vesicles was discovered for the first time in 2007 (Valadi et al. 2007). The majority of vesicular RNAs are small non coding RNA (<200nt) (Nolte'T Hoen et al. 2012). Deep sequencing analysis of shuttled RNA derived from murine immune cells revealed that microRNAs represent only 7,8% of small RNAs which are therefore clearly underrepresented compared to the relative amount of 57,3% within cells (Nolte'T Hoen et al. 2012). On the other hand vesicles were enriched in ribosomal, structural signal recognition particle (SRP) as well as Y-RNA in comparison to its producer cell (Nolte'T Hoen et al. 2012).

The biogenesis, cargo selection and release of extracellular vesicles is still unclear and depends most probably not only on the type of extracellular vesicle, but also on its producer cell, the cellular state and the environmental trigger (Mathivanan, Ji, et al. 2010). By now two pathways participating in the sorting of cargo into vesicles have been identified. On the one hand the endosomal sorting complex required for transport (ESCRT) complex involved in the sorting of cargo into intraluminal vesicles as well as in the pinching of theses vesicles (Gibbings et al. 2009). On the other hand an ESCRT independent pathway where cargo is sorted in ceramide rich microdomains has been proposed (Trajkovic et al. 2008). In regard of miRNAs an involvement of ESCRT (Irion & St Johnston 2007) as well as RNA induced silencing (RISC) complex (Gibbings et al. 2009; Gibbings & Voinnet 2010) and neutral sphingomyelinase 2 (nSMase2) (Kosaka, Iguchi, Yoshioka, et al. 2010), an enzyme necessary for ceramide biosynthesis, have

been shown to be involved in the loading of microRNAs into extracellular vesicles. More recently the group of Sánchez-Madrid has proposed a new mechanism by demonstrating that sumoylated heterogeneous nuclear ribonucleoprotein A2B1 (hnRNPA2B1) recognizes and binds to a specific motif on microRNAs, intended for exosomal secretion, thereby regulating its loading into intraluminal vesicles (Villarroya-Beltri et al. 2013).

The molecular mechanism regulating the transport of MVBs to the lysosomes or the plasma membrane is still incompletely understood. Several studies reported an important role for Ras-related in brain (Rab) proteins, such as Rab 27b (Ostrowski et al. 2010) and Rab 35 (Hsu et al. 2010), which mediate the transport and the docking of MVBs to the plasma membrane. On the other hand not only Rabs but also proteins of the soluble N-ethylmaleimide-sensitive-factor attachment receptor (SNARE) family are known to play an important role in the fusion of MVB with the plasma membrane whereby intraluminal vesicles are released as exosomes (Bobrie et al. 2011). Once extracellular vesicles have been released they were shown to protect and transport their cargo over shorter and longer distances (Mitchell et al. 2008; Chen et al. 2012). Remarkably, the binding of extracellular vesicles to target cells is highly specific (Fevrier & Raposo 2004). This observation gave rise to the assumption that extracellular vesicles contribute to cell-to-cell communication (Mathivanan, Ji, et al. 2010).

Extracellular vesicles are able to signal by interacting with surface receptors of the target cell (Thery et al. 2009) but also through the transfer of vesicular effector molecules into the target cell due to plasma membrane fusion (Montecalvo et al. 2012) or endocytosis (Tian et al. 2010; Svensson et al. 2013). Since extracellular vesicles contain a set of effector molecule like transcription factors and RNAs they rapidly affect the behaviour of the target cell. A recently published study gave evidence that microRNAs are functionally delivered to target cells. In particular it was not only demonstrated that functional vesicular miR-223 is taken up by target cells which were transfected with a luciferase vector containing a miR-223 target seed sequence but also that this uptake reduces the luciferase activity to a similar extent as direct transfection of target cells with pre-miRNA-223 did (Ismail et al. 2013).

Although originally discovered in *in vitro* cultures (Pan & Johnstone 1983) extracellular vesicles were by now found in several body fluids such as blood (Kosaka, Iguchi & Ochiya 2010), plasma (Huang et al. 2013), serum (Gallo et al. 2012), saliva (Gallo et al. 2012), seminal fluid (Bobrie et al. 2011) and breast milk (Admyre et al. 2007).

Additionally a function for extracellular vesicles in physiological but also in pathological processes as for instance in tumour development (Mathivanan, Lim, et al. 2010; Janowska-Wieczorek et al. 2005), infectious diseases (Nanbo et al. 2013), cardiovascular disorders (Zhu & Fan 2011), in activating or repressing the immune response (Bobrie et al. 2011), the blood coagulation process (Müller et al. 2003), in the neuron system (Frühbeis et al. 2012) and in tissue repair (Maguire et al. 2013) has been demonstrated.

Since the composition of extracellular vesicles depends on the cell type but also on its cellular and infectious state, the presence or absence of vesicular components might reflect the health or disease state of tissues (Properzi et al. 2013). For example changes in the vesicular microRNA secretion profile have been reported in patients suffering from colon cancer (Ogata-Kawata et al. 2014). This tumour related secretion profile was reduced after surgical remove of the primary tumour (Ogata-Kawata et al. 2014). Therefore vesicles derived from body fluid are seen as promising candidates for biomarkers of diseases.

5.5 microRNAs

MicroRNAs (miRNAs) are single stranded RNAs and belong to the large group of non-coding RNAs. The first microRNA was discovered more than 20 years ago in Caenorhabditis elegans (C. elegans) where overexpression of lin-4 resulted in an elongated life span (Lee et al. 1993). By now microRNAs have been detected in all eukaryotic cells and typically consist of a unique approximately 21 long nucleotide sequence (Chapman & Carrington 2007). The biogenesis process of microRNAs starts with their transcription mediated by the Polymerase II (Lee et al. 2004) or III (Lee et al. 2003). The resulting pri-microRNA is further cleaved by the Pasha-complex, consisting of the nuclear RNase III enzyme Drosha and Pasha (DGCR8) (Han et al. 2004). Subsequent binding of the Exportin-5–Ran-GTP complex to the synthesized microRNA precursor (pre-microRNA) does not only protect the precursor from degradation but also mediates its translocation from the nucleus to the cytoplasm through nuclear pores (Bohnsack et al. 2004; Zeng & Cullen 2004). Upon hydrolysis of Ran-GTP to Ran-GDP pre-microRNA is released from the Exportin-5-Ran complex in the cytoplasm (Kehlenbach et al. 1999) thereby getting accessible to the Dicer-TAR RNA binding protein (TRBP) complex, which mediates the final cleavage-step to generate mature microRNA (Chendrimada et al. 2005). Mature microRNAs can regulate protein

expression on the posttranscriptional level. Therefore mature microRNA associates with Ago-2 and is loaded into the RISC complex (Gregory et al. 2005). In the following the mature miRNA-RISC complex binds to the 3´untranslated regions of target mRNAs and mediated its degradation, translational repression or deadenylation (Winter et al. 2009).

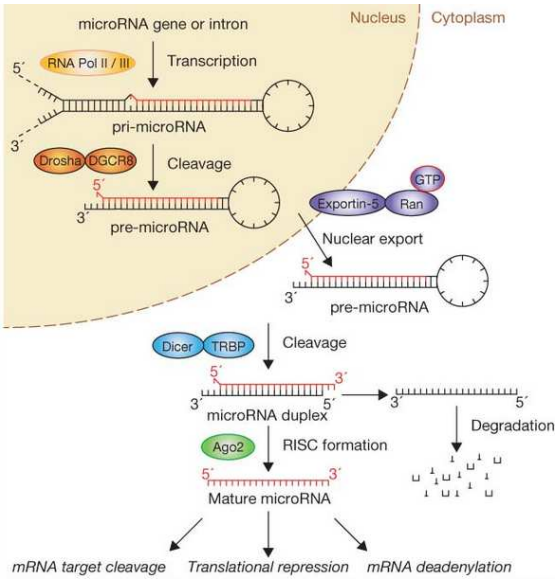

Figure 3: MicroRNA biogenesis

Figure adapted from Winter et al. (Winter et al. 2009), showing a graphical representation of the miRNA biogenesis. Upon transcription pri-microRNA gets cleaved by the Drosha-DGCR8 complex. The cleaved pri-microRNA translocates in association with Exportin-5 into the cytosol where it undergoes a second cleavage step mediated by the by Dicer-TRBP complex. Consequently the mature microRNA is able to bind to its target mRNA in order to inhibit its translation.

MiRNAs can not only repress the translation of one but up to several hundred mRNAs within one pathway and related pathways thereby allowing a rapid control over the cellular behaviour and influencing cellular processes (Winter et al. 2009). Remarkably miRNAs were not only shown to have an influence on cellular processes like differentiation, proliferation, senescence and apoptosis (Thum et al. 2008; Zhao & Srivastava 2007) but also to be deregulated with age (Jung & Suh 2012).

5.5.1 MicroRNAs, longevity and aging

The first microRNAs which were shown to have an influence on the lifespan of an organism were found in the nematode C. elegans. For example lin-4, miR-71 or miR-246 overexpressing nematodes exhibited a prolonged lifespan while organisms having reduced levels of these microRNAs died earlier compared to wild type animals (Boehm & Slack 2005; de Lencastre et al. 2010).

In the fly Drosophila melanogaster (D. melanogaster), a common model organism in developmental biology, miR-34 was shown to be upregulated with age (N. Liu et al. 2012). Furthermore organisms lacking miR-34 exhibited accelerated neuronal degradation and a shortened lifespan, while overexpression of miR-34 extended their life span (N. Liu et al. 2012). Interestingly miR-34 was not only shown to increase with age in D. melanogaster but also in C. elegans and to be upregulated in the murine adult brain possibly fulfilling similar functions like protecting the brain from accelerated aging (X. Li et al. 2011).

While the influence of microRNAs on the lifespan of organisms has already been demonstrated in C. elegans and D. melanogaster, no influence on the lifespan of mammals could be demonstrated so far. However a recent study demonstrated that humans exhibit an altered circulating microRNA expression profile in old age too (ElSharawy et al. 2012). Different aged tissues showed a different microRNA expression profile compared to tissues of young individuals as for instance human skeletal muscles (Drummond et al., 2011), peripheral blood mononuclear cells (Noren Hooten et al., 2010), aged murine livers (Li et al., 2011b) as well as murine and human brains (Persengiev et al. 2011; X. Li et al. 2011). In addition also bone marrow derived stem cells (Hackl et al., 2010), foreskin samples (Hackl et al., 2010) and CD8+ T cell populations (Hackl et al., 2010) of elderly compared to young human donors showed a different microRNA pattern. Hereafter some examples of deregulated miRNAs within aged tissues are given.

Generally adult mesenchymal stem cells are known to play a central role in tissue regeneration but their regeneration capacity and functionality decrease with age (Lepperdinger 2011). Therefore aged MSCs are thought to contribute to the gradually declining regeneration capacity. Alt and coworkers demonstrated, that senescence related genes like p16INK4a are increased in adipose derives MSCs (ASCs) from elderly compared to young donors and that miR-27b, miR-106a, miR-199a and let-7 are deregulated with age in these cells (Alt et al., 2012).
Furthermore Yu and colleagues investigated the differences of bone marrow derived mesenchymal stem cells from young, middle and old rhesus macaques (Yu et al. 2011). They could not only correlated the proliferation and differentiation capacity of isolated stem cells with the age of the corresponding donor but reported on increased levels of

miR-766 and miR-558 as well as decreased levels of let-7f, miR-125b, miR-222, miR-199-3p, miR-23a and miR-221 with age in addition (Yu et al. 2011). As already mentioned above replicative as well as stress induced premature senescence has been shown to lead to a phenomenon called SASP that is characterized by the enhanced secretion of specific effector molecules (Ohtani & Hara 2013). While much is known about intracellular microRNA expression and how this profile changes with *in vitro* as well as *in vivo* aging (Chen et al. 2010), hardly any data is available on the age related changes in the microRNA secretion profile. However first indications that the vesicular miRNA secretion profile is altered with age (Olivieri et al. 2013) and in age associated diseases were already provided for cardiovascular disease (Fichtlscherer et al. 2011), Alzheimer's diseases (Cogswell et al. 2008) and Diabetes mellitus, type 2 (Zampetaki et al. 2010).

5.5.2 MicroRNAs and bone biology

Several studies demonstrated the importance of miRNAs in bone maintenance by showing that upon inhibition of microRNA biogenesis in mature osteoblasts or osteoclasts a high bone mass phenotype in adult mice can be observed (Gaur et al., 2010; Mizoguchi et al., 2010; Sugatani and Hruska, 2009) Other studies report a negative influence of specific microRNAs. For example miR-204 (Huang et al. 2010), miR-705 (L. Liao et al. 2013) and miR-3077-5p (L. Liao et al. 2013) were shown to target Runx-2 resulting in a reduced osteogenesis but an enhanced adipogenic differentiation potential of mesenchymal stem cells. On the other hand miR-93 (Yang et al. 2012), miR-143 (Li et al. 2013) and miR-145 (Jia et al. 2013) were shown to decrease osteogenesis by inhibiting the translation of osterix. Taken together these studies could indicate that microRNAs have a negative influence on bone formation in general. However, this conclusion is misleading since some microRNAs were also found to target negative regulators of osteogenesis. For example miR-15b inhibits the expression of a protein that facilitates the degradation of Runx-2 (Vimalraj et al. 2014) and miR-196a was demonstrated to repress an antagonist of BMP signalling (Kim et al. 2009). Another prominent example for an influential microRNA is miR-138 which was shown to have a negative effect on osteogenic differentiation *in vitro* (Eskildsen et al. 2011) and whose overexpression led to a low bone mass phenotype in mice (Eskildsen et al., 2011). Another interesting study revealed that miR-214 levels increase with age (Xiaogang Wang et al. 2013) and that miR-214 inhibits osteogenic differentiation *in vitro*

(Xiaogang Wang et al. 2013). The great therapeutic potential of microRNAs was demonstrated when mice treated with inhibitors against miR-214 were able to maintain bone mass while aging (X. Wang et al. 2013).

MicroRNAs do not only have a leading part in bone remodelling but also in age related pathologies like osteoporosis. For example miR-133a, which is known to inhibit the translation of Runx-2 (X.-B. Liao et al. 2013) and therefore also osteoblastogenesis, has been proven to be upregulated in monocytes of patients suffering from osteoporosis (Wang et al. 2012) and might therefore pose a diagnostic target. Remarkably Li et al found that silencing of miR-2861 leads to negatively impaired osteogenesis in mice (H. Li et al. 2009). Strikingly they also commented on 2 related human individuals exhibiting a homozygote mutation in miR-2861 and suffering from primary osteoporosis in youth (H. Li et al. 2009).

5.6 Galectin-3

Galectin-3 is a 26 kDa protein consisting of 250 amino acids. These amino acids are arranged in 3 different domains (Leffler et al. 2004). The conserved carbohydrate-recognition domain (CRD) conferring its characteristic carbohydrate binding activity. This domain contains in particular an amino acid sequence which facilitates the recognition and low affinity binding to beta-galactoside as well as a high affinity binding to specific larger oligosaccharides (Yang et al. 1996). Due to this characteristic feature the binding of Galectin-3 to potential partners does not simply depend on the presence of both proteins but also on the presence of specific glycosyltransferases or the glycosylation state of the target protein (Dumic et al. 2006). Furthermore Galectin-3 consists of a collagen α-like domain which separates the CRD domain from the short amino-terminal domain (Dumic et al. 2006). The collagen α-like and the N terminal domain exhibit 6 predicted phosphorylation sites which were shown to influence Galectin-3s subcellular localization as well as its interaction with other proteins (Byrd et al. 2012). For example Galectin-3 was shown to impact on Wnt signalling by stabilizing β-Catenin in colon cancer cells (Song et al. 2009; Shimura et al. 2005). Although the direct mechanism for its β-Catenin protective role was not yet elucidated, indications that Galectin-3s Serine 96 phosphorylation site might play an important role were provided when observing that Serine 96 phosphorylation enhanced TCF4 promotor activity in gastric cancer cells (Kim et al. 2010). Galectin-3 is not only localized in the nucleus (Davidson et al. 2002), in the cytoplasm (Davidson et al. 2002) and the cellular

surface (Guevremont et al. 2004) but was also detected in the extracellular matrix (Ochieng et al. 2002) and in the circulation (Zhao et al. 2009). Its localization does not only depend on the cell cycle (Liu et al. 2002) but also on the cell type (Liu et al. 2002) and as a consequence of its various locations and binding partners, Galectin-3 was shown to have multiple functions (Dumic et al. 2006). For example when present in the nucleus it is involved in pre-mRNA splicing (Dagher et al. 1995) and in controlling the cell cycle by inhibiting cyclin A and E and upregulating the cell cycle inhibitors p21 and p27 (Kim et al. 1999; Inohara et al. 1998). Cytoplasmatic Galectin-3 confers a cellular resistance to apoptosis (Akahani et al. 1997) and seems to be involved in endocytosis (Furtak et al. 2001; Lepur et al. 2012). Then again extracellular Galectin-3 plays an important role in the immune response caused by infectious diseases or allergies due to its binding to IgE and the IgE receptor (Frigeri et al. 1993; Radosavljevic et al. 2012). Furthermore it functions as an receptor for advanced glycosylation end products (AGEs) (Vlassara et al. 1995) and contributes to cell-to-cell (Inohara & Raz 1995) as well as cell-to-matrix contact (Perillo et al. 1998). The extracellular presence of Galectin-3 remains especially enigmatic since it does not exhibit a classical endoplasmic reticulum signal sequence necessary for translocation into the endoplasmic reticulum and Golgi mediated secretion pathway (Menon & Hughes 1999). However, Galectin-3 was recently found in fractions of isolated extracellular vesicles (Théry et al. 2001). Additionally phosphorylation of Galectin-3 by Calpain-4 is necessary for its release (Menon et al. 2011). Furthermore Galectin-3 involvement or deregulation in diseases like cardiovascular diseases (De Boer et al. 2010), prion infection (Jin et al. 2007; Mok et al. 2007) and most prominent in tumour development and progression (Zhao et al. 2009; Yu 2010) was shown.

5.7 Unpublished data leading us to the PhD work presented here

Several groups could already demonstrate that osteoblastogenesis is impaired with age (Kassem & Marie 2011; Roholl et al. 1994) and that this impairment contributes to bone loss in elderly and might subsequently lead to osteoporosis (Föger-Samwald et al. 2014). Since several intrinsic factors influencing the differentiation capacity of MSCs are already known (Shuanhu Zhou et al. 2008) we were interested whether changes in the local or systemic environment of MSCs besides the reduction in growth hormones (Darendeliler et al. 2005) or estrogen (Wilson & Thorp 1998; Joss et al. 1997) impact on the osteogenic differentiation capacity of MSCs. Therefore an experimental *in vitro*

system was established in order to study and compare the impact of multiple environments on the ostegenic differentiation potential of MSCs and to identify components of the aged niche which impact on stem cell functionality. In particular the influence of extracellular vesicles from different donors on the differentiation capacity of MSCs was investigated. For this a fraction containing extracellular vesicles isolated by differential centrifugation from the conditioned medium of endothelial cells after a secretion period of 48h or from human plasma was co-incubated with adipose tissue derived mesenchymal stem cells (ASCs) for 3 days before osteogenic differentiation was induced.

Previous experiments showed that extracellular vesicles isolated from the supernatant of endothelial cells are spherical, approximately 100nm in diameter (Figure 4A) and positive for the typical vesicular membrane spanning marker CD63 (Figure 4B).

A **B**

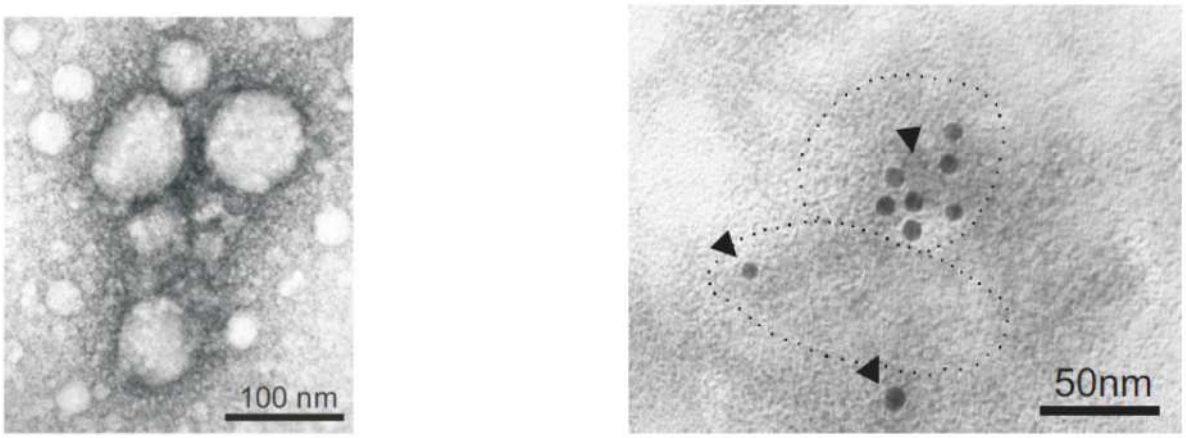

Figure 4: Characterization of EVs isolated from endothelial cell derived supernatants by electron microscopy.

(A) The picture shows the presence of vesicles of 30 – 100nm in diameter isolated by differential centrifugation. The scale bar represents 100nm. **(B)** Isolated immunogold labelled EVs are positive for the vesicular marker CD63. The scale bar represents 50nm.

Exposure of ASCs to EVs isolated from senescent endothelial cell derived supernatant resulted in a decline of osteogenic differentiation capacity compared to cells exposed to vesicles isolated from young quiescent or unexposed cells as quantified by Alizarin Red staining (Figure 5).

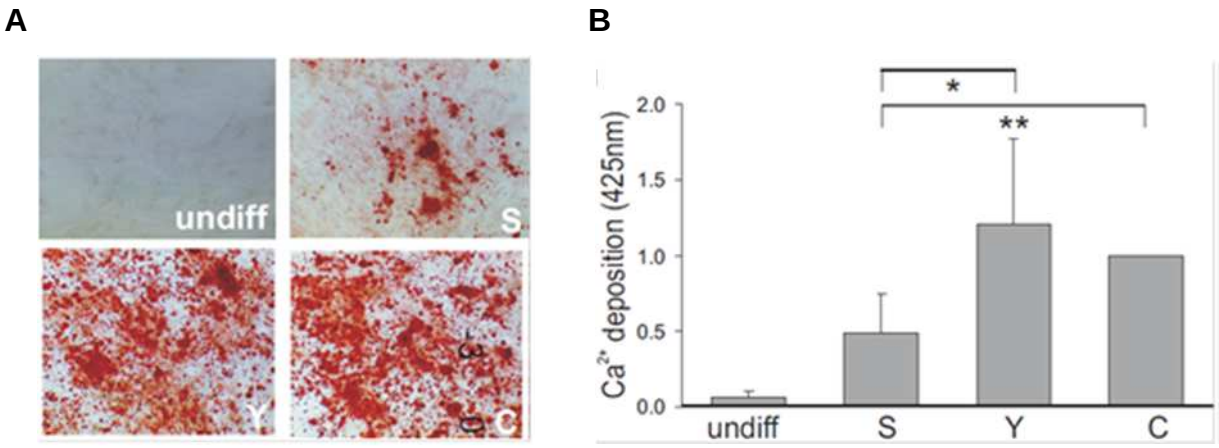

Figure 5: Influence of endothelial derived extracellular vesicles on osteogenic differentiation capacity of ASCs.

(A-B) Mineralization of ASCs after exposure to senescent (S) or young quiescent (Y) endothelially derived EVs as well as of ASCs without exposure to EV (C) or without induction of osteogenic differentiation (undiff) as a control was evaluated by Alizarin Red staining. **(A)** Plate view of Alizarin Red stainings **(B)** The released dye was quantified by microplate reader at 425nm. Mineralization was significantly reduced in ASCs exposed to senescent (S) cell derived EVs compared to cells co-incubated with young quiescent (Y) or no EVs (C).

While searching for factors which are differentially secreted in EVs of young quiescent versus senescent endothelial derived vesicles microRNA-31-5p (miR-31) was found to be enriched in the EV containing fraction of senescent cells compared to the one of young quiescent ASCs as quantified by qPCR (Figure 6).

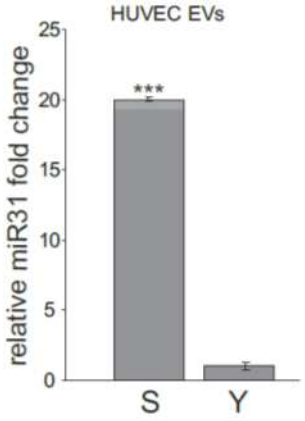

Figure 6: MicroRNA-31 level in senescent versus young quiescent endothelial cell derived extracellular vesicles.

Relative fold change of microRNA-31 (miR-31) levels of extracellular vesicle isolated from the same number of senescent (S) or young quiescent (Y) endothelial cells evaluated by qPCR.

Since miR-31 was shown to be enriched within the anti-osteogenic acting EV fraction isolated from the conditioned medium of senescent ECs, miR-31s effect on osteogenic

differentiation of ASCs was tested. Therefore ASCs were transfected with miR-31 or a non-targeting control. MiR-31 transfected cells showed a significantly reduced osteogenic differentiation potential compared to non-targeting control transfected cells as quantified by Alizarin Red staining (Figure 7).

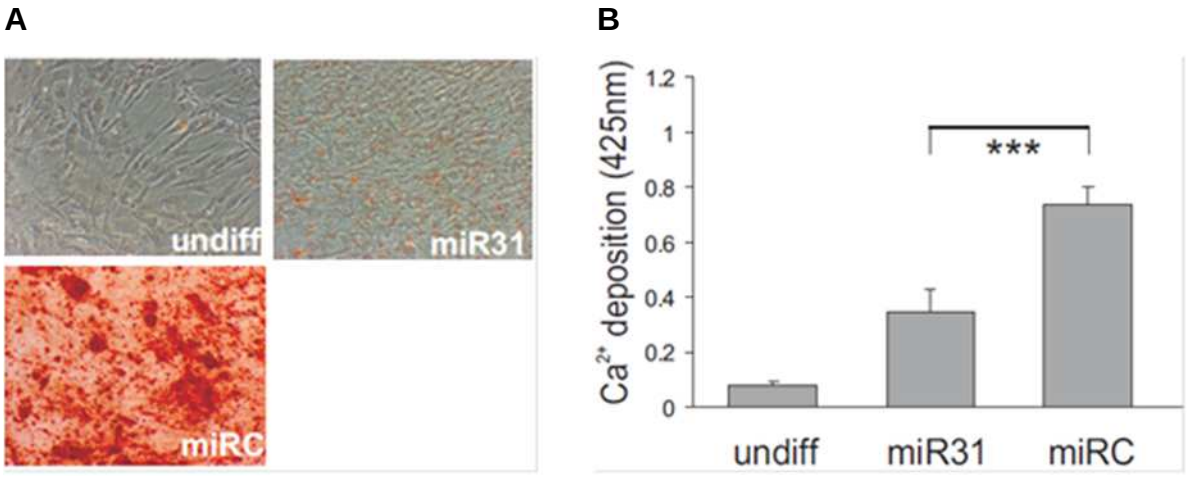

Figure 7: Influence of microRNA-31 (miR-31) overexpression on osteogenic differentiation capacity of ASCs.

(A-B) Mineralization of miR-31 or non-target control (miRC) transfected ASCs as well as of ASCs without induction of osteogenic differentiation (undiff) as a control was evaluated by Alizarin Red staining. **(A)** Plate view of Alizarin Red stainings **(B)** The released dye was quantified by microplate reader at 425nm. Mineralization was significantly reduced in miR-31 transfected ASCs compared to non-target control transfected cells.

Since miR-31 is known to target Frizzled-3 (FZD3) mRNA, a transmembrane protein which is by now thought to be important in the β-Catenin independent Wnt-signalling pathway, the impact of FZD3 on osteogenesis was tested. ASCs transfected with siRNA against FZD3 showed a significantly reduced osteogenic differentiation capacity compared to non-targeting control transfected or untransfected cells (Figure 8).

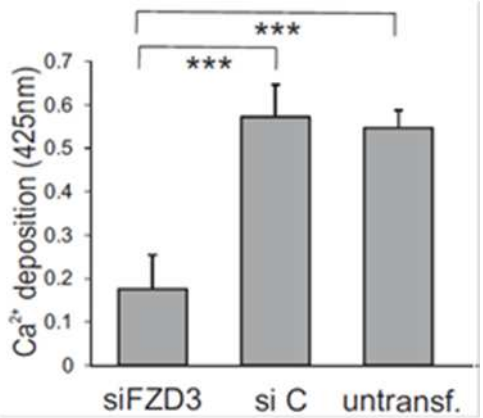

Figure 8: Influence of Frizzled-3 (FZD3) knock down on osteogenic differentiation capacity of ASCs.

Mineralization of siRNA against FZD3 (siFZD3) or non-target control (siC) transfected ASCs as well as of untransfected ASCs (untransf) as a control was evaluated by Alizarin Red stainings. The released dye was quantified by microplate reader at 425nm. Mineralization was significantly reduced in siFZD3 transfected ASCs compared to non-target control (siC) transfected cells.

Since endothelial cells line the blood vessels and senescent endothelial cells are known to accumulate with age *in vivo*, the question rose whether also an isolated fraction containing plasma derived EVs of elderly donors inhibit osteogenic differentiation of ASCs compared to a fraction isolated from young individuals. Plasma derived EVs purified and enriched by differential centrifugation, were spherically formed and of 70 – 120nm in diameter (Figure 9).

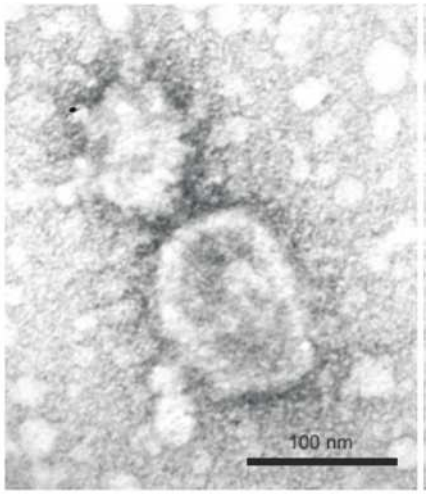

Figure 9: Characterization of plasma derived EVs by electron microscopy.

The picture shows the presence of vesicles of 70 – 120nm in diameter isolated by differential centrifugation. The scale bar represents 100nm

Exposure of ASCs to a fraction of EVs isolated from plasma of elderly resulted in a decline of osteogenic differentiation capacity compared to cells exposed to vesicles isolated from young donors or unexposed cells as quantified by Alizarin Red staining (Figure 10A, B).

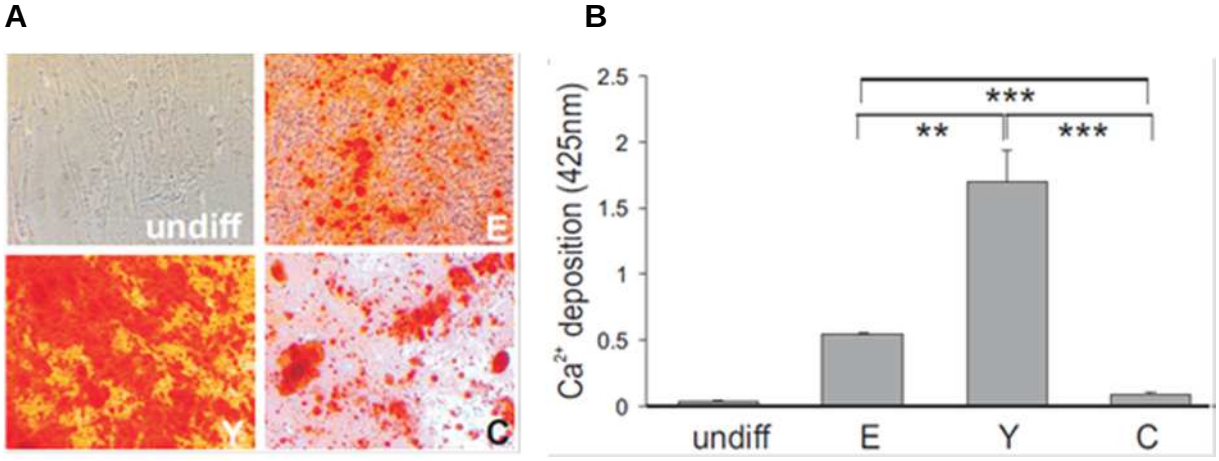

Figure 10: Influence of plasma derived extracellular vesicles on osteogenic differentiation capacity of ASCs.

(A-B) Mineralization of ASCs after exposure to EVs isolated from the plasma of elderly (E) or young (Y) donors as well as of ASCs without exposure to any EV (C) or without induction of osteogenic differentiation (undiff) as a control was evaluated by Alizarin Red stainings. **(A)** Plate view of Alizarin Red stainings. **(B)** The released dye was quantified by microplate reader at 425nm. EVs of elderly donors (E) failed to induce osteogenesis compared to EVs isolated from young individuals (Y). Overall an induction of osteogenesis was observed when ASCs were exposed to plasma derived EVs compared to unexposed ASCs (C).

Summarizing the preliminary data demonstrate that a fraction containing extracellular vesicles isolated from elderly donors fails to induce osteogenic differentiation capacity compared to vesicles derived from young donors and that this inhibitory factors within the fraction might at least in part be provided by senescent endothelial cells since they showed a similar negative effect on osteogenic differentiation capacity as compared to vesicles isolated from young quiescent endothelial cells.

6 Aim

The aim of this study was to identify novel extracellular effector molecules impacting on the osteogenic differentiation process of mesenchymal stem cells in an age dependent way.

7 Material and methods

7.1 Generation of Galectin-3 expression constructs

In order to test the effect of Galectin-3 in osteogenic differentiation a Galectin-3 overexpression construct as well as two constructs overexpressing Galectin-3 mutants exhibiting an Alanine instead of Serine at position 96 in order to destroy the phosphorylation site or an Aspartic Acid instead of Serine at position 96 in order to mimic phosphorylation were prepared.

7.1.1 Cloning

The mammalian expression vector pCMV6-XL4 harbouring the human wild type Galectin-3 cDNA was purchased from Origene. Human Galectin-3 DNA transcript variant I within the pCMV6-XL4 vector was flanked by two NotI restriction sites. Therefore the pCMV6-XL4 plasmid was digested with NotI and the excised cDNA was separated from the vector backbone by agarose gel electrophoresis. After purifying the obtained Galectin-3 cDNA containing insert with the Wizard® SV Gel and PCR Clean-Up Kit (Promega) the n according to manufactures manual, purified Insert was subcloned into the previously NotI digested and dephosphorylated mammalian pcDNA3.1 hygro (+) vector. The design of the Galectin-3 pcDNA3.1 hygro(+) expression construct is graphically outlines in Figure 11**.**

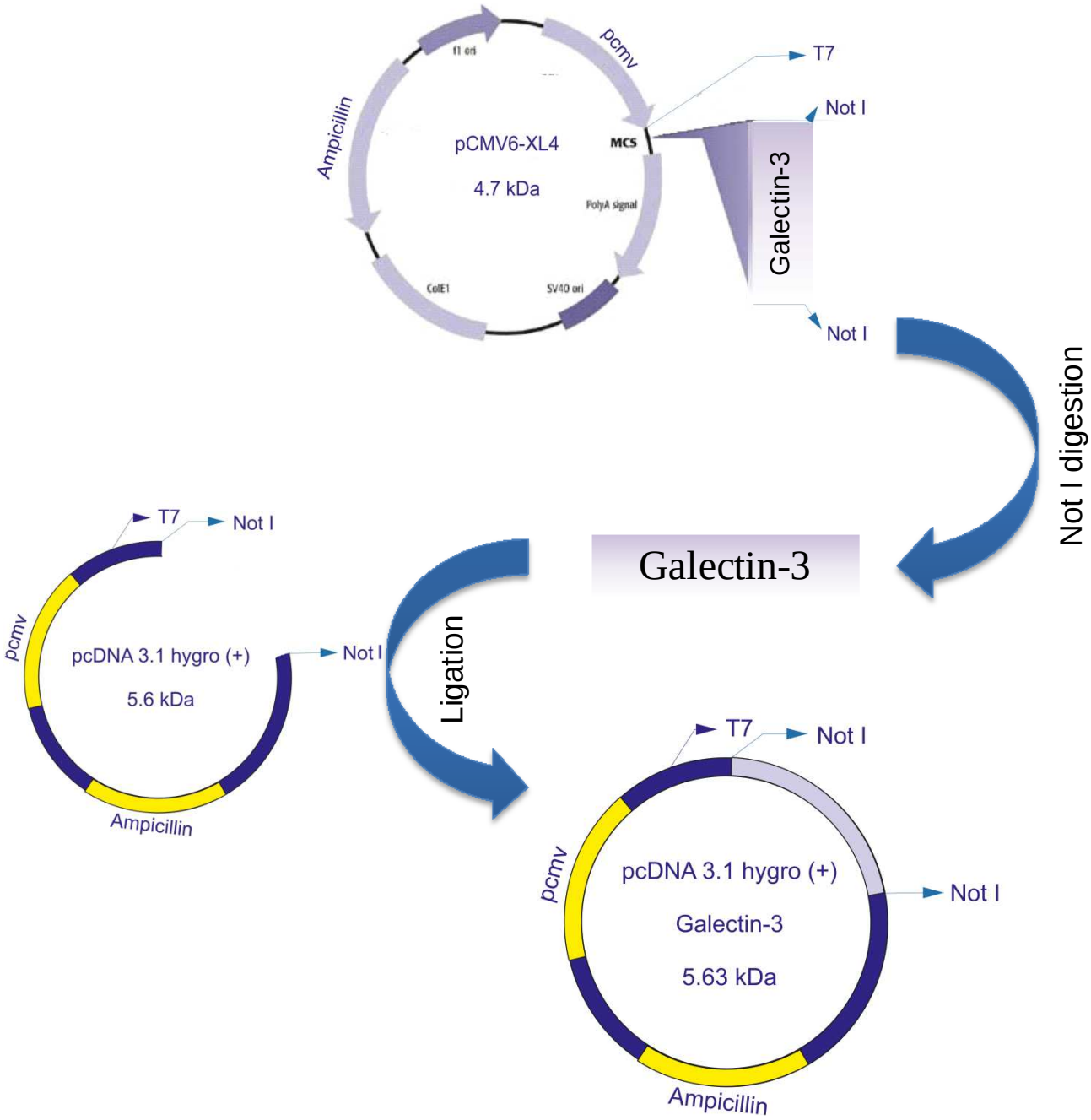

Figure 11: Cloning strategy

The Galectin-3 cDNA containing pCMV6-XL4 expression vector was digested with the aid of the restriction enzyme NotI to isolated Galectin-3 cDNA. The obtained purified insert was subsequently ligated into the previously Not I and dephosphorylated pcDNA 3.1 hygro (+) vector.

7.1.2 Analysis of transformants

The successful insertion of Galectin-3 cDNA was proven with the aid of a NotI restriction enzyme analysis. Furthermore the proper orientation of Galectin-3 was tested by an EcoRI restriction enzyme analysis since not only the multiple coning site of the pcDNA3.1 hygro (+) vector back bone but also the Galectin-3 cDNA exhibit an EcoRI restriction site.

After chemically transforming a plasmid exhibiting the right orientation of Galectin-3 cDNA to the Escherichia Coli strain DH5α, plasmids were isolated from successfully transformed E.coli by plasmid purification by WizardR plus SV minipreps DNA purification system (Promega) according to the manufacturers protocol. Finally the newly generated expression constructs were sequenced with the aid of the T7 primer in order to confirm that the DNA sequence is correct. Sequencing results are found in Appendix D: Sequencing results**.**

7.1.3 Site directed mutagenesis

In order to generate serine 96 (S96) to alanine (S96A) or to aspartic acid (S96D) Galectin-3 mutants the QuikChange Multi Site-Directed Mutagenesis Kit (Agilent technologies) was used according to manufacturer's protocol. Briefly oligonucleotides carring the mutations of interest were designed according to the guidelines of the manual and are listed in Table 1. Next the mutation carrying Galectin-3 plasmids were synthesized. Thereto the Galectin-3 pcDNA3.1 hygro(+) plasmid was denaturated, mutated oligonucleotides were annealed and the primers were extended with the aid of an DNA/DNA polymerase. Afterwards the parental strand was DpnI digested, thereby ensuring that only the newly synthesized mutation harbouring strand remains. Finally the new plasmid was chemically transformed to the Escherichia Coli strain DH5α and the plasmid was subsequently purification by WizardR plus SV minipreps DNA purification system (Promega) according to the manufacturer's protocol. Finally the newly generated expression constructs were sequenced with the aid of the CMV primer in order to analyse the DNA sequence. Sequencing results are shown Appendix D: Sequencing results.

Table 1: Primer sequences for site directed mutagenesis of Galectin-3

	Primer sequence (5´to 3´)
Alanine mutant (S96A) forward	cccatcttctggacagccagctgccaccgga
Alanine mutant (S96A) reverse	tccggtggcagctggctgtccagaagatggg
Aspartic acid mutant (S96D) forward	ctccggtggcatctggctgtccagaagatgggta
Aspartic acid mutant (S96D) reverse	tacccatcttctggacagccagatgccaccggag

7.2 Cell culture

7.2.1 Cell types

7.2.1.1 Human umbilical vein endothelial cells (HUVECs)

Endothelial cells were isolated from human umbilical veins according to the work published by Chang and colleagues (Chang et al. 2005). Adherent HUVECs were grown in T25 or T75 1% gelatine precoated culture flasks (Greiner) in EBM (Lonza) basal medium mixed with EGM Single Quotes (Lonza) and 10% FCS (Sigma) at 37°C in a humidified atmosphere with 5% CO_2. Cells were passaged twice a week at a split ratio of 1:2 to 1:6 according to the growth rate.

7.2.1.2 Human adipose-derived stem cells (ASCs)

Subcutaneous adipose tissue was obtained by liposuction under local anestesia. ASCs were isolated as described before (Wolbank et al. 2009; Wolbank et al. 2007). Briefly adipose tissue was diluted 1:2 in phosphate buffered saline (PBS) buffer and after phase separation the infranatant was discarded. Subsequently the tissue was digested for 1h by collagenase. After the incubation time the digested tissue was centrifuged for 7min at 1180xg and room temperature. Next the adipocyte and collagenase containing supernatant was discarded while the erythrocytes and stem cells containing pellet was resuspended in an erythrocyte lysis buffer and incubated for 10min at 37°C. After the incubation time the tube was centrifuged for 7min at 300xg, the supernatant discarded and the pellet resuspended in PBS. The pellet was washed once more in PBS before it was passed through a 100 and subsequently through a 40µm cell strainer filter. Finally cells were pelleted at 300xg for 7min, resuspended in EGM-2 (Lonza) and seeded in a tissue culture flask and grown at 37°C, 5% CO_2 and 95% air humidity. For subsequent experiments cells were grown in T80 culture flasks (Nunc) in DMEM-low glucose (1%)/HAM´s F-12 (PAA) supplemented with 4mM L-glutamine, 10% fetal calf serum (FCS, Sigma) and 1ng/mL recombinant human basic fibroblast growth factor (rhFGF,

R&D Systems) at 37°C, 5% CO_2 and 95% air humidity. Cells were passaged once a week at a split ratio of 1:3.

7.2.1.3 Peripheral blood mononucleated cells (PBMCs)

PBMCs were isolated from whole blood purchased from Red Cross Vienna by Ficoll gradient centrifugation (StemCell Technologies) in LeucoSep tubes (Greiner Bio-One) according to the manufactures instructions. After isolation PBMCs were grown in culture flasks (Greiner) in RPMI 1640 (PAA) containing 9% FCS (Sigma), 2mM L-glutamine (PAA), 100U/ml penicillin (PAA) and 0,1 mg/ml streptomycin (PAA) at 37°C in a humidified atmosphere with 5% CO_2.

7.2.2 Transfections

ASCs were electroporated using the Neon transfection system (Life technologies) according to the manufactures instruction. Briefly 100000 ASCs were resuspended in 10µl while 700000 HUVECs were resuspended 100µl buffer R. 1µg of DNA or 1µl of 10µM siRNA or miRNA were added to ASCs. On the other hand 5µg of DNA or 5µl of 10µM siRNA or miRNA were added to HUVECs. Subsequently electroporation was performed. Electroporation parameters are listened in Table 2 and details on transfected microRNAs, microRNA inhibitors (a-miRs), siRNAs and corresponding controls are listed in Table 3.

Table 2: Electroporation parameter for transfection of mammalian cells

Cell type	Pulse voltage (V)	Pulse width (ms)	Pulse number
ASCs	1400	10	3
HUVECs	1350	30	1

Cells were transfected with human microRNAs, microRNA inhibitors and there corresponding controls from Ambion or siRNA against Galectin-3 and its corresponding non-targeting control purchased from Dharmacon (Table 3). Three days after transfection, differentiation was started as described before.

Table 3: List of MicroRNA mimics, inhibitors, siRNAs and corresponding controls

Mature miRNA or miRNA inhibitor	RNA sequence	Ordering number
miR-10b-5p	UACCCUGUAGAACCGAAUUUGUG	AM11108
miR-21-5p	UAGCUUAUCAGACUGAUGUUGA	AM10206
miR-22-3p	AAGCUGCCAGUUGAAGAACUGU	AM10203
miR-24-3p	UGGCUCAGUUCAGCAGGAACAG	AM10737
a-miR-31-5p	AGGCAAGAUGCUGGCAUAGCU	AM11465
miR-100-5p	AACCCGUAGAUCCGAACUUGUG	AM10188
miR-148a-3p	UCAGUGCACUACAGAACUUUGU	AM10263
a-miR-328-3p	CUGGCCCUCUCUGCCCUUCCGU	AM10034
miR-637	ACUGGGGGCUUUCGGGCUCUGCGU	AM11545
Pre-miR Negative Control #1		AM17110
a-miR Negative control #1		AM17010
ON-TARGET plus non-targeting pool	UGGUUUACAUGUCGACUAA, UGGUUUACAUGUUGUGUGA, UGGUUUACAUGUUUUCUGA, UGGUUUACAUGUUUUCCUA	D-001810-10-20
ON-TARGET plus SMART pool, human Galectin-3		L-010606-00-005
siGLO		D-001630-01-05

Differentiation assays for adipose tissue derived mesenchymal stem cells

All differentiation experiments were carried out in 24 well cell culture plates.

7.2.2.1 Osteogenic differentiation

For osteogenic differentiation 2000 ASCs per dish of a 24 well culture plate were seeded 3 days before osteogenic differentiation was induced by switching from the growth medium to the osteogenesis medium for up to 3 weeks. The composition of the osteogenesis medium is listened in Table 4.

Table 4: Components of osteogenesis medium

Reagent	Final concentration
DMEM low glucose (1g/l) (PAA)	

FCS (Sigma)	10%
L-Glutamine	4 mM
Dexamethasone (Sigma)	10 nM
Ascorbate-2-phosphate (Sigma)	150 µM
β-Glycerolphosphate (Sigma)	10 mM
1.25 Dihydroxyvitamine D3 (Sigma-Aldrich)	10 nM
Primocin (500x) (Invirtogen)	100 µg/ml

7.2.2.2 Chondrogenic differentiation

For chondrogenic differentiation 10 000 ASCs per dish of an 24 well culture plate were seeded 3 days before chondrogenic differentiation was induced by switching from the growth medium to the chondrogenesis medium for up to 3 weeks. The composition of the chondrogenesis medium is listened in Table 5.

Table 5: Components of chondrogenesis medium

Reagent	Final concentration
DMEM high glucose (4,5g/l):Ham´s F12 1:1 (PAA)	
FCS (Sigma)	10%
Insulin (Sigma)	6 µg/ml
Ascorbate-2-phosphate (Sigma)	200 µM
TGF-β (R&D Systems)	10 ng/ml
Primocin (500x) (Invirtogen)	100 µg/ml

7.2.2.3 Adipogenic differentiation

For adipogenic differentiation 14 000 ASCs per dish of an 24 well culture plate were seeded 3 days before adipogenic differentiation was induced by switching from the growth medium to the adipogenesis medium for up to 2 weeks. The composition of the adipogenesis medium is listened in Table 6.

Table 6: Components of adipogenesis medium

Reagent	Final concentration
DMEM high glucose (4,5g/l) (PAA)	
FCS (Sigma)	10%
L-Glutamine	4 mM
Dexamethason (Sigma)e	1 µM
Indomethacine (Sigma)	60 µM
Hydrocortisone (Sigma)	500 nM
IBMX (Sigma)	500 µM

Primocin (Invirtogen)	100/ml

7.2.3 Isolation of extracellular vesicles

7.2.3.1 Isolation of extracellular vesicles containing fraction V

Extracellular vesicles were either isolated from cell culture supernatant of early passage quiescent, senescent or transfected HUVECs after a secretion period of 48h or from the plasma of healthy human individuals. In the case of plasma samples were diluted in PBS 1:1 before isolation by differential centrifugation and filtration was started. Briefly conditioned cell culture medium or diluted plasma was centrifuged for 15 minutes at 500g and 4°C in order to remove cells. Subsequently the obtained supernatant was centrifuged at 14000g for 15 minutes at 4°C in order to sediment cell debris. In the next step the supernatant was passed through a 0,22 µm filter while the pellet was discarded. In order to isolate extracellular vesicles the filtered supernatant was subsequently centrifuged at 100000 g for 60 minutes at 4°C. While the supernatant was discarded, the pellet containing extracellular vesicles, subsequently referred to as V, was resuspended in growth medium if it was intended for co-incubation with cells, in PBS if they were further purified by immunoprecipitation, in RIPA buffer if vesicular proteins were analysed by Western Blotting or ELISA or directly in TriReagent if RNA analysis were performed subsequently. The composition of the RIPA buffer is listened in Table 7.

Table 7: Components of RIPA buffer

Reagent (Concentration)	Volume [ml]
NaCl (5M)	30
Tris-Cl pH 7,4 (1M)	5.0
NP-40 (20%)	5.0
Sodium deoxycholate (10%)	5.0
SDS (20%)	0.5
ddH2O	50

7.2.3.2 Purification of extracellular vesicles by immunoprecipitation

Coupling of antibodies against CD63 to magnetic beads

The Dynabeads® Antibody Coupling Kit (Invitrogen) kit was used in order to prepare magnetic CD63 monoclonal antibody immunoaffinity capture microbeads (Dynabeads® M-270 Epoxy, Invitrogen) according to the manufacturers protocol.

Briefly 5 mg of magnetic Dynabeads and 1 ml of solution C1 were mixed. The tube was placed on a magnet for 1 minute before the supernatant was carefully discarded. The washed beads were co-incubated with 50µl of monoclonal CD63 antibody (ab8219 Abcam) or 50µl of corresponding mouse IgG1 isotype control (MA1-10406, Thermo scientific) , 200 µl of solution C1 and 250µl of solution C2 on a tube rotator at 37°C over night.

On the next day she tube was placed on a magnet for 1 minute before the supernatant was carefully discarded. Subsequently coupled beads were washed with 800µl of HB, LB, SB buffer and PBS in order to use them immediately.

Depletion of P100 from CD63 positive extracellular vesicles

The isolated extracellular vesicle containing pellet (V) was resuspended in PBS (PAA) and incubated with CD63 antibody coupled Dynabeads for 2 h at 4°C on a tube rotator. In order to obtain the fraction depleted of CD63 positive extracellular vesicles ($CD63^-$) the tube was placed on a magnet for at least 1 minute and the supernatant was carefully transferred to a new 1,5 ml tube. Subsequently extracellular vesicles secreted by $2x10^4$ HUVECs or isolated of 1ml plasma were co-incubated with 2000 ASCs and the remaining supernatant was centrifuged once more at 100 000g for 2h. The obtained pellet was resuspended in RIPA buffer for subsequent protein analysis in order to ensure successful depletion of the CD63 positive vesicular fraction.

The fraction containing CD63 positive extracellular vesicles ($CD63^+$) was eluted by adding 140 µl of citric acid pH=3. The fluid was transferred in a new 1,5 ml tube and immediately mixed with 50 µl of 1M NaOH for neutralization. Subsequently extracellular vesicles secreted by $2x10^4$ HUVECs or isolated of 1ml plasma were co-incubated with 2000 ASCs and the remaining supernatant was centrifuged once more at 100 000g for 2h. The obtained pellet was resuspended in RIPA buffer for subsequent protein analysis in order to ensure successful depletion of the CD63 positive vesicular fraction.

7.2.4 Biological samples

7.2.4.1 Healthy human plasma samples for Galectin-3 experiments

Plasma samples of healthy human female donors were purchased from the Red Cross, Linz, Austria. Donors were female and either younger than 25 or older than 55 years. All donors exhibited normal C reactive protein levels, a body mass index (BMI) of less than 30, were not suffering from diabetes mellitus type II and had blood type A, B or AB.

7.2.4.2 Human plasma samples from patients and health controls for micro-RNA analysis

Plasma samples of patients suffering from a osteoporotic fracture and the corresponding unfractured control individuals were generously provided by Peter Dovjak, Landeskrankenhaus Gmunden, Austria.

7.2.4.3 Galectin-3 knock out mice

Femurs of homozygote Galectin-3 knock out C57black/6 mice as well wild type littermates were generously provided by Prof Tong Liu at the Institute of Biomedical Sciences, Academia Sinica, Taipei, Taiwan. Mice were 17 to 22 weeks old and besides one male couple (18 weeks old) all female. Galectin-3 knock out mice were characterised in detail by Hsu and colleagues as described elsewhere (Hsu et al. 2000).

7.3 Analytical methods

7.3.1 RNA analysis

In order to compare the mRNA levels of typical osteogenic or chondrogenic markers under different conditions or to test for the successful overexpression of certain microRNAs as well as for the knock down of Galectin-3 mRNA or other microRNAs RNA was analysed.

7.3.1.1 Isolation of RNA

7.3.1.1.1 Isolation of intracellular or vesicular RNA

In order to isolate intracellular RNA, the medium was aspirated and the cells were washed twice with PBS (PAA) before cells of one 24 Well were resuspended in 500µl TRI Reagent® (Sigma-Aldrich). In the case of vesicular RNA the obtained pellet after ultracentrifugation was directly resuspended in 500µl TRI Reagent® and transferred into a 1,5ml RNAse free tube (Sarstedt). Subsequently 200µl of Chloroform (Merck) / ml TRI Reagent® were added and mixed for 15 seconds for subsequent RNA extraction. After an incubation time of 3 minutes at room temperature samples were centrifuged at 12000 g for 15 minutes at 4°C for a clean phase separation. . Next the RNA containing aqueous phase was transferred in a new 1,5ml RNAse free tube and 1µl of GlycoBlue™ (Ambion) which is facilitating the RNA precipitation was added. The samples were briefly mixed before 500µl Isopropanol (Merck-Millipore) / ml TRI Reagent® were added to precipitate RNA. After an incubation time of 10 minutes at room temperature, samples were centrifuged at 12000 g for 10 minutes at 4°C. The supernatant was discarded and the RNA containing pellet was washed in 1ml of 70% Ethanol (Merck-Millipore). Therefore the samples were centrifuged at 7500 g for 5 minutes at 4°C. Subsequently the supernatant was discarded and the tubes were shortly spinned in order to aspirate all traces of the remaining Ethanol. Finally the pellet was air dried, resuspended in 20µl of nuclease-free water (NFW) (Qiagen), heated for 10 minutes at 58°C (Thermomixer comfort, Eppendorf) and stored at -80°C upon c-DNA synthesis.

7.3.1.1.2 Isolation of RNA from plasma samples

225µl of plasma was centrifuged at 12 000 g for 5 minutes at 4°C to remove cellular debris. The supernatant was transferred in a new RNAse free 1,5 ml tube (Sarstedt) and mixed with 1 ml Quiazol (Quaigen) and 1µl of RNA spike in kit (Exiquon) for monitoring the sample to sample variation during the isolation process. The solution was mixed for 10 seconds and incubated for 5 minutes at room temperature before 200µl of chloroform were added and mixed for 10 seconds for subsequent extraction. After an incubation time of 3 minutes at room temperature samples were centrifuged at 12000 g for 15 minutes at 4°C for a clean phase separation. Next 650µl of the RNA containing aqueous phase were transferred in a new 1,5ml RNAse free tube and 7µl of 5mg/ml glycogen (Ambion) were added which is facilitating the following RNA precipitation process. The samples were briefly mixed and 975µl of 100% Ethanol (Merck-Millipore) were added to precipitate RNA. By pipetting and inverting the tube several times proper mixing was ensured. Subsequently RNA was isolated with the aid of miRNeasy mini kit (Quiagen) according to manufactures instructions. Briefly the first sample volume of 700µl were transferred to the RNeasy Mini Spin Column (Quiagen) and centrifuged at 13000g for 30 seconds at room temperature. The flow-through was discarded and the remaining sample volume was loaded onto the same column and again spinned at 13000g for 30 seconds at room temperature. The flow through was discarded and the membrane bound RNA was washed once with 700µl RWT (Quiagen) and subsequently 3 times with 500µl RPE buffer (Quiagen) by centrifuging at 13000g for 1 minute at room temperature. Finally the column was transferred to a new RNAse free 1,5 ml tube and centrifuged for 2 minutes at room temperature for at 13000 g. In the last step the column was once more transferred to a new RNAse free 1,5 ml tube and the RNA containing membrane was evenly moistened with 30µl nuclease-free water (Qiagen). In order to elute the RNA the column was placed on a DNase/RNase free low bind 1.5 ml tubes (Eppendorf) and centrifuged at 13000g for 1 minute at room temperature. Until reuse isolated RNA was stored at -80°C.

7.3.1.2 Copy-DNA Synthesis

7.3.1.2.1 cDNA Synthesis for mRNA analysis

Quantitative real time polymerase chain reaction (PCR) is performed by a heat stable DNA dependent DNA polymerase in order to analyse mRNA levels. Therefore isolated

RNA needs to be converted into copyDNA (cDNA) with the aid of a RNA dependent DNA polymerase reversed transcriptase. Thereto RNA concentration was measured at 260nm before maximal 500 ng of RNA per sample were mixed with 2 x RT buffer (Finnzymes), the random hexamer primer set (Finnzymes) and the transcriptase M-Mul V Rnase H+ (Finnzymes) according to manufactures instruction described in Table 8. Subsequently cDNA was synthesized with the aid of the T3 thermocycler (Biometra) according to the cycling protocol described in Table 9.

Table 8: Mix for one mRNA c-DNA synthesis reaction

Reagent	Volume [µl]
2 x RT buffer	10
Random hexamer primer set	1
M-Mul V Rnase H+	2
500 ng of RNA template	x
NFW	7-x

Table 9: Cycling protocol for c-DNA synthesis from mRNA

Step	Temperature [°C]	Time [min.]
1st - Primer extension	25	10
2nd - cDNA synthesis	37	30
3rd - Reaction termination	85	5
4th - Cooling	4	5

7.3.1.2.2 cDNA Synthesis for microRNA analysis

Quantitative real time polymerase chain reaction (PCR) is performed by a heat stable DNA dependent DNA polymerase in order to analyse miRNA levels. Therefore isolated RNA needs to be converted into copyDNA (cDNA) with the aid of a RNA dependent DNA polymerase reversed transcriptase. Thereto RNA concentration was measured at 260nm before maximal 10 ng of RNA per sample were used. Reversed transcription was performed with the aid of TaqMan® MicroRNA reverse transcription kit (Applied Biosystems) CDNA was synthesized with the aid of the T3 thermocycler (Biometra) according to the recipe (Table 9) and the cycling protocol (Table 11) described below.

Table 10: Mix for one miRNA c-DNA synthesis reaction

Reagent (Concentration)	Volume [µl]
RT-Primer (5x)	2.00
Buffer (10x)	1.00
dNTPs (100 mM)	0.10
RNase Inhibitor	0.12
MultiScribe RT polymerase	0.60
Nuclease free water	5.18
cDNA template	1.00

Table 11: Cycling protocol for c-DNA synthesis from miRNA

Step	Temperature [°C]	Time [min.]
1st - Primer extension	16° C	30
2nd - cDNA synthesis	42° C	30
3rd - Reaction termination	85° C	5
4th - Cooling	4° C	5

7.3.1.3 Quantitative real time PCR

7.3.1.3.1 Quantitative real time PCR of mRNAs

In order to determine and compare the relative amounts of specific mRNAs of different samples the 5x HOT FIREPol EvaGreen qPCR mix (Biotium), containing a DNA dependent DNA polymerase as well as a fluorescent dye when bound to double stranded DNA, was used according to manufactures instruction. Therefore cDNA was mixed with the Evagreen reaction buffer as well as the corresponding primer pairs according to Table 12. CDNA was amplified and quantified with the aid of RotorGene2000 (Corbett) according to the cycling protocol in Table 13. Osteogenic differentiation was confirmed by the early osteogenic marker alkaline phosphates (ALP) at day 7, the mid marker osteonectin (ON) at day 14 and the late marker osteocalcin (OC) at day 21 after induction of differentiaiton. Regulation of Galectin-3 and Frizzled-3 during osteogenesis as well as the influence of Galectin-3 on Runx-2 expression were determined with the aid of specific primers as well. In particular Frizzled-3 mRNA levels were analysed at day 3 after induction of osteogenic differentiation. Chondrogenic differentiation potential was quantified by determining the late marker Collagen X and

Aggrecan. All gene expression data obtained were normalized to the housekeeper Glycerinaldehyd-3-phosphat-Dehydrogenase (GAPDH). Primer pairs are listed in Table 14.

Table 12: Mix for one quantitative real time PCR to compare mRNA levels

Reagent	Volume [µl]
Primer sense	0.25
Primer antisense	0.25
Reaction buffer	2.00
NFW	6.50
cDNA template	9.00

Table 13: Cycling protocol for quantitative real time PCR to compare mRNA levels

Step	Temperature [C°]	Time
1st – Hot start PCR	95	15 min.
2nd –Denaturation	95	15 s.
3rd – Primer annealing	60	30 s.
4th – Extension time	72	15 s.
45 repetitions of step 2 – 4		

Table 14: Primer sequences used for quantitative real time PCR

MRNA		Primer sequence (5´to 3´)
GAPDH	forward	TGTGAGGAGGGGAGATTCAG
GAPDH	reverse	CGACCACTTTGTCAAGCTCA
ALP	forward	GCGCAAGAGACACTGAAATATGC
ALP	reverse	TGGTGGAGCTGACCCTTGAG
Runx-2	forward	CTTCACAAATCCTCCCCAAG
Runx-2	reverse	GAATGCGCCCTAAATCACTG
Osteonectin	forward	ATCTTCCCTGTACACTGGCAGTTC
Osteonectin	reverse	CCACTCATCCAGGGCGATGTAC
Osteocalcin	forward	ATCAAAGAGGAGGGGAACCTA
Osteocalcin	reverse	AGGAAGTAGGGTGCCATAACA
Galectin-3	forward	ATGCAAACAGAATTGCTTTAGATT
Galectin-3	reverse	AGTTTGCTGATTTCATTGAGTTTT
Frizzled-3	forward	TGTCGTAGGCTGTGTCAGCGGGC
Frizzled-3	reverse	TCTCTGCACTGCCACTGGGGCTC
Collagen X	forward	CCCTTTTTGCTGCTAGTATCC
Collagen X	reverse	CTGTTGTCCAGGTTTTCCTGGCA
Aggrecan	forward	ACAGCTGGGGACATTAGTGG
Aggrecan	reverse	GTGGAATGCAGAGGTGGTTT
Versican	forward	TGGAATGATGTTCCCTGCAA
Versican	reverse	AAGGTCTTGGCATTTTCTACAACAG

7.3.1.3.2 Quantitative real time PCR of microRNAs

In order to determine and compare the relative amounts of specific miRNAs of different samples the taqman assay (Life technologies), containing a DNA dependent DNA polymerase was used according to manufactures instruction. Therefore cDNA was mixed with the taqman reaction buffer as well as the corresponding fluorescent primer according to Table 15. CDNA was amplified and quantified with the aid of RotorGene2000 (Corbett) according to the cycling protocol listed in Table 16.

Table 15: Mix for one quantitative real time PCR to compare miRNA levels

Reagent	Volume [µl]
Taqman reaction buffer (2x) (Applied Biosystems)	5.0
RT-Primer (20x) (Applied Biosystems)	0.5
cDNA template	1.0
NFW	3.5

Table 16: Cycling protocol for quantitative real time PCR to compare miRNA levels

Step	Temperature [C°]	Time
1st – Hot start	95	15 min.
2nd –Denaturation	95	10 s.
3rd – Primer annealing	60	45 s.
4th – Extension time	72	20 s.
55 repetitions of step 2 – 4		

7.3.2 Protein analysis

7.3.2.1 SDS PAGE and Western blotting

Proteins from cells or from extracellular vesicles were extracted by lysing the samples in sodium dodecyl sulphate (SDS) loading dye containing 5 % Mercaptoethanol. Subsequently protein lysates were sonicated 30 times for 30 seconds with a cooling break of 30 seconds in between (Bioruptor Plus, Diagenode).

Next samples were subjected to 4–15% SDS-polyacrylamide gel electrophoresis (Biorad). Proteins were transferred by semi-dry electroblotting to a PVDF membranes (Biorad) and membranes were blocked in 3% non-fat milk (PBS, 0,1% Tween (VWR), 3% dry-milk) for at least 3 hours at room temperature but not longer than over night at 4°C. Membranes were exposed to antibodies against Galectin-3 (ab2785, Abcam, 1:1000), total β-Catenin (PA5-19469, Thermo Scientific, 1:200), unphosphorylated β-

Catenin (06-734, Millipore, 1:750) or GAPDH (MA5-15738, Pierce 1:5000). Anti-Rabbit-IR-Dye 800 (LiCor, 1:10000) or anti-mouse-IR-Dye® 680RD Donkey anti-Mouse (LiCor, 1:10000) were used for subsequent detection by Odyseey (Licor) infrared image system (LiCor). All antibodies were diluted in 0,1% Tween-20 containing PBS and incubated for at least 1 h at room temperature.

7.3.2.2 Enzyme linked immunoassay

Proteins from cells or from extracellular vesicles were extracted by lysing the samples for 15 minutes at room temperature in RIPA buffer containing 1x phosphatase inhibitor (Roche) and 1x Protease inhibitor (Roche). Subsequently protein lysates were sonicated 30 times for 30 seconds with a halt of 30 seconds in between (Bioruptor Plus, Diagenode).

Vesicular and plasma Galectin-3 concentrations were determined with an enzyme-linked immunoassay (ELISA) kit (Abcam, ab119525) according to manufactures instructions. Briefly the 96 well culture plate precoated with a specific antibody against Galectin-3 was washed 4 times. Next 100µl of standards and 50µl of protein samples or plasma were transferred into the wells and mixed with 50µl biotin antibody solution. After co-incubation for 2h at room temperature and 3 washing steps to remove the unbound proteins 100µl of streptavidin-horseradish peroxidase conjugate were added and incubated for 1h at room temperature. Subsequently each well was washed 3 times before 100µl of 3,3',5,5' - tetramethylbenzidine substrate were added. Finally reaction was stopped after 10 minutes of incubation at room temperature and the concentration of Galectin-3 was quantified by detecting the absorbance at 450nm using 620nm as reference wave length (Tecan Infinity M200 plate reader, Magellan software for analysis of data).

7.3.3 Flow cytometry

In order to determine the transfection efficiency pmaxGFP or siGlow transfected HUVECs or ASCs were harvested 48h after electroporation. Therefore cells were detached with the aid of Trypsin (Sigma), resuspended in the corresponding growth medium and washed two times with PBS (PAA) before flow cytometric analysis was performed. Cells were examined by flow cytometry using a FACS Gallios (Beckman Coulter). Obtained data were analysed with the aid of Kaluza Software.

7.3.4 Analysis of differentiation capacity

7.3.4.1 Analysis of osteogenic differentiation capacity

Alkaline phosphatase activity assay

This assay measures the activity of alkaline phosphatase. Basically p-Nitrophenylphosphate is used as substrate. Upon ALP hydrolysis p-Nitrophenylphosphate is dephosphorylated to yellow coloured p-Nitrophenol whose amount is consequently quantified by detecting the absorbance at 405nm (Tecan Infinity M200 plate reader, Magellan software for analysis of data).

7 days after induction of osteogenesis osteogenesis medium was aspirated and cells were washed 3 times with PBS (PAA). Subsequently 100µl ALP lysis buffer (0,25% v/v Triton X-100 in ALP buffer) were added per dish of a 24 well culture plate and incubated for 1h at room temperature. Next cell lysate was centrifuged for 10 min at 13000xg and 4°C. Next 50µl ALP Buffer A (Table 18) were added per tube and the sample was incubated for 20 minutes at room temperature. During this time, exposure to intense light was avoided. Finally 50µl 0,2M NaOH was added to stop the reaction and absorption was measured at 405nm relative to 620nm.

Table 17: ALP buffer

Reagent	Final concentration
2-amino-2-methyl-1-propanol (Sigma-Aldrich)	0.5 M
Magnesiumchloride (VWR)	2.0 mM
AD	90 ml
Adjust pH to 10.3	
Fill to 100 ml	

Table 18: ALP buffer A

Reagent	Amount
p-Nitrophenylphosphate disodium hexahydrat (Sigma-Aldrich)	7,4 mg
ALP buffer	1 ml

Alizarin Red staining

Alizarin Red S is a calcium binding dye. In order to quantify the degree of mineralization of ASCs, Alizarin Red staining was performed at the end of the differentiation process. Therefore medium was aspirated and cells were washed 3 times with PBS without calcium or magnesium (PAA). Subsequently cells were fixed with 500µl of 70% ethanol

(Merck) per dish of a 24 well culture plate for at least 1h at -20°C. Afterwards ethanol was discarded and cells were washed 3 times with AD. Next deposited calcium was stained with 500µl Alizarin Red staining solution (Table 19) per dish for 10 minutes while shaking. In order to aspirate the excessive dye, cells were washed several times with PBS. The remaining dye was extracted by the addition of 200µl Alizarin Red extraction solution (Table 20) for 30 min at room temperature. Finally the amount of dye was quantified by measuring the absorbance at 425nm (Tecan Infinity M200 plate reader, Magellan software for analysis of data).

Table 19: Alizarin Red staining solution

Reagent	Final concentration
Alizarin Red S (AppliChem)	40 mM
AD	10ml
Adjust pH to 4.2	

Table 20: Alizarin Red extraction solution

Reagent	Final concentration
Sodium Dodecyl Sulfate	0.5 %
HCl	0.1 M
AD	50 ml

7.3.4.2 Analysis of chondrogenic differentiation capacity

Chondrogenic differentiation capacity was quantified by determining the mRNA levels of aggrecan normalized to GAPDH using qPCR. Aggrecan is a proteoglycan necessary for crosslinking collagen, type II and therefore abundant in cartilage. On the other hand mRNA levels of collagen, type X normalized to GAPDH as marker for hypertrophic chondrocytes were quantified by qPCR. Hypertrophic chondrocytes do not produce collagen, type II anymore but facilitate the mineralization of their environment a process known as endochondral ossification.

7.3.4.3 Analysis of adipogenic differentiation capacity

Adipogenic differentiation capacity was quantified with the aid of Infinity Tm triglycerides quantification kit (Microgenics, TR22421) 14 days after induction of adipogenesis. Initally medium was aspirated, cells were washed once with PBS (PAA) and covered with 250µl PBS (PAA) per well. Subsequently the cell surface was manually scratched with a pipette tip and 200µl of cell lysate were transferred in a 1.5ml tube (Sarstedt).

Next cell lysates were sonicated 30 times for 30 seconds with a cooling break of 30 seconds in between (Bioruptor Plus, Diagenode). To quantify the amount of triglycerides 30µl of glycerol (Merck) standards or 30µl of samples were mixed with 200µl Triglyceride Reagent (Microgenics, TR22421) and incubated for 10 min at 37°C. Finally triglyceride content was quantified by measuring the absorbance at 500nm (Tecan Infinity M200 plate reader, Magellan software for analysis of data). In order to normalize the obtained data protein concentration was determined by bicinchoninic acid (BCA) assay. Therefore 25µl of bovine serum albumin (Sigma) standard or 25µl sample were mixed with 200µl working reagent (Pierce ® BCA protein assay kit) for 30 sec and incubated for 30 min. at 37°C. The colour changes from green to purple in proportion to the total protein content. Therefore protein concentration is measured by detecting the absorbance at 562nm (Tecan Infinity M200 plate reader, Magellan software for analysis of data).

7.3.4.4 Analysis of immunomodulatory properties

ASCs or urine derived mesenchymal stem cells (USCs) were seeded at different concentrations ($5x10^4$, $2.5x10^4$,$1.25x10^4$,$0.63x10^4$ or $0.32x10^4$ cells per 96 well tissue culture plate). On the next day stem cell growth medium was aspirated and $5x10^4$ PBMCs suspended in 100µl medium containing no or 2.4 µg/ml phytohemagglutinin (PAH) were added per well for 3 days in order to activate PBMCs. In an attempt to quantify immunomodulatory properties of ASCs or USCs 10µl tetrazolium dye (MTT) were added per well for 4h. After this incubation time 100µl of 10% sodium dodecyl sulfate (SDS) in 0.01 M HCl were added and incubated for 24h. The colour changes to purple in proportion to the metabolic activity and therefore the viable cell number. Consequently metabolic activity was measured by detecting the absorbance at 570nm to 690nm as reference (Tecan Infinity M200 plate reader, Magellan software for analysis of data).

7.3.5 µCT imaging

Femur of Galectin-3 knock out mice as well as corresponding wild type littermates were delivered in 50% ethanol and examined using microCT (µCT 50, Scanco Medical AG). The isotropic scanning resolution was 7,4 µm (70kV, 200 µA, 500ms sample time). Scan timer per femur was about 3 hours. By the use of a bone phantom the scanner

was calibrated. Longitudinal aligned scans were analyzed and reference points were chosen in order to compare samples from different ice. The volume of interest was 1,48mm. Cortical parameters were measured at the middle of the diaphysis, while trabecular parameters were determined 148µm from the distal growth plate in the metaphysis region. Attention has been made to exclude the primary spongia. Cortical thickness as well as trabecular thickness, number and spacing were examined.

7.4 Statistics

Data were tested for Gaussian distribution by using D'Agostino & Pearson omnibus normality test. Subsequent comparison of two groups was performed by unpaired or paired t-test if Gaussian distribution was given or Mann Whitney test if not. If one parameter of more than two groups was compared 1-way-ANOVA and if two parameters in several groups were compared 2-way ANOVA was performed. Depending on the Gaussian distribution either Pearson correlation or Spearman correlation was performed. Analyses were performed with GraphPad Prism 5. The tests were two-tailed with type 1 error probability of 0.05. Data are presented as mean values ± SD.

8 Results

8.1 Influence of extracellular vesicles on differentiation capacity

In previous experiments the influence of plasma derived extracellular vesicles (EVs) on osteogenic differentiation capacity of mesenchymal stem cells was shown to strongly depend on the plasma donors age (Figure 10). In order to confirm this observation and to test whether these extracellular vesicles also impact on chondrogenic or adipogenic differentiation capacity, ASCs of one donor were co-incubated with extracellular vesicles isolated from the plasma of either two donors younger than 25 (Y1, Y2) or two individuals older than 50 years (E1, E2) for three days before differentiation was induced.

ASCs exposed to EVs derived from young donors exhibited significantly increased osteogenic differentiation capacity as quantified by Alizarin Red staining (Figure 12) as well as chondrogenic differentiation potential as analysed by qPCR on Aggrecan (Figure 13C) as compared to cells co-incubated with vesicles isolated from elderly donors. On the other hand neither the adipogenic, as quantified by the triglyceride content (Figure 14B), nor the endochondrial differentiation capacity, as analysed by qPCR on Collagen X (Figure 13B), of ASCs were significantly influenced by the plasma donors age. Pictures of ASCs differentiated into the chondrogenic (Figure 13A) and adipogenic (Figure 14A) lineage were taken at the end of the differentiation process.

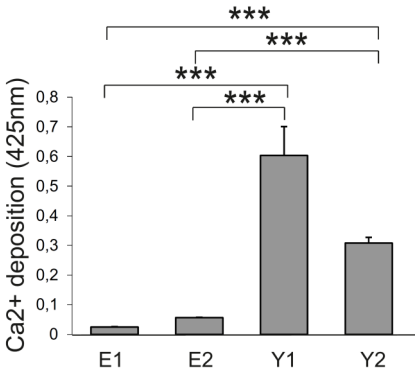

Figure 12: Vesicular impact on osteogenic differentiation capacity of ASCs

Mineralization of ASCs exposed to extracellular vesicles either derived from donors older than 55 years (E1, E2) or from donors younger than 25 years (Y1, Y2).was evaluated by Alizarin Red staining. The released dye was quantified by microplate reader at 425nm. Mineralization was significantly increased in

ASCs exposed to extracellular vesicles of young donors compared to ASCs exposed to vesicles of elderly donors. *:p<0,05; **: p<0.01; ***: p<0.001 in comparison to indicated group. Data are presented as mean values ± SD and were statistically analysed by 1-way ANOVA followed by Bonferroni´s multiple comparison test.

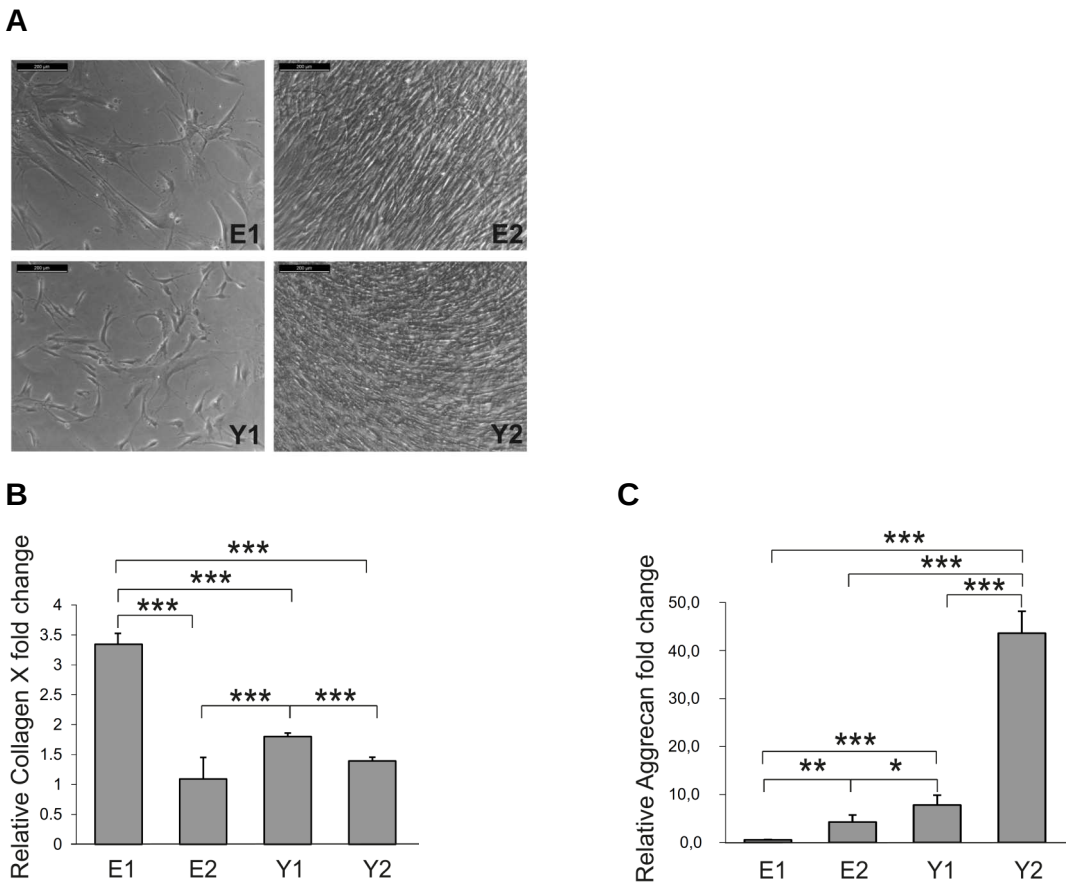

Figure 13: Vesicular impact on chondrogenic differentiation capacity of ASCs.

(A) Bright field microscopy images of ASCs co-incubated with extracellular vesicles either derived from donors older than 55 years (E1, E2) or from donors younger than 25 years (Y1, Y2) at day 21 of chondrogenic differentiation. **(B-C)** Relative fold change of Collagen X **(B)** and Aggrecan **(C)** mRNA level of ASCs at day 21 after induction of chondrogenic differentiation were evaluated by qPCR and normalized to GAPDH. **(B)** There is a significantly increased differentiation capacity of ASCs exposed to extracellular vesicles isolated from the elderly donor E1, but no vesicular effect on Collagen X mRNA expression correlating with the EV donors age can be observed. **(C)** A significant vesicular effect on Aggrecan mRNA expression correlating with the EV donors age was observed.*:p<0,05; **: p<0.01; ***: p<0.001 in comparison to indicated group. Data are presented as mean values ± SD and were statistically analysed by 1-way ANOVA followed by Bonferroni´s multiple comparison test.

A **B**

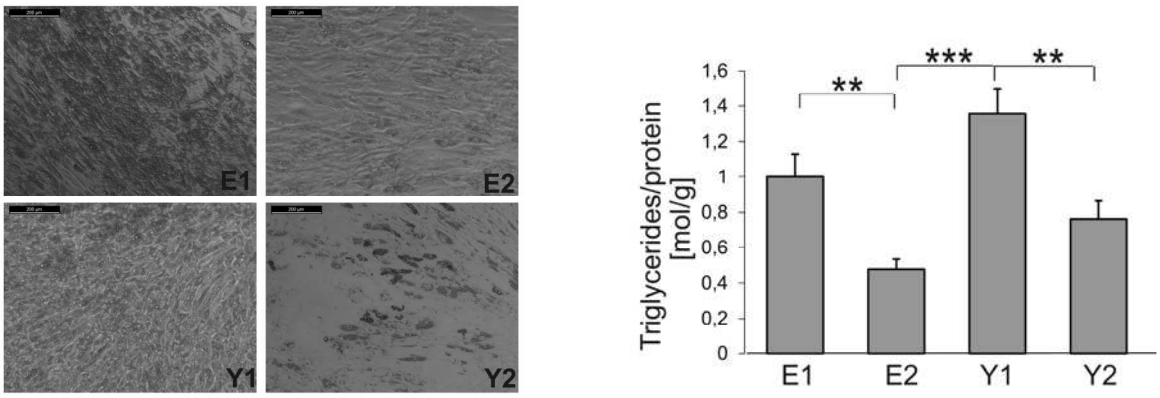

Figure 14: Vesicular impact on adipogenic differentiation capacity of ASCs.

(A) Bright field microscopy images of ASCs co-incubated with extracellular vesicles either derived from donors older than 55 years (E1, E2) or from donors younger than 25 years (Y1, Y2) at day 14 of osteogenic differentiation. **(B)** Content of triglycerides normalized to the amount of protein at day 14 after induction of adipogenic differentiation. No clear vesicular effect on adipogenic differentiation capacity correlating with the EV donors age was observed. ****:** $p<0.01$; *****:** $p<0.001$ in comparison to indicated group. Data are presented as mean values ± SD and were statistically analysed by 1-way ANOVA followed by Bonferroni´s multiple comparison test..

8.2 MicroRNA-31

8.2.1.1 Vesicular shuttling of microRNAs from endothelial cells to stem cells

Since endothelially derived EVs were shown to have a population doubling dependent influence on osteogenesis (Figure 5) and senescent cell derived vesicles were shown to be enriched in anti-osteogenic acting miR-31, a possible transfer of microRNAs by endothelial derived EVs to ASCs was tested for. Therefore young quiescent endothelial cells were transfected with cel-miR39, a microRNA of C. elegans with no homologue in Homo sapiens, by electroporation. 24h post transfection the medium was changed to remove not incorporated cel-miR39 and after a secretion period of 48h extracellular vesicles were isolated by differential centrifugation. Subsequently ASCs were exposed for 1, 12, 24 or 72 hours to EVs secreted by 1,2 x 10^6 ECs or for 72h to EVs secreted by 2,4 x 10^6 ECs. Detection of intracellular cel-miR39 levels of ASCs after the indicated co-incubation time by qPCR reveals an exposure-time (Figure 15A) as well as EV-dose (Figure 15B) dependent uptake compared to EVs isolated from non-targeting control transfected ECs.

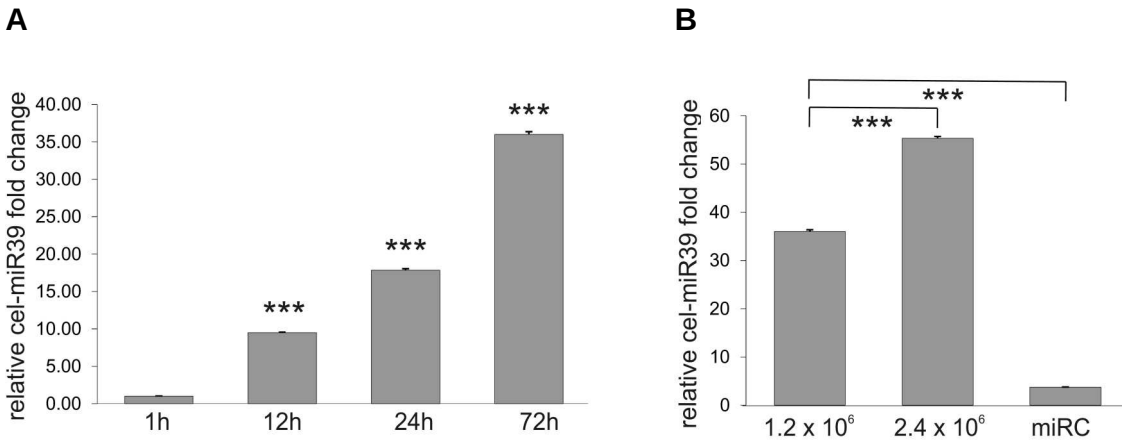

Figure 15:Time and dose dependent delivery of microRNAs by endothelial derived extracellular vesicles to ASCs.

Relative fold change of intracellular cel-miR39 was evaluated by qPCR and normalized to RNU6. **(A)** Intracellular cel-miR39 levels of ASCs after exposure to EVs for 1, 12, 24 or 72 hours. ***: $p<0.001$ in comparison to 1 h control. Data are presented as mean values ± SD and were statistically analysed using unpaired *t* test. **(B)** Intracellular cel-miR39 levels of ASCs after exposure to EVs isolated from 1.2 x 10^6 or 2.4 x 10^6 cel-miR39 transfected endothelial cells or non-targeting control transfected HUVECs (miRC) for 72 hours. *****:** $p<0.001$ in comparison to indicated group. Data are presented as mean values ± SD and

were statistically analysed using one way ANOVA followed by a Bonferroni test to compare every pair of means, n=1.

8.2.1.2 CD63 positive extracellular vesicles inhibit osteogenesis

When isolating the extracellular vesicle containing fraction, subsequently referred to as V, of conditioned media or plasma samples by differential centrifugation, other factors such as protein aggregates might co-pellet during the last ultracentrifugation step. In order to test whether the osteogenesis inhibitory activity is indeed mediated by senescent endothelial cell or elderly plasma derived EVs, extracellular vesicles containing fraction (V) was isolated from endothelial derived supernatant (SN) using differential centrifugation. Therefore SN was centrifuged at 500g for 15minutes followed by a centrifugation step at 14 000 g for 15 minutes. Subsequently the pellet was discarded and the supernatant was passed through a 0.22µm filter before EVs were pelleted at 100 000g for 1h. Subsequently the obtained extracellular vesicle containing pellet (V) was further purified by immunoprecipitation. Therefore the V pellet was resuspended in PBS and spit into two parts. In order to deplete one half from CD63 positive extracellular vesicles it was loaded on magnetic beads coupled to an antibody against CD63, a transmembrane marker which endothelial derived vesicles were already stained positive for (Figure 4B). The second part was co-incubated with magnetic beads coupled to the corresponding isotype antibody control. After an incubation time of 2h at 4°C, the supernatants, subsequently referred to as $CD63^-$ for the fraction depleted of CD63 positive vesicles or tV for the total extracellular vesicle containing fraction, were transferred into new tubes and spinned for 1h at 100 000g. Experimental strategy for identifying the fraction influencing osteogenic differentiation of ASCs is graphically outlines in Figure 16.

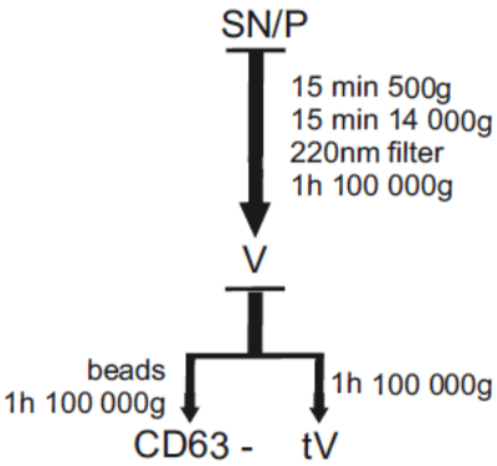

Figure 16: Experimental setup for immunoprecipitation.

The extracellular vesicles containing fraction (V) was isolated from supernatant (SN) or human plasma samples by differential centrifugation starting with a centrifugation at 500g for 15 minutes. Pellet was discarded and the supernatant was centrifuged at 14.000g for 15 minutes. Subsequently the supernatant was transferred into ultracentrifugation tubes through 0.22µm filters and centrifuged for 1h at 100.000g. The supernatant was discarded and the obtained pellet was resuspended in 1ml PBS whereof in each case 500µl were loaded on anti-CD63 or anti-isotype control coupled magnetic beads. Samples were incubated at 4°C for at least 2h under gentle rotation. After the incubation time the beads were placed on a magnet to collect the beads at the tube wall and the supernatant corresponding to the fraction free of CD63 positive vesicles ($CD63^-$) or the one containing still total extracellular vesicles (tEV) were transferred in a new tube. Finally the CD63 negative ($CD63^-$) as well as the total extracellular vesicle containing fraction (tV) were centrifuged at 100.000g for 1h at 4°C and the isolated pellet was resuspended in the corresponding volume of ASC growth medium.

The successful depletion of CD63 positive EVs from the $CD63^-$ fraction compared to the total EV fraction tV (Figure 17 A) or to the CD63 positive ($CD63^+$) fraction (Figure 17B), eluted by lowering the pH to 4, was proven by Western blot analysis.

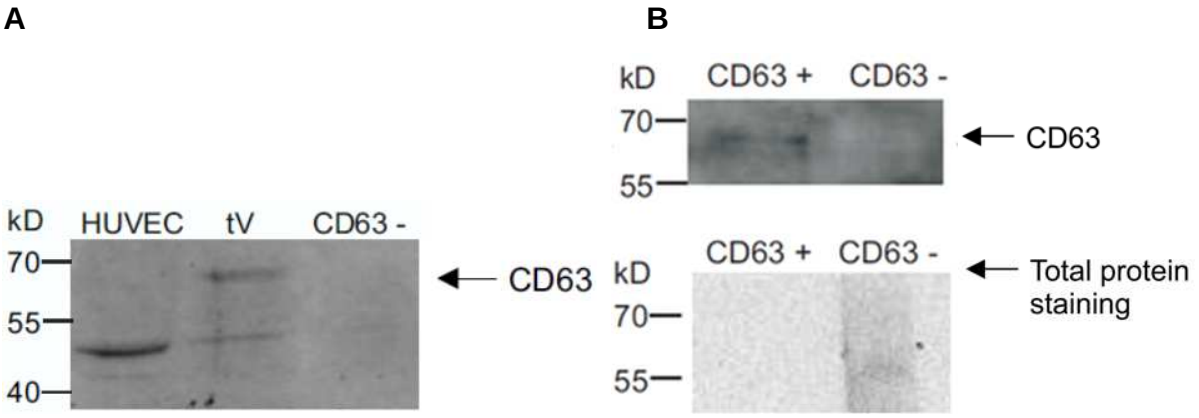

Figure 17: Confirmation of CD63 depletion after immunoprecipitation.

(A) Detection of the vesicular marker CD63 by Western blot in protein lysates derived from endothelial cell (HUVECS) or from the total extracellular vesicle fraction (tV) and the CD63 negative fraction ($CD63^-$) isolated from equal volumes of endothelial cell culture supernatant. **(B) Upper panel:** Western blot of protein lysates derived from the CD63 negative fraction ($CD63^-$) and CD63 positive fraction ($CD63^+$) after separation by magnetic beads based immunoprecipitation detecting CD63. **Lower panel:** Total protein staining by in gel fluorescent detection of proteins lysates of CD63 negative fraction ($CD63^-$) and CD63 positive fraction ($CD63^+$) as loading control.

Since it has been previously shown that the EV containing fraction (V) isolated from senescent endothelial cells is enriched in microRNA-31-5p (miR-31) (Figure 6), and that mir-31-5p negatively impacts on osteogenesis (Figure 7) by targeting Frizzled-3 (FZD3) mRNA (Figure 8), localization of miR-31 within the senescent endothelial cell derived V fraction was investigated. QPCR analysis on miR-31 of the tV compared to the $CD63^-$ immunopurified fraction showed that miR-31 levels are reduced in the $CD63^-$ fraction (Figure 18) indicating that approximately 75% of miR-31 are located within the CD63 positive vesicular fraction.

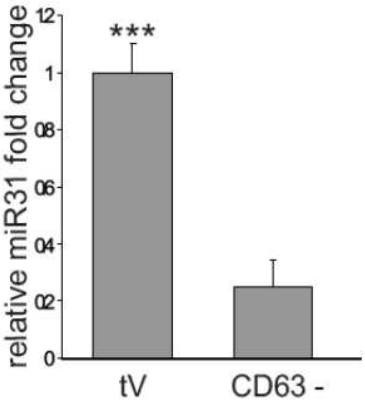

Figure 18: Localization of miR-31 within senescent endothelial cell derived extracellular vesicle fractions.

Relative fold change of microRNA-31 (miR-31) levels of total extracellular vesicle containing fraction (tV) and the CD63 negative fraction ($CD63^-$) evaluated by qPCR. ***: $p<0.001$ in comparison to $CD63^-$ fraction. Data are presented as mean values ± SD and were statistically analysed using unpaired *t* test.

Finally the ability to influence osteogenesis of both fractions after immunoprecipitation was compared. When exposing ASCs to the $CD63^-$ fraction, osteogenic differentiation capacity was not inhibited compared to ASCs co-incubated with the total EV containing fraction (tV) or to unexposed ASCs as quantified by Alizarin Red staining (Figure 19) indicating that the inhibitory activity of the V fraction indeed resides within the CD63 positive vesicular fraction.

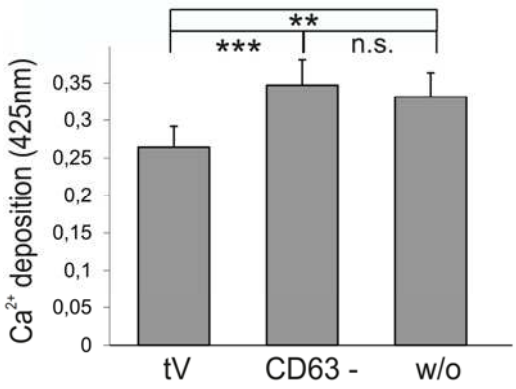

Figure 19: Effects of CD63 positive endothelial derived extracellular vesicles on mineralization capacity of ASCs.

Mineralization of unexposed ASCs or ASCs exposed to the fraction depleted of CD63 positive extracellular vesicles ($CD63^-$) or co-incubated with the total extracellular vesicle fraction (tV).was

evaluated by Alizarin Red staining. The released dye was quantified by microplate reader at 425nm. Mineralization was significantly increased in ASCs exposed to the fraction depleted of CD63 positive extracellular vesicles ($CD63^-$) compared to ASCs co-incubated with the total extracellular vesicle fraction (tV). ns: not significant, **: $p<0.01$, ***: $p<0.001$ in comparison to indicated group. Data are presented as mean values ± SD and were statistically analysed using one way ANOVA followed by a Bonferroni test to compare every pair of means.

In previous experiments extracellular vesicles isolated from the plasma of individuals older than 55 years (Figure 9) where shown to fail to induce osteogenesis (Figure 10) as efficiently as EVs isolated from donors younger than 25 years. In order to test whether the osteogenesis inhibitory activity is mediated by plasma derived EVs or by other factors such as protein aggregates that might co-pellet during the last high-speed ultracentrifugation step the EV containing fraction (V) was isolated from the plasma of a miR-31 high elderly donor by differential centrifugation and subsequently purified by anti-CD63 immunoprecipitation. Experimental strategy for identifying the fraction influencing osteogenic differentiation of ASCs is graphically outlines in Figure 16. When exposing ASCs to the $CD63^-$ fraction, osteogenic differentiation capacity was significantly restored compared to ASCs co-incubated with the total EV containing (tV) faction as quantified by Alizarin Red staining (Figure 20A) as well as by qPCR on ALP mRNA (Figure 20B) indicating that the inhibitory activity of the V fraction indeed resides within the CD63 positive vesicular fraction.

A

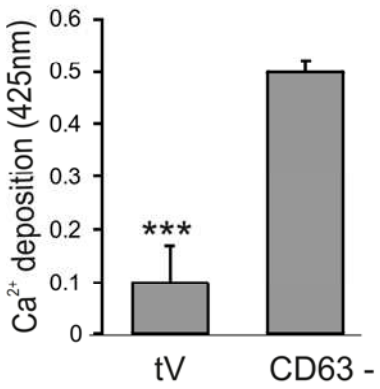

B

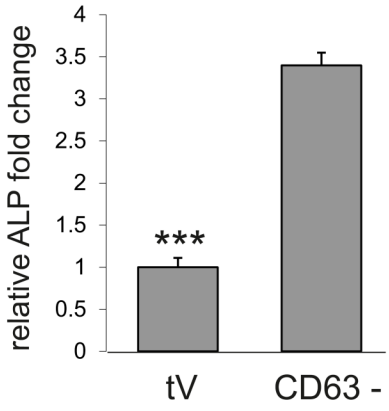

Figure 20: Effects of CD63 positive plasma derived extracellular vesicles on the osteogenic differentiation capacity of ASCs.

(A) Mineralization of ASCs was evaluated by Alizarin Red staining. The released dye was quantified by microplate reader at 425nm. Mineralization was significantly increased in ASCs exposed to the fraction depleted of CD63 positive extracellular vesicles ($CD63^-$) compared to ASCs co-incubated with the total extracellular vesicle fraction (tV). **(B)** Relative fold change of Alkaline Phosphatase (ALP) mRNA levels of ASCs were evaluated by qPCR and normalized to GAPDH. ALP mRNA level was significantly increased in ASCs exposed to the fraction depleted of CD63 positive extracellular vesicles ($CD63^-$) compared to ASCs co-incubated with the total extracellular vesicle fraction (tV). ***: $p<0.001$ in comparison to $CD63^-$ fraction control. Data are presented as mean values ± SD and were statistically analysed using unpaired *t* test.

8.2.1.3 Vesicular miR-31 inhibits osteogenic differentiation capacity

Due to the observation that osteogenesis inhibiting miR-31 is enriched within CD63 positive senescent endothelial cell derived EVs, the question arose whether vesicular miR-31 is conferring the anti-osteogenic effect of senescent endothelial cell derived EVs. Therefore ASCs were transfected with anti-miR-31, a synthetic oligonucleotide complementary to miR-31, 24h before exposing ASCs to senescent endothelial derived extracellular vesicle containing fraction for 3 days. Successful reduction of miR-31 upon anti-miR-31 transfection in ASCs was confirmed by qPCR (Figure 21).

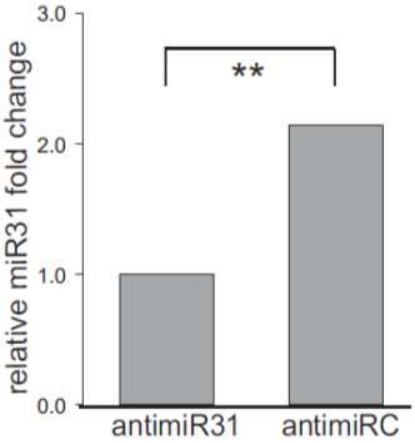

Figure 21: Effects of antimiR-31 transfection on miR-31 levels in ASCs.

Relative fold change of miR-31 was evaluated by qPCR and normalized to RNU6. MiR-31 level was significantly decreased in antimiR-31 transfected ASCs compared to non-targeting control (antimiRC) transfected cells. **: $p<0.01$ in comparison to antimiRC. Data are presented as mean values ± SD and were statistically analysed using unpaired *t* test.

Induction and subsequent quantification of osteogenic differentiation potential revealed that anti-miR-31 transfected cells showed a restored osteogenic differentiation capacity compared to non-targeting control transfected cells when exposed to the extracellular vesicle containing fraction V as quantified by Alizarin Red staining (Figure 22A) and by qPCR on Osteocalcin (Figure 22B). In addition rescued Fzd3 mRNA levels were observed in anti-miR-31 transfected cells exposed to EVs (Figure 22C). In order to exclude the possibility that the observed positive effect of anti-miR-31 transfection before EV exposure results from the reduction of intracellular miR-31 levels, ASCs were transfected with anti-miR-31 or the corresponding non-targeting control without exposing

them to EVs as control. Transfection of ASCs with anti-miR-31 alone showed no significant positive effect on osteogenesis (Figure 22A, B, C).

A

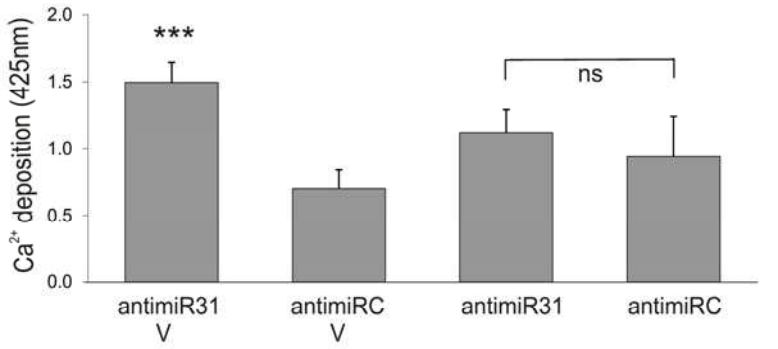

B

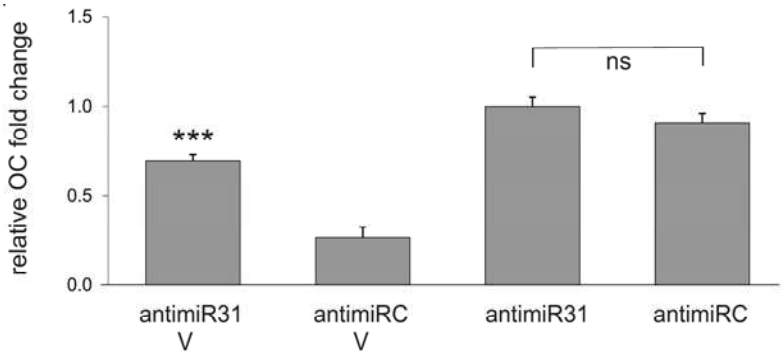

C

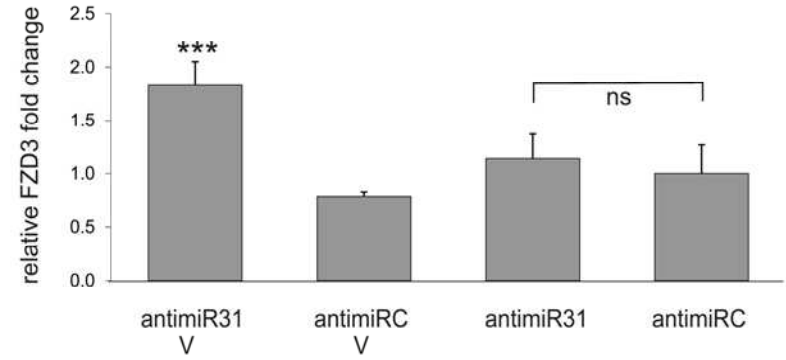

Figure 22: Effects of antimiR-31 transfection on osteogenic differentiation capacity of ASCs with or without exposure to senescent endothelial cell derived extracellular vesicles (V).

(A) Mineralization of ASCs was evaluated by Alizarin Red staining. The released dye was quantified by microplate reader at 425nm. Mineralization was significantly increased in antimiR-31 transfected ASCs exposed to V compared to non-targeting control transfected (antimiRC) cells while there was no significant

difference of Ca^{2+} depositions in antimiR-31 or antimiRC transfected ASCs without exposure to V. **(B-C)** Relative fold change of Osteocalcin (OC) **(B)** and Frizzled -3 (FZD3) **(C)** mRNA level of ASCs were evaluated by qPCR and normalized to GAPDH. OC **(B)** as well as FZD3 **(C)** mRNA levels were significantly increased in antimiR-31 transfected ASCs exposed to EVs compared to non-targeting control transfected (antimiRC) cells while there was no significant difference of OC **(B)** or FZD3 **(C)** mRNA levels in antimiR-31 or antimiRC transfected ASCs without exposure to EV. ns: not significant, ***: $p<0.001$ in comparison to control. Data are presented as mean values ± SD and were statistically analysed using unpaired *t* test, n=4.

Finally we raised the question whether also in the case of plasma derived EVs isolated from elderly miR-31 plays a crucial role in conferring the anti-osteogenic effect. Therefore ASCs were transfected with anti-miR-31 or the corresponding non-targeting control 24h before exposing them the extracellular vesicle containing fraction V fraction isolated from the plasma of a miR-31 high elderly donor. AntimiR-31 transfected cells showed a restored osteogenic differentiation capacity compared to control transfected cells as quantified by Alizarin Red staining (Figure 23A) as well as by qPCR on ALP (Figure 22B) and OC (Figure 22C). Furthermore restored FZD3 mRNA levels were observed in antimiR-31 transfected ASCs (Figure 22D).

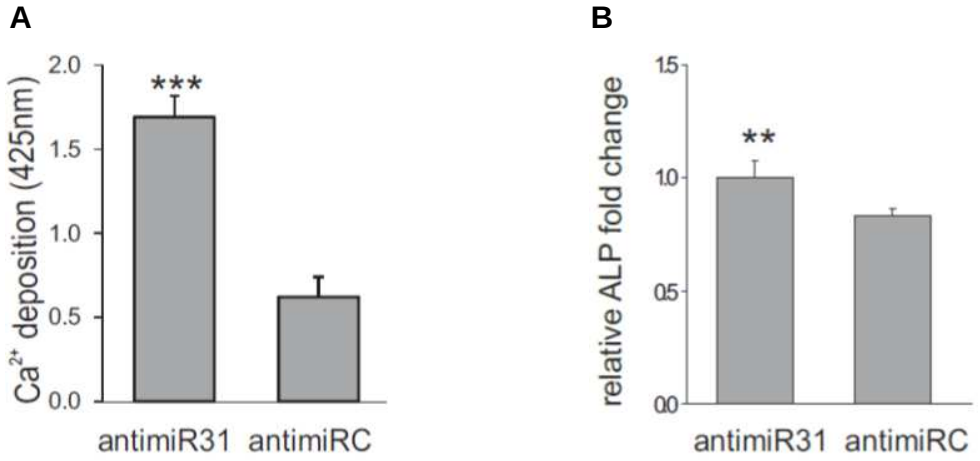

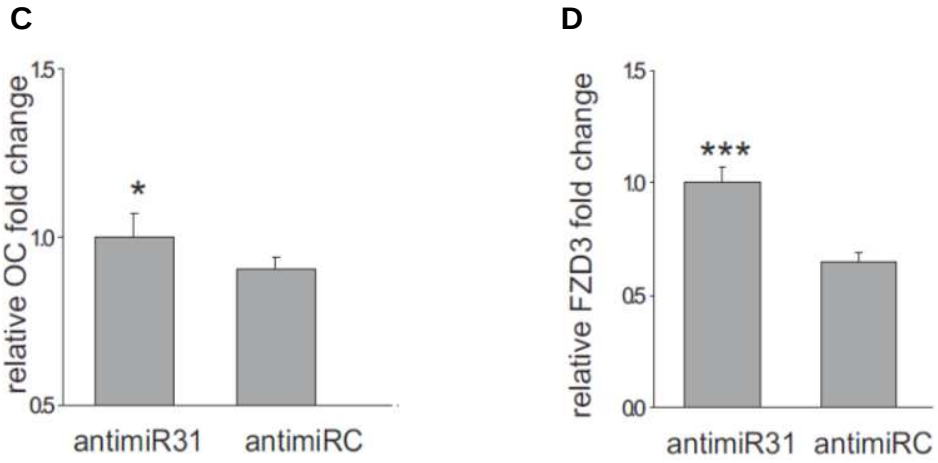

Figure 23: Effects of antimiR-31 transfection on the osteogenic differentiation capacity of ASCs exposed to plasma derived extracellular vesicles of an elderly donor.

(A) Mineralization of ASCs was evaluated by Alizarin Red staining. The released dye was quantified by microplate reader at 425nm. Mineralization was significantly increased in antimiR-31 transfected ASCs exposed to plasma derived EVs compared to non-targeting control transfected (antimiRC) cells. **(B-D)** Relative fold change of Alkaline Phosphatase (ALP) **(B)**, Osteocalcin (OC) **(C)** and Frizzled-3 (FZD3) **(D)** mRNA levels of ASCs were evaluated by qPCR and normalized to GAPDH. ALP, OC and FZD3 mRNA levels were significantly increased in antimiR-31 transfected ASCs exposed to plasma derived EVs compared to control transfected (antimiRC) cells.

*: $p<0.05$, **: $p<0.01$, ***: $p<0.001$ in comparison to control. Data are presented as mean values ± SD and were statistically analysed using unpaired t test , n=4.

8.3 Galectin3

8.3.1.1 Plasma derived CD63 positive extracellular vesicles impact on osteogenesis

The positive impact of the extracellular vesicles containing fraction derived from the plasma of young donors compared to unexposed ASCs or ASCs co-incubated with vesicles derived from elderly donors has already been shown for three donors (Figure 10) in previous experiments and confirmed by an experiment including two more donors per group (Figure 12). In order to test whether the pro-osteogenic activity of this fraction indeed resides within extracellular vesicles or in other effector molecules that might co-pellet the extracellular vesicle containing fraction (V) of a young donor was further purified by anti-CD63 immunoprecipitation as graphically outlined in Figure 16. ASCs were co-incubated for 72h with the fraction depleted of CD63 positive vesicles ($CD63^-$) or the total extracellular vesicle containing fraction (tV). Unexposed ASCs were included as a control. Pictures of ASCs at the end of the incubation time show no vesicular effect on cell morphology (Figure 24A). Upon induction of osteogenesis ASCs co-incubated with the $CD63^-$ fraction failed to facilitate osteogenic differentiation as efficiently as the total EV containing fraction (tV) as quantified by Alizarin Red staining (Figure 24B), ALP activity assay (Figure 24C) as well as by qPCR on ON mRNA (Figure 24D) indicating that the pro-osteogenic activity of the extracellular vesicles containing fraction (V) mainly but not exclusively resides within CD63 positive extracellular vesicles.

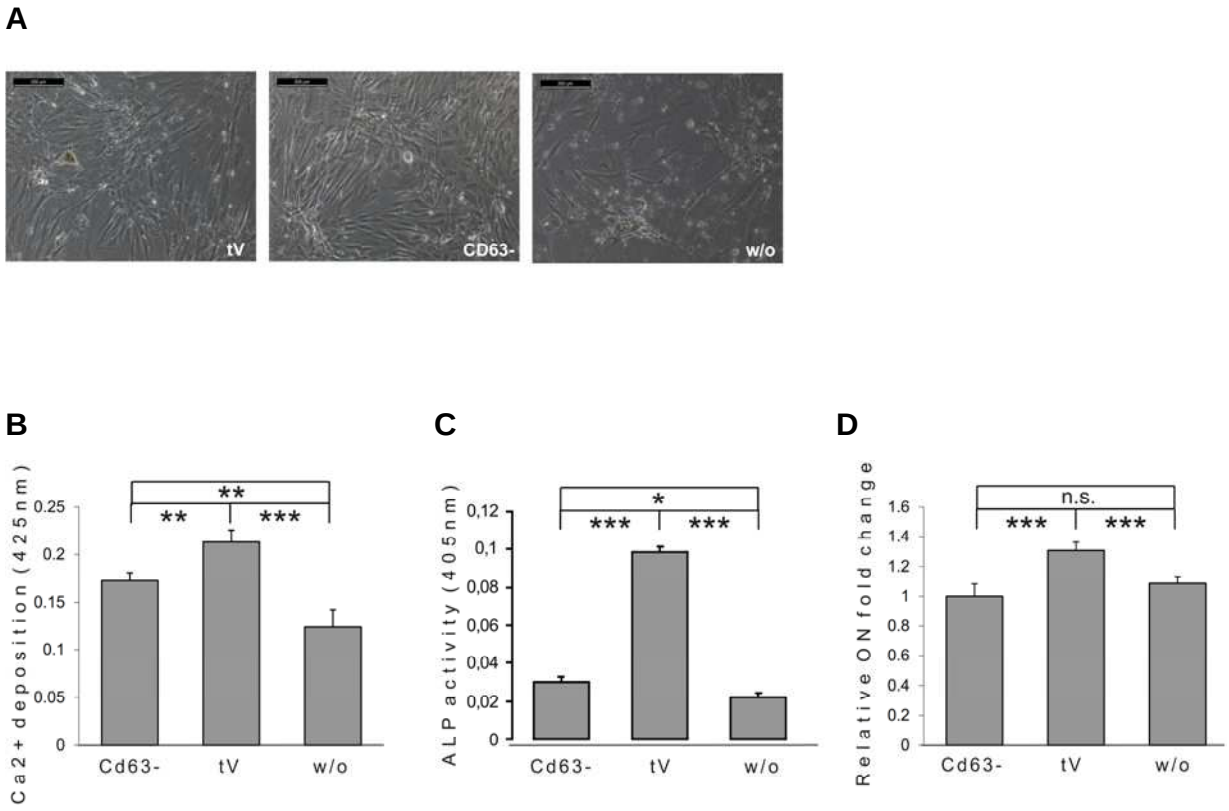

Figure 24: Effects of CD63 positive plasma derived extracellular vesicles of young donors on the osteogenic differentiation capacity of ASCs.

(A) Bright field microscopy images of ASCs exposed to the total extracellular vesicle containing fraction (EV), the fraction depleted of CD63 positive EVs ($CD63^-$) and unexposed ASCs. **(B)** Mineralization of ASCs exposed to the $CD63^-$ fraction, the total EV fraction (tEV) or of unexposed ASCs was evaluated by Alizarin Red staining. The released dye was quantified by microplate reader at 425nm. Osteogenic differentiation was decreased when cells were exposed to the EV fraction depleted of CD63 positive vesicles. **(C)** Alkaline Phosphatase (ALP) activity was quantified by microplate reader at 405nm. Activity was significantly decreased when cells were exposed to the EV fraction depleted of CD63 positive vesicles. **(D)** Relative fold change of Osteonectin (ON) mRNA levels of ASCs were evaluated by qPCR and normalized to GAPDH. ON mRNA levels were significantly decreased when cells were exposed to the EV fraction depleted of CD63 positive vesicles.

ns: not significant, *: $p<0.05$, **: $p<0.01$, ***: $p<0.001$ in comparison to control. Data are presented as mean values ± SD and were statistically analysed using one way ANOVA followed by a Bonferroni test to compare every pair of means , n=4.

8.3.1.2 Galecin-3 and osteogenic differentiation

CD63 positive extracellular vesicles of donors younger than 25 years were shown to have a positive effect on osteogenesis. Consequently we were interested which vesicularly delivered effector molecules are mediating this positive effect. Since Galectin-3 is known to be a component of extracellular vesicles (Hughes 1999) and to impact on β-Catenin degradation (Shimura et al. 2005) we focused on its role in osteogenic differentiation. When testing for Galectin-3 mRNA expression levels during the process of osteogenic differentiation, mRNA level of Galectin-3 peaked at day 9 after inducing osteogenic differentiation compared to undifferentiated cells (Figure 25).

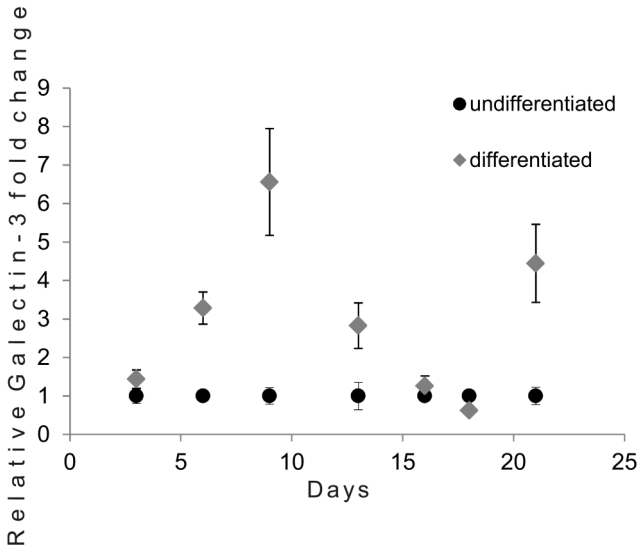

Figure 25: Galectin-3 and osteoblastogenesis

Relative fold change of Galectin-3 mRNA levels over a time course of 21 days of differentiated und undifferentiated ASCs were evaluated by qPCR and normalized to GAPDH. Galectin-3 mRNA transcription was significantly increased and peaked at day 9 in ASCs which were induced to undergo osteogenesis (grey squares) compared to undifferentiated ASCs (black dots). N=4

8.3.1.3 Knock down of Galectin-3 inhibits osteogenic differentiation *in vitro* and *in vivo*

In order to test whether Galectin-3 is not only regulated during osteogenesis but also influencing the differentiation process, Galectin-3 knock down was mediated by siRNA in ASCs. Transfection success was confirmed by comparing intracellular Galectin-3 protein level of siRNA against Galectin-3 and non-targeting control transfected cells using Western blot (Figure 26A). ASCs expressing reduced intracellular Galectin-3 levels showed a significantly decreased osteogenic differentiation capacity as quantified by Alizarin Red staining (Figure 26B), ALP activity assay (Figure 26C) and qPCR on the osteogenic marker Osteonectin (Figure 26C) compared to non-targeting control transfected cells.

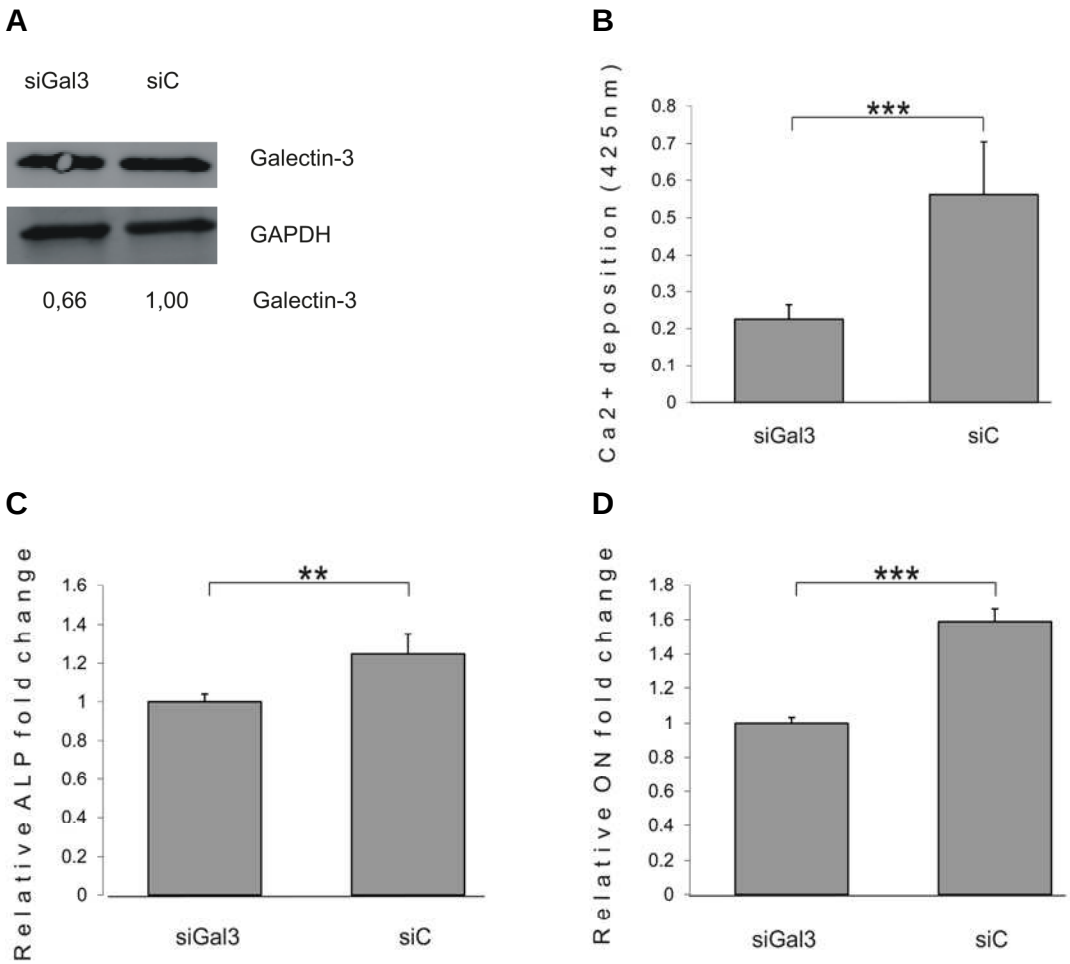

Figure 26: Influence of Galectin-3 knock down on osteogenic differentiation capacity of ASCs.

(A) Detection of total Galectin-3 and GAPDH protein levels by Western blot in protein lysates derived from ASCs transfected with siRNA against Galectin-3 (siGal3) or with the corresponding non-targeting control (siC). **(B)** Mineralization of siGal3 or siC transfected ASCs was evaluated by Alizarin Red staining. The released dye was quantified by microplate reader at 425nm. Osteogenic differentiation was reduced in siGal3 transfected ASCs compared to control transfected cells. **(C)** Alkaline Phosphatase (ALP) activity was quantified by microplate reader at 405nm. Activity was significantly decreased in siGal3 transfected ASCs compared to non-targeting control transfected cells. **(D)** Relative fold change of Osteonectin (ON) mRNA levels of ASCs were evaluated by qPCR and normalized to GAPDH. ON mRNA levels were significantly decreased in siGal3 transfected ASCs compared to non -targeting control transfected cells.
**: $p<0.01$, ***: $p<0.001$ in comparison to control (siC). Data are presented as mean values ± SD and were statistically analysed using unpaired t test , n=4.

.

Since reduced Galectin-3 levels negatively impact on osteogenic differentiation capacity of ASCs *in vitro* we tested whether also Galectin-3 knockout mice exhibit a bone phenotype. Therefore femurs of 6 female Galectin-3 knockout mice and 1 male knock out mouse and their corresponding gender matched wild type littermates were examined by µ-computed tomography. Mice are characterized in Table 21.

Table 21: Characterization of mice in knock out experiments

Date of birth as well as age at sacrifices are listed for all pairs consisting of one Galectin-3 knock out mouse and its age and gender matched corresponding wild type littermate. f=female, m=male

Age at sacrificec	Gender	Date of birth
17 weeks	f	14.01.2014
18 weeks	f	12.06.2013
18 weeks	m	12.06.2013
19 weeks	f	23.12.2013
20 weeks	f	29.09.2013
21 weeks	f	15.09.2013
22 weeks	f	18.06.2013

In particular cortical parameters were measured at femoral mid shaft and trabecular parameters at femoral distal metaphysis

When comparing all trabecular parameters of female knockout mice to their corresponding wild type littermates, Wilcoxon matched pairs test revealed no significant influence of the genetic background on the trabecular bone volume to tissue volume ratio (Figure 27A), the trabecular number (Figure 27B), the trabecular thickness (Figure

27C) or the trabecular separation (Figure 27D). However, further correction for parameters like the weight or the length of these mice might influence statistical analysis. On the other hand examination of femoral cortical thickness of 18 and 22 weeks old couples demonstrated no significant influence of the genetic background as analysed by Wilcoxon matched pairs test (Figure 27E). Due to the small sample number of male littermates only descriptive analysis was performed. Interestingly there seems to be no negative but rather a positive effect of the Galectin-3 knockout in the male mouse compared to its wild type littermate (Figure 27F).

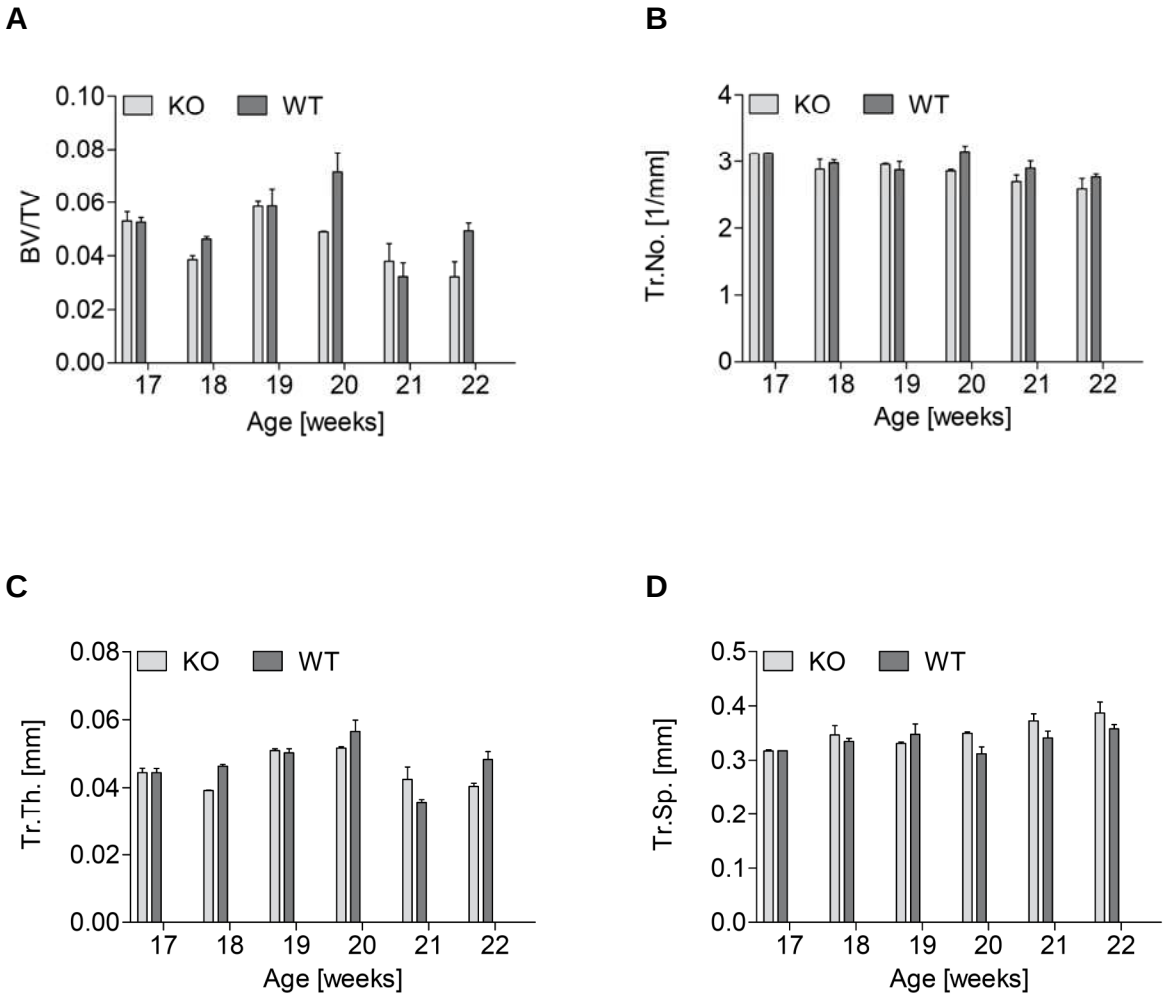

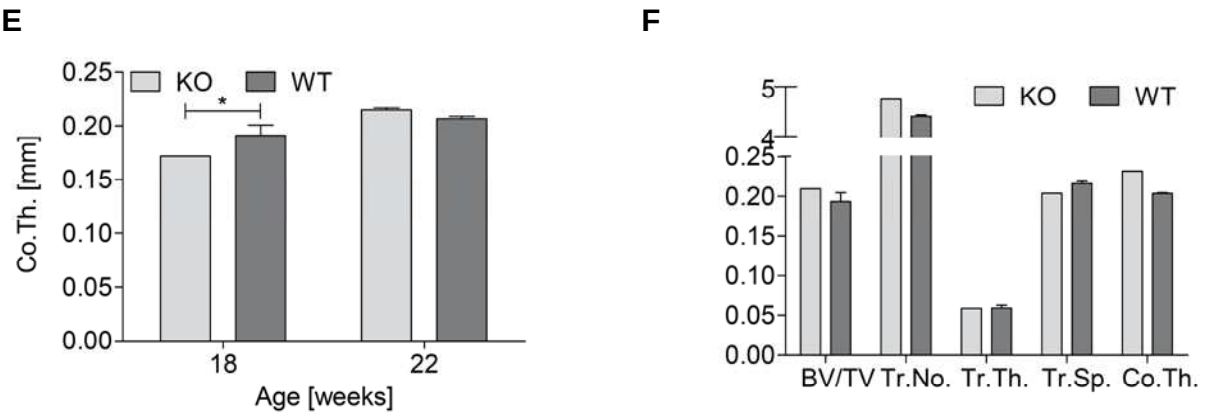

Figure 27: Analysis of femoral bone microarchitecture from 7 Galectin-3 knockout mice compared to corresponding wild type littermates.

(A-E) Trabecular as well as cortical parameters of 17, 18, 19, 20, 21 or 22 weeks old female Galectin-3 knock out (KO) or wild type (WT) littermates. In order to test for the influence of the genetic background Wilcoxon matched pairs test was performed for trabecular parameters such as **(A)** the ratio bone volume to tissue volume (BV/TV), **(B)** number (Tr.No.), **(C)** thickness (Tr.Th), **(D)** separation (Tr.Sp.) as well as **(E)** cortical thickness (Co.Th.). **(F)** Trabecular as well as cortical parameters of 18, weeks old male Galectin-3 knock out (KO) or wild type (WT) couple. Due to the small sample number no statistical analysis was performed.

8.3.1.4 Galectin-3 overexpression boosts osteogenic differentiation *in vitro*

A lack of Galectin-3 inhibits osteogenic differentiation as shown above. Consequently we were interested whether Galectin-3 overexpressing ASCs exhibit an enhanced osteogenic differentiation capacity. Several optimization steps for successful transient transfection of ASCs resulted in a transfection efficiency of more than 90% as analysed by flow cytometry 48h post electroporation (Figure 28A). After optimizing the transfection conditions the effect of Galectin-3 on osteogenesis was investigated by Galectin-3 overexpressing to empty vector control transfected cells. Overexpression of Galectin-3 in Galectin-3 expression construct compared to empty vector control transfected ASCs was confirmed by Western blot (Figure 28B). Galectin-3 overexpressing cells exhibited a significantly increased osteogenic differentiation capacity as quantified by Alizarin Red staining (Figure 28C), ALP activity assay (Figure 28D) and qPCR on Osteonectin (Figure 28E).

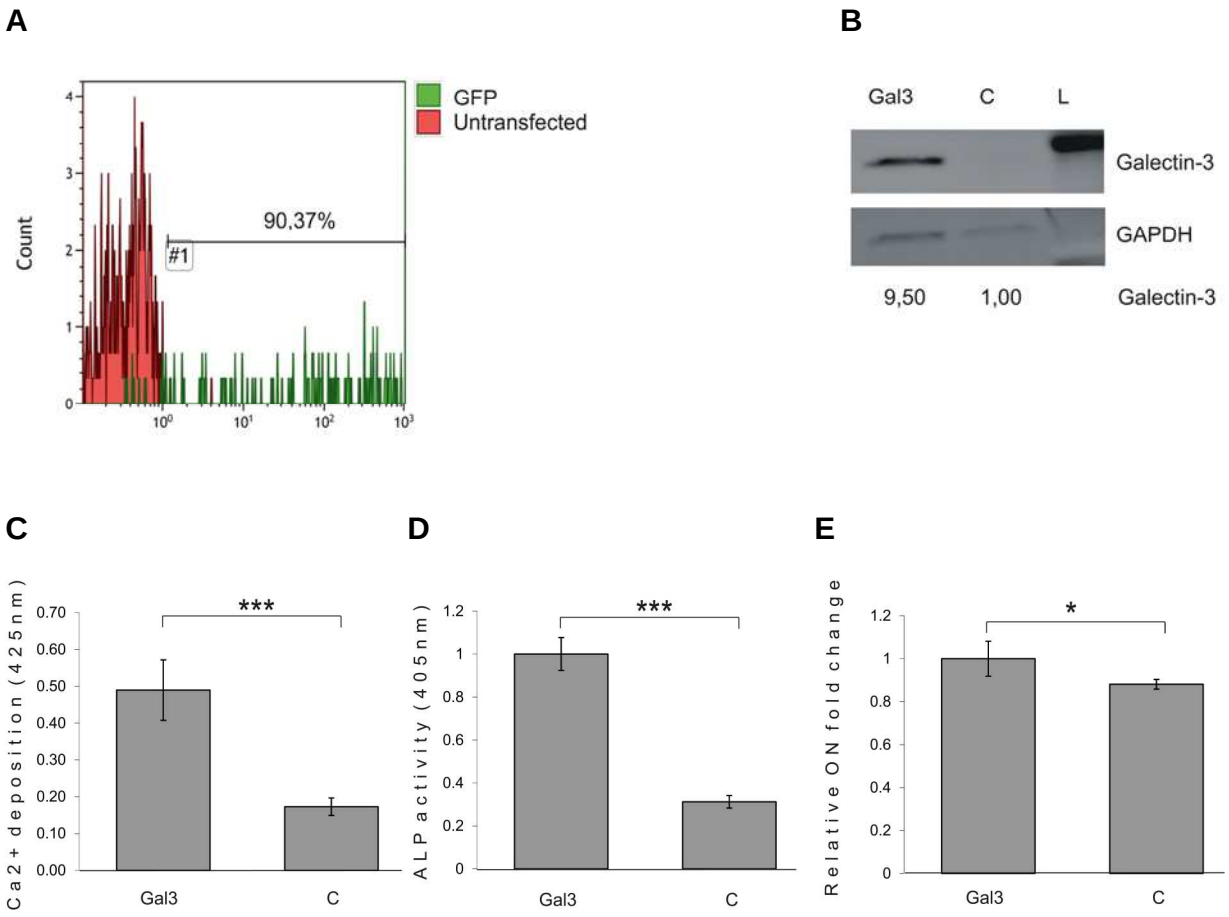

Figure 28: Influence of Galectin-3 overexpression on osteogenic differentiation capacity of ASCs. **(A)**Flow cytometry analysis comparing GFP expression construct transfected ASCs (green population) to untransfected ASCs (red population) shows a transfection efficiency of more than 90%. **(B)** Detection of Galectin-3 normalized to GAPDH protein levels by Western blot in protein lysates derived from ASCs transfected with Galectin-3 overexpression construct (Gal3) or with the corresponding empty vector control (C). The last lane shows the ladder (L) **(C)** Mineralization of Gal3 or control transfected ASCs was evaluated by Alizarin Red staining. The released dye was quantified by microplate reader at 425nm. Osteogenic differentiation was enhanced in Gal3 transfected ASCs compared to control transfected cells**. (D)** Alkaline Phosphatase (ALP) activity was quantified by microplate reader at 405nm. Activity was significantly increased in Gal3 transfected ASCs compared to empty vector control transfected cells**. (E)** Relative fold change of Osteonectin (ON) mRNA levels of ASCs were evaluated by qPCR and normalized to GAPDH. ON mRNA levels were significantly increased in Gal3 transfected ASCs compared to control transfected cells.

*: $p<0.05$, ***: $p<0.001$ in comparison to control (C). Data are presented as mean values ± SD and were statistically analysed using unpaired t test, n=4.

.

8.3.1.5 Galectin-3 and osteogenic differentiation capacity

Since Galectin-3 overexpression impacts on osteogenesis we were curious to see whether intracellular Galectin-3 protein levels of ASCs might be a useful biomarker for their differentiation capacity. Therefore we compared ASCs from 9 different donors. Donor characteristics are listed in detail in Table 22.

Table 22: Characterisation of ASC donors to determine the impact of intracellular Galectin-3

ASCs isolated from adipose tissue of nine different donors (HUF803, 846, 851, 864, 871, 887, 900, 904 and 957) were used in order to determine intracellular Galectin-3 as well as β-Catenin levels and to examine their osteogenic differentiation capacity. The donors gender, year of birth as well as the site of liposuction were cells were isolated from are listed in detail. f=female

Donor No.	Gender	Age at liposuction [years]	Site of liposuction
HUF 803	f	45	femoral
HUF 846	f	21	femoral and abdominal
HUF 851	f	25	femoral
HUF 864	f	35	femoral
HUF 871	f	26	femoral
HUF 887	f	25	femoral
HUF 900	f	48	femoral
HUF 904	f	24	femoral
HUF 957	f	43	knee

Microscopy pictures of ASCs of all donors have been made before protein was extracted or cells were seeded for subsequent induction of osteogenic differentiation to examine donor dependent variations in morphology (Figure 29A). Subsequently their Galectin-3 (Figure 29B) as well as β-Catenin (Figure 29B) protein levels were quantified by Western blotting. Interestingly correlation analysis revealed that Galectin-3 (Figure 29C) as well as β-Catenin (Figure 29D) protein levels significantly correlate with their Ca^{2+} deposition capability. Furthermore the levels of intracellular Galectin-3 and β-Catenin correlated with each other (Figure 29E). Because of the small number of ASCs derived from donors older than 50 years only descriptive analysis of the age dependent influence on intracellular Galectin-3 or β-Catenin protein levels as well as on ASCs osteogenic differentiation capacity can be performed. However, there seems to be a trend towards reduced Galectin-3 (Figure 29F) and β-Catenin (Figure 29G) levels as well as osteogenic differentiation capacity (Figure 29H) of ASCs derived from donors

older than 40 years. In this regard several in vitro and in vivo experiments revealed a reduction in the osteogenic differentiation potential of MSCs isolated from elderly donors as excellently reviewed by Lepperdinger (Lepperdinger 2011).

A

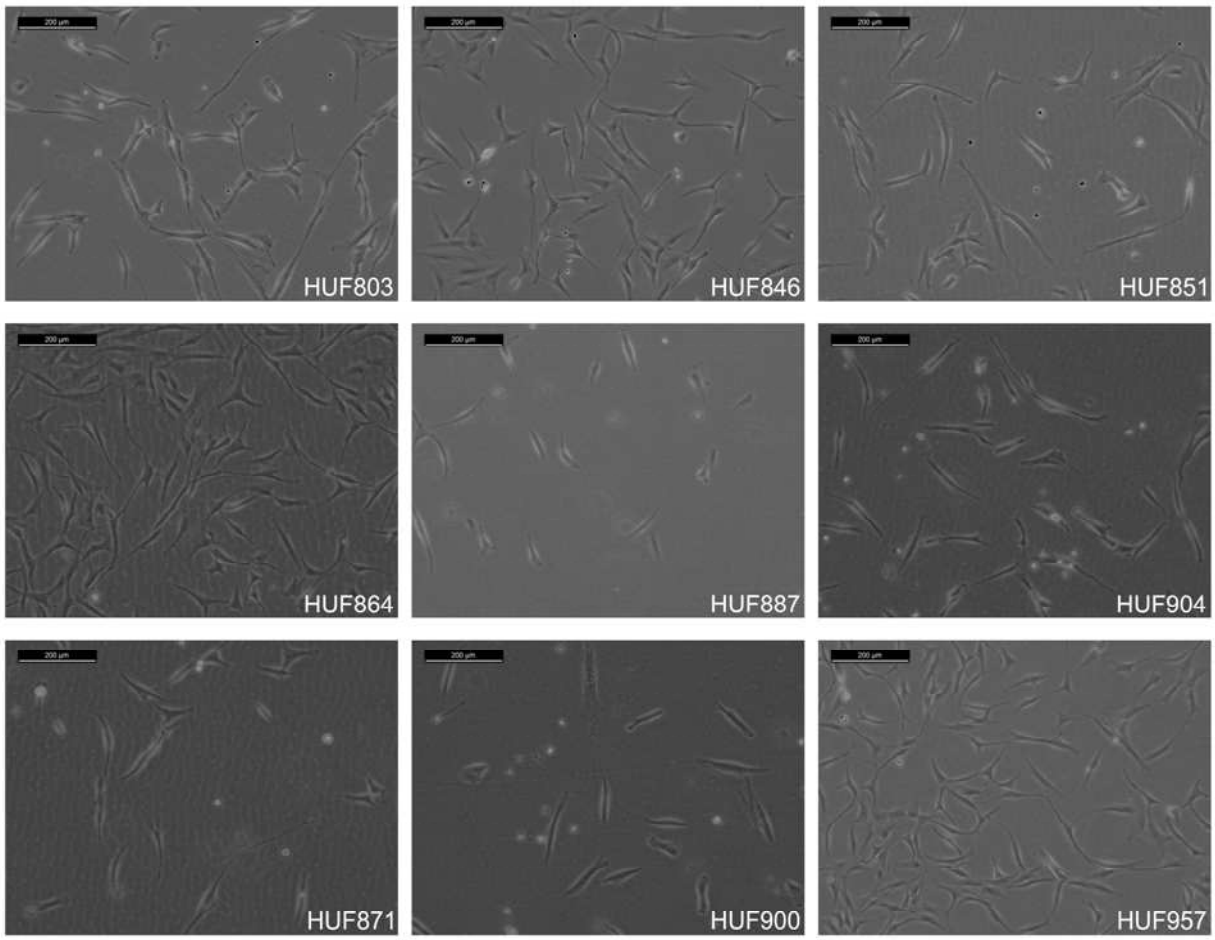

B

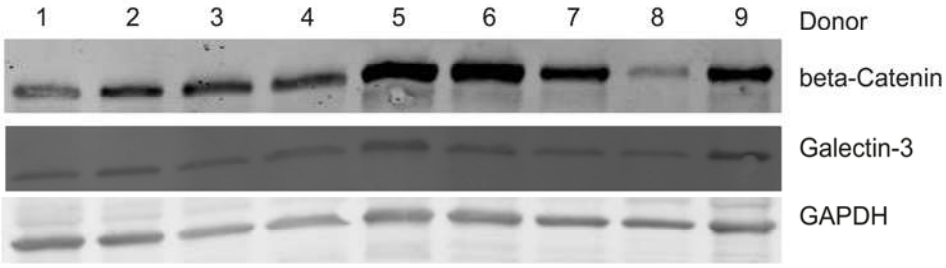

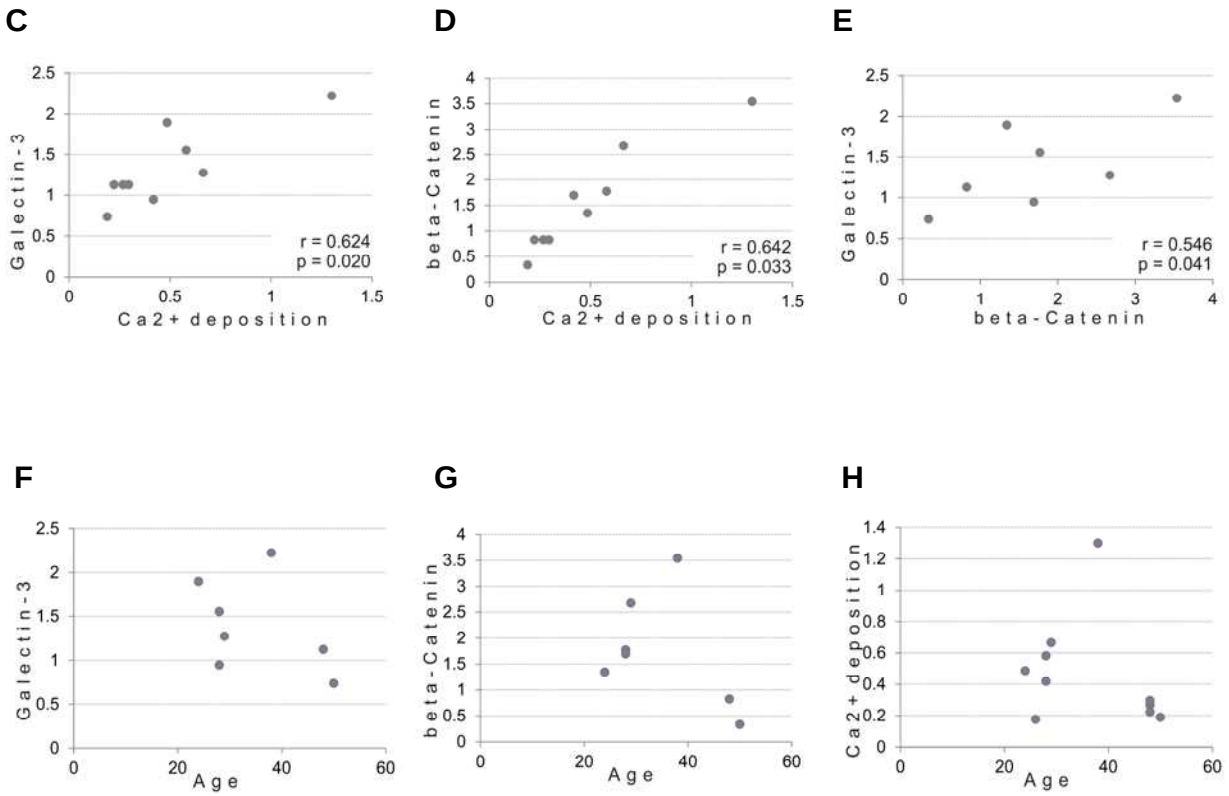

Figure 29: Intracellular Galectin-3 protein levels of ASCs derived from different donors

(A) Bright field microscopy images of ASCs derived from 9 different donors 3 days after toughing. **(B)** Detection of total β-Catenin and Galectin-3 normalized to GAPDH protein levels by Western blot in protein lysates derived from ASCs isolated from 9 different donors before induction of osteogenic differentiation. **(C)** Spearman correlation of Galectin-3 protein levels before induction of osteogenic differentiation and mineralization capacity of ASCs. **(D)** Spearman correlation of β-Catenin protein levels before induction of osteogenic differentiation and mineralization capacity of ASCs. **(E)** Pearson correlation of Galectin-3 protein levels and β-Catenin protein levels. **(F)** Comparison of intracellular Galectin-3 protein levels of ASCs from different donors to the corresponding donors age reveals a trend towards downregulated Galectin-3 levels of donors older than 40 years. **(G)** Comparison of intracellular β-Catenin protein levels of ASCs from different donors to the corresponding donors age reveals a trend towards downregulated β-Catenin levels of donors older than 40 years. **(H)** Comparison of the mineralization capacity of ASCs from different donors after induction of osteogenesis to the corresponding donors age reveals a trend towards downregulated osteogenic differentiation capacity of donors older than 40. N=9

8.3.1.6 Vesicular Galectin-3 *in vivo* and its impact on osteogenesis *in vitro*

8.3.1.6.1 Galectin-3 protein levels of plasma derived extracellular vesicles

Summarizing we found that CD63 positive extracellular vesicles isolated from the plasma of young individuals as well as enhanced levels of intracellular Galectin-3 in ASCs facilitate osteogenesis. Consequently the question arose whether there are age dependent differences in the amount of vesicularly secreted Galectin-3. Therefore we confirmed the presence of Galectin-3 within plasma derived CD63 positive extracellular vesicles purified by anti-CD63 immunoprecipitation using Western blot (Figure 30A). Subsequent analysis of vesicular as well as total plasma Galectin-3 protein levels by ELISA revealed a significant reduction of Galectin-3 protein levels in individuals older than 55 years compared to donors younger than 25 years (Figure 30B). In addition a highly significant correlation of vesicular and plasma Galectin-3 protein levels was confirmed by Spearman correlation (Figure 30C).

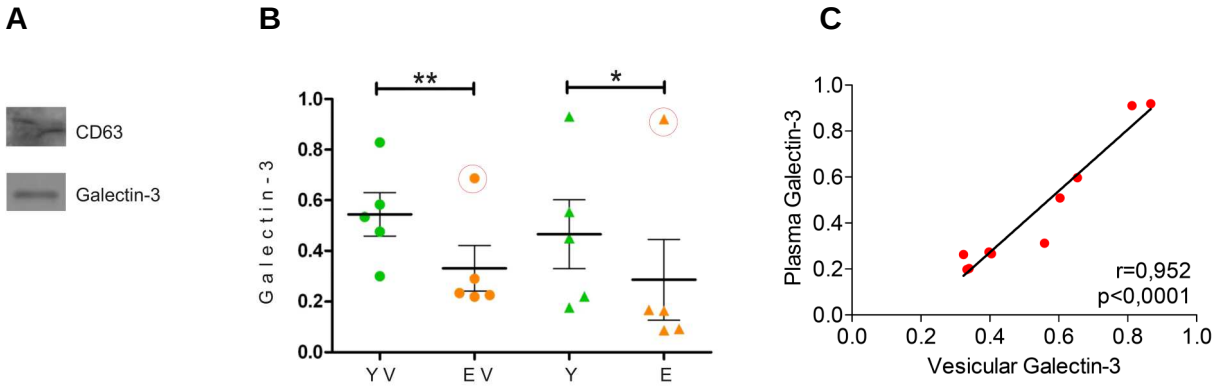

Figure 30: Plasma derived vesicular Galectin-3 levels

(A) Detection of Galectin-3 and CD63 protein by Western blot in protein lysates derived from anti-CD63 immunopurified plasma derived extracellular vesicles. **(B)** Galectin-3 protein levels in extracellular vesicles of donors younger than 25 (YV) or older than 50 years (EV) as well as total plasma levels of young (Y) and elderly (E) donors were analysed by ELSIA. Vesicular and total plasma Galectin-3 protein levels significantly decrease with age. Grubbs´ analysis identified an outlier in the elderly population (highlighted in red) who was excluded from subsequent statistical analysis. *: $p<0.05$, **: $p<0.01$ in comparison to protein levels of elderly. Data are presented as mean values ± SD and were statistically analysed using Mann-Whitney test since D'Agostino & Pearson omnibus normality test did reveal that data are not Gaussian distributed **(C)** Spearman correlation analysis of vesicular as well as total plasma Galectin-3 protein level reveals a highly significant ($p<0,001$) linear connectivity. Spearman correlation coefficient: $r= 0.952$. N=10.

8.3.1.6.2 Applicability of the *in vitro* test system

By now the positive effect of extracellular vesicles derived from young donors on osteogenesis and their enrichment in pro-osteogenic acting Galectin-3 has been demonstrated. Next we tested whether levels of vesicularly secreted Galectin-3 influence osteogenic differentiation capacity as well. While searching for an appropriate *in vitro* vesicle producing cell system we tested endothelial cells for their usefulness since endothelially derived EVs were already shown before to have an influence on osteogenesis (Figure 5) and to be able to transfer microRNAs to ASCs (Figure 15). Consequently we were interested whether also proteins or coding RNA might be transferred by this mechanism.

Therefore young quiescent endothelial cells were transfected with pmaxGFP, a green fluorescent proteins (GFP) overexpressing construct, by electroporation. GFP is a protein with no homolog in Homo sapiens. 24h post transfection the medium was changed to aspirate remaining plasmids and after a secretion period of 48h extracellular vesicles were isolated by differential centrifugation. Subsequently ASCs were exposed for 72 hours to EVs before osteogenesis was induced. The experimental design is graphically outlined in Figure 31.A. Figure 31.B shows GFP expressing pmaxGFP transfected HUVECs as compared to untransfected cells. Analysing the transfection efficiency by flow cytometry revealed that 99% of all viable cells were successfully transfected (Figure 31C). In order to demonstrate that extracellular vesicles derived from transfected HUVECs indeed contain GFP, purified vesicles were analysed for their mRNA (Figure 31D) as well as protein content (Figure 31E). Vesicles isolated from pmaxGFP transfected cells encapsulated high levels of GFP mRNA compared to untransfected HUVECs but no GFP protein was detected in comparison to normal ASCs as negative and GFP expressing HUVECs as positive control. After co-incubation of ASCs with EVs for 72h fluorescence microscopy images were taken. ASCs exposure to EVs isolated from GFP expressing HUVECs exhibited an intracellular GFP signal (Figure 31F) as well as enhanced intracellular GFP mRNA levels (Figure 31G) compared to cells exposed to vesicles of untransfected endothelial cells indicating that endothelially derived vesicles do not only transfer their mRNA to ASCs but that the delivered messages are not degraded but indeed translated by the host cell. Finally we wanted to test whether HUVECs secrete Galectin-3 containing extracellular vesicles and

might therefore qualify as a possible *in vivo* source of vesicular Galectin-3 in plasma. Immunopurification of endothelial derived EVs by the aid of anti-CD63 revealed that Galectin-3 is indeed vesicularly secreted by these cells (Figure 31H).

A

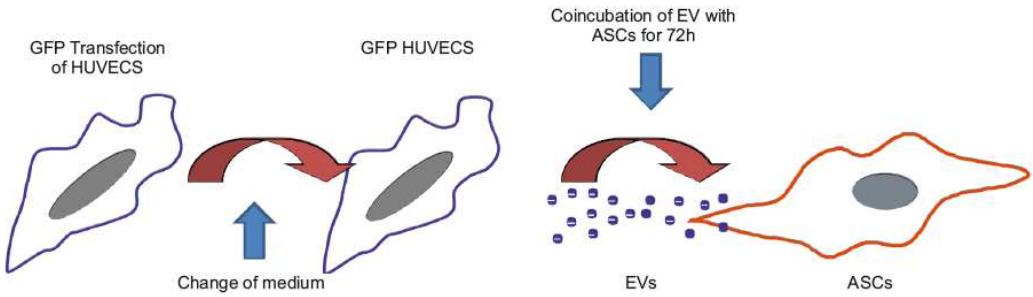
GFP Transfection of HUVECS
GFP HUVECS
Coincubation of EV with ASCs for 72h
Change of medium
EVs
ASCs

B

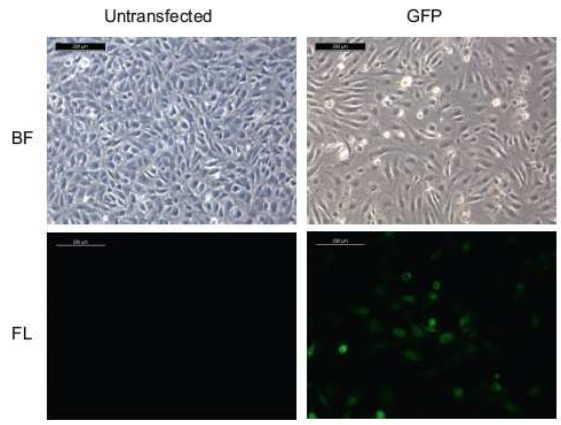
Untransfected
GFP
BF
FL

C

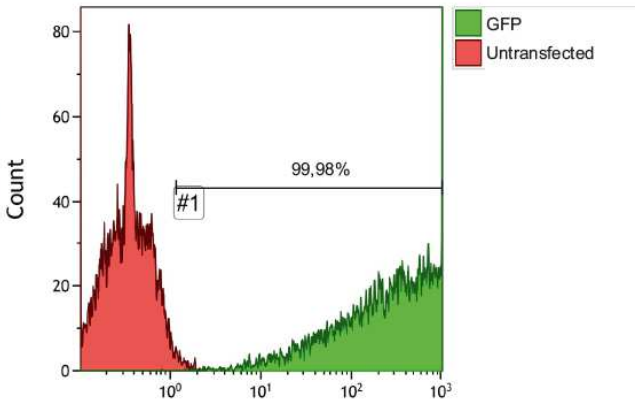
GFP
Untransfected
Count
99,98%
#1
0
20
40
60
80
10^0
10^1
10^2
10^3

D

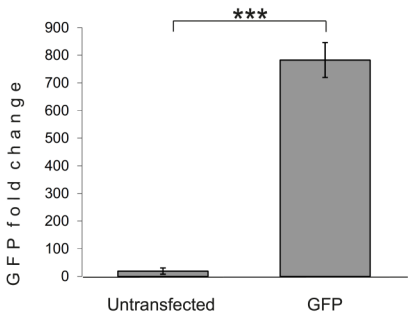
***
GFP fold change
0
100
200
300
400
500
600
700
800
900
Untransfected
GFP

E

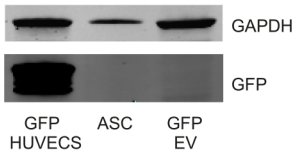
GAPDH
GFP
GFP HUVECS
ASC
GFP EV

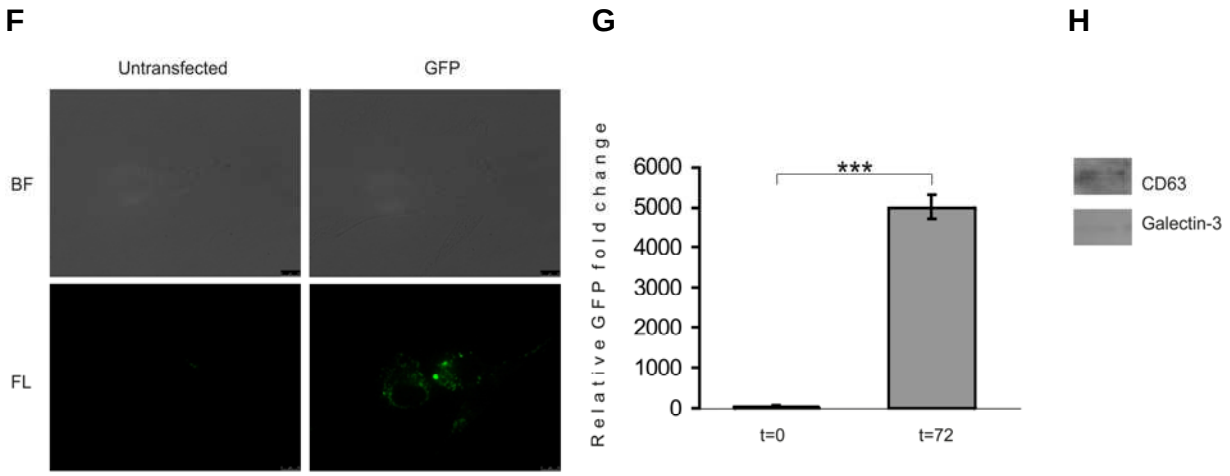

Figure 31: Transfer of endothelial derived genetic information to ASCs by extracellular vesicles.
(A) Schematic outline of experimental design: Endothelial cells (ECs) were transfected with a GFP overexpression construct (GFP) or not transfected (untransfected). 24h post transfection the medium was changed and after an additional secretion period of 48h EVs were isolated by differential centrifugation. Isolated EVs derived from transfected or untransfected cells were co-incubated with ASCs for 72h. **(B)** Bright field (BF) and fluorescence (FL) microscopy images of endothelial cells transfected with a GFP overexpression construct (GFP) or untransfected cells (untransfected) as control. **(C)** Flow cytometry analysis comparing GFP transfected ECs (green population) to untransfected ECs (red population) demonstrates a transfection efficiency of more than 99%. **(D)** Relative fold change of GFP mRNA levels within EVs normalized to the number of donor cells were evaluated by qPCR. **(E)** Detection of GFP and GAPDH protein levels by Western blot in protein lysates derived from endothelial cells transfected with GFP overexpression construct (GFP HUVECs), ASCs before exposure to EVs or EVs isolated from GFP HUVECs (GFP EV). **(F)** Bright field (BF) and fluorescence (FL) microscopy images of ASCs after exposure to EVs isolated from GFP expressing HUVECs (GFP) or untransfected cells (untransfected) for 72h. **(G)** Relative fold change of GFP mRNA levels of ASCs were evaluated by qPCR and normalized to GAPDH. GFP mRNA levels were significantly increased in cells after exposure for 3 days to EVs isolated from GFP expressing HUVECs (72h) as compared to the ASCs before co-incubation with EVs (t=0). **(H)** Detection of Galectin-3 and CD63 protein by Western blot in protein lysates derived from anti-CD63 immunoprecipitated endothelial derived extracellular vesicles.
***: $p<0.001$ in comparison to control. Data are presented as mean values ± SD and were statistically analysed using unpaired t test , n=4.
.

8.3.1.6.3 Vesicular Galectin-3 levels impact on osteogenic differentiation capacity

In order to test whether vesicular Galectin-3 levels impact on osteogenesis of ASCs, HUVECS were transfected with siRNA against Galectin-3 or the corresponding non-targeting control. After 24h the medium was changed in order to remove not cellularly incorporated siRNA. Subsequently vesicles were isolated after an additional secretion period of 48h. Taking account of small differences in the number of vesicle producing donor cells after transfection, the appropriate volume of extracellular vesicles was added to ASCs for 72h. Subsequently osteogenic differentiation was induced. ASCs exposed to extracellular vesicles isolated from siRNA transfected HUVECS exhibited a reduced osteogenic differentiation capacity as quantified by Alizarin Red staining (Figure 32A) and by qPCR on the early osteogenic marker ALP (Figure 32B).

On the other hand osteogenesis was significantly increased as quantified by Alizarin Red staining (Figure 32C) and by qPCR on ALP (Figure 32D) when ASCs were exposed to vesicles derived from Galectin-3 overexpressing cells as compared to cells co-incubated with extracellular vesicles derived from empty vector control transfected HUVECs. Summarizing these data indicate that vesicular Galectin-3 levels indeed impact on osteogenesis.

A

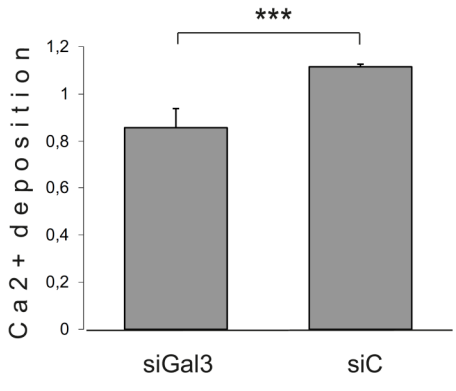

B

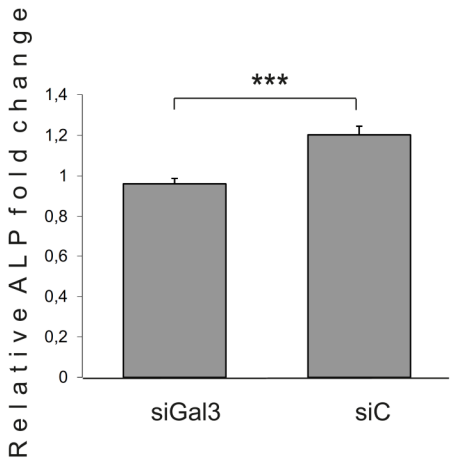

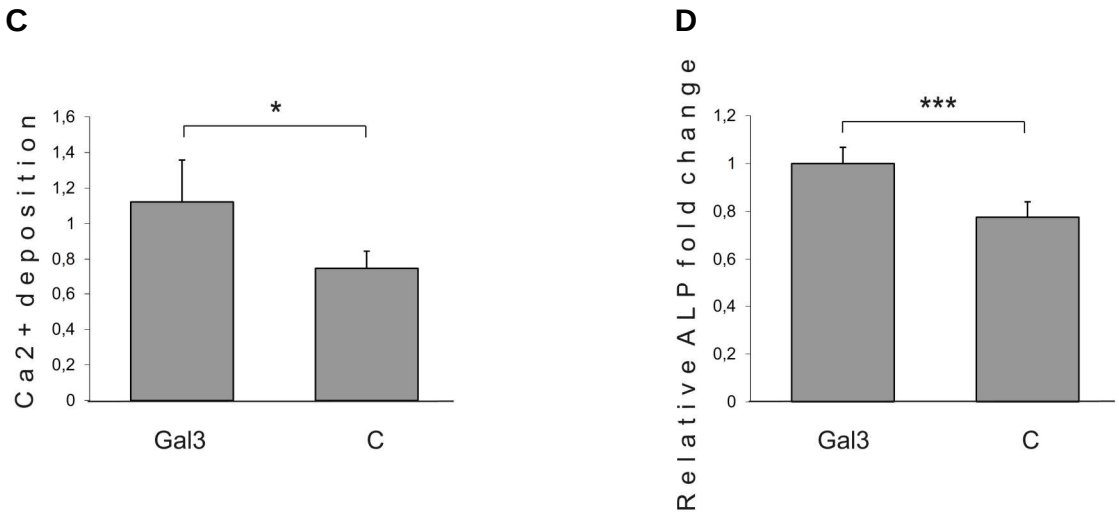

Figure 32: Vesicular Galectin-3 impacts on osteogenesis

(A) Mineralization of ASCs exposed to siRNA against Galectin-3 (siGal3) or corresponding non-targeting control (siC) transfected endothelial cells was evaluated by Alizarin Red staining. The released dye was quantified by microplate reader at 425nm. Osteogenic differentiation was reduced in ASCs co-incubated with vesicles derived from HUVECs expressing less Galectin-3 (siGal3) as compared to cells exposed to extracellular vesicles of control transfected HUVECs (siC). **(D)** Relative fold change of alkaline phosphatase (ALP) mRNA levels of ASCs were evaluated by qPCR and normalized to GAPDH. ALP mRNA levels were significantly reduced in ASCs exposed to vesicles derived from HUVECs exhibiting reduced levels of Galectin-3. **(C)** Mineralization of ASCs exposed to Galectin-3 plasmid (Gal-3) or empty vector (C) transfected endothelial cells was evaluated by Alizarin Red stainings. The released dye was quantified by microplate reader at 425nm. Osteogenic differentiation was enhanced in ASCs co-incubated with vesicles derived from Galectin-3 overexpressing HUVECs as compared to cells exposed to extracellular vesicles of empty vector transfected HUVECs. **(D)** Relative fold change of alkaline phosphatase (ALP) mRNA levels of ASCs were evaluated by qPCR and normalized to GAPDH. ALP mRNA levels were significantly increased in ASCs exposed to vesicles derived from Galectin-3 overexpressing HUVECs.

*: $p<0.05$, ***: $p<0.001$ in comparison to control. Data are presented as mean values ± SD and were statistically analysed using unpaired t test , n=4.

.

8.3.1.7 Molecular mechanism of Galectin-3s osteogenesis facilitating activity

8.3.1.7.1 Galectin-3 influences Runx-2 expression levels

Since Runx-2 is known to be a key transcription factor in the osteogenic differentiation process we wanted to test whether Galectin-3 overexpression has an effect on Runx-2 expression. Therefore ASCs were transfected with the Galectin-3 overexpression plasmid or the corresponding empty vector as control. Transfection success was confirmed by Western blot (Figure 33A). Again Galectin-3 overexpression in ASCs led to an enhanced mineralization capacity as quantified by Alizarin Red staining (Figure 33B) and to increased ALP m-RNA levels as quantified by qPCR (Figure 33C). When testing for Runx-2 mRNA levels during the process of osteogenesis Galectin-3 overexpressing cells exhibited an earlier induction of Runx-2 as compared to empty vector control transfected cells at day 4 after induction of osteogenic differentiation, while at later time points the levels converge on a same level (Figure 33D).

A

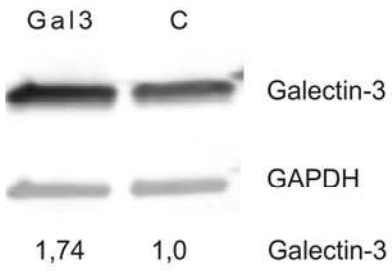

B

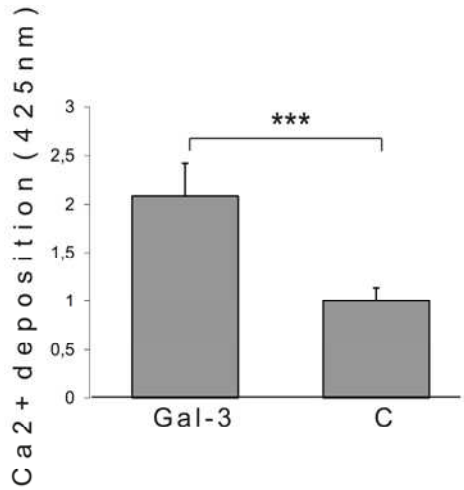

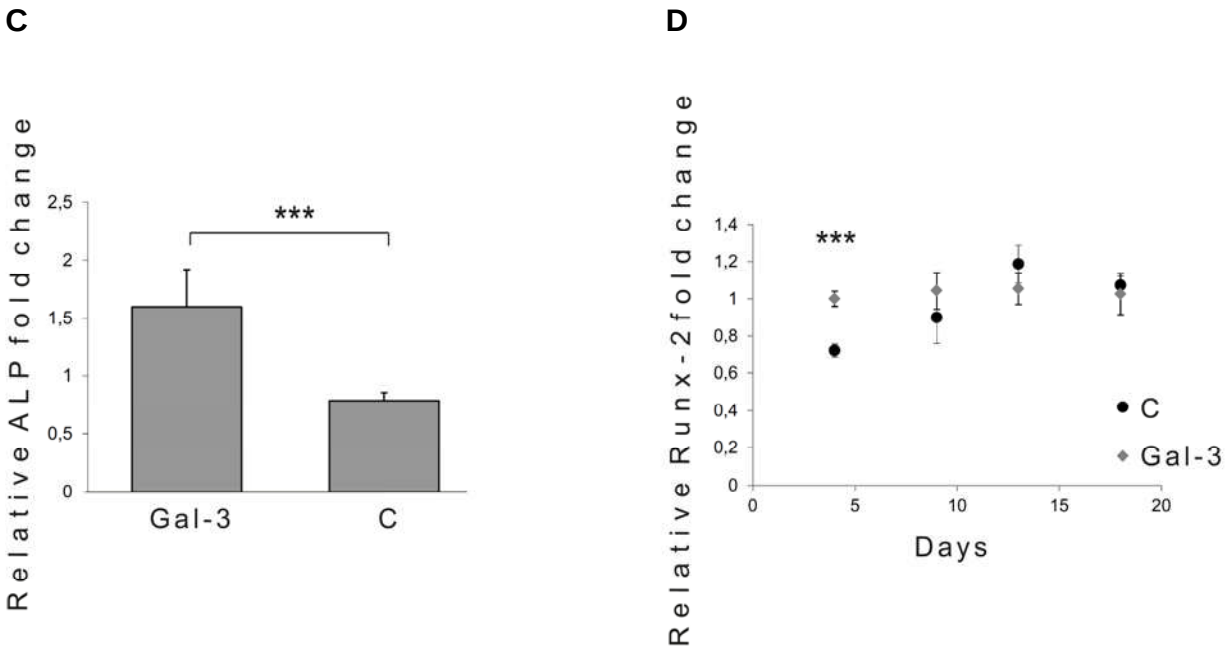

Figure 33: Galectin-3 influences Runx-2

(A) Detection of Galectin-3 normalized to GAPDH protein levels by Western blot in protein lysates derived from ASCs transfected with Galectin-3 overexpression construct (Gal3) or with the corresponding empty vector control (C). **(B)** Mineralization of Galectin-3 overexpressing or control ASCs was evaluated by Alizarin Red staining. The released dye was quantified by microplate reader at 425nm. Osteogenic differentiation was enhanced in Galectin-3 overexpressing ASCs (Gal3) compared to empty vector control transfected cells (C). **(C)** Relative fold change of ALP mRNA of Galectin-3 overexpressing or control transfected ASCs was evaluated by qPCR and normalized to GAPDH. ALP mRNA levels were significantly increased in ASCs transfected with a Galectin-3 overexpression construct (Gal-3) compared to empty vector control transfected ASCs (C). **(D)** Relative fold change of Runx-2 mRNA levels during osteogenic differentiation over a time course of 18 days. Runx-2 mRNA levels of Galectin-3 overexpressing (Gal-3) or control transfected cells (C) were evaluated by qPCR and normalized to GAPDH. Runx-2 mRNA transcription was already significantly increased at day 4 of differentiation in Galectin-3 overexpressing ASCs (Gal3) compared to empty vector control transfected cells (C) Levels of empty vector control transfected cells are displayed as black dots and data obtained from Galectin-3 overexpressing cells as grey dots.

***: $p<0.001$ in comparison to control (C). Data are presented as mean values ± SD and were statistically analysed using unpaired t test , n=4.

.

8.3.1.7.2 Serine 96 phosphorylated Galectin-3 and its impact on β-Catenin degradation

Galectin-3 influences the expression of Runx-2 (Figure 33) and has previously been described to impact on the degradation process of β-Catenin possibly by its Serine 96 phosphorylation site. Therefore we tested whether Serine 96 to alanine, in order to mimic unphosphorylated protein, or Serine 96 to aspartic acid, to simulate phosphorylation, Galectin-3 mutants impact on osteogenic differentiation capacity similarly to the wild type protein. In addition we also tested for their influence on cellular β-Catenin levels. Three independent experiments with ASCs isolated from two different donors (HUF846, HUF864) were performed. Donors are characterised in Table 23.

Table 23: Characterisation of ASC donors for Galectin-3 mutant experiments

ASCs isolated from adipose tissues of two different donors (HUF846 and 864) were used in order to examine the effect on their osteogenic differentiation capacities upon transfection with wild type or mutant Galectin-3 expression constructs. The donors number, gender, year of birth as well as the site of liposuction were cells were subsequently isolated from are listed. f=female,

Donor ID.	Gender	Age at liposuction [years]	Site of liposuction
HUF 846	f	21	femoral and abdominal
HUF 864	f	35	femoral

Successful overexpression of Galectin-3 wild type (G) as well as its serine 96 to alanine (A) and serine 96 to aspartic acid (D) mutants was checked by Western blot. While donor HUF846 exhibited increased Galectin-3 protein levels under all protein expressing conditions compared to empty vector control transfected cells (C) (Figure 34A), overexpression of mutant D in Donor HUF864 did not lead to enhanced Galectin-3 expression levels in the first experiment (Figure 34B). Therefore experiments on ASCs derived from donor HUF864 were performed again and in this case overexpression turned out to work properly (Figure 34C). When testing for the effect of Galectin-3 wild type overexpression on β-Catenin protein levels no trend was observable. While overexpression of Galectin-3 in ASCs from donor HUF846 led to decreased β-Catenin levels (Figure 34A), 3.9 fold overexpression of Galectin-3 in ASCs derived from donor HUF864 resulted in enhanced β-Catenin levels (Figure 34B) while a 1.74 fold increase of Galectin-3 caused slightly reduced β-Catenin levels in the second experiment (Figure

34C). However, successful overexpression of Galectin-3 mutants consistently led to reduced β-Catenin levels under all experimental conditions (Figure 34A, B, C). When testing for the osteogenic differentiation capacity, overexpression of wild type Galectin-3 resulted in an enhanced mineralization capacity in all experiments on ASCs from donor HUF864 (Figure 34D) but did not reach significance in cells obtained from HUF846. Overexpression of both Galectin-3 mutants caused a decrease in osteogenic differentiation capacity compared to wild type Galectin-3 overexpressing cells under all experimental conditions emphasizing the importance of a functional Serine 96 phosphorylation site for Galectin-3s pro-osteogenic effect.

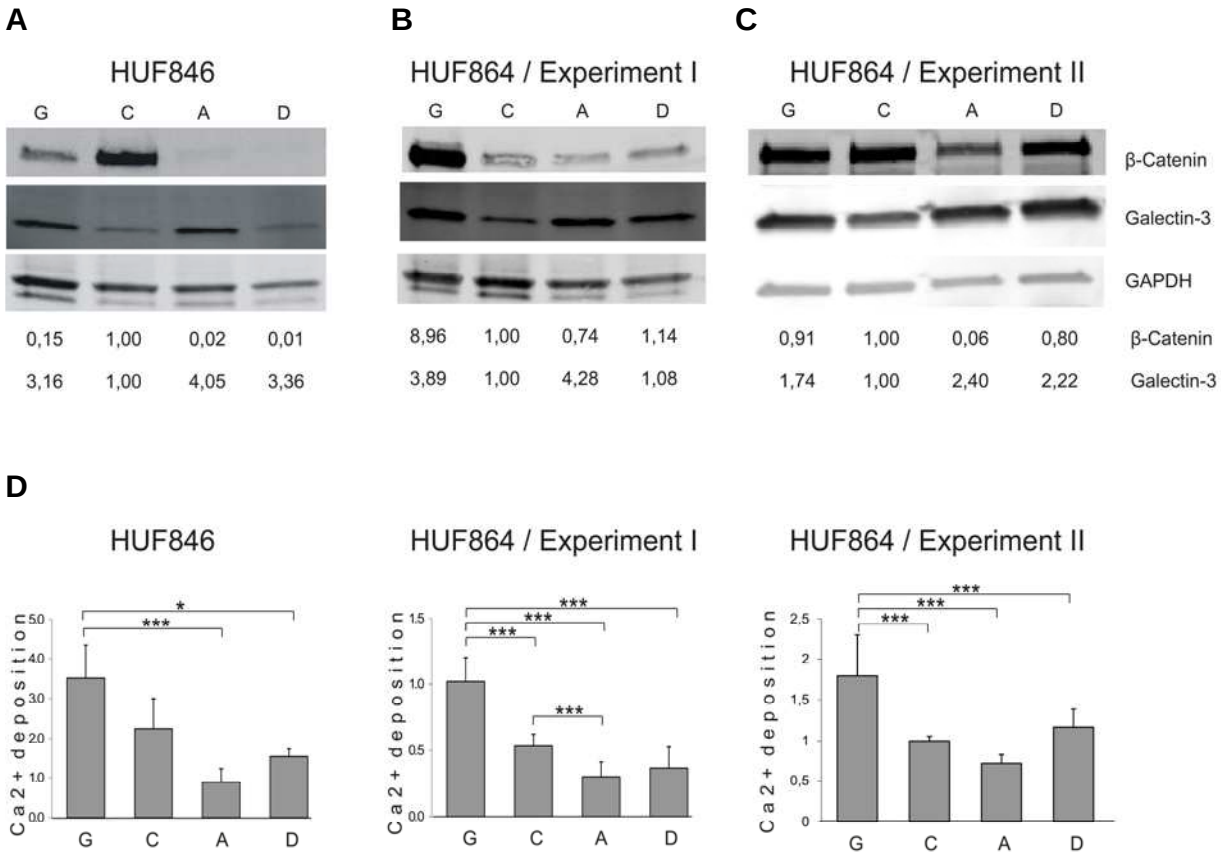

Figure 34: Influence of Serine 96 Galectin-3 mutants on osteogenic differentiation capacity.
ASCs derived from two different donors (donor I, donor II) were used. **(A)** Detection of total β-Catenin and Galectin-3 normalized to GAPDH protein levels by Western blot in protein lysates derived G, C, A and D ASCs of donor I. Galectin-3 overexpression as well as a reduction of β-Catenin in G, A and D cells was confirmed as compared to C cells. **(B)** Detection of total β-Catenin and Galectin-3 normalized to GAPDH protein levels by Western blot in protein lysates derived G, C, A and D ASCs of donor II. Galectin-3 overexpression in G and A but not in D cells was confirmed as compared to C cells. Increased levels of β-

Catenin in G cells but a reduction in A cells was observed. **(C)** Detection of total β-Catenin and Galectin-3 normalized to GAPDH protein levels by Western blot in protein lysates derived G, C, A and D ASCs of donor II in a second experiment. Galectin-3 overexpression and a reduction in β-Catenin levels was confirmed in G, A and D cells as compared to C ASCs. **(D)** Mineralization of G, C, A and D ASCs derived from two different donors was evaluated by Alizarin Red staining. The released dye was quantified by microplate reader at 425nm. Osteogenic differentiation was enhanced in G ASCs compared to C cells but did only reach significance in cells derived from donor II. Furthermore A and D ASCs exhibited a reduced differentiation capacity in contrast to G cells under all experimental conditions.* $p<0.05$; ***: $p<0.001$ in comparison to indicated control (C). Data are presented as mean values ± SD and were statistically analysed by one way ANOVA followed by a Bonferroni test to compare every pair of means.
C…Empty vector transfected ASCs, G…Wild type Galectin-3 plasmid transfected cells, A…Serine 96 to Alanine Galectin- 3 mutant expression plasmid transfected cells, D…Serine 96 to Aspartic acid Galectin- 3 mutant plasmid transfected cells

8.4 MicroRNAs and osteoporosis

In a first step the secretory levels of 175 microRNAs were analysed in 7 patients suffering from a femoral neck osteoporotic fracture as well as 7 unfractured aged matched controls. Donors are characterised in detail in

Table 24.

Table 24: Characterisation of plasma donors.

Samples from 7 patients suffering from an osteoporotic fracture (femoral neck) and 7 unfractured donors (unfractured) were analysed. The donors age, the body mass index (BMI), the T-score as measured by femoral and vertebral DEXA, levels of $1.25(OH)_2$ Vitamin D and parathyroid hormone (PTH) as well as the elapsed time between the surgery and blood sampling are listed in detail.

Donor	Fracture	Age (years)	BMI	T-score	Hydoxy-Vitamin D (µg/l)	PTH (ng/L)	Sampling day post surgery
1	Femoral neck	62	17,30	n/a	9,9	20	9
2	Femoral neck	64	27,89	n/a	10,1	59	12
3	Femoral neck	82	23,14	-0,3	21,9	39	10
4	Femoral neck	72	19,49	n/a	14,1	44	17
5	Femoral neck	71	25,46	-2,5	24,3	32	10
6	Femoral neck	87	25,10	-0,4	6,2	137	7
7	Femoral neck	69	25,04	n/a	18,5	n/a	14
8	Unfractured	78	28,00	-1,4	21,7	40	
9	Unfractured	70	32,30	1,1	26,8	33	
10	Unfractured	67	31,60	2,3	13,2	37	
11	Unfractured	69	27,30	-1,0	9,9	65	
12	Unfractured	80	28,00	3,0	43,8	33	
13	Unfractured	72	24,50	-1,6	11,9	48	
14	Unfractured	61	35,50	-1,1	13,1	41	

In order to compare both groups values of each parameter were tested for Gaussian distribution by D'Agostino & Pearson omnibus normality test. Besides the hormone levels for parathyroid hormone (PTH) ($p<0,001$) and $1.25(OH)_2$ Vitamin D ($p<0,001$) all parameters were not significantly Gaussian distributed. Subsequently unpaired t-tests in the case of PTH and $1.25(OH)_2$ Vitamin D as well as Mann Whitney tests for the remaining parameters were performed. No significant differences were observed between the fractured and the unfractured group regarding the age (Figure 35A), PTH (Figure 35B) and $1.25(OH)_2$ Vitamin D (Figure 35C) levels as well as the T-score (Figure

35D). However, both groups differed significantly in the body mass index (BMI) (Figure 35E).

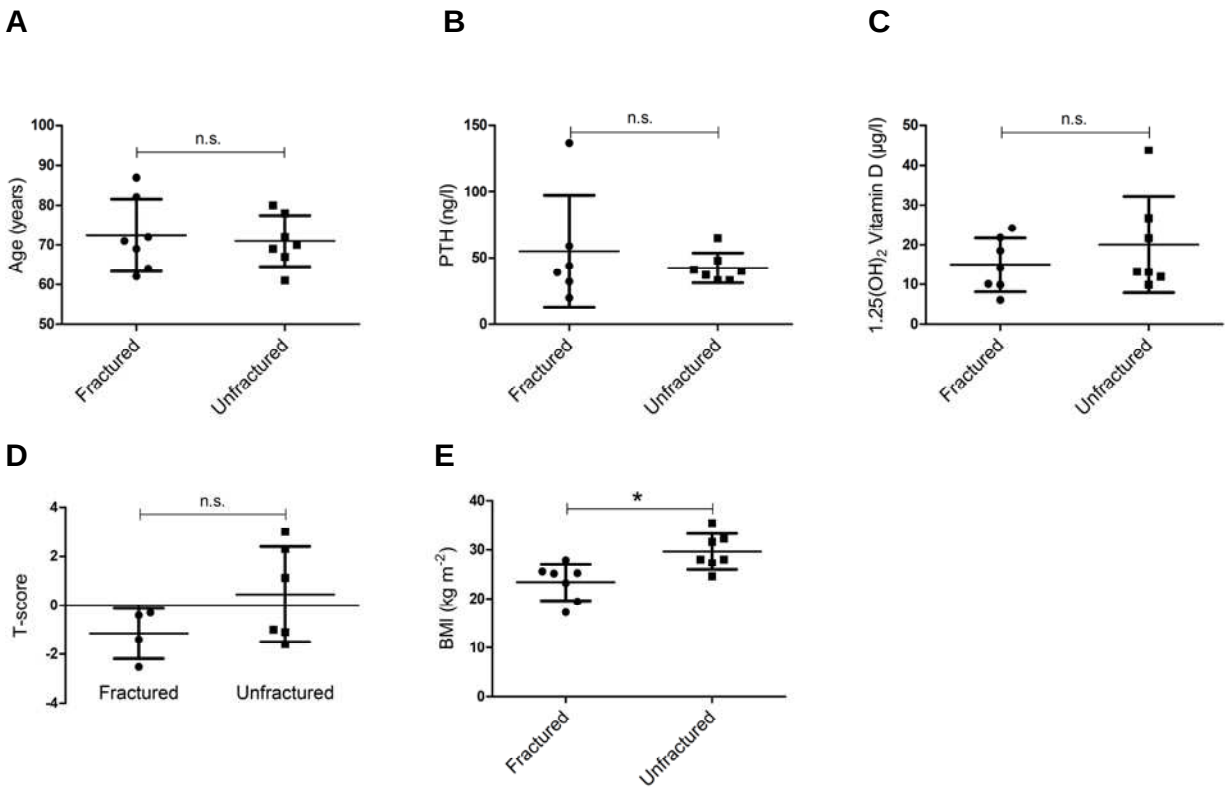

Figure 35: Statistical comparison of fractured vs. unfractured group

(A-E) Statistical analysis by two tailed unpaired t-test in the case of PTH and 1.25(OH)2 Vitamin D or two tailed Mann Whitney tests for the remaining parameters. No significant differences in fractured patients compared to unfractured individuals were observed in regard of **(A)** age, **(B)** PTH**, (C)** 1.25$(OH)_2$ Vitamin D, and **(D)** T-score. **(E)** Both groups differed significantly in body mass index (BMI)**. (A-E)** Data are presented as mean values ± SD and were statistically analysed using unpaired t-test or Mann Whitney tests. n.s.: not significant; * = p<0,05, n=14.

Tests for correlation between the T-score, the BMI and both hormone levels revealed no significant correlation between PTH and 1.25$(OH)_2$ Vitamin D levels as analysed by Pearson correlation. In addition the T-score neither significantly correlated with BMI and PTH nor with 1.25$(OH)_2$ Vitamin D levels as tested by Spearman correlation analysis (Figure 36).

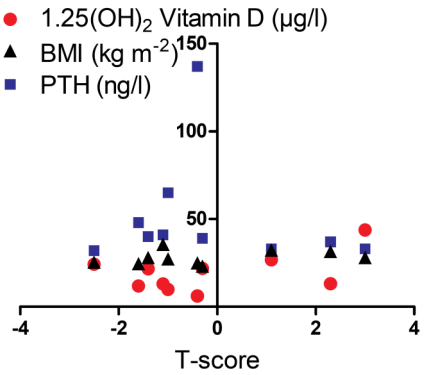

Figure 36: Graphical display of parameters from patients and unfractured individuals.
Body mass index (BMI), PTH and 1.25(OH)2 Vitamin D levels are blotted against the corresponding T-score for each donor. N=14

Pearson correlation of all 175 analysed microRNAs against miR-451a-5p, a typical marker for haemolysis, was performed and 10 significantly correlating microRNAs were identified and excluded from further statistical analysis. Subsequent explorative data analysis with the aid of principal components analysis and hierarchical clustering did not identify distinct patterns in the dataset (data not shown). However statistical analysis on the expression levels by unpaired t-test revealed 5 differentially secreted microRNAs. While miR-10a-5p (miR-10a), 10b-5p (miR-10b) and miR-22-3p (miR-22) have been shown to be upregulated miR-133b and miR-328-3p were significantly downregulated in fractured patients compared to unfractured individuals. Subsequent test for Gaussian distribution confirmed that all 5 differently regulated microRNAs passed the Shapiro-Wik normality test (data not shown)

In order to investigate whether these microRNAs have an effect on osteoblastogenesis in vitro, ASCs of three different donors (HUF803, 812, 851) were transfected with the microRNAs which were found to be upregulated in fractured patients besides miR-10a since it differs only in one nucleotide from miR-10b and is less abundant in plasma samples compared to miR-10b. Furthermore ASCs were transfected with microRNA-inhibitors against miR-328 (a-miR-328). MicroRNA inhibitors are complementary to the mature microRNA. Therefore they bind to their target and inhibit its activity (Weiler et al. 2006). We did not transfect ASCs with an inhibitor against miR-133b since miR-133b is a muscle cell specific microRNA and therefore only expressed at very low levels in

ASCs (Koutsoulidou et al. 2011; Trompeter et al. 2013). All three ASC donors are characterized in Table 25.

Table 25: Characterisation of ASC donors for transfection experiments

ASCs isolated from adipose tissues of three different donors (HUF803, 812 and 851) were used in order to examine the effect on their osteogenic differentiation capacities upon transfection with various microRNAs or microRNA inhibitors. The donors gender, year of birth as well as the site of liposuction were cells were subsequently isolated from are listed in detail. f=female, m=male

Donor number	Gender	Age at liposuction [years]	Site of liposuction
HUF 803	f	45	femoral
HUF 812	f	39	femoral and abdominal
HUF 851	f	25	femoral

Since a recently published paper analysed circulating microRNA levels in sera of osteoporotic patients and unfractured age matched controls we decided to test a choice of those differentially expressed candidates on their effect on osteoblastogenesis as well (Seeliger et al. 2014). In particular miR-21-5p (miR-21), miR-24-3p (miR-24) and miR-100-5p (miR-100) which were shown to be upregulated in the serum as well as in the bone tissue of osteoporotic patients and miR-148a-3p (miR-148a) which was only upregulated in the serum of patients was tested (Seeliger et al. 2014). Since miR-637 is known to inhibit bone formation by targeting Runx-2 and Osterix (Zhang et al. 2011), we included this microRNA in our transfection experiments as a control although neither this nor the study of Seeliger and colleagues demonstrated that this microRNA is deregulated in patients suffering from osteoporosis (Seeliger et al. 2014).

In order to quantify the influence of microRNA transfection on osteogenesis ALP activity assay, Alizarin Red staining and qPCRs on Osteonectin as well as Osteocalcin were performed in ASCs of three donors. ALP activity as well as Alizarin Red staining data strongly correlated with each other as analysed by Spearman correlation ($p<0,001$, $r=0,825$). However, neither OC nor ON mRNA fold change levels revealed a significant correlation to the mineralization capacity or the ALP activity. Therefore only ALP activity as well as Alizarin Red staining data were considered for subsequent interpretation

(Figure 37A). Statistical analysis by 2-way ANOVA to test whether the donor or the type of transfected microRNA has a significant influence on the mineralization capacity or the ALP activity revealed that both parameters have a highly significant influence ($p<0,001$) on the osteogenic differentiation process (Figure 37B).

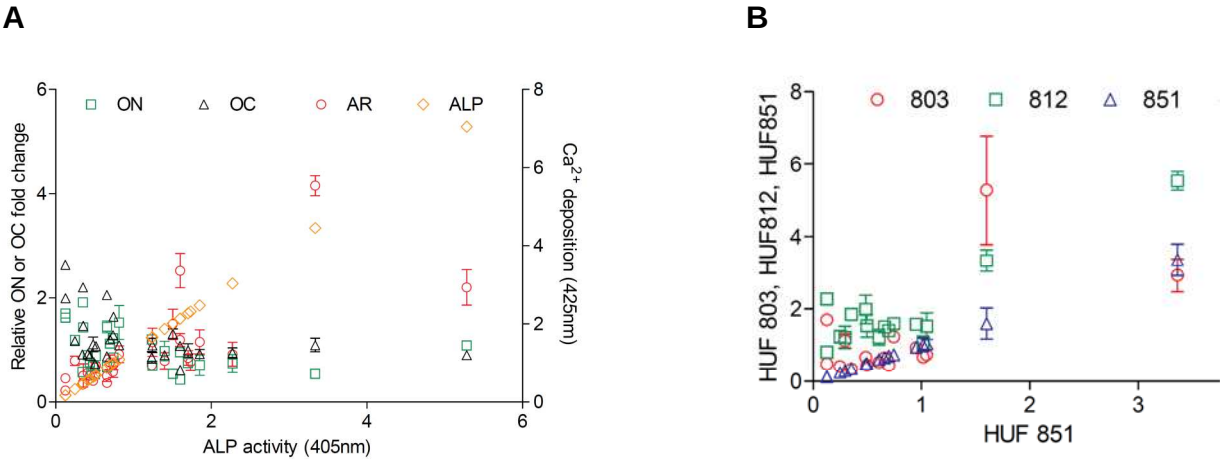

Figure 37: Correlation analysis upon microRNA transfections of ASCs from three different donors
ASCs of three different donors (HUF803, 812 and 851) were transfected with miR-10b,, miR-21, miR-22, miR-24, miR-100, miR-148a, anti-miR-328 as well as miR-637. All data are displayed relative to corresponding non-targeting control transfection **(A)** Ca^{2+} deposition evaluated by Alizarin Red stainings as well as relative fold change of ON and OC analysed by qPCR were blotted against corresponding Alkaline Phosphatase (ALP) activity. Analysis by Spearman correlation revealed a significant correlation of ALP activity and Ca^{2+} deposition but no correlation of OC and ON mRNA levels with ALP activity or Ca^{2+} deposition. **(B)** ALP activity and Ca^{2+} deposition quantified by Alizarin Red stainings of donor HUF803, HUF812 or HUF851 transfected with different microRNAs were blotted against the corresponding parameters of HUF851 transfected cells. 2 way ANOVA reveals that the transfected micro-RNA as well as the donor have a significant influence on ALP activity as well as on Alizarin Red levels. N=14

In particular miR-637 transfection success was confirmed by qPCR (Figure 38A, B). However, miR-637 transfected ASCs deriving from donor HUF812 exhibited a significantly enhanced differentiation capacity compared to non-targeting control transfected cells as quantified by ALP activity assay (Figure 38C) and Alizarin Red staining (Figure 38D). This observation is in contrast to the results obtained from donor HUF803 and HUF851 as well as to literature (Figure 38C, D) (Zhang et al. 2011). Therefore data from this donor were not considered furthermore.

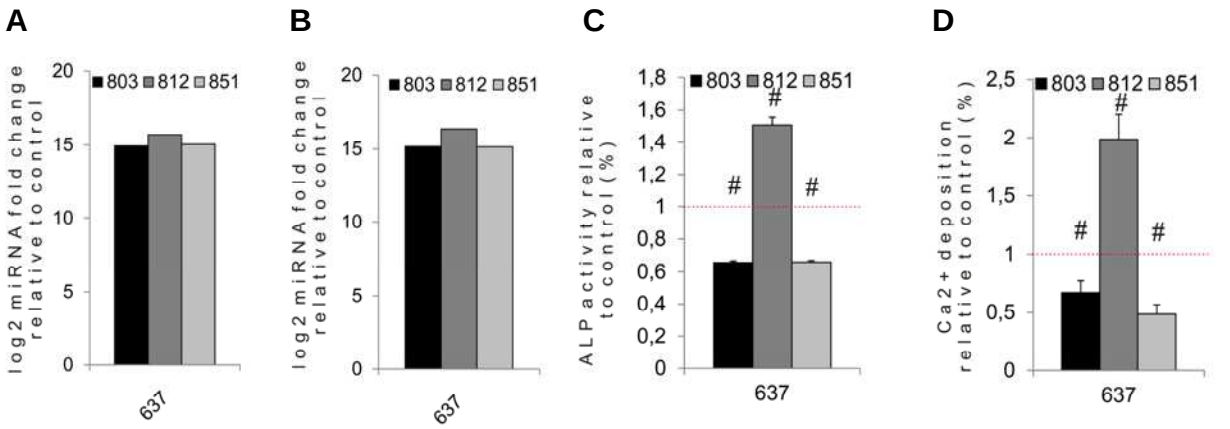

Figure 38: MiR-637 transfection

(A-B) Transfection success was confirmed by qPCR. Therefore obtained miR-637 cycle numbers of miR-637 or non-targeting control transfected cells were normalized to corresponding **(A)** RNU6 or **(B)** 5S cycle numbers as reference RNA. Data are displayed as log2 miRNA 637 fold changes relative to non-targeting control. **(C)** Alkaline Phosphatase (ALP) activities of all miR-637 transfected cells was quantified by microplate reader at 405nm and normalized to corresponding non-targeting control transfected cells **(D)** Mineralization of transfected ASCs of three different donors was evaluated by Alizarin Red stainings. The released dye was quantified by microplate reader at 425nm and normalized to corresponding non-targeting control transfected cells. (C-D) #: $p<0.001$ in comparison to non-targeting control transfected cells. Data are presented as mean values ± SD and were statistically analysed using Bonferroni test. N=3

Next, transfection success of the remaining RNA transfections in cells deriving from donor HUF803 or HUF851 was controlled. By the use of U6 as reference RNA all RNA transfected cells exhibited at least an two-fold increase or downregulation of the corresponding microRNA compared to non-targeting control transfected cells (Figure 39A). The same holds true when using 5S as reference RNA besides for miR-21 transfected cells of HUF851 (Figure 39B). MiR-10b and miR-100 overexpressing ASCs of both donors exhibited a reduced differentiation capacity while transfection of miR-148a led to enhanced osteogenesis as quantified by ALP activity assay (Figure 39C) as well as Alizarin Red staining (Figure 39D) Furthermore miR-21, miR-24 and miR-328 overexpression caused a significant reduction of ostegenic differentiation in one of two donors as quantified by ALP activity assay (Figure 39C) and Alizarin Red staining (Figure 39D). Finally miR-22 transfected ASCs did not show a clear trend towards impaired osteoblastogenesis (Figure 39C, D).

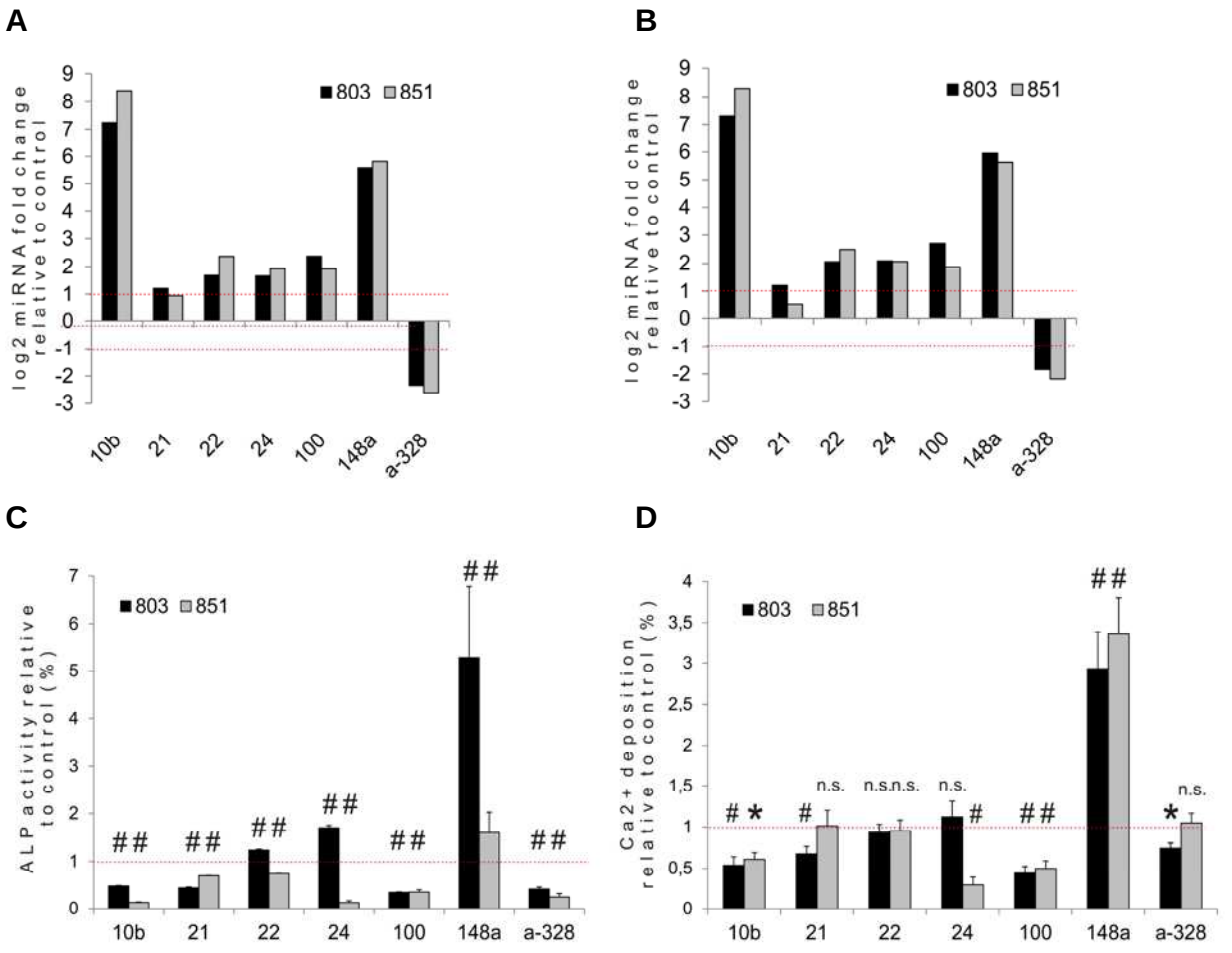

Figure 39: Influence of osteoporosis associated microRNA overexpression on osteogenic differentiation capacity of ASCs.

ASCs of two different donors (HUF803 and HUF851) were transfected with miR-10b (10b), miR-21 (21), miR-22 (22), miR-24 (24), miR-100 (100), miR-148a (148a) and an inhibitor against miR-328 (a-328). All data are displayed relative to corresponding non-targeting control transfection **(A-B)** Relative fold change of indicated microRNA in miR-10b, 21, 22, 24, 100, 148-a as well as miR-328 inhibitor transfected cells compared to non-targeting control transfected cells derived from two different donors (HUF803 and HUF 851) was evaluated by qPCR and normalized to **(A)** U6 or **(B)** 5S. Transfection success was confirmed under all experimental conditions besides in miR-21 transfected cells of donor HUF851 when using 5S as reference RNA. **(C)** Alkaline Phosphatase (ALP) activity was quantified by microplate reader at 405nm and normalized to corresponding non-targeting control transfected cells **(D)** Mineralization of transfected ASCs was evaluated by Alizarin Red stainings. The released dye was quantified by microplate reader at 425nm and normalized to corresponding non-targeting control transfected cells. **(C-D)** n.s.: not significant, +: $p<0.05$, *: $p<0.01$, #: $p<0.001$ in comparison to non-targeting control transfected cells. Data are presented as mean values ± SD and were statistically analysed using Bonferroni test. N=2

9 Discussion

Mesenchymal stem cells make up an important part of the organisms repair system (Caplan 2007). Reduced commitment of MSCs towards the osteogenic but also the chondrogenic lineage with age has already been reported. For example in rats an accumulation of preosteoblastic cells coupled with a decreased number of mature osteoblasts with age was observed , suggesting that impaired osteoblastogenesis is a potential mechanism for age-related impaired bone formation (Roholl et al. 1994). This hypothesis is further supported by the work of Föger-Samwald and colleagues who recently reported on a reduced expression of osteoblastogenesis relevant genes like Runx-2 and Osterix in hip biopsies of male patients suffering from age-related osteoporosis (Föger-Samwald et al. 2014). Similar to the gradual decline of osteogenic differentiation potential a reduction in the chondrogenic differentiation capacity of stem cells isolated from old rats has been observed (Zheng et al. 2007). Taken together these investigations suggest that the reduced replacement of specialised bone and cartilage forming cells indeed contributes to a decline in tissue functionality *in vivo*. Nowadays stem cell based therapies are thought to have a great therapeutic potential and are already in clinics (Le Blanc et al. 2004; Otsuru et al. 2012; Okamoto & Watanabe 2004). Therefore understanding the biology and the aging process of MSCs is of particular importance in order to identify factors that impact on their regenerative power especially in the case of elderly hosts in order to improve the therapeutic outcome.

But which factors cause the age associated functional decline of MSCs? Besides several known intrinsic factors which have been demonstrated to impact on stem cells functionality (Shuanhu Zhou et al. 2008) first indications that also extrinsic factors of the systemic or local environment might contribute to this loss have been provided. Evidence accumulates that cell based therapies such as muscle transplantations are less efficient in elderly compared to young hosts (Carlson & Faulkner 1989). Secondly, when connecting the blood vessels of an elderly mouse to the circulation of a young mouse the regenerative capacity of the aged animal was improoved (Conboy et al. 2005; Katsimpardi et al. 2014; Kaiser 2014; Sinha et al. 2014) and finally transplanted embryonic stem cells were not able to efficiently persist in the tissue of elderly individuals compared to young ones (Carlson & Conboy 2007). Taken together these studies indicate that environmental factors impact on stem cell functionality as well.

However, only a few secreted factors such as estrogen (Wilson & Thorp 1998) or growth hormones (Corpas et al. 1993) are known to contribute to the decline in bone anabolism caused by the aged systemic environment. Additionally influencial secreted factors might be provided by extracellular vesicles (EVs) since they are dectectable in most body fluids (Mathivanan, Ji, et al. 2010) for example in the blood (Gallo et al. 2012) and are known to stabilize and protect their cargo efficiently from degradation (Chen et al. 2008; Mitchell et al. 2008). Furthermore cargo selection (Kowal et al. 2014) as well as delivery (Fevrier & Raposo 2004) by EVs was reported to be highly specific leading to the assumption that EVs contribute to cell non-autonomous cell-to-cell communication. Although their biogenesis, exact biological relevance as well as their cargo selection and cell targeting mechanism are still not completely elucidated several studies could demonstrate that the cargo of EVs changes in disease such as in cancer (Kharaziha et al. 2012) or Alzheimer's disease (Bellingham et al. 2012).

Therefore the effect of EVs isolated from conditioned medium of "*in vitro* aged" senescent endothelial cells or isolated from the plasma of elderly donors on the differentiation capacity of ASCs was investigated. The data presented indicates that extracellular vesicles have a donor-age dependent influence on the osteogenic as well as on the chondrogenic differentiation capacity of ASCs. While searching for vesicular factors that contribute to the inhibitory activity of EVs isolated from the plasma of elderly individuals on osteogenesis we found that pro-osteogenic Galectin-3 is absent while anti-osteogenic acting miR-31 is enriched in vesicles circulating in the plasma of elderly.

9.1 Applicability of endothelial cells as *in vitro* EV production system

Circulating EVs in the peripheral blood derive from several different cell types, mainly from immune cells while, current estimates suggest that only up to 8% of EVs are released by endothelial cells in young mice (Hunter et al. 2008). However, it has suggested that the percentage of MVs secreted by platelets is actually overestimated due to wrong sample handling and that the amount of endothelial derived vesicles has a larger share in human plasma than initially expected. In addition a study revealed that senescent fibroblasts secrete increased amounts of EVs in comparison to proliferating cells (Lehmann et al. 2008), suggesting that in older organisms the relative amount of endothelial derived EVs might be even higher due to an accumulation of senescent

endothelial cells with age (Erusalimsky 2009; Erusalimsky & Kurz 2006; Minamino & Komuro 2007). The underlying mechanism of enhanced EV release in senescence might be explained by the observation that cellular senescence triggering p53 was shown to facilitate the secretion of exosomes (Yu et al. 2006).

Nevertheless, the pressing question if circulating EVs interact with MSCs located in the bone tissue remained. Anatomically the bone remodelling compartment is highly vascularized (Marcus et al. 2010). Consequently MSCs within the bone might be easily accessible for circulating vesicles. Secondly osteoprogenitor cells have been identified in the peripheral circulation, where they might interact with circulating EVs (Eghbali-Fatourechi et al. 2005). Thirdly it has been confirmed that some MSCs are pericytes (Blocki et al. 2013; Shi & Gronthos 2003; Crisan et al. 2008) and therefore in close proximity to endothelial cells as well as to the vasculature. In the latter case the endothelial secretome might not only contribute to the systemic but also to the local environment of mesenchymal stem cells.

Finally it was still unclear if endothelial derived EVs have the ability to interact with mesenchymal stem cells at all, since it has been previously shown that the interaction between extracellular vesicles and target cells is highly specific (Fevrier & Raposo 2004). *In vitro* experiments confirmed that EVs secreted by GFP or cel-miR39 transfected endothelial cells deliver their species foreign cargo to human ASCs.

In summary endothelial cells might as well qualify as a powerful source of released factors that contribute to the systemic and local environment of MSCs.

9.2 Galectin-3

Galectin-3 plays a decisive role in bone, cartilage and adipose tissue remodelling suggesting that it might play an important role in stem cell commitment. *In vivo* experiments revealed age-dependent increased adiposity in Galectin-3 knock out mice (Pejnovic et al. 2013; Pang et al. 2013) and a role of Galectin-3 in preadipocyte proliferation (Kiwaki et al. 2007). Reduced levels of Galectin-3 did not only seem to be critical in regard of adipose tissue formation (Pejnovic et al. 2013) but also for the survival of chondrocytes (Kiwaki et al. 2007), since Galectin-3 deficiency seems to facilitate chondrocyte death while intracellular Galectin-3 was shown to contribute to chondrocyte survival (Boileau et al. 2008). In regard of bone remodelling the presence of Galectin-3 was reported to inhibit the formation and maturation of a murine osteoclast

precursor cell line *in vitro* (Y.-J. J. Li et al. 2009). Considering anabolic bone formation Galectin-3 was confirmed to be important in the late stage of osteoblast maturation (Aubin et al. 1996) and that its expression is mediated by Runx-2 (Stock et al. 2003), an important transcription factor in osteogenesis. In contrast to the last-mentioned reports we observed that Galectin-3 does not only play a critical role in the late stage of osteoblast maturation but that increased levels of Galectin-3 have a positive effect on ASCs, the progenitor cells of osteoblasts, since Galectin-3 overexpression in ASCs led to an early induction of ALP and Runx-2 at day 4 of osteogenic differentiation. Supportingly siRNA against Galectin-3 reduced osteogenic differentiation capacity of ASCs *in vitro*.

While searching for pro-osteogenic factors in vesicles of young individuals, we found that Galectin-3 is enriched within CD63 positive plasma derived EVs of young individuals and that human vesicular Galectin-3 plasma levels decrease with age. Furthermore we demonstrated that the amount of vesicularly delivered Galectin-3 indeed impacts on osteogenic differentiation capacity of ASCs. In regard of circulating Galectin-3 levels several studies already reported that Galectin-3 protein levels in body fluids significantly correlate with the donors state of health in several diseases such as various types of cancer (Inohara et al. 2008; Sakaki et al. 2008; Saussez et al. 2008; Vereecken et al. 2009; Vereecken & Heenen 2006; Xie et al. 2012; Yu 2010), systemic sclerosis (Koca et al. 2013), inflammatory diseases (Ten Oever et al. 2013), Alzheimer´s disease (X Wang et al. 2013), Diabetes mellitus, type 2 (Jin et al. 2013) or chronic heart failure (Lin et al. 2009).The origin of Galectin-3 carrying CD63 positive MVs within the circulation is still not clear but we identified endothelial cells as a possible source, as they are secreting vesicular Galectin-3 *in vitro*.

In order to elucidate the underlying molecular mechanism of Galectin-3s pro-osteogenic activity we focused on its influence on β-Catenin since Galectin-3 has also been implicated in β-Catenin dependent Wnt signalling in the context of β-Catenin stabilization (Song et al. 2009) and Wnt signalling is known to be critical for osteogenesis (Baron & Kneissel 2013). Notably, it was recently demonstrated that Galectin-3 contributes to vascular calcification by stabilising β-Catenin (Menini et al. 2013).

Although we showed that a functional Serine 96 phosphorylation site of Galetin-3 is necessary for its pro-osteogenic effect, we could not attribute this effect to its proposed

machanism of β-Catenin stabilization (Song et al. 2009). This might have several reasons. On the one hand we cannot exclude the possibility that mutations in Serine 96 have an effect on the total confirmation of Galectin-3 and thereby rather mimick a knock down of Galectin-3 instead of a loss of function through the mutation of the Serine 96 phosphorylation site. Additionally analysis of the nuclear fraction instead of the whole cell lysate might have made clear proofs of the effects of Galectin-3 mutants on β-Catenin stabilization.

In order to estimate the biological and clinical relevance of our *in vitro* findings trabecular as well as cortical microarchitecture of bones derived from Galectin-3 knock out mice were examined. Although mice are a good model system to study bone biology in mammals, several differences to humans are subsequently outlined. Firstly, humans reach their peak bone mass with sexual maturity and maintain it for a couple of years before cortical as well as trabecular bone become weaker (Marcus et al. 2010). In contrast, mice mature sexually by the age of 6 – 8 weeks (Jilka 2013) but reach their peak bone mass with 4-6 months, after puberty (Jilka 2013). Consequently the bones which were examined in this study might derive from sexually but maybe not completely skeletally matured mice. Secondly, compared to humans no decrease in estrogen (Almeida et al. 2007) or testosterone (Anon 1977) is observed in aged mice, indicating that the age related reduction in bone strength in mice is not caused by sex steroid deficiency but rather age associated. Thirdly, trabecular bone remodelling was demonstrated to be slower (0,1% remodelled /day) (Parfitt 2002) and to require more time (12 – 18 times more) (Han et al. 1997) in humans compared to mice (0,7% remodelled/day) (Weinstein et al. 1998). And finally while cortical bones of mice are vascularized they are not organized in osteons like human bones (Parfitt 1994).
When characterising bone biology in C57BL/6 mice it was revealed, that the femur stops growing at the age of 6 months (Glatt et al. 2007). The bones investigated in this work were thusly derived from mice that were still in growth. Investigations regarding the age related changes in BMD of this inbred strains revealed a gradual decrease of BMD in male and female mice from the age of 16 months (Almeida et al. 2007; Yuan et al. 2009). Although BMD does not start to decrease before the age of 16 months, femoral trabecular bone mass was reported to decline already from the age of 3 months (Halloran et al. 2002; Glatt et al. 2007). Remarkably, this bone loss was demonstrated to be faster in female compared to male mice (Halloran et al. 2002; Glatt et al. 2007).

Quite contrary to these suggestions, we could not observe changes in trabecular bone volume normalized to tissue volume when comparing 17 to 22 weeks old female wild type mice. However, the age difference of the mice might not be significant enough in order to the data from literature. Furthermore, C57BL/6 mice are known to exhibit a decreased trabecular number and connectivity with age while trabecular thickness does not change (Halloran et al. 2002; Glatt et al. 2007).

With age the cortical bone of humans becomes thinner and more porous (Glatt et al. 2007; Han et al. 1997). Despite the differences in the cortical organization of human and murine bone cortical bone of C57BL/6 mice at the age of 18 months was shown to become more porous while no differences were observed in young mice of 6 months (Jilka 2013).

Our investigations on the femoral microarchitecture of Galectin-3 knock out mice revealed that female Galectin-3 knock out mice did not differ significantly in trabecular parameters from their wild type littermates. However parameters like body weight or length were not taken into account at this stage. Interestingly a trend towards improved bone parameters was observed in the 18 weeks old male Galectin-3 knock out mouse. Unfortunately data on cortical thickness in female and male mice were inconclusive due to the small sample number indicating that more animals need to be examined.

Taken together, our studies in combination with previous reports indicates an important role for Galectin-3 during bone remodelling. Increased Galectin-3 levels *in vivo* might lead to an enhanced formation of osteoblasts resulting in an improved bone formation. Circulating Galectin-3 might represent a novel marker of biological aging and reduced vesicular protein levels might contribute to the negative effect of the aged systemic environment on stem cell biology. Therefore, our findings suggest that Galectin-3 might be a valuable plasma-based biomarker for a systemic environment that does not facilitate osteogenic differentiation.

9.3 MicroRNA-31

While microRNA-31 is mainly known for tis role in cancers such as breast (Valastyan et al. 2009), oral (C. J. Liu et al. 2012) head and neck (Odar et al. 2012) carcinoma as well as prostate (Feng et al. 2013), colorectal (Slaby et al. 2008), colon (Cottonham et al. 2010), lung (Tan et al. 2011), cervical (Y. Li et al. 2011) and gastric (Zhang et al. 2010) cancer and myeloid leukaemia (Seca et al. 2010) microRNA-31 also effects the

osteogenic differentiation potential of mesenchymal stem cells. MiR-31-5p (miR-31) was shown to target the two key regulators of osteogenesis Runx-2 and Osterix (Deng et al. 2013) but also enhances osteoclast formation and activity (Mizoguchi et al. 2013). In addition the *in vivo* relevance of miR-31 in bone formation was confirmed by an improved critical size defect repair capacity of transplanted mesenchymal stem cells transfected with an inhibitor against miR-31 (Deng et al. 2014).

Additionally to our preliminary data this series of experiments shows that CD63 positive extracellular vesicles and not co-pelleting protein aggregates or other impurities isolated from the conditioned medium of senescent endothelial cells mediate the observed inhibitory effect on osteogenesis in ASCs. Consistently with our *in vitro* data we confirmed that ex vivo derived CD63 positive extracellular vesicles isolated from the plasma of elderly individuals harbour the inhibitory activity. Finally we attributed the anti-osteogenic effect of senescent cell or elderly plasma derived EVs to increased vesicular miR-31 levels.

Taken together this data supports our hypothesis that extracellular vesicles are part of the endothelial SASP. CD63 positive extracellular vesicles isolated from the conditioned medium of senescent but not from quiescent early passage endothelial cells are enriched in anti-osteogenic miR-31. Since CD63 positive vesicles enriched in miR-31 were also found in the plasma of elderly and in the case of osteoporotic donors they might contribute to impaired osteoblastogenesis *in vivo* as well. Consequently high levels of vesicular miR-31 might add to the negative effect of the aged systemic environment on stem cell differentiation. Therefore, our findings suggest that vesicular miR-31 might be a valuable plasma-based biomarker for a systemic environment that does not facilitate osteogenic differentiation.

9.4 Deregulated microRNAs in osteoporotic fractures

The influence of microRNAs on bone formation and resorption as well as the need for a better fracture risk assessment has already been outlined in the introduction. However the question remains whether changes in the plasma microRNA profile of patients suffering from osteoporosis compared to healthy age matched controls are observable. In order to address this question plasma level of 157 microRNAs were analysed in 7 post-traumatic osteoporotic patients as well as 7 unfractured age matched control individuals. Analysis for differential microRNA expression revealed 5 differentially secreted microRNAs. While miR-10a, 10b and miR-22 have been shown to be upregulated miR-133b and miR-328 were significantly downregulated in femoral fractured patients. When evaluating the effect of miR-10b and miR-22 overexpression as well as of miR-328 knock down on osteoblastogenesis a significant inhibition of osteogenesis in all miR-10b overexpressing donors was observed while only one miR-328 inhibitor transfected donor exhibited a reduced differentiation capacity. MiR-10b was already confirmed to be downregulated in the course of osteogenic differentiation of induced pluripotent stem cells (Okamoto et al. 2012) indicating that it might have an antagonistic effect on osteogenesis. Indeed we confirmed that miR-10b overexpression in ASCs negatively impairs osteoblastogenesis.

Surprisingly overexpression of miR-22 did not clearly impaired osteogenesis although miR-22 has been reported to promote osteogenesis in ASCs by targeting HDAC6, an inhibitor of osteogenic differentiation (Huang et al. 2012).

Additionally to the microRNAs we found to be differentially expressed in hip fractured osteoporotic patients compared to age matched controls in this study, Seelinger and colleagues recently published another set of microRNAs that is differentially regulated in sera and bone biopsies of patients suffering from a osteoporotic hip fracture (Seeliger et al. 2014). In order to test whether these microRNAs have an effect on osteoblastogenesis, ASCs were additionally transfected with miR-21, miR-24, miR-100 or miR-148a. While miR-100 caused a strong reduction of osteoblastogenesis in both donors, miR-148a was demonstrated to have an accelerating effect on osteogenesis. The inhibition of osteoblastogenesis by overexpressing miR-100 is in agreement with studies published earlier showing that miR-100bs anti-osteogenic effect in ASCs is mediated by targeting bone morphogenetic protein receptor type II (BMPR2) (Zeng et al. 2012). MiR-148a is already known to enhance osteoclastogenesis (Cheng et al.

2012) but nothing was reported on its effect on osteoblastogenesis by now. However, knock down of miR-148a in ovariectomized and shame operated control mice resulted in a higher bone mass compared to corresponding control animals indicating that miR-148a has a negative effect on bone remodelling *in vivo* (Cheng et al. 2012). Supportingly increased miR-148a levels were detected in PBMCs of patients suffering from Lupus who exhibit a low BMD (Cheng et al. 2013).

MiR-21 was shown to have a positive effect on the activity of osteoclasts (Sugatani et al. 2011). Furthermore reduced levels of miR-21 lead to apoptosis of osteoclasts (Sugatani & Hruska 2013). In contrast to previous investigations which demonstrated that miR-21 accelerates osteogenic differentiation of mesenchymal stem cells (Mei et al. 2013), miR-21 transfection reduced the mineralization capability in one successfully transiently transfected donor in our experiments. Finally previous investigations report that Runx-2 binds to and thereby inhibits the expression of the miR-24a-27a-24 cluster (Hassan et al. 2010) indicating that those microRNAs might operate against osteoblastogenesis. We confirmed this hypothesis since miR-24 overexpression reduced the mineralization ability in one of two donors. Taken together all deregulated microRNAs in patients suffering from osteoporosis were shown to have a negative influence on osteoblastogenesis *in vitro* besides miR-22, which did not show a clear impact and miR-148a which had a positive effect. However, miR-148a was demonstrated to act on osteoclasts by accelerating their differentiation (Cheng et al. 2013). Considering the effect of miR-148a on bone biology in *in vivo* experiments its impact on osteoclasts seems to be dominant over the consistently observed pro-osteoblastogenic effect in our study.

However the pressing question why this study revealed a different microRNA signature for patients suffering from an osteoperotic fracture compared to unfractured individuals compared to Seeligers work remains. In order to find an answer a closer look at the study designs might explain the differences. Firstly, samples of this work have been taken several days after surgery while in the other report blood was already drawn during surgery. Secondly, in contrast to our study were groups were divided in osteoprotic fractured and unfractured patients, Seeliger and colleagues classified the donors as osteoporotic or not osteoporotic according to their BMD levels measured by dual x-ray absorptiometry (DXA). Thirdly, obtained µ-Array data of this work were normalized to the volume of serum the RNAs were isolated from by the aid of spike-in RNAs. In contrast the group of van Griensven normalized their data to SNORD96a and

RNU6. SNORD96a as well as RNU6 are two frequently used reverence RNAs in order to normalize intracellular RNAs (Peltier & Latham 2008). However, normalization of circulating microRNAs is more challenging since there is no validated reference gene so far (Kang et al. 2012). And finally while Seeliger et al. analysed the profile of 83 microRNAs, 157 microRNAs were examined in this study. In particular the results chapter of Seeliger and colleagues shows that miR-22 and miR-328 were not included in their arrays. Furthermore they could not detect the levels of miR-10a, miR-10b and miR-133b. Taken together the different aims of the studies led to a completely different study design of both works. While Seeliger and colleagues were looking for a microRNA signature correlating with the BMD, the point of this study was to identify a microRNA profile for a better fracture risk assessment. Consequently the valuable data of both studies are not conflicting but rather complementary.

In summary, this study confirms that patients suffering from an osteoporotic fracture exhibit a changed microRNA secretion profile compared to unfractured aged matched control individuals and establishes the basis for further investigations in order to identify a microRNA profile for the early diagnosis of osteoporosis.

10 List of tables

11 List of figures

12 References

Aarden, E.M., Burger, E.H. & Nijweide, P.J., 1994. Function of osteocytes in bone. *Journal of Cellular Biochemistry*, 55, pp.287–299.

Adachi, T. et al., 2009. Osteocyte calcium signaling response to bone matrix deformation. *Journal of Biomechanics*, 42, pp.2507–2512.

Admyre, C. et al., 2007. Exosomes with immune modulatory features are present in human breast milk. *Journal of immunology (Baltimore, Md.□: 1950)*, 179, pp.1969–1978.

Akahani, S. et al., 1997. Galectin-3: a novel antiapoptotic molecule with a functional BH1 (NWGR) domain of Bcl-2 family. *Cancer research*, 57, pp.5272–5276.

Almeida, M. et al., 2007. Skeletal involution by age-associated oxidative stress and its acceleration by loss of sex steroids. *The Journal of biological chemistry*, 282, pp.27285–27297.

Van Amerongen, R., Mikels, A. & Nusse, R., 2008. Alternative wnt signaling is initiated by distinct receptors. *Science signaling*, 1, p.re9.

Anon, 1977. Hormone Production by the Pituitary and Testes of Male C57BL/6J Mice During Aging. *Endocrinology*, 101(4), pp.1310–1317. Available at: http://dx.doi.org/10.1210/endo-101-4-1310.

Anon, 1997. Who are candidates for prevention and treatment for osteoporosis? *Osteoporosis international□: a journal established as result of cooperation between the European Foundation for Osteoporosis and the National Osteoporosis Foundation of the USA*, 7(1), pp.1–6. Available at: http://www.ncbi.nlm.nih.gov/pubmed/9102057 [Accessed July 8, 2014].

Ash, P., Loutit, J.F. & Townsend, K.M., 1980. Osteoclasts derived from haematopoietic stem cells. *Nature*, 283, pp.669–670.

Aubin, J.E. et al., 1996. Expression and regulation of galectin 3 in rat osteoblastic cells. *J Cell Physiol*, 169(3), pp.468–480. Available at: http://www.ncbi.nlm.nih.gov/pubmed/8952696.

Baker, D.J. et al., 2011. Clearance of p16Ink4a-positive senescent cells delays ageing-associated disorders. *Nature*, 479(7372), pp.232–236. Available at: http://www.ncbi.nlm.nih.gov/entrez/query.fcgi?cmd=Retrieve&db=PubMed&dopt=Citation&list_uids=22048312.

Baron, R. & Kneissel, M., 2013. WNT signaling in bone homeostasis and disease: from human mutations to treatments. *Nature medicine*, 19(2), pp.179–92. Available at: http://www.ncbi.nlm.nih.gov/pubmed/23389618 [Accessed May 27, 2014].

Baron, R. & Rawadi, G., 2007. Targeting the Wnt/beta-catenin pathway to regulate bone formation in the adult skeleton. *Endocrinology*, 148, pp.2635–2643.

Bartel, D.P., 2009. MicroRNAs: target recognition and regulatory functions. *Cell*, 136(2), pp.215–233.

Belik, R. et al., 2008. Improvements in culturing exfoliated urothelial cells in vitro from human urine. *Journal of toxicology and environmental health. Part A*, 71(13-14), pp.923–9.

Bellingham, S.A. et al., 2012. Exosomes: vehicles for the transfer of toxic proteins associated with neurodegenerative diseases? *Front Physiol*, 3, p.124. Available at: http://www.ncbi.nlm.nih.gov/pubmed/22563321.

Bennett, C.N. et al., 2005. Regulation of osteoblastogenesis and bone mass by Wnt10b. *Proceedings of the National Academy of Sciences of the United States of America*, 102, pp.3324–3329.

Bennett, C.N. et al., 2007. Wnt10b increases postnatal bone formation by enhancing osteoblast differentiation. *Journal of bone and mineral research□: the official journal of the American Society for Bone and Mineral Research*, 22, pp.1924–1932.

Bernardes de Jesus, B. et al., 2012. Telomerase gene therapy in adult and old mice delays aging and increases longevity without increasing cancer. *EMBO Mol Med*. Available at: http://www.ncbi.nlm.nih.gov/entrez/query.fcgi?cmd=Retrieve&db=PubMed&dopt=Citation&list_uids=22585399.

Bharadwaj, S. et al., 2011. Characterization of urine-derived stem cells obtained from upper urinary tract for use in cell-based urological tissue engineering. *Tissue engineering. Part A*, 17(15-16), pp.2123–32.

Bharadwaj, S. et al., 2013. Multipotential differentiation of human urine-derived stem cells: potential for therapeutic applications in urology. *Stem cells (Dayton, Ohio)*, 31(9), pp.1840–56.

Bierman, E.L., 1978. The effect of donor age on the in vitro life span of cultured human arterial smooth-muscle cells. *In vitro*, 14(11), pp.951–5. Available at: http://www.ncbi.nlm.nih.gov/pubmed/730203 [Accessed July 8, 2014].

Le Blanc, K. et al., 2004. Treatment of severe acute graft-versus-host disease with third party haploidentical mesenchymal stem cells. *Lancet*, 363(9419), pp.1439–41. Available at: http://www.ncbi.nlm.nih.gov/pubmed/15121408 [Accessed June 7, 2014].

Blocki, A. et al., 2013. Not All MSCs Can Act as Pericytes: Functional In Vitro Assays to Distinguish Pericytes from Other Mesenchymal Stem Cells in Angiogenesis. *Stem Cells Dev*, 22(17), pp.2347–2355. Available at: http://www.ncbi.nlm.nih.gov/pubmed/23600480.

Bobrie, A. et al., 2011. Exosome secretion: molecular mechanisms and roles in immune responses. *Traffic*, 12(12), pp.1659–1668. Available at: http://www.ncbi.nlm.nih.gov/pubmed/21645191.

Boehm, M. & Slack, F., 2005. A developmental timing microRNA and its target regulate life span in C. elegans. *Science*, 310(5756), pp.1954–1957. Available at: http://www.ncbi.nlm.nih.gov/pubmed/16373574.

De Boer, R.A., Yu, L. & Van Veldhuisen, D.J., 2010. Galectin-3 in cardiac remodeling and heart failure. *Current Heart Failure Reports*, 7, pp.1–8.

Bohnsack, M.T., Czaplinski, K. & Gorlich, D., 2004. Exportin 5 is a RanGTP-dependent dsRNA-binding protein that mediates nuclear export of pre-miRNAs. *RNA (New York, N.Y.)*, 10, pp.185–191.

Boileau, C. et al., 2008. Intracellular localisation of galectin-3 has a protective role in chondrocyte survival. *Ann Rheum Dis*, 67(2), pp.175–181. Available at: http://www.ncbi.nlm.nih.gov/pubmed/17545192.

Bonewald, L.F., 2013. Osteocytes. In *Primer on the Metabolic Bone Diseases and Disorders of Mineral Metabolism*. pp. 34–41. Available at: http://dx.doi.org/10.1002/9781118453926.ch4.

Bonjour, J.P. et al., 1994. Peak bone mass. In *Osteoporosis International*.

Booth, A.M. et al., 2006. Exosomes and HIV Gag bud from endosome-like domains of the T cell plasma membrane. *The Journal of cell biology*, 172, pp.923–935.

Boskey, A.L., 2007. Mineralization of Bones and Teeth. *Elements*, 3, pp.385–391.

Boskey, A.L. & Coleman, R., 2010. Aging and Bone. , 89(12), pp.1333–1348.

Bouillon, R. & Suda, T., 2014. Vitamin D: calcium and bone homeostasis during evolution. *BoneKEy reports*, 3, p.480. Available at: http://www.nature.com/bonekeyreports/2014/140108/bonekey2013214/full/bonekey2013214.html [Accessed July 9, 2014].

Braig, M. et al., 2005. Oncogene-induced senescence as an initial barrier in lymphoma development. *Nature*, 436(7051), pp.660–5. Available at: http://www.ncbi.nlm.nih.gov/pubmed/16079837 [Accessed June 10, 2014].

Bruce, S.A., Deamond, S.F. & Ts'o, P.O., 1986. In vitro senescence of Syrian hamster mesenchymal cells of fetal to aged adult origin. Inverse relationship between in vivo donor age and in vitro proliferative capacity. *Mechanisms of ageing and development*, 34(2), pp.151–73. Available at: http://www.ncbi.nlm.nih.gov/pubmed/3724250 [Accessed July 8, 2014].

Byrd, J.C., Mazurek, N. & Bresalier, R.S., 2012. Post-Translational Modification of Galectin-3 and Its Role in Biological Function. In *Galectins and Disease Implications for Targeted Therapeutics*. ACS Symposium Series. American

Chemical Society, pp. 137–151 SE – 8. Available at: http://dx.doi.org/10.1021/bk-2012-1115.ch008.

Campisi, J. & d'Adda di Fagagna, F., 2007. Cellular senescence: when bad things happen to good cells. *Nat Rev Mol Cell Biol*, 8(9), pp.729–740. Available at: http://www.ncbi.nlm.nih.gov/entrez/query.fcgi?cmd=Retrieve&db=PubMed&dopt=Citation&list_uids=17667954.

Cao, J.J. et al., 2005. Aging increases stromal/osteoblastic cell-induced osteoclastogenesis and alters the osteoclast precursor pool in the mouse. *Journal of bone and mineral research : the official journal of the American Society for Bone and Mineral Research*, 20(9), pp.1659–68. Available at: http://www.ncbi.nlm.nih.gov/pubmed/16059637 [Accessed July 8, 2014].

Caplan, A.I., 2007. Adult mesenchymal stem cells for tissue engineering versus regenerative medicine. *Journal of Cellular Physiology*, 213, pp.341–347.

Carlson, B.M. & Faulkner, J.A., 1989. Muscle transplantation between young and old rats: age of host determines recovery. *The American journal of physiology*, 256, pp.C1262–C1266.

Carlson, M.E. & Conboy, I.M., 2007. Loss of stem cell regenerative capacity within aged niches. *Aging Cell*, 6, pp.371–382.

Cefalu, C.A., 2004. Is bone mineral density predictive of fracture risk reduction? *Current medical research and opinion*, 20(3), pp.341–349.

Chang, M.W. et al., 2005. Comparison of early passage, senescent and hTERT immortalized endothelial cells. *Exp Cell Res*, 309(1), pp.121–136. Available at: http://www.ncbi.nlm.nih.gov/pubmed/15964568.

Chapman, E.J. & Carrington, J.C., 2007. Specialization and evolution of endogenous small RNA pathways. *Nature reviews. Genetics*, 8, pp.884–896.

Chavez-Munoz, C. et al., 2013. Transdifferentiation of adipose-derived stem cells into keratinocyte-like cells: engineering a stratified epidermis. *PloS one*, 8(12), p.e80587.

Chen, L.H. et al., 2010. MicroRNA and aging: a novel modulator in regulating the aging network. *Ageing Res Rev*, 9 Suppl 1, pp.S59–66. Available at: http://www.ncbi.nlm.nih.gov/pubmed/20708718.

Chen, X. et al., 2008. Characterization of microRNAs in serum: a novel class of biomarkers for diagnosis of cancer and other diseases. *Cell Res*, 18(10), pp.997–1006. Available at: http://www.ncbi.nlm.nih.gov/entrez/query.fcgi?cmd=Retrieve&db=PubMed&dopt=Citation&list_uids=18766170.

Chen, X. et al., 2012. Horizontal transfer of microRNAs: molecular mechanisms and clinical applications. *Protein Cell*, 3(1), pp.28–37. Available at: http://www.ncbi.nlm.nih.gov/pubmed/22314808.

Chen, Y. et al., 2007. Beta-catenin signaling pathway is crucial for bone morphogenetic protein 2 to induce new bone formation. *The Journal of biological chemistry*, 282, pp.526–533.

Chendrimada, T.P. et al., 2005. TRBP recruits the Dicer complex to Ago2 for microRNA processing and gene silencing. *Nature*, 436, pp.740–744.

Cheng, P. et al., 2013. MiR-148a regulates osteoclastogenesis by targeting V-maf musculoaponeurotic fibrosarcoma oncogene homolog B. *Journal of Bone and Mineral Research*, 28, pp.1180–1190.

Cheng, P. et al., 2012. MiR-148a regulates osteoclastogenesis via targeting MAFB. *J Bone Miner Res*, pp.1–31. Available at: http://www.ncbi.nlm.nih.gov/pubmed/23225151.

Cogswell, J.P. et al., 2008. Identification of miRNA changes in Alzheimer's disease brain and CSF yields putative biomarkers and insights into disease pathways. *J Alzheimers Dis*, 14(1), pp.27–41. Available at: http://www.ncbi.nlm.nih.gov/pubmed/18525125.

Collado, M. et al., 2005. Tumour biology: senescence in premalignant tumours. *Nature*, 436(7051), p.642. Available at: http://www.ncbi.nlm.nih.gov/pubmed/16079833 [Accessed June 10, 2014].

Conboy, I.M. et al., 2005. Rejuvenation of aged progenitor cells by exposure to a young systemic environment. *Nature*, 433(7027), pp.760–764. Available at: http://www.ncbi.nlm.nih.gov/entrez/query.fcgi?cmd=Retrieve&db=PubMed&dopt=Citation&list_uids=15716955.

Conboy, I.M. & Rando, T.A., 2005. Aging, stem cells and tissue regeneration: lessons from muscle. *Cell Cycle*, 4(3), pp.407–410. Available at: http://www.ncbi.nlm.nih.gov/pubmed/15725724.

Coppé, J.-P. et al., 2008. *Senescence-associated secretory phenotypes reveal cell-nonautonomous functions of oncogenic RAS and the p53 tumor suppressor.*,

Coppé, J.-P. et al., 2010. The senescence-associated secretory phenotype: the dark side of tumor suppression. *Annual review of pathology*, 5, pp.99–118.

Cornelius, E.A., 1972. Increased incidence of lymphomas in thymectomized Mice - evidence for an immunological theory of aging. *Experientia*, 28(4), p.459. Available at: http://dx.doi.org/10.1007/BF02008340.

Corpas, E., Harman, S.M. & Blackman, M.R., 1993. Human growth hormone and human aging. *Endocr Rev*, 14(1), pp.20–39. Available at: http://www.ncbi.nlm.nih.gov/pubmed/8491152.

Cottonham, C.L., Kaneko, S. & Xu, L., 2010. miR-21 and miR-31 converge on TIAM1 to regulate migration and invasion of colon carcinoma cells. *The Journal of biological chemistry*, 285, pp.35293–35302.

Courtois-Cox, S. et al., 2006. A negative feedback signaling network underlies oncogene-induced senescence. *Cancer cell*, 10(6), pp.459–72. Available at: http://www.pubmedcentral.nih.gov/articlerender.fcgi?artid=2692661&tool=pmcentrez&rendertype=abstract [Accessed May 27, 2014].

Crisan, M. et al., 2008. A perivascular origin for mesenchymal stem cells in multiple human organs. *Cell Stem Cell*, 3(3), pp.301–313. Available at: http://www.ncbi.nlm.nih.gov/pubmed/18786417.

Dagher, S.F., Wang, J.L. & Patterson, R.J., 1995. Identification of galectin-3 as a factor in pre-mRNA splicing. *Proceedings of the National Academy of Sciences of the United States of America*, 92, pp.1213–1217.

Darendeliler, F. et al., 2005. Bone age progression during the first year of growth hormone therapy in pre-pubertal children with idiopathic growth hormone deficiency, Turner syndrome or idiopathic short stature, and in short children born small for gestational age: analysis of data fr. *Horm Res*, 63(1), pp.40–47. Available at: http://www.ncbi.nlm.nih.gov/pubmed/15627781.

Davalos, A.R. et al., 2010. Senescent cells as a source of inflammatory factors for tumor progression. *Cancer Metastasis Rev*, 29(2), pp.273–283. Available at: http://www.ncbi.nlm.nih.gov/pubmed/20390322.

Davidovic, M. et al., 2010. Old age as a privilege of the “selfish ones”. *Aging and disease*, 1, pp.139–46. Available at: http://www.pubmedcentral.nih.gov/articlerender.fcgi?artid=3295027&tool=pmcentrez&rendertype=abstract.

Davidson, P.J. et al., 2002. Shuttling of galectin-3 between the nucleus and cytoplasm. *Glycobiology*, 12, pp.329–337.

Deng, Y. et al., 2013. Effects of a miR-31, Runx2, and Satb2 Regulatory Loop on the Osteogenic Differentiation of Bone Mesenchymal Stem Cells. *Stem Cells Dev*, 22, pp.2278–86. Available at: http://www.ncbi.nlm.nih.gov/pubmed/23517179.

Deng, Y. et al., 2014. Repair of critical-sized bone defects with anti-miR-31-expressing bone marrow stromal stem cells and poly(glycerol sebacate) scaffolds. *European cells & materials*, 27, pp.13–24; discussion 24–5. Available at: http://www.ncbi.nlm.nih.gov/pubmed/24425157.

Dimri, G.P. et al., 1995. A biomarker that identifies senescent human cells in culture and in aging skin in vivo. *Proceedings of the National Academy of Sciences of the United States of America*, 92(20), pp.9363–7. Available at: http://www.pubmedcentral.nih.gov/articlerender.fcgi?artid=40985&tool=pmcentrez&rendertype=abstract [Accessed May 27, 2014].

Dominici, M. et al., 2006. Minimal criteria for defining multipotent mesenchymal stromal cells. The International Society for Cellular Therapy position statement. *Cytotherapy*, 8(4), pp.315–7. Available at: http://www.ncbi.nlm.nih.gov/pubmed/16923606 [Accessed May 24, 2014].

Dong, S. et al., 2012. MicroRNAs regulate osteogenesis and chondrogenesis. *Biochemical and Biophysical Research Communications*, 418, pp.587–591.

Dumic, J., Dabelic, S. & Flögel, M., 2006. Galectin-3: An open-ended story. *Biochimica et Biophysica Acta - General Subjects*, 1760, pp.616–635.

Eghbali-Fatourechi, G.Z. et al., 2007. Characterization of circulating osteoblast lineage cells in humans. *Bone*, 40(5), pp.1370–1377. Available at: http://www.ncbi.nlm.nih.gov/pubmed/17320497.

Eghbali-Fatourechi, G.Z. et al., 2005. Circulating osteoblast-lineage cells in humans. *N Engl J Med*, 352(19), pp.1959–1966. Available at: http://www.ncbi.nlm.nih.gov/pubmed/15888696.

ElSharawy, A. et al., 2012. Genome-wide miRNA signatures of human longevity. *Aging Cell*, 11(4), pp.607–616. Available at: http://www.ncbi.nlm.nih.gov/pubmed/22533606.

Erusalimsky, J.D., 2009. Vascular endothelial senescence: from mechanisms to pathophysiology. *J Appl Physiol*, 106(1), pp.326–332. Available at: http://www.ncbi.nlm.nih.gov/entrez/query.fcgi?cmd=Retrieve&db=PubMed&dopt=Citation&list_uids=19036896.

Erusalimsky, J.D. & Kurz, D.J., 2006. Endothelial cell senescence. *Handb Exp Pharmacol*, (176 Pt 2), pp.213–248. Available at: http://www.ncbi.nlm.nih.gov/pubmed/17001772.

Eskildsen, T. et al., 2011. MicroRNA-138 regulates osteogenic differentiation of human stromal (mesenchymal) stem cells in vivo. *Proc Natl Acad Sci U S A*, 108(15), pp.6139–6144. Available at: http://www.ncbi.nlm.nih.gov/pubmed/21444814.

Fevrier, B. & Raposo, G., 2004. Exosomes: Endosomal-derived vesicles shipping extracellular messages. *Current Opinion in Cell Biology*, 16, pp.415–421.

Fais, S. et al., 2013. Exosomes: The ideal nanovectors for biodelivery. *Biological Chemistry*, 394, pp.1–15.

Feldser, D.M. & Greider, C.W., 2007. Short telomeres limit tumor progression in vivo by inducing senescence. *Cancer cell*, 11(5), pp.461–9. Available at: http://www.pubmedcentral.nih.gov/articlerender.fcgi?artid=1945093&tool=pmcentrez&rendertype=abstract [Accessed June 10, 2014].

Feng, J. et al., 2013. Screening biomarkers of prostate cancer by integrating microRNA and mRNA microarrays. *Genet Test Mol Biomarkers*, 17(11), pp.807–813. Available at: http://www.ncbi.nlm.nih.gov/pubmed/23984644.

Fichtlscherer, S., Zeiher, A.M. & Dimmeler, S., 2011. Circulating MicroRNAs: Biomarkers or mediators of cardiovascular diseases? *Arteriosclerosis, Thrombosis, and Vascular Biology*, 31, pp.2383–2390.

Fine, J.-D. et al., 2008. The classification of inherited epidermolysis bullosa (EB): Report of the Third International Consensus Meeting on Diagnosis and Classification of EB. *Journal of the American Academy of Dermatology*, 58(6), pp.931–50.

Föger-Samwald, U. et al., 2014. Molecular evidence of osteoblast dysfunction in elderly men with osteoporotic hip fractures. *Experimental gerontology*, 57C, pp.114–121. Available at: http://www.ncbi.nlm.nih.gov/pubmed/24862290 [Accessed July 7, 2014].

Friedenstein, A.J. et al., 1974. Stromal cells responsible for transferring the microenvironment of the hemopoietic tissues. Cloning in vitro and retransplantation in vivo. *Transplantation*, 17(4), pp.331–40. Available at: http://www.ncbi.nlm.nih.gov/pubmed/4150881 [Accessed June 5, 2014].

Frigeri, L.G., Zuberi, R.I. & Liu, F.T., 1993. Epsilon BP, a beta-galactoside-binding animal lectin, recognizes IgE receptor (Fc epsilon RI) and activates mast cells. *Biochemistry*, 32, pp.7644–7649.

Frühbeis, C., Fröhlich, D. & Krämer-Albers, E.-M., 2012. Emerging Roles of Exosomes in Neuron–Glia Communication. *Frontiers in Physiology*, 3.

Furtak, V., Hatcher, F. & Ochieng, J., 2001. Galectin-3 mediates the endocytosis of beta-1 integrins by breast carcinoma cells. *Biochemical and biophysical research communications*, 289, pp.845–850.

Galli, C., Passeri, G. & Macaluso, G.M., 2010. Osteocytes and WNT: the mechanical control of bone formation. *Journal of dental research*, 89, pp.331–343.

Gallo, A. et al., 2012. The majority of microRNAs detectable in serum and saliva is concentrated in exosomes. *PloS one*, 7(3), p.e30679. Available at: http://www.pubmedcentral.nih.gov/articlerender.fcgi?artid=3302865&tool=pmcentrez&rendertype=abstract [Accessed June 13, 2014].

Gibbings, D. & Voinnet, O., 2010. Control of RNA silencing and localization by endolysosomes. *Trends Cell Biol*, 20(8), pp.491–501. Available at: http://www.ncbi.nlm.nih.gov/pubmed/20630759.

Gibbings, D.J. et al., 2009. Multivesicular bodies associate with components of miRNA effector complexes and modulate miRNA activity. *Nat Cell Biol*, 11(9), pp.1143–1149. Available at: http://www.ncbi.nlm.nih.gov/pubmed/19684575.

Glatt, V. et al., 2007. Age-related changes in trabecular architecture differ in female and male C57BL/6J mice. *Journal of bone and mineral research□: the official journal of the American Society for Bone and Mineral Research*, 22, pp.1197–1207.

Gordon, M.D. & Nusse, R., 2006. Wnt signaling: multiple pathways, multiple receptors, and multiple transcription factors. *The Journal of biological chemistry*, 281(32), pp.22429–33. Available at: http://www.ncbi.nlm.nih.gov/pubmed/16793760 [Accessed May 24, 2014].

Gregory, R.I. et al., 2005. Human RISC couples microRNA biogenesis and posttranscriptional gene silencing. *Cell*, 123, pp.631–640.

Guan, J. et al., 2014. Biological characteristics of human Urine derived Stem Cells: potential for cell-based therapy in neurology. *Tissue engineering. Part A*.

Guevremont, M. et al., 2004. Galectin-3 surface expression on human adult chondrocytes: a potential substrate for collagenase-3. *Ann Rheum Dis*, 63(6), pp.636–643. Available at: http://www.ncbi.nlm.nih.gov/pubmed/15140769.

Hackl, M. et al., 2010. miR-17, miR-19b, miR-20a and miR-106a are down-regulated in human aging. *Aging Cell*, 9(2), pp.291–296. Available at: http://www.ncbi.nlm.nih.gov/entrez/query.fcgi?cmd=Retrieve&amp.

Halloran, B.P. et al., 2002. Changes in Bone Structure and Mass With Advancing Age in the Male C57BL/6J Mouse. *Journal of Bone and Mineral Research*, 17(6), pp.1044–1050. Available at: http://dx.doi.org/10.1359/jbmr.2002.17.6.1044.

Hamann, A., Jablonski-Westrich, D. & Thiele, H.G., 1986. Contact interaction between lymphocytes is a general event following activation and is mediated by LFA-1. *European journal of immunology*, 16(7), pp.847–50.

Hampel, B. et al., 2005. Apoptosis resistance of senescent human fibroblasts is correlated with the absence of nuclear IGFBP-3. *Aging cell*, 4(6), pp.325–30. Available at: http://www.ncbi.nlm.nih.gov/pubmed/16300485 [Accessed July 8, 2014].

Han, J. et al., 2004. The Drosha-DGCR8 complex in primary microRNA processing. *Genes & development*, 18, pp.3016–3027.

Han, Z.H. et al., 1997. Effects of ethnicity and age or menopause on the remodeling and turnover of iliac bone: implications for mechanisms of bone loss. *Journal of bone and mineral research□: the official journal of the American Society for Bone and Mineral Research*, 12, pp.498–508.

Hanai, J. et al., 1999. Interaction and functional cooperation of PEBP2/CBF with Smads. Synergistic induction of the immunoglobulin germline Calpha promoter. *The Journal of biological chemistry*, 274, pp.31577–31582.

Hassan, M.Q. et al., 2010. A network connecting Runx2, SATB2, and the miR-23a~27a~24-2 cluster regulates the osteoblast differentiation program. *Proceedings of the National Academy of Sciences of the United States of America*, 107, pp.19879–19884.

Hayflick, L., 1965. The limited in vitro lifetime of human diploid cells strains. *Exp Cell Res*, 37, pp.614–636.

Heemst, D. van, 2010. Insulin, IGF-1 and longevity. *Aging and Disease*, 1, pp.147–57. Available at: http://www.pubmedcentral.nih.gov/articlerender.fcgi?artid=3543749&tool=pmcentrez&rendertype=abstract\nhttp://www.ncbi.nlm.nih.gov/pmc/articles/PMC3295030/.

Henriksen, K. et al., 2007. Osteoclasts prefer aged bone. *Osteoporosis International*, 18, pp.751–759.

Herbig, U. et al., 2006. Cellular senescence in aging primates. *Science*, 311(5765), p.1257. Available at: http://www.ncbi.nlm.nih.gov/pubmed/16456035.

Herskind, A.M. et al., 1996. The heritability of human longevity: a population-based study of 2872 Danish twin pairs born 1870-1900. *Human genetics*, 97(3), pp.319–23. Available at: http://www.ncbi.nlm.nih.gov/pubmed/8786073 [Accessed July 8, 2014].

Hsu, C. et al., 2010. Regulation of exosome secretion by Rab35 and its GTPase-activating proteins TBC1D10A-C. *J Cell Biol*, 189(2), pp.223–232. Available at: http://www.ncbi.nlm.nih.gov/pubmed/20404108.

Hsu, D.K. et al., 2000. Targeted disruption of the galectin-3 gene results in attenuated peritoneal inflammatory responses. *The American journal of pathology*, 156, pp.1073–1083.

Huang, J. et al., 2010. MicroRNA-204 regulates Runx2 protein expression and mesenchymal progenitor cell differentiation. *Stem Cells*, 28, pp.357–364.

Huang, S. et al., 2012. Upregulation of miR-22 promotes osteogenic differentiation and inhibits adipogenic differentiation of human adipose tissue-derived mesenchymal stem cells by repressing HDAC6 protein expression. *Stem Cells Dev*, 21(13), pp.2531–2540. Available at: http://www.ncbi.nlm.nih.gov/pubmed/22375943.

Huang, X. et al., 2013. Characterization of human plasma-derived exosomal RNAs by deep sequencing. *BMC genomics*, 14, p.319. Available at: http://www.pubmedcentral.nih.gov/articlerender.fcgi?artid=3653748&tool=pmcentrez&rendertype=abstract.

Hughes, R.C., 1999. Secretion of the galectin family of mammalian carbohydrate-binding proteins. *Biochimica et Biophysica Acta - General Subjects*, 1473, pp.172–185.

Hunter, M.P. et al., 2008. Detection of microRNA expression in human peripheral blood microvesicles. *PLoS One*, 3(11), p.e3694. Available at: http://www.ncbi.nlm.nih.gov/pubmed/19002258.

Inohara, H. et al., 2008. Cytoplasmic and serum galectin-3 in diagnosis of thyroid malignancies. *Biochem Biophys Res Commun*, 376(3), pp.605–610. Available at: http://www.ncbi.nlm.nih.gov/pubmed/18809382.

Inohara, H., Akahani, S. & Raz, A., 1998. Galectin-3 stimulates cell proliferation. *Exp Cell Res*, 245(2), pp.294–302. Available at: http://www.ncbi.nlm.nih.gov/pubmed/9851870.

Inohara, H. & Raz, A., 1995. Functional evidence that cell surface galectin-3 mediates homotypic cell adhesion. *Cancer Res*, 55(15), pp.3267–3271. Available at: http://www.ncbi.nlm.nih.gov/pubmed/7542167.

Irion, U. & St Johnston, D., 2007. bicoid RNA localization requires specific binding of an endosomal sorting complex. *Nature*, 445(7127), pp.554–558. Available at: http://www.ncbi.nlm.nih.gov/pubmed/17268469.

Ismail, N. et al., 2013. Macrophage microvesicles induce macrophage differentiation and miR-223 transfer. *Blood*, 121, pp.984–995.

Janowska-Wieczorek, A. et al., 2005. Microvesicles derived from activated platelets induce metastasis and angiogenesis in lung cancer. *Int J Cancer*, 113(5), pp.752–760. Available at: http://www.ncbi.nlm.nih.gov/pubmed/15499615.

Jaskelioff, M. et al., 2011. Telomerase reactivation reverses tissue degeneration in aged telomerase-deficient mice. *Nature*, 469(7328), pp.102–106. Available at: http://www.ncbi.nlm.nih.gov/pubmed/21113150.

Jeyapalan, J.C. et al., 2007. Accumulation of senescent cells in mitotic tissue of aging primates. *Mechanisms of ageing and development*, 128(1), pp.36–44. Available at: http://www.pubmedcentral.nih.gov/articlerender.fcgi?artid=3654105&tool=pmcentrez&rendertype=abstract [Accessed June 4, 2014].

Jia, J. et al., 2013. MiR-145 suppresses osteogenic differentiation by targeting Sp7. *FEBS Letters*, 587, pp.3027–3031.

Jilka, R.L., 2013. The relevance of mouse models for investigating age-related bone loss in humans. *Journals of Gerontology - Series A Biological Sciences and Medical Sciences*, 68, pp.1209–1217.

Jin, J.K. et al., 2007. Galectin-3 expression is correlated with abnormal prion protein accumulation in murine scrapie. *Neurosci Lett*, 420(2), pp.138–143. Available at: http://www.ncbi.nlm.nih.gov/pubmed/17531384.

Jin, K., 2010. Modern Biological Theories of Aging. *Aging and disease*, 1(2), pp.72–74. Available at: http://www.pubmedcentral.nih.gov/articlerender.fcgi?artid=2995895&tool=pmcentrez&rendertype=abstract.

Jin, Q.H. et al., 2013. Serum galectin-3: a risk factor for vascular complications in type 2 diabetes mellitus. *Chin Med J (Engl)*, 126(11), pp.2109–2115. Available at: http://www.ncbi.nlm.nih.gov/pubmed/23769567.

Johnell, O. & Kanis, J.A., 2006. An estimate of the worldwide prevalence and disability associated with osteoporotic fractures. *Osteoporosis international□: a journal established as result of cooperation between the European Foundation for Osteoporosis and the National Osteoporosis Foundation of the USA*, 17(12), pp.1726–33. Available at: http://www.ncbi.nlm.nih.gov/pubmed/16983459 [Accessed May 26, 2014].

Joss, E.E. et al., 1997. Growth promotion and Turner-specific bone age after therapy with growth hormone and in combination with oxandrolone: when should therapy be started in Turner syndrome? *Horm Res*, 47(3), pp.102–109. Available at: http://www.ncbi.nlm.nih.gov/pubmed/9050948.

Jung, H.J. & Suh, Y., 2012. MicroRNA in Aging: From Discovery to Biology. *Curr Genomics*, 13(7), pp.548–557. Available at: http://www.ncbi.nlm.nih.gov/pubmed/23633914.

Kaiser, J., 2014. Aging. “Rejuvenation factor” in blood turns back the clock in old mice. *Science (New York, N.Y.)*, 344(6184), pp.570–1. Available at: http://www.ncbi.nlm.nih.gov/pubmed/24812376 [Accessed July 8, 2014].

Kang, K. et al., 2012. Identification of circulating miRNA biomarkers based on global quantitative real-time PCR profiling. *Journal of Animal Science and Biotechnology*, 3, p.4.

Kanis, J.A., 2002. Diagnosis of osteoporosis and assessment of fracture risk. *Lancet*, 359(9321), pp.1929–36. Available at: http://www.ncbi.nlm.nih.gov/pubmed/12057569 [Accessed June 3, 2014].

Kanis, J.A. et al., 2013. European guidance for the diagnosis and management of osteoporosis in postmenopausal women. *Osteoporosis international: a journal established as result of cooperation between the European Foundation for Osteoporosis and the National Osteoporosis Foundation of the USA*, 24(1), pp.23–57.

Kanis, J.A. et al., 1997. Guidelines for diagnosis and management of osteoporosis. The European Foundation for Osteoporosis and Bone Disease. *Osteoporosis international□: a journal established as result of cooperation between the European Foundation for Osteoporosis and the National Osteoporosis Foundation of the USA*, 7(4), pp.390–406. Available at: http://www.ncbi.nlm.nih.gov/pubmed/9373575 [Accessed July 8, 2014].

Kapinas, K., Kessler, C.B. & Delany, A.M., 2009. miR-29 suppression of osteonectin in osteoblasts: regulation during differentiation and by canonical Wnt signaling. *Journal of cellular biochemistry*, 108(1), pp.216–224.

Karsenty, G. & Wagner, E.F., 2002. Reaching a genetic and molecular understanding of skeletal development. *Developmental cell*, 2, pp.389–406. Available at: papers://c03f5996-50cd-4258-bcbc-2560b56b0b72/Paper/p234.

Kassem, M. & Marie, P.J., 2011. Senescence-associated intrinsic mechanisms of osteoblast dysfunctions. *Aging Cell*, 10(2), pp.191–197. Available at: http://www.ncbi.nlm.nih.gov/pubmed/21210937.

Katsimpardi, L. et al., 2014. Vascular and neurogenic rejuvenation of the aging mouse brain by young systemic factors. *Science (New York, N.Y.)*, 344(6184), pp.630–4. Available at: http://www.ncbi.nlm.nih.gov/pubmed/24797482 [Accessed May 23, 2014].

Kehlenbach, R.H. et al., 1999. A role for RanBP1 in the release of CRM1 from the nuclear pore complex in a terminal step of nuclear export. *The Journal of cell biology*, 145, pp.645–657.

Kharaziha, P. et al., 2012. Tumor cell-derived exosomes: A message in a bottle. *Biochim Biophys Acta*, 1826(1), pp.103–111. Available at: http://www.ncbi.nlm.nih.gov/pubmed/22503823.

Kim, H.R. et al., 1999. Cell cycle arrest and inhibition of anoikis by galectin-3 in human breast epithelial cells. *Cancer Res*, 59(16), pp.4148–4154. Available at: http://www.ncbi.nlm.nih.gov/pubmed/10463621.

Kim, S.J. et al., 2010. Galectin-3 increases gastric cancer cell motility by up-regulating fascin-1 expression. *Gastroenterology*, 138(3), pp.1032–1035. Available at: http://www.ncbi.nlm.nih.gov/pubmed/19818782.

Kim, Y.J. et al., 2009. miR-196a regulates proliferation and osteogenic differentiation in mesenchymal stem cells derived from human adipose tissue. *Journal of bone and mineral research□: the official journal of the American Society for Bone and Mineral Research*, 24, pp.816–825.

Kiwaki, K. et al., 2007. Galectin-3 stimulates preadipocyte proliferation and is up-regulated in growing adipose tissue. *Obesity (Silver Spring)*, 15(1), pp.32–39. Available at: http://www.ncbi.nlm.nih.gov/pubmed/17228029.

Kobayashi, H. et al., 2000. Multilineage differentiation of Cbfa1-deficient calvarial cells in vitro. *Biochemical and biophysical research communications*, 273, pp.630–636.

Koca, S.S. et al., 2013. Serum galectin-3 level in systemic sclerosis. *Clin Rheumatol*. Available at: http://www.ncbi.nlm.nih.gov/pubmed/23912642.

Kogure, T. et al., 2011. Intercellular nanovesicle-mediated microRNA transfer: a mechanism of environmental modulation of hepatocellular cancer cell growth. *Hepatology*, 54(4), pp.1237–1248. Available at: http://www.ncbi.nlm.nih.gov/pubmed/21721029.

Kohn, A.D. & Moon, R.T., Wnt and calcium signaling: beta-catenin-independent pathways. *Cell calcium*, 38(3-4), pp.439–46. Available at: http://www.ncbi.nlm.nih.gov/pubmed/16099039 [Accessed May 30, 2014].

Komori, T., 2005. Regulation of skeletal development by the Runx family of transcription factors. *Journal of Cellular Biochemistry*, 95, pp.445–453.

Kopen, G.C., Prockop, D.J. & Phinney, D.G., 1999. Marrow stromal cells migrate throughout forebrain and cerebellum, and they differentiate into astrocytes after injection into neonatal mouse brains. *Proceedings of the National Academy of Sciences of the United States of America*, 96(19), pp.10711–6. Available at: http://www.pubmedcentral.nih.gov/articlerender.fcgi?artid=17948&tool=pmcentrez&rendertype=abstract [Accessed June 5, 2014].

Kosaka, N., Iguchi, H., Yoshioka, Y., et al., 2010. Secretory mechanisms and intercellular transfer of microRNAs in living cells. *J Biol Chem*, 285(23), pp.17442–17452. Available at: http://www.ncbi.nlm.nih.gov/pubmed/20353945.

Kosaka, N., Iguchi, H. & Ochiya, T., 2010. Circulating microRNA in body fluid: a new potential biomarker for cancer diagnosis and prognosis. *Cancer Sci*, 101(10), pp.2087–2092. Available at: http://www.ncbi.nlm.nih.gov/pubmed/20624164.

Koutsoulidou, A. et al., 2011. Expression of miR-1, miR-133a, miR-133b and miR-206 increases during development of human skeletal muscle. *BMC developmental biology*, 11, p.34.

Kowal, J., Tkach, M. & Théry, C., 2014. Biogenesis and secretion of exosomes. *Current Opinion in Cell Biology*, 29, pp.116–125. Available at: http://linkinghub.elsevier.com/retrieve/pii/S095506741400057X [Accessed June 23, 2014].

Kozhevnikova, M.N., Mikaelian, A.S. & Starostin, V.I., 2008. [Molecular and genetic regulation of osteogenic differentiation of mesenchymal stromal cells]. *Izv Akad Nauk Ser Biol*, (3), pp.261–271. Available at: http://www.ncbi.nlm.nih.gov/pubmed/18668714.

Kuznetsov, S.A. et al., 2009. Enumeration of the colony-forming units-fibroblast from mouse and human bone marrow in normal and pathological conditions. *Stem cell research*, 2(1), pp.83–94. Available at: http://www.pubmedcentral.nih.gov/articlerender.fcgi?artid=2753860&tool=pmcentrez&rendertype=abstract [Accessed July 8, 2014].

Lang, R. et al., 2013. Self-renewal and differentiation capacity of urine-derived stem cells after urine preservation for 24 hours. I. Kerkis, ed. *PloS one*, 8(1), p.e53980.

Lazzerini Denchi, E. et al., 2005. Deregulated E2F activity induces hyperplasia and senescence-like features in the mouse pituitary gland. *Molecular and cellular biology*, 25(7), pp.2660–72. Available at: http://www.pubmedcentral.nih.gov/articlerender.fcgi?artid=1061636&tool=pmcentrez&rendertype=abstract [Accessed July 8, 2014].

Lee, E.H. et al., 2008. Disruption of the non-canonical WNT pathway in lung squamous cell carcinoma. *Clin Med Oncol*, 2008(2), pp.169–179. Available at: http://www.ncbi.nlm.nih.gov/pubmed/20401333.

Lee, E.J. et al., 2008. Systematic evaluation of microRNA processing patterns in tissues, cell lines, and tumors. *RNA (New York, N.Y.)*, 14(1), pp.35–42.

Lee, K.S. et al., 2000. Runx2 is a common target of transforming growth factor beta1 and bone morphogenetic protein 2, and cooperation between Runx2 and Smad5 induces osteoblast-specific gene expression in the pluripotent mesenchymal precursor cell line C2C12. *Molecular and cellular biology*, 20(23), pp.8783–92. Available at: http://www.pubmedcentral.nih.gov/articlerender.fcgi?artid=86511&tool=pmcentrez&rendertype=abstract [Accessed July 9, 2014].

Lee, R.C., Feinbaum, R.L. & Ambros, V., 1993. The C. elegans heterochronic gene lin-4 encodes small RNAs with antisense complementarity to lin-14. *Cell*, 75(5), pp.843–854. Available at: http://www.ncbi.nlm.nih.gov/pubmed/8252621.

Lee, Y. et al., 2004. MicroRNA genes are transcribed by RNA polymerase II. *The EMBO journal*, 23, pp.4051–4060.

Lee, Y. et al., 2003. The nuclear RNase III Drosha initiates microRNA processing. *Nature*, 425(6956), pp.415–419. Available at: http://dx.doi.org/10.1038/nature01957.

Leffler, H. et al., 2004. Introduction to galectins. *Glycoconj J*, 19(7-9), pp.433–440. Available at: http://www.ncbi.nlm.nih.gov/pubmed/14758066.

Lehmann, B.D. et al., 2008. Senescence-associated exosome release from human prostate cancer cells. *Cancer Res*, 68(19), pp.7864–7871. Available at: http://www.ncbi.nlm.nih.gov/pubmed/18829542.

De Lencastre, A. et al., 2010. MicroRNAs both promote and antagonize longevity in C. elegans. *Curr Biol*, 20(24), pp.2159–2168. Available at: http://www.ncbi.nlm.nih.gov/pubmed/21129974.

Lepperdinger, G., 2011. Inflammation and mesenchymal stem cell aging. *Current Opinion in Immunology*, 23, pp.518–524.

Lepur, A. et al., 2012. Galectin-3 endocytosis by carbohydrate independent and dependent pathways in different macrophage like cell types. *Biochim Biophys Acta*, 1820(7), pp.804–818. Available at: http://www.ncbi.nlm.nih.gov/pubmed/22450157.

Li, E. et al., 2013. miR-143 suppresses osteogenic differentiation by targeting Osterix. *Molecular and Cellular Biochemistry*, pp.1–6.

Li, H. et al., 2009. A novel microRNA targeting HDAC5 regulates osteoblast differentiation in mice and contributes to primary osteoporosis in humans. *J Clin*

Invest, 119(12), pp.3666–3677. Available at: http://www.ncbi.nlm.nih.gov/pubmed/19920351.

Li, X. et al., 2011. Circulatory miR34a as an RNAbased, noninvasive biomarker for brain aging. *Aging (Albany NY)*, 3(10), pp.985–1002. Available at: http://www.ncbi.nlm.nih.gov/pubmed/22064828.

Li, Y. et al., 2011. Progressive miRNA expression profiles in cervical carcinogenesis and identification of HPV-related target genes for miR-29. *Journal of Pathology*, 224, pp.484–495.

Li, Y.-J.J. et al., 2009. A possible suppressive role of galectin-3 in upregulated osteoclastogenesis accompanying adjuvant-induced arthritis in rats. *Lab Invest*, 89(1), pp.26–37. Available at: http://www.ncbi.nlm.nih.gov/pubmed/19015643 [Accessed June 1, 2014].

Li, Z. et al., 2008. A microRNA signature for a BMP2-induced osteoblast lineage commitment program. *Proceedings of the National Academy of Sciences of the United States of America*, 105(37), pp.13906–13911.

Liao, L. et al., 2013. Redundant miR-3077-5p and miR-705 mediate the shift of mesenchymal stem cell lineage commitment to adipocyte in osteoporosis bone marrow. *Cell death & disease*, 4, p.e600. Available at: http://www.pubmedcentral.nih.gov/articlerender.fcgi?artid=3641352&tool=pmcentrez&rendertype=abstract.

Liao, X.-B. et al., 2013. MiR-133a modulates osteogenic differentiation of vascular smooth muscle cells. *Endocrinology*, 154, pp.3344–52. Available at: http://www.ncbi.nlm.nih.gov/pubmed/23798596.

Lin, Y.H. et al., 2009. The relationship between serum galectin-3 and serum markers of cardiac extracellular matrix turnover in heart failure patients. *Clin Chim Acta*, 409(1-2), pp.96–99. Available at: http://www.ncbi.nlm.nih.gov/pubmed/19747906.

Liu, C.J. et al., 2012. Exploiting salivary miR-31 as a clinical biomarker of oral squamous cell carcinoma. *Head Neck*, 34(2), pp.219–224. Available at: http://www.ncbi.nlm.nih.gov/pubmed/22083872.

Liu, D. & Hornsby, P.J., 2007. Senescent human fibroblasts increase the early growth of xenograft tumors via matrix metalloproteinase secretion. *Cancer Res*, 67(7), pp.3117–3126. Available at: http://www.ncbi.nlm.nih.gov/pubmed/17409418.

Liu, F.T., Patterson, R.J. & Wang, J.L., 2002. Intracellular functions of galectins. *Biochim Biophys Acta*, 1572(2-3), pp.263–273. Available at: http://www.ncbi.nlm.nih.gov/pubmed/12223274.

Liu, G., Pareta, R.A., et al., 2013. Skeletal myogenic differentiation of urine-derived stem cells and angiogenesis using microbeads loaded with growth factors. *Biomaterials*, 34(4), pp.1311–26.

Liu, G., Wang, X., et al., 2013. The effect of urine-derived stem cells expressing VEGF loaded in collagen hydrogels on myogenesis and innervation following after subcutaneous implantation in nude mice. *Biomaterials*, 34(34), pp.8617–29.

Liu, N. et al., 2012. The microRNA miR-34 modulates ageing and neurodegeneration in Drosophila. *Nature*, 482(7386), pp.519–523. Available at: http://www.ncbi.nlm.nih.gov/pubmed/22343898.

Ljungquist, B. et al., 1998. The effect of genetic factors for longevity: a comparison of identical and fraternal twins in the Swedish Twin Registry. *The journals of gerontology. Series A, Biological sciences and medical sciences*, 53(6), pp.M441–6. Available at: http://www.ncbi.nlm.nih.gov/pubmed/9823748 [Accessed July 8, 2014].

Lykken, D.T. et al., 1993. Heritability of interests: a twin study. *The Journal of applied psychology*, 78, pp.649–661.

Mackenbach, J.P. & Looman, C.W., 2013. Life expectancy and national income in Europe, 1900-2008: an update of Preston's analysis. *International journal of epidemiology*, 42(4), pp.1100–10. Available at: http://www.ncbi.nlm.nih.gov/pubmed/23920140 [Accessed July 8, 2014].

Maguire, G. et al., 2013. Stem cell released molecules and exosomes in tissue engineering. In *Procedia Engineering*. pp. 270–278.

Manolagas, S.C. & Parfitt, A.M., 2010. What old means to bone. *Trends in endocrinology and metabolism: TEM*, 21(6), pp.369–74. Available at: http://www.pubmedcentral.nih.gov/articlerender.fcgi?artid=2880220&tool=pmcentrez&rendertype=abstract [Accessed July 8, 2014].

Marcellini, S., Henriquez, J.P. & Bertin, A., 2012. Control of osteogenesis by the canonical Wnt and BMP pathways in vivo: cooperation and antagonism between the canonical Wnt and BMP pathways as cells differentiate from osteochondroprogenitors to osteoblasts and osteocytes. *BioEssays: news and reviews in molecular, cellular and developmental biology*, 34(11), pp.953–962.

Marcus, R. et al., 2010. *Fundamentals of Osteoporosis*, Elsevier Inc.

Martin, G.M., Sprague, C.A. & Epstein, C.J., 1970. Replicative life-span of cultivated human cells. Effects of donor's age, tissue, and genotype. *Laboratory investigation; a journal of technical methods and pathology*, 23(1), pp.86–92. Available at: http://www.ncbi.nlm.nih.gov/pubmed/5431223 [Accessed July 8, 2014].

Mathivanan, S., Lim, J.W., et al., 2010. Proteomics analysis of A33 immunoaffinity-purified exosomes released from the human colon tumor cell line LIM1215 reveals a tissue-specific protein signature. *Mol Cell Proteomics*, 9(2), pp.197–208. Available at: http://www.ncbi.nlm.nih.gov/pubmed/19837982.

Mathivanan, S., Ji, H. & Simpson, R.J., 2010. Exosomes: extracellular organelles important in intercellular communication. *J Proteomics*, 73(10), pp.1907–1920. Available at: http://www.ncbi.nlm.nih.gov/pubmed/20601276.

Mavilio, F. et al., 2006. Correction of junctional epidermolysis bullosa by transplantation of genetically modified epidermal stem cells. *Nature medicine*, 12(12), pp.1397–402.

Mei, Y. et al., 2013. MiR-21 modulates the ERK-MAPK signaling pathway by regulating SPRY2 expression during human mesenchymal stem cell differentiation. *Journal of Cellular Biochemistry*, 114, pp.1374–1384.

Melton, L.J. et al., 1992. Perspective. How many women have osteoporosis? *Journal of bone and mineral research□: the official journal of the American Society for Bone and Mineral Research*, 7(9), pp.1005–10. Available at: http://www.ncbi.nlm.nih.gov/pubmed/1414493 [Accessed June 13, 2014].

Menini, S. et al., 2013. The galectin-3/RAGE dyad modulates vascular osteogenesis in atherosclerosis. *Cardiovasc Res*. Available at: http://www.ncbi.nlm.nih.gov/pubmed/23975852.

Menon, R.P. & Hughes, R.C., 1999. Determinants in the N-terminal domains of galectin-3 for secretion by a novel pathway circumventing the endoplasmic reticulum-Golgi complex. *Eur J Biochem*, 264(2), pp.569–576. Available at: http://www.ncbi.nlm.nih.gov/pubmed/10491105.

Menon, S., Kang, C.M. & Beningo, K.A., 2011. Galectin-3 secretion and tyrosine phosphorylation is dependent on the calpain small subunit, Calpain 4. *Biochem Biophys Res Commun*, 410(1), pp.91–96. Available at: http://www.ncbi.nlm.nih.gov/pubmed/21640083.

Minamino, T. & Komuro, I., 2007. Vascular cell senescence: contribution to atherosclerosis. *Circ Res*, 100(1), pp.15–26.

Mitchell, P.S. et al., 2008. Circulating microRNAs as stable blood-based markers for cancer detection. *Proc Natl Acad Sci U S A*, 105(30), pp.10513–10518. Available at: http://www.ncbi.nlm.nih.gov/pubmed/18663219.

Mizoguchi, F. et al., 2013. miR-31 controls osteoclast formation and bone resorption by targeting RhoA. *Arthritis research & therapy*, 15, p.R102. Available at: http://www.ncbi.nlm.nih.gov/pubmed/24004633.

Mok, S.W. et al., 2007. Role of galectin-3 in prion infections of the CNS. *Biochem Biophys Res Commun*, 359(3), pp.672–678. Available at: http://www.ncbi.nlm.nih.gov/pubmed/17555713.

Montecalvo, A. et al., 2012. Mechanism of transfer of functional microRNAs between mouse dendritic cells via exosomes. *Blood*, 119(3), pp.756–766. Available at: http://www.ncbi.nlm.nih.gov/pubmed/22031862.

Müller, I. et al., 2003. Intravascular tissue factor initiates coagulation via circulating microvesicles and platelets. *The FASEB journal□: official publication of the Federation of American Societies for Experimental Biology*, 17, pp.476–478.

Nanbo, A. et al., 2013. Exosomes Derived from Epstein-Barr Virus-Infected Cells Are Internalized via Caveola-Dependent Endocytosis and Promote Phenotypic Modulation in Target Cells. *Journal of virology*, 87, pp.10334–47. Available at: http://www.ncbi.nlm.nih.gov/pubmed/23864627.

Van Niel, G. et al., 2006. Exosomes: a common pathway for a specialized function. *J Biochem*, 140(1), pp.13–21. Available at: http://www.ncbi.nlm.nih.gov/pubmed/16877764.

Nishida, S. et al., 1999. Number of osteoprogenitor cells in human bone marrow markedly decreases after skeletal maturation. *Journal of bone and mineral metabolism*, 17(3), pp.171–7. Available at: http://www.ncbi.nlm.nih.gov/pubmed/10757676 [Accessed May 27, 2014].

Nolte'T Hoen, E.N.M. et al., 2012. Deep sequencing of RNA from immune cell-derived vesicles uncovers the selective incorporation of small non-coding RNA biotypes with potential regulatory functions. *Nucleic Acids Research*, 40, pp.9272–9285.

Ochieng, J., Furtak, V. & Lukyanov, P., 2002. Extracellular functions of galectin-3. *Glycoconjugate Journal*, 19, pp.527–535.

Odar, K. et al., 2012. Differential expression of microRNAs miR-21, miR-31, miR-203, miR-125a-5p and miR-125b and proteins PTEN and p63 in verrucous carcinoma of the head and neck. *Histopathology*, 61, pp.257–265.

Oei, L. et al., 2013. High bone mineral density and fracture risk in type 2 diabetes as skeletal complications of inadequate glucose control: the Rotterdam Study. *Diabetes care*, 36(6), pp.1619–28. Available at: http://www.pubmedcentral.nih.gov/articlerender.fcgi?artid=3661786&tool=pmcentrez&rendertype=abstract [Accessed July 8, 2014].

Ten Oever, J. et al., 2013. Circulating galectin-3 in infections and non-infectious inflammatory diseases. *Eur J Clin Microbiol Infect Dis*. Available at: http://www.ncbi.nlm.nih.gov/pubmed/23828453.

Ogata-Kawata, H. et al., 2014. Circulating Exosomal microRNAs as Biomarkers of Colon Cancer. *PloS one*, 9, p.e92921. Available at: http://dx.plos.org/10.1371/journal.pone.0092921.

Ohtani, N. & Hara, E., 2013. Roles and mechanisms of cellular senescence in regulation of tissue homeostasis. *Cancer Sci*, 104(5), pp.525–530. Available at: http://www.ncbi.nlm.nih.gov/pubmed/23360516.

Okamoto, H. et al., 2012. Involvement of microRNAs in regulation of osteoblastic differentiation in mouse induced pluripotent stem cells. *PLoS ONE*, 7.

Okamoto, R. & Watanabe, M., 2004. Molecular and clinical basis for the regeneration of human gastrointestinal epithelia. *Journal of gastroenterology*, 39(1), pp.1–6. Available at: http://www.ncbi.nlm.nih.gov/pubmed/14767727 [Accessed July 8, 2014].

Olivieri, F. et al., 2013. Circulating inflamma-miRs in aging and age-related diseases. *Front Genet*, 4, p.121. Available at: http://www.ncbi.nlm.nih.gov/pubmed/23805154.

Ostrowski, M. et al., 2010. Rab27a and Rab27b control different steps of the exosome secretion pathway. *Nat Cell Biol*, 12(1), pp.13–19. Available at: http://www.ncbi.nlm.nih.gov/pubmed/19966785.

Otsuru, S. et al., 2012. Transplanted bone marrow mononuclear cells and MSCs impart clinical benefit to children with osteogenesis imperfecta through different mechanisms. *Blood*, 120(9), pp.1933–41. Available at: http://www.pubmedcentral.nih.gov/articlerender.fcgi?artid=3433095&tool=pmcentrez&rendertype=abstract [Accessed May 27, 2014].

Otto, F. et al., 1997. Cbfa1, a candidate gene for cleidocranial dysplasia syndrome, is essential for osteoblast differentiation and bone development. *Cell*, 89, pp.765–771.

Pan, B.T. & Johnstone, R.M., 1983. Fate of the transferrin receptor during maturation of sheep reticulocytes in vitro: selective externalization of the receptor. *Cell*, 33(3), pp.967–978. Available at: http://www.ncbi.nlm.nih.gov/pubmed/6307529.

Panel, N.C.D., 2001. Osteoporosis prevention, diagnosis, and therapy. *JAMA□: the journal of the American Medical Association*, 285(6), pp.785–95. Available at: http://www.ncbi.nlm.nih.gov/pubmed/11176917 [Accessed May 31, 2014].

Pang, J. et al., 2013. Increased adiposity, dysregulated glucose metabolism and systemic inflammation in Galectin-3 KO mice. *PLoS One*, 8(2), p.e57915. Available at: http://www.ncbi.nlm.nih.gov/pubmed/23451284.

Parfitt, a M., 2002. Misconceptions (2): turnover is always higher in cancellous than in cortical bone. *Bone*, 30(6), pp.807–9. Available at: http://www.ncbi.nlm.nih.gov/pubmed/12052445.

Parfitt, A.M., 1994. Osteonal and Hemi-Osteonal remodeling: The spatial and temporal framework for signal traffic in adult human bone. *Journal of Cellular Biochemistry*, 55, pp.273–286.

Park, W.Y. et al., 2001. Gene profile of replicative senescence is different from progeria or elderly donor. *Biochemical and biophysical research communications*, 282, pp.934–939.

Pasco, J.A. et al., 2006. The population burden of fractures originates in women with osteopenia, not osteoporosis. *Osteoporosis international□: a journal established as result of cooperation between the European Foundation for Osteoporosis and the*

National Osteoporosis Foundation of the USA, 17(9), pp.1404–9. Available at: http://www.ncbi.nlm.nih.gov/pubmed/16699736 [Accessed July 8, 2014].

Păunescu, V. et al., 2007. In vitro differentiation of human mesenchymal stem cells to epithelial lineage. *Journal of cellular and molecular medicine*, 11(3), pp.502–8.

Pejnovic, N.N. et al., 2013. Galectin-3 deficiency accelerates high-fat diet-induced obesity and amplifies inflammation in adipose tissue and pancreatic islets. *Diabetes*, 62(6), pp.1932–1944. Available at: http://www.ncbi.nlm.nih.gov/pubmed/23349493.

Peltier, H.J. & Latham, G.J., 2008. Normalization of microRNA expression levels in quantitative RT-PCR assays: identification of suitable reference RNA targets in normal and cancerous human solid tissues. *RNA (New York, N.Y.)*, 14, pp.844–852.

Perillo, N.L., Marcus, M.E. & Baum, L.G., 1998. Galectins: versatile modulators of cell adhesion, cell proliferation, and cell death. *J Mol Med (Berl)*, 76(6), pp.402–412. Available at: http://www.ncbi.nlm.nih.gov/pubmed/9625297.

Persengiev, S. et al., 2011. Genome-wide analysis of miRNA expression reveals a potential role for miR-144 in brain aging and spinocerebellar ataxia pathogenesis. *Neurobiol Aging*, 32(12), p.2316 e17–27. Available at: http://www.ncbi.nlm.nih.gov/pubmed/20451302.

Petersen, B.E. et al., 1999. Bone marrow as a potential source of hepatic oval cells. *Science (New York, N.Y.)*, 284(5417), pp.1168–70. Available at: http://www.ncbi.nlm.nih.gov/pubmed/10325227 [Accessed July 8, 2014].

Van der Plas, A. & Nijweide, P.J., 1992. Isolation and purification of osteocytes. *Journal of bone and mineral research□: the official journal of the American Society for Bone and Mineral Research*, 7, pp.389–396.

Properzi, F., Logozzi, M. & Fais, S., 2013. Exosomes: the future of biomarkers in medicine. *Biomarkers in medicine*, 7(5), pp.769–78. Available at: http://www.ncbi.nlm.nih.gov/pubmed/24044569.

Radosavljevic, G. et al., 2012. The roles of Galectin-3 in autoimmunity and tumor progression. *Immunol Res*, 52(1-2), pp.100–110. Available at: http://www.ncbi.nlm.nih.gov/pubmed/22418727.

Reynoso, R. et al., 2012. HIV-1 induces telomerase activity in monocyte-derived macrophages, possibly safeguarding one of its reservoirs. *Journal of Virology*, 86(19), pp.10327–37.

Rodier, F. & Campisi, J., 2011. Four faces of cellular senescence. *The Journal of cell biology*, 192, pp.547–556.

Roholl, P.J. et al., 1994. Evidence for a diminished maturation of preosteoblasts into osteoblasts during aging in rats: an ultrastructural analysis. *J Bone Miner Res*, 9(3),

pp.355–366. Available at: http://www.ncbi.nlm.nih.gov/pubmed/8191929 [Accessed June 4, 2014].

De Rosa, L. et al., 2013. Long-Term Stability and Safety of Transgenic Cultured Epidermal Stem Cells in Gene Therapy of Junctional Epidermolysis Bullosa. *Stem Cell Reports*, 2(1), pp.1–8.

Rubin, K.H. et al., 2013. Comparison of different screening tools (FRAX®, OST, ORAI, OSIRIS, SCORE and age alone) to identify women with increased risk of fracture. A population-based prospective study. *Bone*, 56(1), pp.16–22.

Sacchetti, B. et al., 2007. Self-renewing osteoprogenitors in bone marrow sinusoids can organize a hematopoietic microenvironment. *Cell*, 131(2), pp.324–36. Available at: http://www.ncbi.nlm.nih.gov/pubmed/17956733 [Accessed May 27, 2014].

Sahota, O. et al., 2004. The relationship between vitamin D and parathyroid hormone: calcium homeostasis, bone turnover, and bone mineral density in postmenopausal women with established osteoporosis. *Bone*, 35(1), pp.312–9. Available at: http://www.ncbi.nlm.nih.gov/pubmed/15207772 [Accessed July 8, 2014].

Sakaki, M. et al., 2008. Serum level of galectin-3 in human bladder cancer. *J Med Invest*, 55(1-2), pp.127–132. Available at: http://www.ncbi.nlm.nih.gov/pubmed/18319555.

Sarkar, D. et al., 2004. Human polynucleotide phosphorylase (hPNPaseold-35): a potential link between aging and inflammation. *Cancer research*, 64(20), pp.7473–8. Available at: http://www.ncbi.nlm.nih.gov/pubmed/15492272 [Accessed July 10, 2014].

Saussez, S. et al., 2008. Serum galectin-1 and galectin-3 levels in benign and malignant nodular thyroid disease. *Thyroid*, 18(7), pp.705–712. Available at: http://www.ncbi.nlm.nih.gov/pubmed/18630998.

Scadden, D.T., 2006. The stem-cell niche as an entity of action. *Nature*, 441, pp.1075–1079.

Schneider, E.L. & Mitsui, Y., 1976. The relationship between in vitro cellular aging and in vivo human age. *Proceedings of the National Academy of Sciences of the United States of America*, 73(10), pp.3584–8. Available at: http://www.pubmedcentral.nih.gov/articlerender.fcgi?artid=431162&tool=pmcentrez&rendertype=abstract [Accessed July 8, 2014].

Seca, H. et al., 2010. miR signatures and the role of miRs in acute myeloid leukaemia. *European Journal of Cancer*, 46, pp.1520–1527.

Seeliger, C. et al., 2014. Five Freely Circulating miRNAs and Bone Tissue miRNAs are Associated with Osteoporotic Fractures. *Journal of bone and mineral research : the official journal of the American Society for Bone and Mineral Research*, pp.1–30. Available at: http://www.ncbi.nlm.nih.gov/pubmed/24431276.

Serrano, M. et al., 1997. Oncogenic ras provokes premature cell senescence associated with accumulation of p53 and p16INK4a. *Cell*, 88(5), pp.593–602. Available at: http://www.ncbi.nlm.nih.gov/pubmed/9054499 [Accessed July 1, 2014].

Shi, S. et al., 2002. Bone formation by human postnatal bone marrow stromal stem cells is enhanced by telomerase expression. *Nature biotechnology*, 20(6), pp.587–91. Available at: http://www.ncbi.nlm.nih.gov/pubmed/12042862 [Accessed July 8, 2014].

Shi, S. & Gronthos, S., 2003. Perivascular niche of postnatal mesenchymal stem cells in human bone marrow and dental pulp. *J Bone Miner Res*, 18(4), pp.696–704. Available at: http://www.ncbi.nlm.nih.gov/pubmed/12674330.

Shimura, T. et al., 2005. Implication of galectin-3 in Wnt signaling. *Cancer Res*, 65(9), pp.3535–3537. Available at: http://www.ncbi.nlm.nih.gov/pubmed/15867344.

Da Silva Meirelles, L., Chagastelles, P.C. & Nardi, N.B., 2006. Mesenchymal stem cells reside in virtually all post-natal organs and tissues. *Journal of cell science*, 119(Pt 11), pp.2204–13. Available at: http://www.ncbi.nlm.nih.gov/pubmed/16684817 [Accessed May 27, 2014].

Simonsen, J.L. et al., 2002. Telomerase expression extends the proliferative life-span and maintains the osteogenic potential of human bone marrow stromal cells. *Nature biotechnology*, 20(6), pp.592–6. Available at: http://www.ncbi.nlm.nih.gov/pubmed/12042863 [Accessed July 8, 2014].

Simpson, R.J. et al., 2009. Exosomes: proteomic insights and diagnostic potential. *Expert Rev Proteomics*, 6(3), pp.267–283. Available at: http://www.ncbi.nlm.nih.gov/pubmed/19489699.

Simpson, R.J., Jensen, S.S. & Lim, J.W., 2008. Proteomic profiling of exosomes: current perspectives. *Proteomics*, 8(19), pp.4083–4099. Available at: http://www.ncbi.nlm.nih.gov/entrez/query.fcgi?cmd=Retrieve&db=PubMed&dopt=Citation&list_uids=18780348.

Sinha, I. et al., 2014. Testosterone is essential for skeletal muscle growth in aged mice in a heterochronic parabiosis model. *Cell and tissue research*. Available at: http://www.ncbi.nlm.nih.gov/pubmed/24859218 [Accessed May 27, 2014].

Siris, E.S. et al., 2004. Bone mineral density thresholds for pharmacological intervention to prevent fractures. *Archives of internal medicine*, 164(10), pp.1108–12. Available at: http://www.ncbi.nlm.nih.gov/pubmed/15159268 [Accessed July 8, 2014].

Slaby, O. et al., 2008. Altered expression of miR-21, miR-31, miR-143 and miR-145 is related to clinicopathologic features of colorectal cancer. *Oncology*, 72, pp.397–402.

Song, S. et al., 2009. Galectin-3 mediates nuclear beta-catenin accumulation and Wnt signaling in human colon cancer cells by regulation of glycogen synthase kinase-

3beta activity. *Cancer Res*, 69(4), pp.1343–1349. Available at: http://www.ncbi.nlm.nih.gov/pubmed/19190323.

Sornay-Rendu, E. et al., 2005. Identification of osteopenic women at high risk of fracture: the OFELY study. *Journal of bone and mineral research□: the official journal of the American Society for Bone and Mineral Research*, 20(10), pp.1813–9. Available at: http://www.ncbi.nlm.nih.gov/pubmed/16160738 [Accessed July 5, 2014].

Van Staa, T.P. et al., 2001. Epidemiology of fractures in England and Wales. *Bone*, 29(6), pp.517–22. Available at: http://www.ncbi.nlm.nih.gov/pubmed/11728921 [Accessed July 8, 2014].

Stein, G. et al., 1994. Altered Regulation of Cell Cycle Genes and Proteins in Senescent Human Diploid Fibroblasts. In V. Hu, ed. *The Cell Cycle SE - 30*. GWUMC Department of Biochemistry Annual Spring Symposia. Springer US, pp. 251–262. Available at: http://dx.doi.org/10.1007/978-1-4615-2421-2_30.

Stenderup, K. et al., 2003. Aging is associated with decreased maximal life span and accelerated senescence of bone marrow stromal cells. *Bone*, 33(6), pp.919–926. Available at: http://www.ncbi.nlm.nih.gov/pubmed/14678851.

Stenderup, K. et al., 2001. Number and proliferative capacity of osteogenic stem cells are maintained during aging and in patients with osteoporosis. *Journal of bone and mineral research□: the official journal of the American Society for Bone and Mineral Research*, 16(6), pp.1120–9. Available at: http://www.ncbi.nlm.nih.gov/pubmed/11393789 [Accessed June 28, 2014].

Stevens, J.R. et al., 2010. Wnt10b deficiency results in age-dependent loss of bone mass and progressive reduction of mesenchymal progenitor cells. *Journal of Bone and Mineral Research*, 25, pp.2138–2147.

Stock, M. et al., 2003. Expression of galectin-3 in skeletal tissues is controlled by Runx2. *J Biol Chem*, 278(19), pp.17360–17367. Available at: http://www.ncbi.nlm.nih.gov/pubmed/12604608.

Sugatani, T. & Hruska, K.A., 2013. Down-regulation of miR-21 biogenesis by estrogen action contributes to osteoclastic apoptosis. *Journal of Cellular Biochemistry*, 114, pp.1217–1222.

Sugatani, T., Vacher, J. & Hruska, K.A., 2011. A microRNA expression signature of osteoclastogenesis. *Blood*, 117, pp.3648–3657.

Svensson, K.J. et al., 2013. Exosome Uptake Depends on ERK1/2-Heat Shock Protein 27 Signaling and Lipid Raft-mediated Endocytosis Negatively Regulated by Caveolin-1. *J Biol Chem*, 288, pp.17713–17724. Available at: http://www.ncbi.nlm.nih.gov/pubmed/23653359.

Török, T.L., 2007. Electrogenic Na+/Ca2+-exchange of nerve and muscle cells. *Progress in Neurobiology*, 82, pp.287–347.

Tan, X. et al., 2011. A 5-MicroRNA Signature for Lung Squamous Cell Carcinoma Diagnosis and hsa-miR-31 for Prognosis. *Clinical Cancer Research*, 17, pp.6802–6811.

Teitelbaum, S.L., 2000. Bone resorption by osteoclasts. *Science (New York, N.Y.)*, 289, pp.1504–1508.

Théry, C. et al., 2001. Proteomic analysis of dendritic cell-derived exosomes: a secreted subcellular compartment distinct from apoptotic vesicles. *J Immunol*, 166(12), pp.7309–7318. Available at: http://www.ncbi.nlm.nih.gov/pubmed/11390481.

Thery, C., Ostrowski, M. & Segura, E., 2009. Membrane vesicles as conveyors of immune responses. *Nat Rev Immunol*, 9(8), pp.581–593. Available at: http://www.ncbi.nlm.nih.gov/entrez/query.fcgi?cmd=Retrieve&db=PubMed&dopt=Citation&list_uids=19498381.

Thum, T., Catalucci, D. & Bauersachs, J., 2008. MicroRNAs: novel regulators in cardiac development and disease. *Cardiovasc Res*, 79(4), pp.562–570. Available at: http://www.ncbi.nlm.nih.gov/pubmed/18511432.

Tian, T. et al., 2010. Visualizing of the cellular uptake and intracellular trafficking of exosomes by live-cell microscopy. *J Cell Biochem*, 111(2), pp.488–496. Available at: http://www.ncbi.nlm.nih.gov/pubmed/20533300.

TILL, J.E. & McCULLOCH, E.A., 1961. A direct measurement of the radiation sensitivity of normal mouse bone marrow cells. *Radiation research*, 14, pp.213–22. Available at: http://www.ncbi.nlm.nih.gov/pubmed/13776896 [Accessed May 29, 2014].

Tomkinson, A. et al., 1997. The death of osteocytes via apoptosis accompanies estrogen withdrawal in human bone. *J Clin Endocrinol Metab*, 82(9), pp.3128–3135. Available at: http://www.ncbi.nlm.nih.gov/pubmed/9284757.

Trajkovic, K. et al., 2008. Ceramide triggers budding of exosome vesicles into multivesicular endosomes. *Science*, 319(5867), pp.1244–1247. Available at: http://www.ncbi.nlm.nih.gov/pubmed/18309083.

Trams, E.G. et al., 1981. Exfoliation of membrane ecto-enzymes in the form of micro-vesicles. *Biochimica et biophysica acta*, 645, pp.63–70.

Trompeter, H.-I. et al., 2013. MicroRNAs miR-26a, miR-26b, and miR-29b accelerate osteogenic differentiation of unrestricted somatic stem cells from human cord blood. *BMC genomics*, 14, p.111. Available at: http://www.pubmedcentral.nih.gov/articlerender.fcgi?artid=3637629&tool=pmcentrez&rendertype=abstract.

Uccelli, A., Moretta, L. & Pistoia, V., 2008. Mesenchymal stem cells in health and disease. *Nature reviews. Immunology*, 8(9), pp.726–36. Available at: http://www.ncbi.nlm.nih.gov/pubmed/19172693 [Accessed May 29, 2014].

Undale, A. et al., 2010. Circulating osteogenic cells: characterization and relationship to rates of bone loss in postmenopausal women. *Bone*, 47(1), pp.83–92. Available at: http://www.pubmedcentral.nih.gov/articlerender.fcgi?artid=2891408&tool=pmcentrez&rendertype=abstract [Accessed June 4, 2014].

Valadi, H. et al., 2007. Exosome-mediated transfer of mRNAs and microRNAs is a novel mechanism of genetic exchange between cells. *Nat Cell Biol*, 9(6), pp.654–659. Available at: http://www.ncbi.nlm.nih.gov/entrez/query.fcgi?cmd=Retrieve&db=PubMed&dopt=Citation&list_uids=17486113.

Valastyan, S. et al., 2009. A pleiotropically acting microRNA, miR-31, inhibits breast cancer metastasis. *Cell*, 137(6), pp.1032–1046. Available at: http://www.ncbi.nlm.nih.gov/pubmed/19524507.

Vasikaran, S. et al., 2011. Markers of bone turnover for the prediction of fracture risk and monitoring of osteoporosis treatment: a need for international reference standards. *Osteoporosis international: a journal established as result of cooperation between the European Foundation for Osteoporosis and the National Osteoporosis Foundation of the USA*, 22(2), pp.391–420.

Ventura, A. et al., 2007. Restoration of p53 function leads to tumour regression in vivo. *Nature*, 445(7128), pp.661–5. Available at: http://www.ncbi.nlm.nih.gov/pubmed/17251932 [Accessed May 27, 2014].

Vereecken, P. et al., 2009. Evaluation of the prognostic significance of serum galectin-3 in American Joint Committee on Cancer stage III and stage IV melanoma patients. *Melanoma Res*, 19(5), pp.316–320. Available at: http://www.ncbi.nlm.nih.gov/pubmed/19581819.

Vereecken, P. & Heenen, M., 2006. Serum galectin-3 in advanced melanoma patients: a hypothesis on a possible role in melanoma progression and inflammation. *J Int Med Res*, 34(1), pp.119–120. Available at: http://www.ncbi.nlm.nih.gov/pubmed/16604833.

Verkaar, F. & Zaman, G.J.R., 2010. A model for signaling specificity of Wnt/Frizzled combinations through co-receptor recruitment. *FEBS Letters*, 584, pp.3850–3854.

Villarroya-Beltri, C. et al., 2013. Sumoylated hnRNPA2B1 controls the sorting of miRNAs into exosomes through binding to specific motifs. *Nature communications*, 4, p.2980. Available at: http://www.nature.com/ncomms/2013/131220/ncomms3980/full/ncomms3980.html.

Vimalraj, S., Partridge, N.C. & Selvamurugan, N., 2014. A Positive Role of microRNA-15b on Regulation of Osteoblast Differentiation. *Journal of cellular physiology*, pp.1–35. Available at: http://www.ncbi.nlm.nih.gov/pubmed/24435757.

Vlassara, H. et al., 1995. Identification of galectin-3 as a high-affinity binding protein for advanced glycation end products (AGE): a new member of the AGE-receptor complex. *Molecular medicine (Cambridge, Mass.)*, 1, pp.634–646.

Wang, X. et al., 2013. Elevated Galectin-3 Levels in the Serum of Patients With Alzheimer's Disease. *Am J Alzheimers Dis Other Demen*. Available at: http://www.ncbi.nlm.nih.gov/pubmed/23823143.

Wang, X. et al., 2013. miR-214 targets ATF4 to inhibit bone formation. *Nat Med*, 19(1), pp.93–100. Available at: http://www.ncbi.nlm.nih.gov/pubmed/23223004.

Wang, Y. et al., 2012. MiR-133a in human circulating monocytes: a potential biomarker associated with postmenopausal osteoporosis. *PLoS One*, 7(4), p.e34641. Available at: http://www.ncbi.nlm.nih.gov/pubmed/22506038.

Weiler, J., Hunziker, J. & Hall, J., 2006. Anti-miRNA oligonucleotides (AMOs): ammunition to target miRNAs implicated in human disease? *Gene therapy*, 13, pp.496–502.

Weilner, S. et al., 2012. Secretion of microvesicular miRNAs in cellular and organismal aging. *Exp Gerontol*. Available at: http://www.ncbi.nlm.nih.gov/pubmed/23283304.

Weilner, S. et al., 2013. Secretion of microvesicular miRNAs in cellular and organismal aging. *Experimental Gerontology*, 48(7), pp.626–633.

Weinstein, R.S. et al., 1998. Inhibition of osteoblastogenesis and promotion of apoptosis of osteoblasts and osteocytes by glucocorticoids. Potential mechanisms of their deleterious effects on bone. *The Journal of clinical investigation*, 102, pp.274–282.

Westin, E.R. et al., 2011. The p53/p21(WAF/CIP) pathway mediates oxidative stress and senescence in dyskeratosis congenita cells with telomerase insufficiency. *Antioxid Redox Signal*, 14(6), pp.985–997. Available at: http://www.ncbi.nlm.nih.gov/pubmed/21087144.

Wieser, M. et al., 2008. hTERT alone immortalizes epithelial cells of renal proximal tubules without changing their functional characteristics. *Am J Physiol Renal Physiol.*, 4, pp.1365–1375.

Van Wijnen, A.J. et al., 2013. MicroRNA functions in osteogenesis and dysfunctions in osteoporosis. *Current osteoporosis reports*, 11(2), pp.72–82.

Wilson, S. & Thorp, B.H., 1998. Estrogen and cancellous bone loss in the fowl. *Calcif Tissue Int*, 62(6), pp.506–511. Available at: http://www.ncbi.nlm.nih.gov/pubmed/9576978.

Winter, J. et al., 2009. Many roads to maturity: microRNA biogenesis pathways and their regulation. *Nature cell biology*, 11, pp.228–234.

Wolbank, S. et al., 2007. Dose-dependent immunomodulatory effect of human stem cells from amniotic membrane: a comparison with human mesenchymal stem cells from adipose tissue. *Tissue Eng*, 13(6), pp.1173–1183. Available at: http://www.ncbi.nlm.nih.gov/pubmed/17518752.

Wolbank, S. et al., 2009. Telomerase immortalized human amnion- and adipose-derived mesenchymal stem cells: maintenance of differentiation and immunomodulatory characteristics. *Tissue Eng Part A*, 15(7), pp.1843–1854. Available at: http://www.ncbi.nlm.nih.gov/pubmed/19125642.

Wu, S. et al., 2011. Implantation of autologous urine derived stem cells expressing vascular endothelial growth factor for potential use in genitourinary reconstruction. *The Journal of urology*, 186(2), pp.640–7.

Xie, L. et al., 2012. The expressions and clinical significances of tissue and serum galectin-3 in pancreatic carcinoma. *J Cancer Res Clin Oncol*, 138(6), pp.1035–1043. Available at: http://www.ncbi.nlm.nih.gov/pubmed/22367363.

Yang, D.G., Liu, L. & Zheng, X.Y., 2008. Cyclin-dependent kinase inhibitor p16(INK4a) and telomerase may co-modulate endothelial progenitor cells senescence. *Ageing Res Rev*, 7(2), pp.137–146. Available at: http://www.ncbi.nlm.nih.gov/pubmed/18343732.

Yang, L. et al., 2012. miR-93/Sp7 function loop mediates osteoblast mineralization. *Journal of Bone and Mineral Research*, 27, pp.1598–1606.

Yang, R.Y., Hsu, D.K. & Liu, F.T., 1996. Expression of galectin-3 modulates T-cell growth and apoptosis. *Proc Natl Acad Sci U S A*, 93(13), pp.6737–6742. Available at: http://www.ncbi.nlm.nih.gov/pubmed/8692888.

Yu, J.M. et al., 2011. Age-related changes in mesenchymal stem cells derived from rhesus macaque bone marrow. *Aging Cell*, 10(1), pp.66–79. Available at: http://www.ncbi.nlm.nih.gov/pubmed/20969724.

Yu, L.G., 2010. Circulating galectin-3 in the bloodstream: An emerging promoter of cancer metastasis. *World J Gastrointest Oncol*, 2(4), pp.177–180. Available at: http://www.ncbi.nlm.nih.gov/pubmed/21160594.

Yu, X., Harris, S.L. & Levine, A.J., 2006. The regulation of exosome secretion: a novel function of the p53 protein. *Cancer Res*, 66(9), pp.4795–4801. Available at: http://www.ncbi.nlm.nih.gov/pubmed/16651434.

Yuan, R. et al., 2009. Aging in inbred strains of mice: Study design and interim report on median lifespans and circulating IGF1 levels. *Aging Cell*, 8, pp.277–287.

Zaharieva, I.T. et al., 2013. Dystromirs as serum biomarkers for monitoring the disease severity in duchenne muscular dystrophy. *PloS one*, 8(11), p.e80263.

Zampetaki, A. et al., 2010. Plasma microRNA profiling reveals loss of endothelial miR-126 and other microRNAs in type 2 diabetes. *Circ Res*, 107(6), pp.810–817. Available at: http://www.ncbi.nlm.nih.gov/pubmed/20651284.

Zeng, Y. et al., 2012. MicroRNA-100 regulates osteogenic differentiation of human adipose-derived mesenchymal stem cells by targeting BMPR2. *FEBS Letters*, 586, pp.2375–2381.

Zeng, Y. & Cullen, B.R., 2004. Structural requirements for pre-microRNA binding and nuclear export by Exportin 5. *Nucleic Acids Research*, 32, pp.4776–4785.

Zhang, J. -f. et al., 2011. MiR-637 maintains the balance between adipocytes and osteoblasts by directly targeting Osterix. *Molecular Biology of the Cell*, 22, pp.3955–3961.

Zhang, Y. et al., 2010. Down-regulation of miR-31 expression in gastric cancer tissues and its clinical significance. *Medical oncology (Northwood, London, England)*, 27, pp.685–689.

Zhang, Y. et al., 2008. Urine derived cells are a potential source for urological tissue reconstruction. *The Journal of urology*, 180(5), pp.2226–33.

Zhao, Q. et al., 2009. Circulating galectin-3 promotes metastasis by modifying MUC1 localization on cancer cell surface. *Cancer Res*, 69(17), pp.6799–6806. Available at: http://www.ncbi.nlm.nih.gov/pubmed/19690136.

Zhao, X. et al., 2013. MicroRNAs regulate bone metabolism. *Journal of bone and mineral metabolism*.

Zhao, Y. & Srivastava, D., 2007. A developmental view of microRNA function. *Trends Biochem Sci*, 32(4), pp.189–197. Available at: http://www.ncbi.nlm.nih.gov/pubmed/17350266.

Zheng, H. et al., 2007. Impact of aging on rat bone marrow-derived stem cell chondrogenesis. *The journals of gerontology. Series A, Biological sciences and medical sciences*, 62(2), pp.136–48. Available at: http://www.ncbi.nlm.nih.gov/pubmed/17339639 [Accessed July 8, 2014].

Zhou, S. et al., 2008. Age-related intrinsic changes in human bone-marrow-derived mesenchymal stem cells and their differentiation to osteoblasts. *Aging Cell*, 7(3), pp.335–343. Available at: http://www.ncbi.nlm.nih.gov/pubmed/18248663.

Zhou, S. et al., 2008. Age-related intrinsic changes in human bone-marrow-derived mesenchymal stem cells and their differentiation to osteoblasts. *Aging cell*, 7(3), pp.335–43. Available at: http://www.pubmedcentral.nih.gov/articlerender.fcgi?artid=2398731&tool=pmcentrez&rendertype=abstract [Accessed June 4, 2014].

Zhou, T. et al., 2012. Generation of human induced pluripotent stem cells from urine samples. *Nature Protocols*, 7(12), pp.2080–9.

Zhou, T. et al., 2011. Generation of induced pluripotent stem cells from urine. *Journal of the American Society of Nephrology□: JASN*, 22(7), pp.1221–8.

Zhu, H. & Fan, G.C., 2011. Extracellular/circulating microRNAs and their potential role in cardiovascular disease. *Am J Cardiovasc Dis*, 1(2), pp.138–149. Available at: http://www.ncbi.nlm.nih.gov/pubmed/22059153.

Appendix A: Abbreviations

A

A	Adenine
aa	Amino acids
AD	Acqua distillata
ALP	Alkaline Phosphatase
ASC	Adipose tissue derived mesenchymal stem cells

B

bp	Base pairs
BMD	Bone mineral density
BMI	Body mass index
BMP2	Bone morphogenic protein 2
BSA	Bovine serum albumin
BV/TV	Bone volume to tissue volume

C

C	Cytosine
C. elegans	Caenorhabditis elegans
Ca^{2+}	Calcium
CIP	Calf intestine alkaline phosphatase
Co.Th.	Cortical thickness

D

DNA	Deoxyribonucleic acid
dNTPs	Deoxynucleotide triphosphates
DXA	Dual-energy X-ray absorptiometry

E

EC	Endothelial cells
EV	Extracellular vesicles
E.coli	Escherichia coli
E.g.	Exempli gratia

ELISA	Enzyme-linked immunoassay
ESCRT	Endosomal sorting complex required for transport

F

FCS	Fetal calf serum
Fzd3	Frizzled 3

G

G	Guanine
Gal3	Galectin-3
GAPDH	Gyceraldehydes-3-phosphate-dehydrogenase
GFP	Green fluorescent protein
GSK-3β	Glycogen synthase kinase 3 β

H

HSC	Hematopoietic stem cells
HUVECs	Human umbilical vein endothelial cells

M

MRNA	Messenger RNA
MiRNA	MicroRNA
miR-31	MicroRNA 31
Min.	Minute
MSC	Mesenchymal stem cells

N

NFW	Nuclease free water
nm	Nanometers

O

OC	Osteocalcin
OD	optical density
ON	Osteonectin

P

PBS	Phosphate buffered saline
PCR	Polymerase chain reaction
PD	Population doubling
PBMCs	Peripheral blood mononucleated cells
PTH	Parathyroid hormone

Q

qPCR	Quantitative real time polymerase chain reaction

R

RNA	Ribonucleic acid
RISC	RNA induced silencing complex
Runx-2	Runt related transcription factor-2

S

SASP	Senescence associated secretory phenotype
SDS	Sodium dodecyl sulphate
SDS-PAGE	SDS polyacrylamide gel electrophoresis
Sec.	Second
siGal	siRNA against Galectin-3

T

T	Thymine
Tr.No.	Trabecular number
Tr.Sp.	Trabecular separation
Tr.Th.	Trabecular thickness

V

V	Volt

W

Wnt	Wingless-type MMTV integration site family

Appendix B: Vector maps

pcDNA 3.1/Hygro(+):

Length: 5597 bp

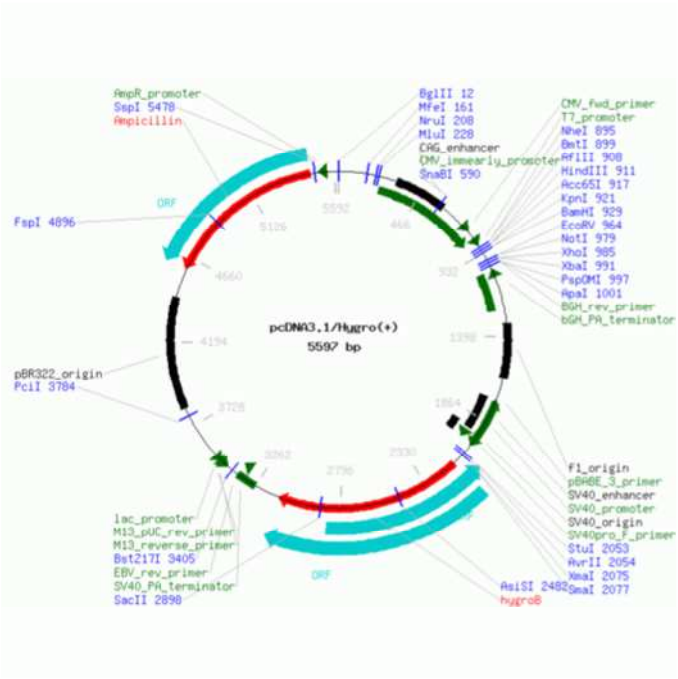

Figure 40: Vector map pcDNA 3.1/Hygro(+)

pCMV6-XL4

Length: 4707 bp

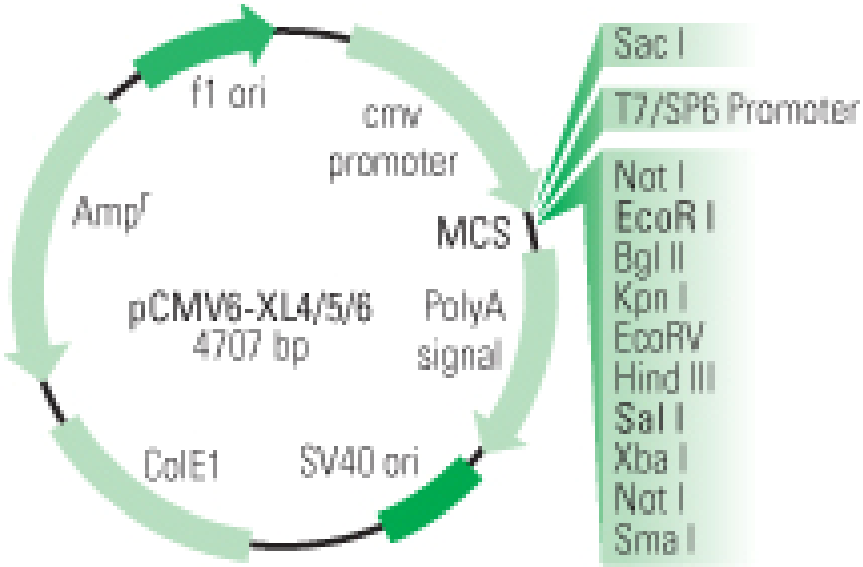

Figure 41: Vector map pCMV6-XL4

pmaxGFP:

Length: 3486 bp

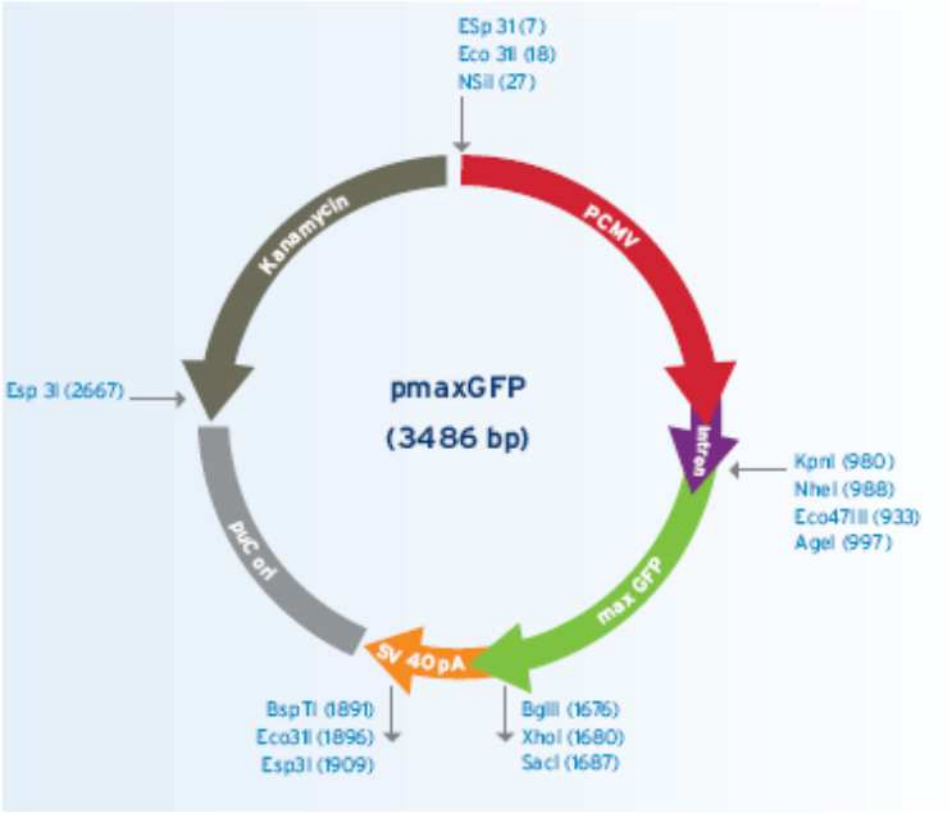

Figure 42: Vector map pmaxGFP

Appendix C: Molecular weight marker

Molecular weight marker for agarose gel electrophoresis:

GeneRuler™ 1kb DNA Ladder, 0,5µg/µl (Fermentas)

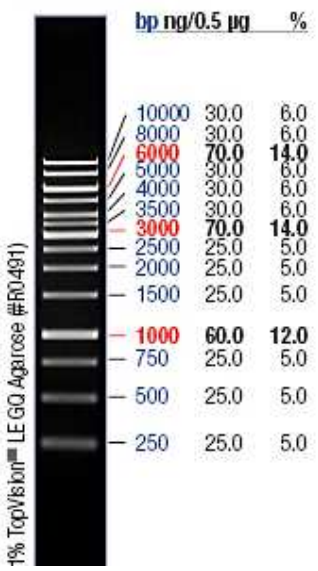

Figure 43: GeneRuler™ 1 kb DNA Ladder, 0,5 µg/lane, 8 cm length gel, 1 X TAE, 7 V/cm, 45 Min

Molecular weight marker for Western blotting:

See Blue ® Plus 2 marker, company: Invitrogen

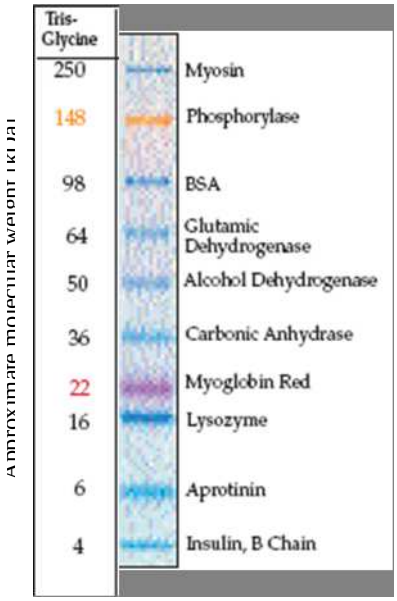

Figure 44: See Blue® Plus 2 marker, Bis-Tris 4-12% gel, Tris-Glycine electrophoresis buffer

Appendix D: Sequencing results

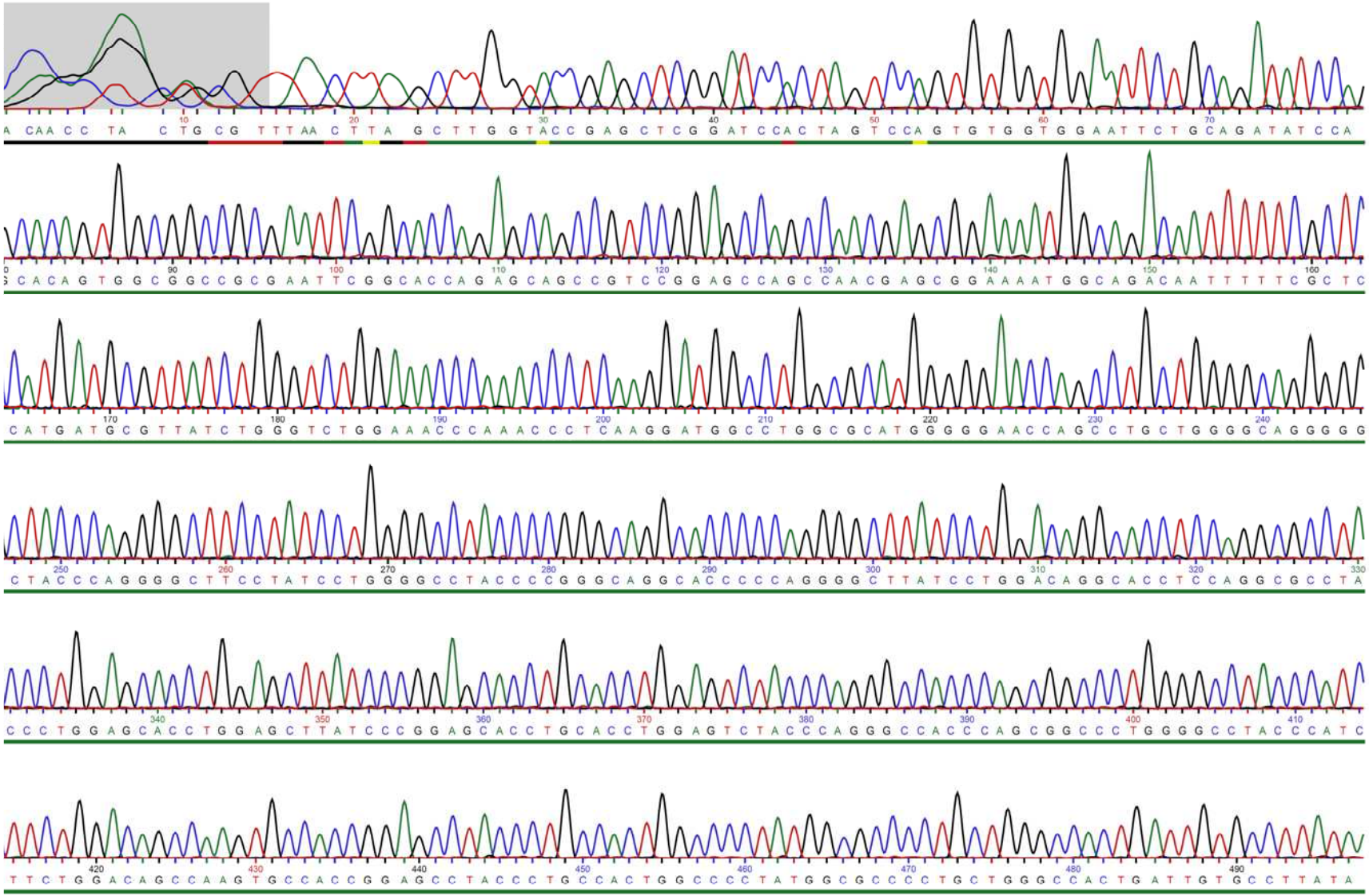

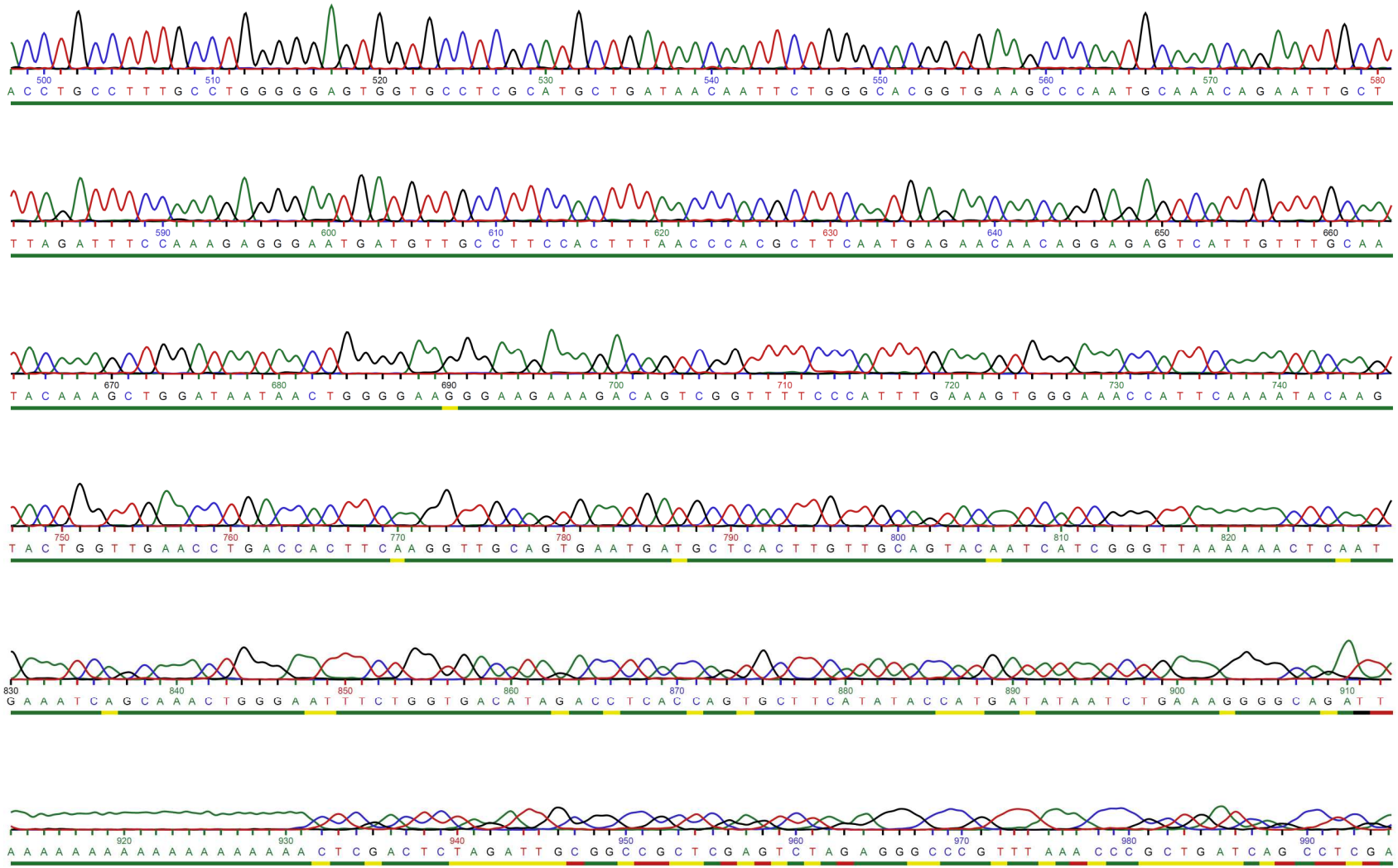
500 510 520 530 540 550 560 570 580
A C C T G C C T T T G C C T G G G G G A G T G G T G C C T C G C A T G C T G A T A A C A A T T C T G G G C A C G G T G A A G C C C A A T G C A A A C A G A A T T G C T
590 600 610 620 630 640 650 660
T T A G A T T T C C A A A G A G G G A A T G A T G T T G C C T T C C A C T T T A A C C C A C G C T T C A A T G A G A A C A A C A G G A G A G T C A T T G T T T G C A A
670 680 690 700 710 720 730 740
T A C A A A G C T G G A T A A T A A C T G G G G A A G G G A A G A A A G A C A G T C G G T T T T C C C A T T T G A A A G T G G G A A A C C A T T C A A A A T A C A A G
750 760 770 780 790 800 810 820
T A C T G G T T G A A C C T G A C C A C T T C A A G G T T G C A G T G A A T G A T G C T C A C T T G T T G C A G T A C A A T C A T C G G G T T A A A A A A C T C A A T
830 840 850 860 870 880 890 900 910
G A A A T C A G C A A A C T G G G A A T T T C T G G T G A C A T A G A C C T C A C C A G T G C T T C A T A T A C C A T G A T A T A A T C T G A A A G G G G C A G A T T
920 930 940 950 960 970 980 990
A A A A A A A A A A A A A A A A A A A A C T C G A C T C T A G A T T G C G G C C G C T C G A G T C T A G A G G G C C C G T T T A A A C C C G C T G A T C A G C C T C G A

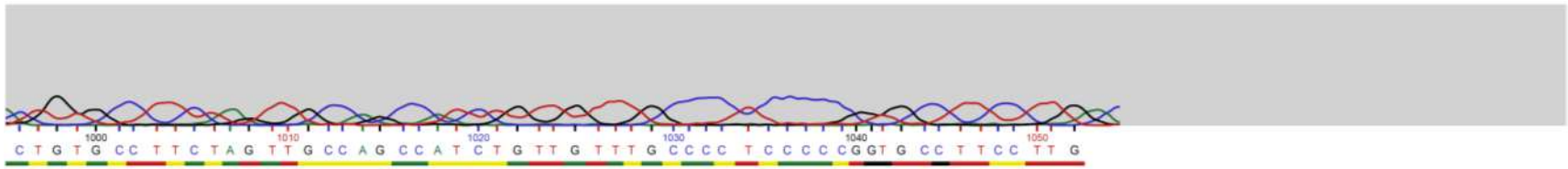

Figure 45: Sequencing result of Galectin-3 pcDNA.3.1 hygro (+) expression construct

Primer: **T7**

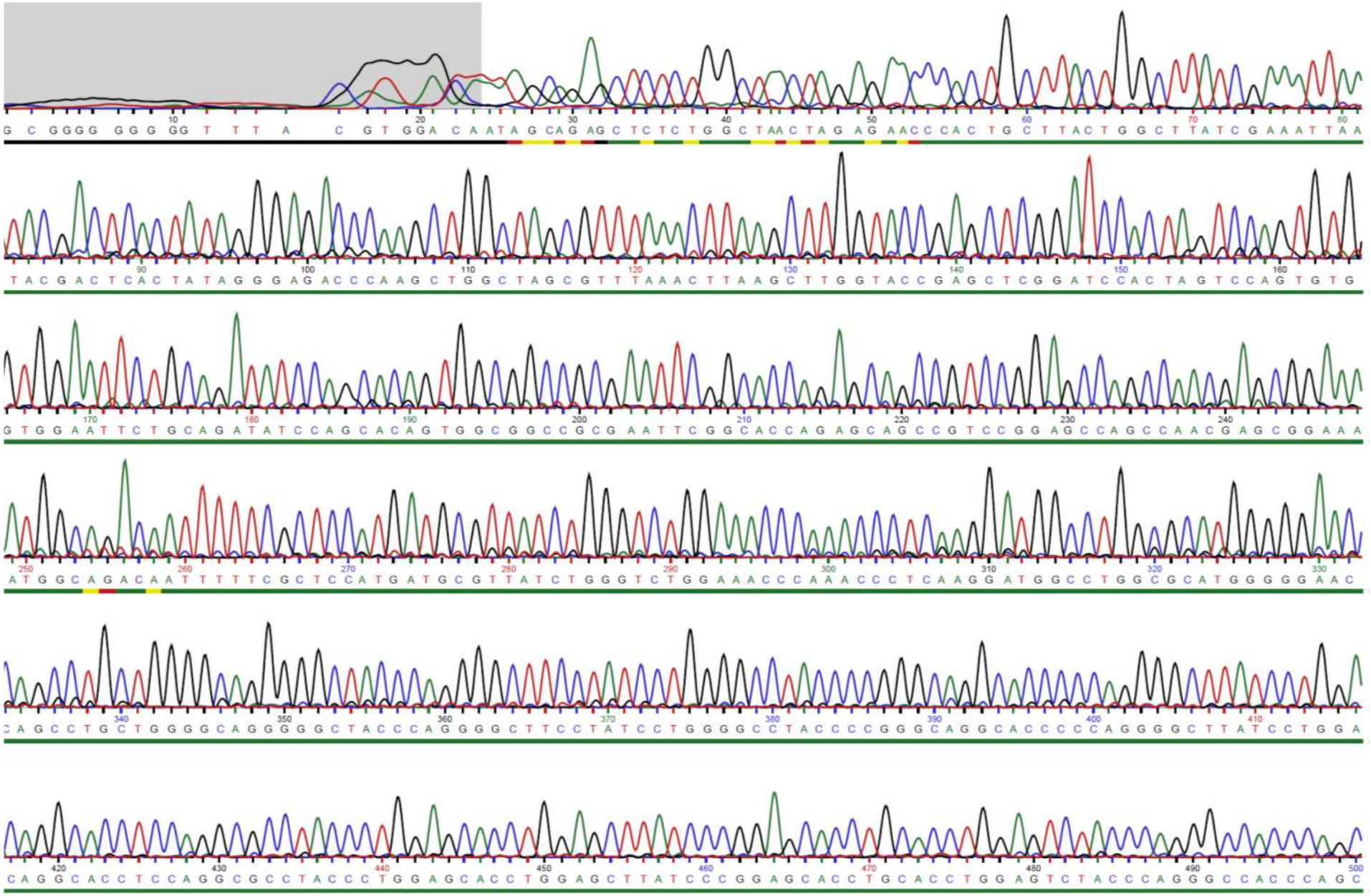

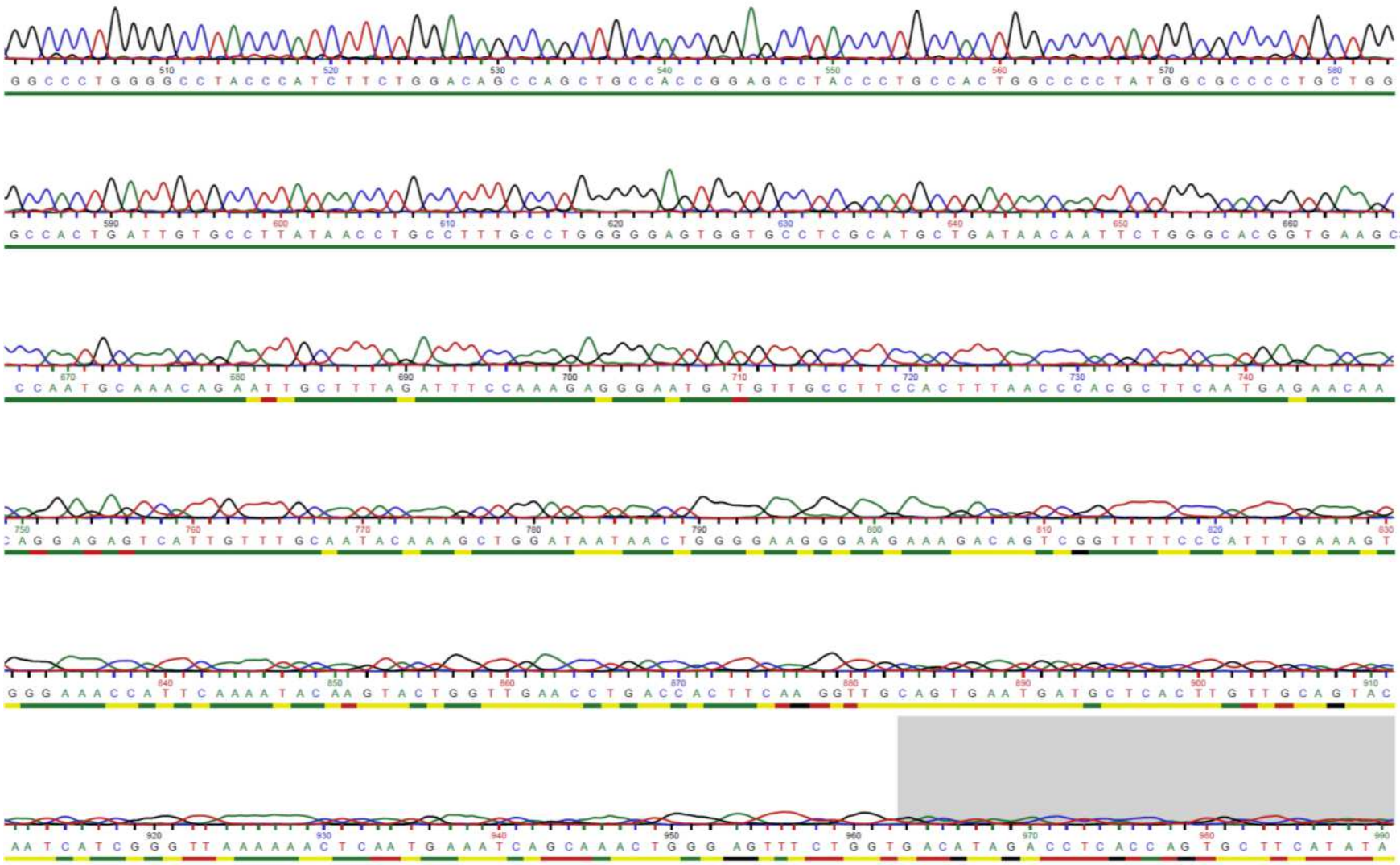

Figure 46: Sequencing result of Serine 96 to Alanine Galectin-3 mutant pcDNA.3.1 hygro (+) expression construct

Primer: **CMV**

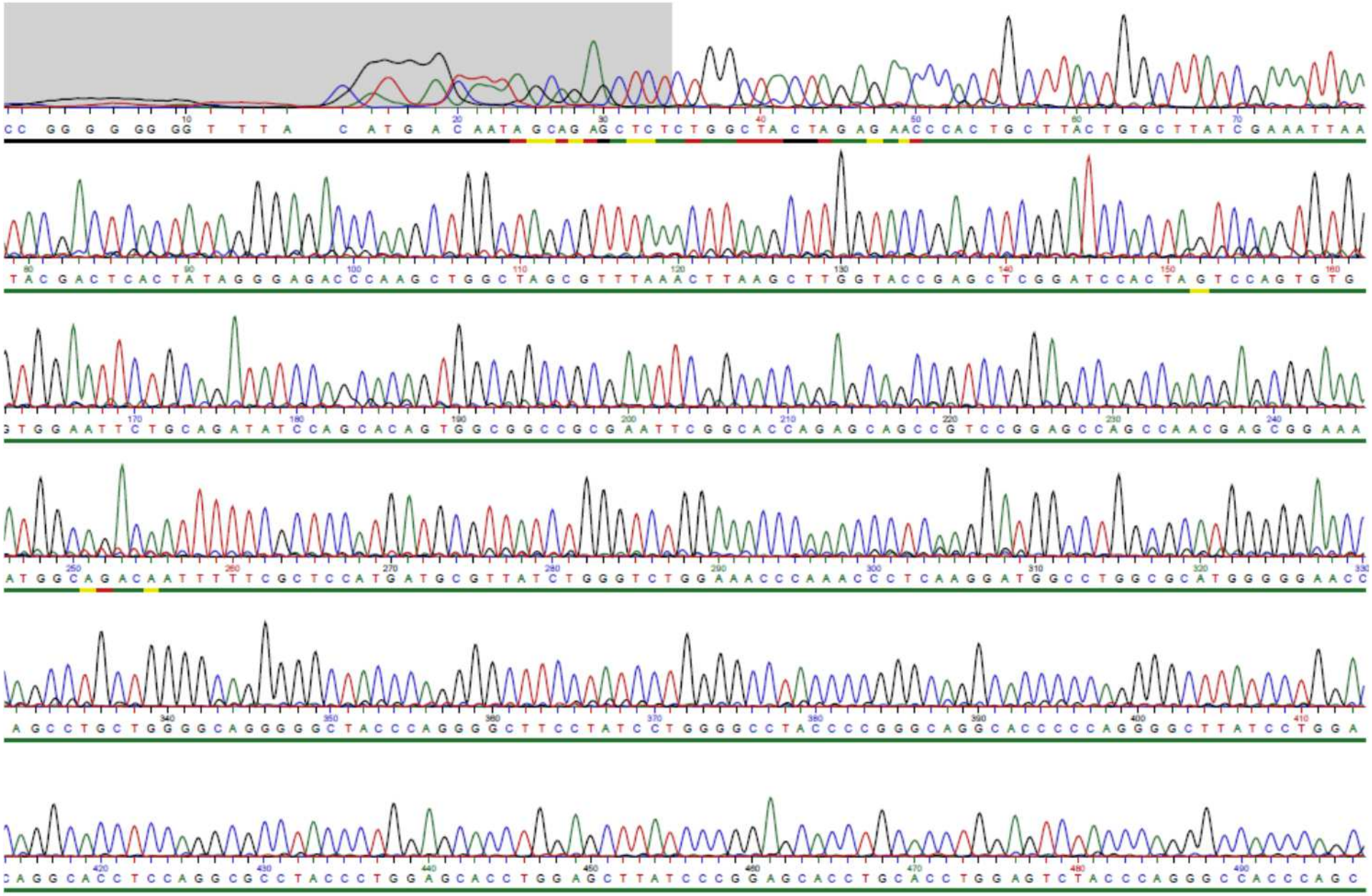

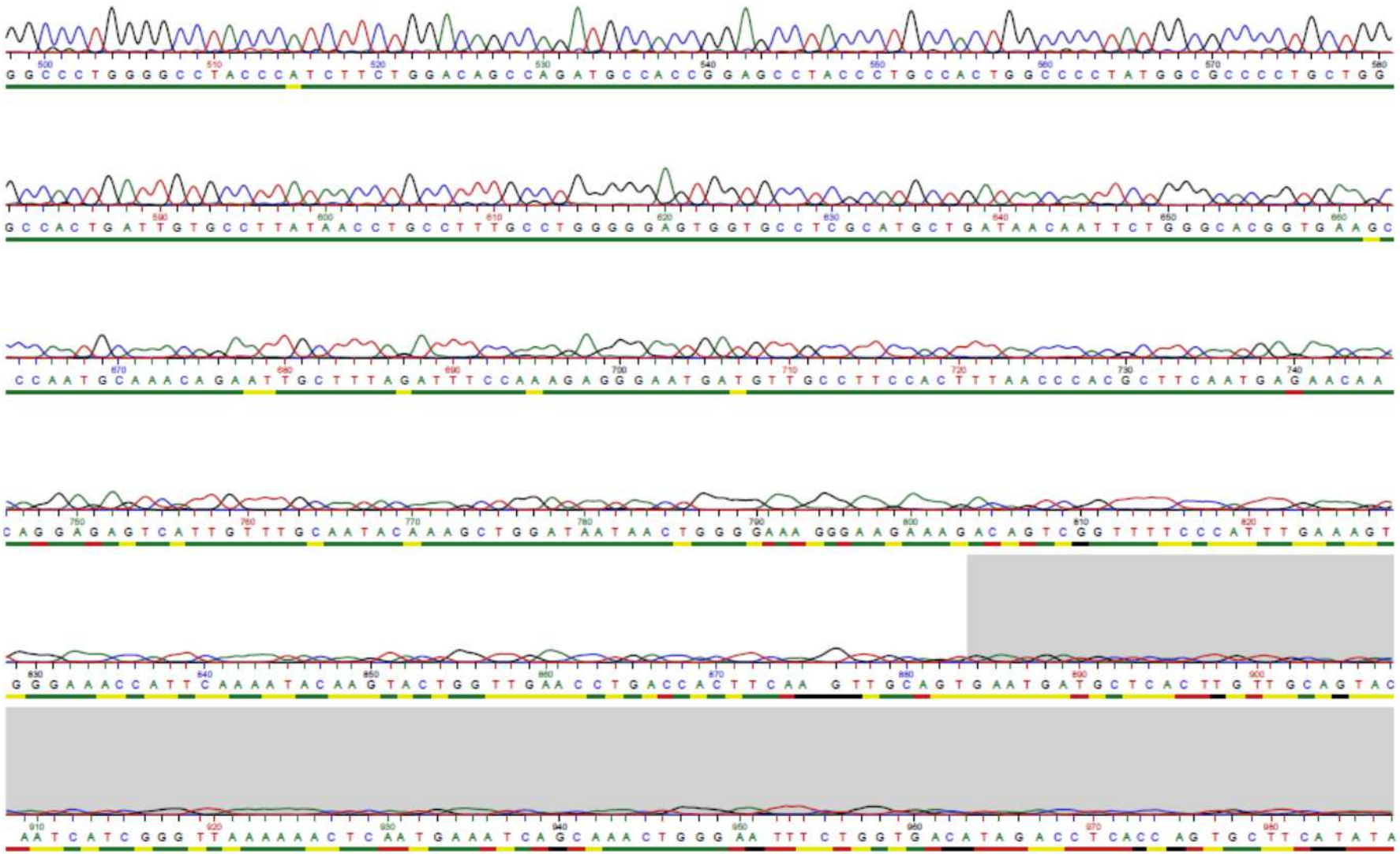

Figure 47: Sequencing result of Serine 96 to Aspartic acid Galectin-3 mutant pcDNA.3.1 hygro (+) expression construct

Primer: **CMV**

Appendix E: Published and accepted manuscripts

Secretion of microvesicular miRNAs in cellular and organismal aging

Sylvia Weilner[a,b] Elisabeth Schraml[a] Heinz Redl[b] Regina Grillari-Voglauer[a,c] and Johannes Grillari,[c]*

[a]BOKU, VIBT, University of Natural Resources and Life Sciences, Department of Biotechnology, Vienna, Austria
[b]Ludwig Boltzmann Institute for Clinical and Experimental Traumatology, Austrian Cluster for Tissue Regeneration, Vienna, Austria
[c]Evercyte GmbH, Vienna, Austria

*Corresponding author at: Muthgasse 18, A-1190 Vienna, Austria. Tel.: + 43 1 47654 6230; fax: + 43 1 3697615. Email: johannes.grillari@boku.ac.at

Abstract

Changes of factors circulating in the systemic environment during human aging have been investigated for a long time. Only recently however, miRNAs have been found to be secreted into the systemic and tissue environments where they are protected from RNAses by either carrier proteins or by being packaged into microvesicles. These miRNAs are then taken up by recipient cells, changing the cellular behavior by the classical miRNA induced silencing of target mRNAs. The origin of circulating miRNAs, however, is in most instances unclear, but senescent cells emerge as a possible source of such secreted miRNAs. Since differences in the circulating miRNAs have been found in a variety of age-associated diseases, and accumulation of senescent cells in the elderly emerges as a possible detrimental factor in aging, it is well conceivable that these miRNAs might contribute to the functional decline observed during aging of organisms.

Therefore, we here give an overview on current knowledge on microvesicular secretion of miRNAs, changes of the systemic and tissue environments during aging

of cells and organisms. Finally, we summarize current knowledge on miRNAs that are found to be specific for age-associated diseases.

Abbreviations: ESCRT, endosomal sorting complex required for transport; ILV, intraluminal vesicles; miRNA, microRNA; mRNA, messenger RNA; MVB, multivesicular bodies; MSC, mesenchymal stem cell; PM, plasma membrane; Rab, Ras-related in brain; RISC, RNA-induced silencing complex; rRNA, ribosomal RNA; SASP, senescence-associated secretory phenotype

Highlights

► miRNAs are secreted within microvesicles. ► Little is known about miRNA secretion in cellular and organismal aging. ► miRNA secretion is altered in age associated diseases.

Introduction

Although much progress has been achieved in aging research over the past decades, the individual heterogeneity of the aging process in humans still remains puzzling and one of the major challenges for our societies. It is therefore mandatory to improve our understanding of the normal aging process, as aging is the substrate on which age-associated diseases will grow. Such a functional understanding on a molecular level might help to design strategies for prevention and therapy of the age-related losses in cell, tissue and organism functionalities.

Here we will summarize current knowledge on the secretion of miRNAs and their potential impact on cellular and organismal aging processes.

Cellular senescence, organismal aging, and the systemic environment

Cellular senescence

Senescent cells have been widely studied as a model system of aging ever since the replicative limit of normal human somatic cells in culture had been described by Hayflick more than four decades ago (Hayflick, 1965). Senescent cells are characterized by a combination of changes in cell behavior, structure and functions including an irreversible growth arrest, resistance to apoptosis and alteration in gene expression (Campisi and d'Adda di Fagagna, 2007). Moreover, a senescent phenotype is also induced by various physico-chemical stressors that induce DNA damage and chromatin disruption as well as by oncogenic signals (Cabrera et al.,

1992; Maruyama et al., 2009). Since senescent cells never re-enter the cell cycle, cellular senescence is suggested to prevent malignant transformation of potentially mutated cells and thus contributes to tumor suppression. In contrast, senescent cells persist within tissues and are not eliminated by apoptosis, and their altered functional profile alters tissue microenvironments in ways that can promote both cancer and aging phenotypes (Krtolica and Campisi, 2002; Rodier et al., 2007). Recently it was shown that premalignant mammary epithelial cells exposed to senescent human fibroblasts in mice irreversibly lose differentiated properties, become invasive and undergo full malignant transformation (Parrinello et al., 2005).

Cellular senescence in vivo

By now, the presence and age-related accumulation of senescent cells in vivo have become well accepted (Campisi and d'Adda di Fagagna, 2007; Campisi and Sedivy, 2009) and it is well established that senescent cells in vivo contribute to age-associated diseases like atherosclerosis (Erusalimsky, 2009; Erusalimsky and Skene, 2009; Minamino and Komuro, 2007). Moreover it was shown that cellular senescence limits the extent of fibrosis following liver damage and underscores the interplay between senescent cells and the tissue microenvironment (Krizhanovsky et al., 2008).

In spite of these variously good and bad effects of cellular senescence, recent studies support the idea that accumulation of senescent cells with the aging of organisms accelerates age-associated diseases and loss of tissue function (Baker et al., 2011). In addition, the reactivation of telomerase in mice delays the onset of loss of tissue functionality (Jaskelioff et al., 2011), and even increases mouse life span (Bernardes de Jesus et al., 2012).

Senescent cells and their microenvironment

Besides the altered functionality of the cells themselves, detrimental effects of senescent cells might be due to an altered secretion phenotype. Indeed, senescent cells develop a senescence-associated secretory phenotype (SASP), where cytokines, extracellular matrix proteins and proteases, as well as other factors that alter the behavior of neighboring cells have been found. The senescent secretome of fibroblasts has been well established by the identification of various secreted factors that contribute to senescence like insulin-like growth factor binding protein 7 (IGFBP7) (Wajapeyee et al., 2008), interleukin-8 (IL-8) receptor binding chemokines (Acosta et al., 2008a, 2008b), IL-6 (Kuilman and Peeper, 2009), but also key

components of the Wnt pathway, insulin-like growth factor 1 (IGF1), transforming growth factor-β (TGFβ), and plasmin (Kuilman and Peeper, 2009). The SASP includes inflammatory cytokines that are thought to drive aging and age-related disease (Finch and Crimmins, 2004). Indeed, some SASP factors, when chronically present, can disrupt tissue structure and differentiation (Parrinello et al., 2005), and others can promote malignant phenotypes in nearby premalignant cells (Bavik et al., 2006; Coppé et al., 2008; Krtolica et al., 2001; Liu and Hornsby, 2007). On the other hand, some SASP factors may be beneficial. For example, some reinforce the senescence growth arrest in an autocrine manner (Acosta et al., 2008b; Kuilman and Peeper, 2009; Kuilman et al., 2008). Others may allow damaged cells to communicate their compromised state (Rodier et al., 2009) in order to stimulate tissue repair or limit pathology (Krizhanovsky et al., 2008).

Senescent cells, the systemic environment and miRNAs

Accumulation of damage in cells and tissues has been accepted as one of the major driving forces of aging and age related diseases (Kirkwood, 2005). Several systemic factors have been found to change with age so far, among them chemokines like chemokine (C–C motif) ligand 11 (CCL11), whose levels correlate with neurogenesis (Villeda et al., 2011), and hormones like the growth hormone (Corpas et al., 1993) as well as the sulfated form of dehydroepiandrosterone (Baulieu, 1996).

In most tissues, there is an age-related decline in stem cell functionality but not a depletion of stem cells. Their ability to self-renew and differentiate is essential for homeostasis and regeneration of tissue and organs. The functionality of these cells declines with age (Rando, 2006). One factor that contributes to this functional decline is the systemic environment of old organisms (Conboy et al., 2005). This decline in functionality might be either due to factors that actively inhibit successful tissue regeneration or due to the absence of promoting factors in the elderly. In contrast, factors present in the systemic environment of young animals promote successful tissue regeneration (Matsumoto et al., 2009).

Such factors are still largely unknown, but some are slowly emerging. Among these are proteins, Wnt, TGF-β (Carlson et al., 2009) and IGF-1 signaling molecules (Mayack et al., 2010) that are suspected to be factors contributing to the functional decline. However, the source of such factors is currently unknown. It can be imagined that any other types of endocrine and inflammatory signaling molecules by their presence or absence might contribute to such an impairment of tissue functionality.

Recently, such “endocrine” functions have been attributed to miRNAs, as miRNAs are not only found intracellularly, but are also detectable outside of the cells, including various body fluids (e.g., serum, plasma, saliva, urine and milk) (Chen et al., 2012), where they circulate unimpeded by RNAses due to association with protective proteins or by being packaged into microvesicles (Viaud et al., 2008). But how are miRNAs generated, and how do they end up in microvesicles?

Microvesicular miRNAs

MicroRNA biogenesis and turnover

MiRNAs comprise a large family of ~ 21-nucleotide-long RNAs that have emerged as key post-transcriptional regulators of gene expression and have revolutionized our comprehension of the post-transcriptional regulation of gene expression. miRNAs are processed from primary transcripts (pri-miRNAs), which are either transcribed by RNA polymerase II from independent genes or represent introns of protein-coding genes. Pri-miRs are then processed to precursor miRNAs (pre-miRs) by the RNA endonucleases Drosha and Pasha and are exported to the cytoplasm where dicer cuts the pre-miRs into the mature miRNA duplexes. The mode of action in silencing depends on the recognition of target mRNAs by single stranded miRNAs that get incorporated into the RNA induced silencing complex (RISC). Binding may depend on the “seed” region consisting of nucleotides 2–8 of the miRNA only. One miRNA is able to regulate up to hundred mRNA targets and therefore seems to orchestrate a large variety of cellular processes similar to transcription factors (Lim et al., 2005; Stefani and Slack, 2008), but also in concert with transcription factors forming feed forward loops (Shalgi et al., 2007).

In contrast to miRNA biogenesis, turnover of miRNAs has received only limited attention to date. It is generally thought that miRNAs represent highly stable molecules and, experimentally using RNA polymerase II inhibitors or depletion of miRNA processing enzymes, have indicated that the half-lives of miRNAs in cell lines or in organs such as liver or heart correspond to many hours or even days (Gatfield et al., 2009; Großhans and Chatterjee, 2010; Krol et al., 2010; van Rooij et al., 2007). miRNA stability is influenced by the 3′ end sequence motif or modification that mark miRNAs for degradation or protect them against exonucleolytic activity, depending on the specific miRNAs and the tissues. In liver cells, a single adenine residue added to

the 3′ end of miR-122 prevents trimming and protects the miRNA against exonucleolytic degradation (Katoh et al., 2009).

Microvesicles

It was long believed that the way of communication between cells and tissues depends to a large extent on protein-based signaling systems exemplified by soluble secreted factors like cytokines, chemokines, neurotransmitter, enzymes and hormones. In principle there were two classes of signaling systems described. One system depends on direct cell–cell contact (also known as juxtacrine signaling) exemplified by the formation of gap junctions, intercellular bridges or synaptic connections. On the other hand a second contact independent system has been described. In the latter case soluble factors are either secreted into the intercellular space where they are able to effect nearby cells (also known as paracrine signaling) or into the circulation where they can cover long distances and affect faraway recipient cells (also known as endocrine signaling).

With the recent discovery of microvesicles a new mechanism of cell communication participating in the contact independent system was proposed. Microvesicles are vesicles which bud from a cellular membrane and contain, depending on their origin, proteins, mRNAs, miRNAs and/or DNA (Mathivanan et al., 2010a). In contrast to the abovementioned and well understood protein-based signaling systems, microvesicles have the advantage that they deliver not only one but multiple (potentially synergistic) messages, whereby they might be able to influence and change the cellular behavior at several stages of protein expression allowing rapid control over targeted cells.

Microvesicles were found to be produced by various cells e.g. by dentritic cells, mast cells, B-cells, T-cells, platelets, but also in neurons, oligodentrocytes, epithelial cells, endothelial cells, embryonic fibroplast cells, microglia, neuroglial cells and several tumor cell lines to name but a few (Hu et al., 2012; Mathivanan et al., 2010a). Furthermore they were also found in several body fluids such as serum, plasma, urine, ocular fluids, amniotic fluid, ascites, broncheoalveolar lavage, cerebrospinal fluid, seminal plasma, breast milk, tears and saliva (Cocucci et al., 2009; Hu et al., 2012; Mathivanan et al., 2010a; Pant et al., 2012; Zhu and Fan, 2011).

The Babylonian language problem

To date, three different types of microvesicles seem to crystallize out of a plethora of names (Table 1): ectosomes, exosomes and apoptotic blebs. In principle they are

distinguished by their size, shape, density, origin as well as protein membrane composition (Mathivanan et al., 2010a; Thery et al., 2009).

However, no commonly accepted nomenclature for microvesicles has yet been established, resulting in a confusing and confounding terminology. For example several names such as microparticles, microvesicles, nanoparticles, shedding microvesicles, ectosomes, exosomes, exosome-like vesicles, dexosomes, texosomes, oncosomes, apoptotic blebs, apoptotic bodies, to name a few were used for a mixed population of microvesicles. Only recently, we have begun to understand that in body fluids different species of vesicles exist and that we need to isolate them based on differences in composition, size or shape as done in a couple of recent reports (Mathivanan et al., 2010b). Therefore, a close look on the performed isolation method of vesicles is highly recommended when reading literature and a commonly agreed terminology would be highly welcome.

Biogenesis of microvesicles

Exosomes

Exosomes are small cup shaped membrane vesicles of 30–100 nm in diameter which originate from the endosomal compartment (Simpson et al., 2008, 2009). The name goes back to 1983, when Pan and Johnstone described microvesicles responsible for externalizing receptors during erythrocyte maturation, which are formed by inward budding of vesicles into the late endosomal compartment (Pan and Johnstone, 1983). Such inward budding of the late endosomal limiting membrane, is by now known to encapsulate cytosolic ‘cargo’ into intraluminal vesicles (ILV) whereby large multivesicular bodies (MVB) are formed (van Niel et al., 2006). MVBs enriched in ILV can either fuse with lysosomes, if their content is intended for degradation or with the plasma membrane whereby ILVs are released into the extracellular space as “exosomes” (Simpson et al., 2009).

Although it is still unknown how the formation of MVBs works on a molecular basis, mechanisms have been proposed.

The first requires the ESCRT (endosomal sorting complex required for transport) machinery to comprise mainly mono ubiquitinated cargo for lysosomal degradation (Babst, 2005). The formation of the second type of MVBs is based on an alternative mechanism involving lipid rafts enriched in sphingolipid ceramide (Trajkovic et al., 2008). The third mechanism was proposed by Rana et al. assuming that proteins are

incorporated by special membrane domains resistant to detergents because of their lipid composition and enriched in tetraspanin (Rana and Zöller, 2011).

Whichever mechanism or combination of mechanisms will be operative, several necessary components for exosome formation have by now been identified, e.g., Ras-related in brain 27a (Rab27a) which influences the size of MVBs (Ostrowski et al., 2010), Rab27b which is controlling the direction of MVBs (Ostrowski et al., 2010), Rab35 which contributes to the docking of exosomes to the plasma membrane (Hsu et al., 2010), hepatocyte growth factor receptor substrate (Hrs) which is necessary for ILV formation (Razi and Futter, 2006), soluble N-ethylmaleimide-sensitive-factor attachment receptors (SNAREs) having a role in the fusion process of MVBs and the cellular plasma membrane (Bobrie et al., 2011) and myosins (Pant et al., 2012).

Ectosomes

Stein and Luzio defined ectosomes as right-side-out-orientated vesicles containing cytosolic components which are released from the surface of polymorphonuclear leucocytes attacked by a complement (Stein and Luzio, 1991). Today the term “ectosomes” is used in a more general way and defined as microvesicles which directly bud from the cellular plasma membrane. Ectosomes are of irregular shape and vary in size between 100 and 1000 µm (Mathivanan et al., 2010a). In contrast to the plasma membrane that they originate from, they expose phospholipid phospatidylserine (PS) on their surface (Zwaal and Schroit, 1997). Furthermore they contain metalloproteinases, which were shown to influence the extracellular space thereby promoting tumor metastasis and invasion, selectins and integrins (Coppé et al., 2008; Mathivanan et al., 2010a).

Ectosomes are continuously produced by many if not all cells in vitro but the stimulating agents, which are able to enhance their production, vary between the different cell types (Sadallah et al., 2011). In addition they contain proteins, mRNAs and miRNAs. The composition depends on cell type, cellular state, and stimulating agent (Cocucci and Meldolesi, 2011).

For the shedding of ectosomes a local disassembly of the cytoskeleton as well as the vesicle abscission process is necessary (Cocucci and Meldolesi, 2011). Therefore increasing cytosolic Ca^{2+} concentrations, activated p38 MAPK Curtis et al. (2009), acid sphingomyelinase (Bianco et al., 2009) and the Rho–ROCK axis (Pinner and Sahai, 2008) as well as the regulative enzymes calpain, a calcium-dependent

cytosolic protease (Miyoshi et al., 1996), flippase, floppase, scramblase and gelosin were shown to be involved (Enjeti et al., 2008).

Apoptotic blebs

Apoptotic blebs are released by cells during the late stage of apoptosis through pinching off from the cellular plasma membrane (Beyer and Pisetsky, 2010). The abscission of apoptotic blebs is performed through the intracellular increase of the hydrostatic pressure followed by the cellular contraction with the aid of actomyosin (Charras et al., 2005, 2008). They are greater than 50 nm in diameter and of irregular shape (Mathivanan et al., 2010a). They contain proteins, mRNAs, miRNAs as well as DNA and expose phosphatidylserine (Théry et al., 2001).

Packaging of miRNAs into vesicles and releasing to the cellular environment

In 2007 Valadi and coworkers were the first to show that miRNAs, besides mRNAs and proteins, are packaged into microvesicles (Valadi et al., 2007). Surprisingly, the miRNA content of microvesicles does not necessarily correspond to the cytosolic repertoire of miRNAs, as the miRNA profile of hepatocellular cancer cells and their microvesicles does differ (Kogure et al., 2011). Only 134 of 424 cellular detectable miRNAs were also found in the exosomes of hepatocellular cancer cells. Of these 134 vesicular miRNAs, 25 were higher and 30 miRNAs were less expressed compared to the intracellular miRNA expression levels. Interestingly, 11 miRNAs were solely identified in microvesicles, strongly suggesting that a specific and controlled packaging mechanism needs to exist (Kogure et al., 2011).

So far, only the first indications on this mechanism are known from studies using human monocytes, where mRNAs, miRNAs and components of the RNA-induced silencing complexes (RISCs) are concentrated in GW-bodies, which are distinct foci within the cytoplasm where many necessary proteins for miRNA gene silencing accumulate. These GW-bodies accumulate at the membrane of late endosomes and MVBs which might facilitate the loading of RNA into exosomes thereby contributing to intercellular transport or post-transcriptional control of intracellular miRNA levels (Gibbings and Voinnet, 2010). Although all components of RISC were found to be localized at the membranes of late endosomes and MVBs, only trinucleotide repeat containing 6 (TNRC6), pre-miRNAs, fragments of pre-miRNA stem loops and miRNAs were found to be enriched within exosomes (Chen et al., 2010; Gibbings et al., 2009). It is known that TNRC6 directly binds to Argonaute (Ago) thereby initiating

the mRNA decay (Chen et al., 2009). A mutant of TNRC6 lacking, in its C-terminus, caused a reduced miRNA activity and the accumulation of miRISC (AGO, miRNA, mRNA and TNRC6) indicating that its C-terminus might be necessary for the dissociation of miRISC (Zekri et al., 2009). Poly(A) binding protein (PABP) which potentially binds at the C-terminus of TNRC6 was shown to bind directly to tumor susceptibility gene 101 (TSG101) thereby providing the link between the RISC complex and exosomes (Schlundt et al., 2009).

Interestingly similar inhibiting effects on miRISC dissociation and reduced levels of exosomal TNRC6 were observed when ESCRT was knocked out, suggesting that ESCRT is necessary for sorting TNRC6 into exosomes (Gibbings et al., 2009). In addition ESCRT II might have a role in sorting miRNA into exosomes since it is able to bind RNA directly (Irion and St Johnston, 2007). Summarizing functional links between miRNAs and the ESCRT machinery, where RISC as well as the ESCRT complex might work together in a common pathway to load miRNAs into exosomes were found.

In contrast, neutral sphingomyelinase 2 (nSMase2), which is regulating the biosynthesis of ceramide, but not the ESCRT machinery is necessary for the production of exosomes and their enclosed miRNAs in human T cells (Mittelbrunn et al., 2011). This indicates that the uptake of miRNAs by the aid of the ESCRT machinery may not be the only miRNA loading mechanism and might depend on the cell type and condition.

Packaging of miRNAs into ectosomes is currently even less understood. It is assumed that ectosomes shed from plasma membrane regions enriched in lipid rafts and that proteins, mRNAs and miRNAs supposed to be packaged into ectosomes, accumulate at these regions (Cocucci and Meldolesi, 2011). However, there are several independent studies indicating that ectosomes mainly contain mRNAs and show lower levels of miRNAs compared to exosomes. Skog et al. determined in 2008 by bioanalyzer that ectosomes originating from glioblastoma cells predominantly contain mRNAs and barely miRNAs (Skog et al., 2008).

In any case, packaging of miRNAs into vesicles is a key step for protecting the miRNAs against the ubiquitous RNAses in the extracellular space, clearly necessary for the stability of extracellular miRNAs, which are reportedly more resistant against extreme temperatures, extreme pHs, prolonged storage and freeze–thaw cycles (Chen et al., 2008; Mitchell et al., 2008).

Microvesicular miRNAs: uptake mechanisms by target cell

After packaging miRNAs into microvesicles, they can be transported through the interstitium or even the peripheral blood (Hunter et al., 2008). Interestingly microvesicular miRNAs were also found in serum (Skog et al., 2008), breast milk (Kosaka et al., 2010) and saliva (Michael et al., 2010). Recently it was shown that engineered microvesicles expressing a neuron specific peptide fused to the surface marker CD107b, are even able to cross the blood–brain barrier and to deliver siRNA to murine neurons, microglia and oligodendrocytes after their intravenous injection (Alvarez-Erviti et al., 2011).

The first RNAs to be proven as functionally delivered and translated by microvesicles were mRNAs originating from mouse mast cells. Their vesicular transport to human mast cells resulted in the expression of three mouse proteins in human cells (Valadi et al., 2007).

In terms of miRNAs, by now several independent studies demonstrate, that functional microvesicular miRNAs are taken up by targeted cells in a sufficient amount to repress the translation of target genes. For example in 2010 the group of Pegtel observed a microvesicular transport of miR-150 from THP-1 to HMEC-1 cells and the consequent silencing of its target c-Myb in the recipient cells (Zhang et al., 2010).

These results also make clear that our current transfection procedures might work so well since they just mimic the natural transfer of RNA and DNA species via microvesicles. But how are the microvesicular miRNAs then taken up by the target cells? There are two mechanisms that have been observed so far.

Plasma membrane fusion

Exosomes can be transferred between dendritic cells (DC) and are taken up by membrane fusion. Through the expression of a GFP-tagged exosomal surface marker protein by the cells of origin, the recipient plasma membrane exhibited fluorescing GFP patterns after exosomal uptake. This is taken as a proof that vesicles are taken up by membrane fusion (Montecalvo et al., 2012).

Endocytosis

By live-cell microscopy Tian et al. observed that microvesicles from rat PC-12 cells can be efficiently taken up by endocytosis and consequently transferred to the perinuclear region probably mediated by the cytoskeleton (Tian et al., 2010). Similarly, we recently observed a reduced uptake of microvesicles originating from

endothelial cells by human mesenchymal stem cells (MSCs), when endocytosis of MSCs was blocked by the overexpression of a dominant negative dynamin construct (K44A) (Schraml et al., unpublished data).

Functional consequences of microvesicular miRNA uptake

Several functions of microvesicles were demonstrated in recent years including effects on cell growth, proliferation, development, differentiation and cell death as well as on coagulation, the immunological processes, viral infections, prion infections and cancer progression (Janowska-Wieczorek et al., 2005; Vlassov et al., 2012; Zhu and Fan, 2011). By now, several examples exist showing that the transfer of miRNAs to target cells results in changes of the target cell behavior strongly indicating that microvesicular miRNAs do indeed make part of the cell to cell communication system. Such examples come mainly from studies in the cancer field, where microvesicles isolated from the highly metastatic gastric cancer cell line AZ-P7a secrete increased levels of the let-7 miRNA family compared to low metastatic AZ-521. Let-7 miRNAs are known to function in tumor suppression since they target the oncogenes RAS and HMGA2. It is assumed, that metastatic AZ-P7a cells release let-7 miRNAs via microvesicles in order to get rid of this tumor suppressive miRNAs and to maintain their own tumorigenesis (Ohshima et al., 2010).

Similarly, several examples in the immune system exist. Unidirectional transfer of miRNA within CD63 positive exosomes, derived from T cells to antigen-presenting cells was shown (Mittelbrunn et al., 2011). Furthermore miRNAs circulating in human breast milk might support the development of the infants' immune system (Kosaka et al., 2010) and miRNA transfer by microvesicles seems also important in viral infection or defense (Pegtel et al., 2010).

Aging, senescence and microvesicular miRNAs

Recently, it has been reported that in both replicative and cell damage-driven senescence, cells increase overall secretion, termed SASP, which is characterized by the secretion of a wide variety of factors, including peptide hormones, as well as the release of microvesicles (Acosta et al., 2008a, 2008b; Campisi, 2008; Campisi and d'Adda di Fagagna, 2007). Of note, this secretory activity and microvesicle formation in senescent cells is also regulated by p53 (Yu et al., 2006).

It is known that miRNAs have some influence on the aging process (Gorospe and Abdelmohsen, 2011; Hackl et al., 2010), but little is known in regard to the systemic environment. So far, several studies have compared samples from young versus healthy elderly individuals of different species from worm to human tissues in regard to the intra-cellular miRNA expression profile. Indeed, different expression levels of several miRNAs have been found with age, e.g., the miR-17-92 cluster (Hackl et al., 2010) let-7 (Peng et al., 2012) and miR-34a (Li et al., 2011). Upregulation of specific miRNAs seems to induce senescence in cells, among them miR-34a in human cells (Christoffersen et al., 2010), miR-203 in melanoma cells (Noguchi et al., 2012) and miR-101, miR-137 and miR-668 in keratinocytes (Shin et al., 2011).

While not much has been published on miRNA secretion during the process of aging, it becomes increasingly clear that miRNAs might be biomarkers of several age-associated diseases. Since several of these diseases seem to be connected to the increase of senescent cells, we summarize in the following the current knowledge on miRNAs that have been found in the serum or plasma of such patients (Fig. 1).

Microvesicular miRNAs in age-associated diseases

The promises of miRNAs as diagnostics and therapeutics are very high even if we are only at the beginning of developing this RNA species into biomedical tools. Still, we are convinced that the need for personalized medicine will boost the search and identification of single miRNAs and/or miRNA signatures characterizing specific patients and thus will help in guiding therapies. This seems an urgent need considering that 90% of the available drugs are efficient only in 40% of the patients.

Cardiovascular disease

Cardiovascular diseases are the primary cause of death and cause for many conditions that severely impact on the quality of life at old age. Endothelial cells seem to counteract this as they secrete microvesicles, containing miR-143 and miR-145 that are taken up by VSMC preventing VSMC de-differentiation (Hergenreider et al., 2012). Injection of vesicles containing both miRNAs into ApoE−/− mice then indeed resulted in reduced atherosclerotic lesion formation (Hergenreider et al., 2012). In addition, it was found that deregulation of both miRNAs contributes to aberrant VSMC plasticity occurring during vascular diseases (Jakob and Landmesser, 2012).

During atherosclerosis, miR-126 has been found to be secreted via apoptotic blebs by endothelial cells. This in turn enhances the production of the anti-inflammatory

chemokine CXCL12 as well as its receptor CXCR4 and promotes the recruitment of endothelial progenitor cells supposedly as a protective mechanism, where the progenitor cells help to maintain tissue homeostasis (Zernecke et al., 2009). The protective role of miR-126 was demonstrated also in vivo when apoptotic blebs enriched in miR-126 originating from human umbilical vein endothelial cells (HUVECs) were injected into high fat diet ApoE−/− mice, resulting in a reduced lesion size and macrophage accumulation through CXCR4 expression (Zernecke et al., 2005).

Counterintuitively, downregulation of miR-126 in the plasma of patients suffering from coronary artery disease has been reported (Fichtlscherer et al., 2011). It might be speculated, that the targeted transport of vesicular miRNAs to the sites of atherosclerotic lesions could cause a reduced detection of freely circulating miRNA levels (Zhu and Fan, 2011).

Moreover microvesicles also protect against progression of chronic kidney damage by inhibiting capillary refraction, glomerulosclerosis, and tubulointerstitial fibrosis by delivering pro-angiogenic miR-126 and miR-296 (Cantaluppi et al., 2012).

In any case, these studies taken together indicate that endothelially derived miRNA carrying microvesicles might contribute to the progression of atherosclerosis.

Neurodegenerative diseases

Alzheimer's disease is the most frequent neurodegenerative disease in humans. It is characterized by the incident of amyloid plaques, which are insoluble extracellular depositions containing amyloid beta peptide (Aβ) (Cai et al., 1993). In Alzheimer's patients, typical exosomal markers were found to be located at sites of amyloid plaques (Rajendran et al., 2006), giving a first indication that microvesicles might be involved in neurodegenerative diseases. Indeed, microvesicles have been shown to be secreted by several neuronal cell types, thereby contributing to the physiology and synaptic plasticity of the central nervous system (Bellingham et al., 2012). It is also of note, that microvesicles have been found to be able to pass the blood–brain barrier and to deliver functional siRNA to neurons (Alvarez-Erviti et al., 2011), which opens up the possibility of cross talk via this usually very tight and selective barrier.

Furthermore, microvesicles from Alzheimer's patients have been found to be enriched in Aβ, its precursor protein APP and some components of γ-secretase and might thereby contribute to the spread of Alzheimer's disease (Vella et al., 2008). Surprisingly, microvesicles isolated from the cerebrospinal fluid of diseased patients

contain around 60 differentially expressed miRNAs compared to healthy controls (Cogswell et al., 2008). So far it is unclear, if these miRNAs might in consequence also be involved in the pathogenic mechanisms of Alzheimer's disease, but the findings again support the importance of microvesicular miRNAs which might serve at least as biomarkers of diseases like Alzheimer's disease.

Diabetes mellitus, type 2 (T2DM)

The number of patients suffering from T2DM is dramatically increasing in developed and developing countries (Zimmet et al., 2001).

First indications of deregulated microvesicular miRNAs in plasma of patients suffering from T2DM compared to healthy age and sex matched controls are available and provide a potential diagnostic signature containing 5 miRNAs, including reduced miR-126 level (Zampetaki et al., 2010).

Interestingly, it was already demonstrated that increased miR-126 level promote vascular endothelial growth factor (VEGF) signaling and has a positive effect on vascular protection (Zernecke et al., 2009). It is known that the monocytes of patients suffering from T2DM exhibit reduced VEGF sensitivity which is contributing to an impaired collateral vessel development. This effect might be due to a reduced microvesicular transport of miR-126 to monocytes (Zampetaki et al., 2010).

Osteoporosis

So far, no study has addressed secreted miRNA in bone disorders of the elderly, however, it is conceivable that miRNAs will be associated with this disease as well, since several miRNAs are known to be regulated during osteogenic differentiation (reviewed by Schraml and Grillari, 2012).

Recently our group could show that microvesicles originating from senescent endothelial cells are taken up by MSCs thereby inhibiting osteogenesis via miR-31 delivery Weilner, Schraml and Grillari, unpublished observations. Additionally, circulating miR-31 levels were also found to be significantly increased in plasma of donors older than 55 as well as in patients suffering from osteopenia compared to donors younger than 25 years Weilner, Schraml and Grillari, unpublished observations.

These results might provide a link between the age associated incidence of reduced bone healing or osteopenia and accumulating senescent endothelial cells with age in vivo.

Concluding remarks

The still quite recent identification of secreted and/or microvesicular miRNAs in the systemic environment, in interstitial fluids or other body fluids poses a formidable tool to identify and use miRNAs as diagnostic signatures. Developing such signatures is of high concern as personalized medication and therapy depends on “personalized” diagnostic tools. The here presented examples of miRNAs that are associated or sometimes even causally linked to age-associated diseases might provide such a toolbox of biomarkers. As small non-coding RNAs have been used in clinical trials by now, miRNAs will certainly also find applications as therapeutic targets. Especially for those miRNAs that circulate in the systemic environment, drug targeting might be comparably easy due to good accessibility in the blood.

Acknowledgments

This work has been supported by the GEN-AU Project 820982 “Non-coding RNAs” and the FWF project P 24498-B20 of the Austrian Science Fund, and CE.R.I.E.S. to JG, as well as grants from the Herzfelder'sche Familienstiftung to RGV.

References

Acosta J.C., O'Loghlen A., Banito A., Guijarro M.V., Augert A., Raguz S., Fumagalli M., Da Costa M., Brown C., Popov N., Takatsu Y., Melamed J., d'Adda di Fagagna F., Bernard D., Hernando E., Gil J. Chemokine signaling via the CXCR2 receptor reinforces senescence. Cell. 2008;133:1006–1018.[PubMed: 18555777]

Acosta J.C., O'Loghlen A., Banito A., Raguz S., Gil J. Control of senescence by CXCR2 and its ligands. Cell Cycle. 2008;7:2956–2959.[PubMed: 18838863]

Alvarez-Erviti L., Seow Y., Yin H., Betts C., Lakhal S., Wood M.J. Delivery of siRNA to the mouse brain by systemic injection of targeted exosomes. Nat. Biotechnol. 2011;29:341–345.[PubMed: 21423189]

Babst M. A protein's final ESCRT. Traffic. 2005;6:2–9.[PubMed: 15569240]

Baker D.J., Wijshake T., Tchkonia T., LeBrasseur N.K., Childs B.G., van de Sluis B., Kirkland J.L., van Deursen J.M. Clearance of p16Ink4a-positive senescent cells delays ageing-associated disorders. Nature. 2011;479:232–236.[PubMed: 22048312]

Baulieu E.E. Dehydroepiandrosterone (DHEA): a fountain of youth? J. Clin. Endocrinol. Metab. 1996;81:3147–3151.[PubMed: 8784058]

Bavik C., Coleman I., Dean J.P., Knudsen B., Plymate S., Nelson P.S. The gene expression program of prostate fibroblast senescence modulates neoplastic epithelial cell proliferation through paracrine mechanisms. Cancer Res. 2006;66:794–802.[PubMed: 16424011]

Bellingham S.A., Guo B.B., Coleman B.M., Hill A.F. Exosomes: vehicles for the transfer of toxic proteins associated with neurodegenerative diseases? Front. Physiol. 2012;3:124.[PubMed: 22563321]

Bernardes de Jesus B., Vera E., Schneeberger K., Tejera A.M., Ayuso E., Bosch F., Blasco M.A. Telomerase gene therapy in adult and old mice delays aging and increases longevity without increasing cancer. EMBO Mol. Med. 2012;4:691–704.[PubMed: 22585399]

Beyer C., Pisetsky D.S. The role of microparticles in the pathogenesis of rheumatic diseases. Nat. Rev. Rheumatol. 2010;6:21–29.[PubMed: 19949432]

Bianco F., Perrotta C., Novellino L., Francolini M., Riganti L., Menna E., Saglietti L., Schuchman E.H., Furlan R., Clementi E., Matteoli M., Verderio C. Acid sphingomyelinase activity triggers microparticle release from glial cells. EMBO J. 2009;28:1043–1054.[PubMed: 19300439]

Bobrie A., Colombo M., Raposo G., Théry C. Exosome secretion: molecular mechanisms and roles in immune responses. Traffic. 2011;12:1659–1668.[PubMed: 21645191]

Cabrera T., Garrido V., Concha A., MartÃn J., Esquivias J., Oliva M.R., Ruiz-Cabello F., Serrano S., Garrido F. HLA molecules in basal cell carcinoma of the skin. Immunobiology. 1992;185:440–452.[PubMed: 1452215]

Cai X.D., Golde T.E., Younkin S.G. Release of excess amyloid beta protein from a mutant amyloid beta protein precursor. Science. 1993;259:514–516.[PubMed: 8424174]

Campisi J. Aging and cancer cell biology, 2008. Aging Cell. 2008;7:281–284.[PubMed: 18331618]

Campisi J., d'Adda di Fagagna F. Cellular senescence: when bad things happen to good cells. Nat. Rev. Mol. Cell Biol. 2007;8:729–740.[PubMed: 17667954]

Campisi J., Sedivy J. How does proliferative homeostasis change with age? What causes it and how does it contribute to aging? J. Gerontol. A Biol. Sci. Med. Sci. 2009;64:164–166.[PubMed: 19228778]

Cantaluppi V., Gatti S., Medica D., Figliolini F., Bruno S., Deregibus M.C., Sordi A., Biancone L., Tetta C., Camussi G. Microvesicles derived from endothelial progenitor cells protect the kidney from ischemia–reperfusion injury by microRNA-dependent reprogramming of resident renal cells. Kidney Int. 2012;82:412–427.[PubMed: 22495296]

Carlson M.E., Conboy M.J., Hsu M., Barchas L., Jeong J., Agrawal A., Mikels A.J., Agrawal S., Schaffer D.V., Conboy I.M. Relative roles of TGF-beta1 and Wnt in the systemic regulation and aging of satellite cell responses. Aging Cell. 2009;8:676–689.[PubMed: 19732043]

Charras G.T., Yarrow J.C., Horton M.A., Mahadevan L., Mitchison T.J. Non-equilibration of hydrostatic pressure in blebbing cells. Nature. 2005;435:365–369.[PubMed: 15902261]

Charras G.T., Coughlin M., Mitchison T.J., Mahadevan L. Life and times of a cellular bleb. Biophys. J. 2008;94:1836–1853.[PubMed: 17921219]

Chen X., Ba Y., Ma L., Cai X., Yin Y., Wang K., Guo J., Zhang Y., Chen J., Guo X., Li Q., Li X., Wang W., Wang J., Jiang X., Xiang Y., Xu C., Zheng P., Zhang J., Li R., Zhang H., Shang X., Gong T., Ning G., Zen K., Zhang C.Y. Characterization of microRNAs in serum: a novel class of biomarkers for diagnosis of cancer and other diseases. Cell Res. 2008;18:997–1006.[PubMed: 18766170]

Chen C.Y., Zheng D., Xia Z., Shyu A.B. Ago-TNRC6 triggers microRNA-mediated decay by promoting two deadenylation steps. Nat. Struct. Mol. Biol. 2009;16:1160–1166.[PubMed: 19838187]

Chen T.S., Lai R.C., Lee M.M., Choo A.B., Lee C.N., Lim S.K. Mesenchymal stem cell secretes microparticles enriched in pre-microRNAs. Nucleic Acids Res. 2010;38:215–224.[PubMed: 19850715]

Chen X., Liang H., Zhang J., Zen K., Zhang C.Y. Horizontal transfer of microRNAs: molecular mechanisms and clinical applications. Protein Cell. 2012;3:28–37.[PubMed: 22314808]

Christoffersen N.R., Shalgi R., Frankel L.B., Leucci E., Lees M., Klausen M., Pilpel Y., Nielsen F.C., Oren M., Lund A.H. p53-independent upregulation of miR-34a during oncogene-induced senescence represses MYC. Cell Death Differ. 2010;17:236–245.[PubMed: 19696787]

Cocucci E., Meldolesi J. Ectosomes. Curr. Biol. 2011;21:R940–R941.[PubMed: 22153157]

Cocucci E., Racchetti G., Meldolesi J. Shedding microvesicles: artefacts no more. Trends Cell Biol. 2009;19:43–51.[PubMed: 19144520]

Cogswell J.P., Ward J., Taylor I.A., Waters M., Shi Y., Cannon B., Kelnar K., Kemppainen J., Brown D., Chen C., Prinjha R.K., Richardson J.C., Saunders A.M., Roses A.D., Richards C.A. Identification of miRNA changes in Alzheimer's disease brain and CSF yields putative biomarkers and insights into disease pathways. J. Alzheimers Dis. 2008;14:27–41.[PubMed: 18525125]

Conboy I., Conboy M., Wagers A., Girma E., Weissman I., Rando T. Rejuvenation of aged progenitor cells by exposure to a young systemic environment. Nature. 2005;433:760–764.[PubMed: 15716955]

Coppé J., Patil C., Rodier F., Sun Y., Muñoz D., Goldstein J., Nelson P., Desprez P., Campisi J. Senescence-associated secretory phenotypes reveal cell-nonautonomous functions of oncogenic RAS and the p53 tumor suppressor. PLoS Biol. 2008;6:2853–2868.[PubMed: 19053174]

Corpas E., Harman S.M., Blackman M.R. Human growth hormone and human aging. Endocr. Rev. 1993;14:20–39.[PubMed: 8491152]

Curtis A.M., Wilkinson P.F., Gui M., Gales T.L., Hu E., Edelberg J.M. p38 mitogen-activated protein kinase targets the production of proinflammatory endothelial microparticles. J. Thromb. Haemost. 2009;7:701–709.[PubMed: 19192109]

Enjeti A.K., Lincz L.F., Seldon M. Microparticles in health and disease. Semin. Thromb. Hemost. 2008;34:683–691.[PubMed: 19085769]

Erusalimsky J.D. Vascular endothelial senescence: from mechanisms to pathophysiology. J. Appl. Physiol. 2009;106:326–332.[PubMed: 19036896]

Erusalimsky J.D., Skene C. Mechanisms of endothelial senescence. Exp. Physiol. 2009;94:299–304.[PubMed: 18931048]

Fichtlscherer S., Zeiher A.M., Dimmeler S. Circulating microRNAs: biomarkers or mediators of cardiovascular diseases? Arterioscler. Thromb. Vasc. Biol. 2011;31:2383–2390.[PubMed: 22011751]

Finch C.E., Crimmins E.M. Inflammatory exposure and historical changes in human life-spans. Science. 2004;305:1736–1739.[PubMed: 15375259]

Gatfield D., Le Martelot G., Vejnar C.E., Gerlach D., Schaad O., Fleury-Olela F., Ruskeepää A.L., Oresic M., Esau C.C., Zdobnov E.M., Schibler U. Integration of microRNA miR-122 in hepatic circadian gene expression. Genes Dev. 2009;23:1313–1326.[PubMed: 19487572]

Gibbings D., Voinnet O. Control of RNA silencing and localization by endolysosomes. Trends Cell Biol. 2010;20:491–501.[PubMed: 20630759]

Gibbings D.J., Ciaudo C., Erhardt M., Voinnet O. Multivesicular bodies associate with components of miRNA effector complexes and modulate miRNA activity. Nat. Cell Biol. 2009;11:1143–1149.[PubMed: 19684575]

Gorospe M., Abdelmohsen K. MicroRegulators come of age in senescence. Trends Genet. 2011;27:233–241.[PubMed: 21592610]

Großhans H., Chatterjee S. MicroRNases and the regulated degradation of mature animal miRNAs. Adv. Exp. Med. Biol. 2010;700:140–155.[PubMed: 21627036]

Hackl M., Brunner S., Fortschegger K., Schreiner C., Micutkova L., Mück C., Laschober G., Lepperdinger G., Sampson N., Berger P., Herndler-Brandstätter D., Wieser M., Kühnel H., Strasser A., Rinnerthaler M., Breitenbach M., Mildner M., Eckhart L., Tschachler E., Trost A., Bauer J., Papak C., Trajanoski Z., Scheideler M., Grillari-Voglauer R., Grubeck-Loebenstein B., Jansen-Dürr P., Grillari J. miR-17, miR-19b, miR-20a and miR-106a are down-regulated in human aging. Aging Cell. 2010;9:291–296.[PubMed: 20089119]

Hayflick L. The limited in vitro lifetime of human diploid cells strains. Exp. Cell Res. 1965;37:614–636.[PubMed: 14315085]

Hergenreider E., Heydt S., Tréguer K., Boettger T., Horrevoets A.J., Zeiher A.M., Scheffer M.P., Frangakis A.S., Yin X., Mayr M., Braun T., Urbich C., Boon R.A., Dimmeler S. Atheroprotective communication between endothelial cells and smooth muscle cells through miRNAs. Nat. Cell Biol. 2012;14:249–256.[PubMed: 22327366]

Hsu C., Morohashi Y., Yoshimura S., Manrique-Hoyos N., Jung S., Lauterbach M.A., Bakhti M., Grønborg M., Möbius W., Rhee J., Barr F.A., Simons M. Regulation of exosome secretion by Rab35 and its GTPase-activating proteins TBC1D10A-C. J. Cell Biol. 2010;189:223–232.[PubMed: 20404108]

Hu G., Drescher K.M., Chen X.M. Exosomal miRNAs: biological properties and therapeutic potential. Front. Genet. 2012;3:56.[PubMed: 22529849]

Hunter M.P., Ismail N., Zhang X., Aguda B.D., Lee E.J., Yu L., Xiao T., Schafer J., Lee M.L., Schmittgen T.D., Nana-Sinkam S.P., Jarjoura D., Marsh C.B. Detection of microRNA expression in human peripheral blood microvesicles. PLoS One. 2008;3:e3694.[PubMed: 19002258]

Irion U., St Johnston D. Bicoid RNA localization requires specific binding of an endosomal sorting complex. Nature. 2007;445:554–558.[PubMed: 17268469]

Jakob P., Landmesser U. Role of microRNAs in stem/progenitor cells and cardiovascular repair. Cardiovasc. Res. 2012;93:614–622.[PubMed: 22135162]

Janowska-Wieczorek A., Wysoczynski M., Kijowski J., Marquez-Curtis L., Machalinski B., Ratajczak J., Ratajczak M.Z. Microvesicles derived from activated platelets induce metastasis and angiogenesis in lung cancer. Int. J. Cancer. 2005;113:752–760.[PubMed: 15499615]

Jaskelioff M., Muller F.L., Paik J.H., Thomas E., Jiang S., Adams A.C., Sahin E., Kost-Alimova M., Protopopov A., Cadinanos J., Horner J.W., Maratos-Flier E., Depinho R.A. Telomerase reactivation reverses tissue degeneration in aged telomerase-deficient mice. Nature. 2011;469:102–106.[PubMed: 21113150]

Katoh T., Sakaguchi Y., Miyauchi K., Suzuki T., Kashiwabara S., Baba T. Selective stabilization of mammalian microRNAs by 3′ adenylation mediated by the cytoplasmic poly(A) polymerase GLD-2. Genes Dev. 2009;23:433–438.[PubMed: 19240131]

Kirkwood T.B. Understanding the odd science of aging. Cell. 2005;120:437–447.[PubMed: 15734677]

Kogure T., Lin W.L., Yan I.K., Braconi C., Patel T. Intercellular nanovesicle-mediated microRNA transfer: a mechanism of environmental modulation of hepatocellular cancer cell growth. Hepatology. 2011;54:1237–1248.[PubMed: 21721029]

Kosaka N., Izumi H., Sekine K., Ochiya T. microRNA as a new immune-regulatory agent in breast milk. Silence. 2010;1:7.[PubMed: 20226005]

Krizhanovsky V., Yon M., Dickins R.A., Hearn S., Simon J., Miething C., Yee H., Zender L., Lowe S.W. Senescence of activated stellate cells limits liver fibrosis. Cell. 2008;134:657–667.[PubMed: 18724938]

Krol J., Busskamp V., Markiewicz I., Stadler M.B., Ribi S., Richter J., Duebel J., Bicker S., Fehling H.J., Schübeler D., Oertner T.G., Schratt G., Bibel M., Roska B., Filipowicz W. Characterizing light-regulated retinal microRNAs reveals rapid turnover as a common property of neuronal microRNAs. Cell. 2010;141:618–631.[PubMed: 20478254]

Krtolica A., Campisi J. Cancer and aging: a model for the cancer promoting effects of the aging stroma. Int. J. Biochem. Cell Biol. 2002;34:1401–1414.[PubMed: 12200035]

Krtolica A., Parrinello S., Lockett S., Desprez P.Y., Campisi J. Senescent fibroblasts promote epithelial cell growth and tumorigenesis: a link between cancer and aging. Proc. Natl. Acad. Sci. U.S.A. 2001;98:12072–12077.[PubMed: 11593017]

Kuilman T., Peeper D.S. Senescence-messaging secretome: SMS-ing cellular stress. Nat. Rev. Cancer. 2009;9:81–94.[PubMed: 19132009]

Kuilman T., Michaloglou C., Vredeveld L.C., Douma S., van Doorn R., Desmet C.J., Aarden L.A., Mooi W.J., Peeper D.S. Oncogene-induced senescence relayed by an interleukin-dependent inflammatory network. Cell. 2008;133:1019–1031.[PubMed: 18555778]

Li X., Khanna A., Li N., Wang E. Circulatory miR34a as an RNAbased, noninvasive biomarker for brain aging. Aging (Albany NY) 2011;3:985–1002.[PubMed: 22064828]

Lim L.P., Lau N.C., Garrett-Engele P., Grimson A., Schelter J.M., Castle J., Bartel D.P., Linsley P.S., Johnson J.M. Microarray analysis shows that some microRNAs downregulate large numbers of target mRNAs. Nature. 2005;433:769–773.[PubMed: 15685193]

Liu D., Hornsby P.J. Senescent human fibroblasts increase the early growth of xenograft tumors via matrix metalloproteinase secretion. Cancer Res. 2007;67:3117–3126.[PubMed: 17409418]

Maruyama J., Naguro I., Takeda K., Ichijo H. Stress-activated MAP kinase cascades in cellular senescence. Curr. Med. Chem. 2009;16:1229–1235.[PubMed: 19355881]

Mathivanan S., Ji H., Simpson R.J. Exosomes: extracellular organelles important in intercellular communication. J. Proteomics. 2010;73:1907–1920.[PubMed: 20601276]

Mathivanan S., Lim J.W., Tauro B.J., Ji H., Moritz R.L., Simpson R.J. Proteomics analysis of A33 immunoaffinity-purified exosomes released from the human colon tumor cell line LIM1215 reveals a tissue-specific protein signature. Mol. Cell. Proteomics. 2010;9:197–208.[PubMed: 19837982]

Matsumoto Y., Adams V., Walther C., Kleinecke C., Brugger P., Linke A., Walther T., Mohr F., Schuler G. Reduced number and function of endothelial progenitor cells in patients with aortic valve stenosis: a novel concept for valvular endothelial cell repair. Eur. Heart J. 2009;30:346–355.[PubMed: 19010796]

Mayack S.R., Shadrach J.L., Kim F.S., Wagers A.J. Systemic signals regulate ageing and rejuvenation of blood stem cell niches. Nature. 2010;463:495–500.[PubMed: 20110993]

Michael A., Bajracharya S.D., Yuen P.S., Zhou H., Star R.A., Illei G.G., Alevizos I. Exosomes from human saliva as a source of microRNA biomarkers. Oral Dis. 2010;16:34–38.[PubMed: 19627513]

Minamino T., Komuro I. Vascular cell senescence: contribution to atherosclerosis. Circ. Res. 2007;100:15–26.[PubMed: 17204661]

Mitchell P.S., Parkin R.K., Kroh E.M., Fritz B.R., Wyman S.K., Pogosova-Agadjanyan E.L., Peterson A., Noteboom J., O'Briant K.C., Allen A., Lin D.W., Urban N., Drescher C.W., Knudsen B.S., Stirewalt D.L., Gentleman R., Vessella R.L., Nelson P.S., Martin D.B., Tewari M. Circulating microRNAs as stable blood-based markers for cancer detection. Proc. Natl. Acad. Sci. U. S. A. 2008;105:10513–10518.[PubMed: 18663219]

Mittelbrunn M., Gutiérrez-Vázquez C., Villarroya-Beltri C., González S., Sánchez-Cabo F., González M., Bernad A., Sánchez-Madrid F. Unidirectional transfer of microRNA-loaded exosomes from T cells to antigen-presenting cells. Nat. Commun. 2011;2:282.[PubMed: 21505438]

Miyoshi H., Umeshita K., Sakon M., Imajoh-Ohmi S., Fujitani K., Gotoh M., Oiki E., Kambayashi J., Monden M. Calpain activation in plasma membrane bleb formation during tert-butyl hydroperoxide-induced rat hepatocyte injury. Gastroenterology. 1996;110:1897–1904.[PubMed: 8964416]

Montecalvo A., Larregina A.T., Shufesky W.J., Stolz D.B., Sullivan M.L., Karlsson J.M., Baty C.J., Gibson G.A., Erdos G., Wang Z., Milosevic J., Tkacheva O.A., Divito S.J., Jordan R., Lyons-Weiler J., Watkins S.C., Morelli A.E. Mechanism of transfer of functional microRNAs between mouse dendritic cells via exosomes. Blood. 2012;119:756–766.[PubMed: 22031862]

Noguchi S., Mori T., Otsuka Y., Yamada N., Yasui Y., Iwasaki J., Kumazaki M., Maruo K., Akao Y. Anti-oncogenic microrna-203 induces senescence by targeting E2F3 in human melanoma cells. J. Biol. Chem. 2012;287:11769–11777.[PubMed: 22354972]

Ohshima K., Inoue K., Fujiwara A., Hatakeyama K., Kanto K., Watanabe Y., Muramatsu K., Fukuda Y., Ogura S., Yamaguchi K., Mochizuki T. Let-7 microRNA family is selectively secreted into the extracellular environment via exosomes in a metastatic gastric cancer cell line. PLoS One. 2010;5:e13247.[PubMed: 20949044]

Ostrowski M., Carmo N.B., Krumeich S., Fanget I., Raposo G., Savina A., Moita C.F., Schauer K., Hume A.N., Freitas R.P., Goud B., Benaroch P., Hacohen N., Fukuda M., Desnos C., Seabra M.C., Darchen F., Amigorena S., Moita L.F., Thery C. Rab27a and Rab27b control different steps of the exosome secretion pathway. Nat. Cell Biol. 2010;12:19–30. (sup pp. 1–13) [PubMed: 19966785]

Pan B.T., Johnstone R.M. Fate of the transferrin receptor during maturation of sheep reticulocytes in vitro: selective externalization of the receptor. Cell. 1983;33:967–978.[PubMed: 6307529]

Pant S., Hilton H., Burczynski M.E. The multifaceted exosome: biogenesis, role in normal and aberrant cellular function, and frontiers for pharmacological and biomarker opportunities. Biochem. Pharmacol. 2012;83:1484–1494.[PubMed: 22230477]

Parrinello S., Coppe J.P., Krtolica A., Campisi J. Stromal–epithelial interactions in aging and cancer: senescent fibroblasts alter epithelial cell differentiation. J. Cell Sci. 2005;118:485–496.[PubMed: 15657080]

Pegtel D.M., Cosmopoulos K., Thorley-Lawson D.A., van Eijndhoven M.A., Hopmans E.S., Lindenberg J.L., de Gruijl T.D., Würdinger T., Middeldorp J.M. Functional delivery of viral miRNAs via exosomes. Proc. Natl. Acad. Sci. U.S.A. 2010;107:6328–6333.[PubMed: 20304794]

Peng C.H., Liu J.H., Woung L.C., Lin T.J., Chiou S.H., Tseng P.C., Du W.Y., Cheng C.K., Hu C.C., Chien K.H., Chen S.J. MicroRNAs and cataracts: correlation among let-7 expression, age and the severity of lens opacity. Br. J. Ophthalmol. 2012;96:747–751.[PubMed: 22334139]

Pinner S., Sahai E. PDK1 regulates cancer cell motility by antagonising inhibition of ROCK1 by RhoE. Nat. Cell Biol. 2008;10:127–137.[PubMed: 18204440]

Rajendran L., Honsho M., Zahn T.R., Keller P., Geiger K.D., Verkade P., Simons K. Alzheimer's disease beta-amyloid peptides are released in association with exosomes. Proc. Natl. Acad. Sci. U.S.A. 2006;103:11172–11177.[PubMed: 16837572]

Rana S., Zöller M. Exosome target cell selection and the importance of exosomal tetraspanins: a hypothesis. Biochem. Soc. Trans. 2011;39:559–562.[PubMed: 21428939]

Rando T. Stem cells, ageing and the quest for immortality. Nature. 2006;441:1080–1086.[PubMed: 16810243]

Razi M., Futter C.E. Distinct roles for Tsg101 and Hrs in multivesicular body formation and inward vesiculation. Mol. Biol. Cell. 2006;17:3469–3483.[PubMed: 16707569]

Rodier F., Campisi J., Bhaumik D. Two faces of p53: aging and tumor suppression. Nucleic Acids Res. 2007;35:7475–7484.[PubMed: 17942417]

Rodier F., Coppé J.P., Patil C.K., Hoeijmakers W.A., Muñoz D.P., Raza S.R., Freund A., Campeau E., Davalos A.R., Campisi J. Persistent DNA damage signalling triggers senescence-associated inflammatory cytokine secretion. Nat. Cell Biol. 2009;11:973–979.[PubMed: 19597488]

Sadallah S., Eken C., Schifferli J.A. Ectosomes as modulators of inflammation and immunity. Clin. Exp. Immunol. 2011;163:26–32.[PubMed: 21039423]

Schlundt A., Sticht J., Piotukh K., Kosslick D., Jahnke N., Keller S., Schuemann M., Krause E., Freund C. Proline-rich sequence recognition: II. Proteomics analysis of Tsg101 ubiquitin-E2-like variant (UEV) interactions. Mol. Cell. Proteomics. 2009;8:2474–2486.[PubMed: 19542561]

Schraml E., Grillari J. From cellular senescence to age-associated diseases: the miRNA connection. Longev. Healthspan. 2012;1(10) (3 December 2012) [PMCID: PMC3922944]

Schraml, E., Weilner, S., Wassermann, K., Wieser, M., Messner, P., Schneider, K., Micutkova, L., Fortschegger, K., Maier, A.B., Westendorp, R., Resch, H., Wolbank, S., Redl, H., Jansen-Dürr, P., Pietschmann, P., Grillari-Voglauer, R., Grillari, J., unpublished data. MicroRNA-31 is secreted by senescent endothelial cells and inhibits osteogenic differentiation of mesenchymal stem cells.

Shalgi R., Lieber D., Oren M., Pilpel Y. Global and local architecture of the mammalian microRNA-transcription factor regulatory network. PLoS Comput. Biol. 2007;3:e131.[PubMed: 17630826]

Shin K.H., Pucar A., Kim R.H., Bae S.D., Chen W., Kang M.K., Park N.H. Identification of senescence-inducing microRNAs in normal human keratinocytes. Int. J. Oncol. 2011;39:1205–1211.[PubMed: 21725593]

Simpson R.J., Jensen S.S., Lim J.W. Proteomic profiling of exosomes: current perspectives. Proteomics. 2008;8:4083–4099.[PubMed: 18780348]

Simpson R.J., Lim J.W., Moritz R.L., Mathivanan S. Exosomes: proteomic insights and diagnostic potential. Expert Rev. Proteomics. 2009;6:267–283.[PubMed: 19489699]

Skog J., WÃ¼rdinger T., van Rijn S., Meijer D.H., Gainche L., Sena-Esteves M., Curry W.T., Jr., Carter B.S., Krichevsky A.M., Breakefield X.O. Glioblastoma microvesicles transport RNA and proteins that promote tumour growth and provide diagnostic biomarkers. Nat. Cell Biol. 2008;10:1470–1476.[PubMed: 19011622]

Stefani G., Slack F.J. Small non-coding RNAs in animal development. Nat. Rev. Mol. Cell Biol. 2008;9:219–230.[PubMed: 18270516]

Stein J.M., Luzio J.P. Ectocytosis caused by sublytic autologous complement attack on human neutrophils. The sorting of endogenous plasma-membrane proteins and lipids into shed vesicles. Biochem. J. 1991;274(Pt 2):381–386.[PubMed: 1848755]

Théry C., Boussac M., Véron P., Ricciardi-Castagnoli P., Raposo G., Garin J., Amigorena S. Proteomic analysis of dendritic cell-derived exosomes: a secreted subcellular compartment distinct from apoptotic vesicles. J. Immunol. 2001;166:7309–7318.[PubMed: 11390481]

Thery C., Ostrowski M., Segura E. Membrane vesicles as conveyors of immune responses. Nat. Rev. Immunol. 2009;9:581–593.[PubMed: 19498381]

Tian T., Wang Y., Wang H., Zhu Z., Xiao Z. Visualizing of the cellular uptake and intracellular trafficking of exosomes by live-cell microscopy. J. Cell. Biochem. 2010;111:488–496.[PubMed: 20533300]

Trajkovic K., Hsu C., Chiantia S., Rajendran L., Wenzel D., Wieland F., Schwille P., Brügger B., Simons M. Ceramide triggers budding of exosome vesicles into multivesicular endosomes. Science. 2008;319:1244–1247.[PubMed: 18309083]

Valadi H., Ekström K., Bossios A., Sjöstrand M., Lee J.J., Lötvall J.O. Exosome-mediated transfer of mRNAs and microRNAs is a novel mechanism of genetic exchange between cells. Nat. Cell Biol. 2007;9:654–659.[PubMed: 17486113]

van Niel G., Porto-Carreiro I., Simoes S., Raposo G. Exosomes: a common pathway for a specialized function. J. Biochem. 2006;140:13–21.[PubMed: 16877764]

van Rooij E., Sutherland L.B., Qi X., Richardson J.A., Hill J., Olson E.N. Control of stress-dependent cardiac growth and gene expression by a microRNA. Science. 2007;316:575–579.[PubMed: 17379774]

Vella L.J., Sharples R.A., Nisbet R.M., Cappai R., Hill A.F. The role of exosomes in the processing of proteins associated with neurodegenerative diseases. Eur. Biophys. J. 2008;37:323–332.[PubMed: 18064447]

Viaud S., Ullrich E., Zitvogel L., Chaput N. Exosomes for the treatment of human malignancies. Horm. Metab. Res. 2008;40:82–88.[PubMed: 18283625]

Villeda S.A., Luo J., Mosher K.I., Zou B., Britschgi M., Bieri G., Stan T.M., Fainberg N., Ding Z., Eggel A., Lucin K.M., Czirr E., Park J.S., Couillard-Després S., Aigner L., Li G., Peskind E.R., Kaye J.A., Quinn J.F., Galasko D.R., Xie X.S., Rando T.A.,

Wyss-Coray T. The ageing systemic milieu negatively regulates neurogenesis and cognitive function. Nature. 2011;477:90–94.[PubMed: 21886162]

Vlassov A.V., Magdaleno S., Setterquist R., Conrad R. Exosomes: current knowledge of their composition, biological functions, and diagnostic and therapeutic potentials. Biochim. Biophys. Acta. 2012;1820:940–948.[PubMed: 22503788]

Wajapeyee N., Serra R.W., Zhu X., Mahalingam M., Green M.R. Oncogenic BRAF induces senescence and apoptosis through pathways mediated by the secreted protein IGFBP7. Cell. 2008;132:363–374.[PubMed: 18267069]

Yu X., Harris S.L., Levine A.J. The regulation of exosome secretion: a novel function of the p53 protein. Cancer Res. 2006;66:4795–4801.[PubMed: 16651434]

Zampetaki A., Kiechl S., Drozdov I., Willeit P., Mayr U., Prokopi M., Mayr A., Weger S., Oberhollenzer F., Bonora E., Shah A., Willeit J., Mayr M. Plasma microRNA profiling reveals loss of endothelial miR-126 and other microRNAs in type 2 diabetes. Circ. Res. 2010;107:810–817.[PubMed: 20651284]

Zekri L., Huntzinger E., Heimstädt S., Izaurralde E. The silencing domain of GW182 interacts with PABPC1 to promote translational repression and degradation of microRNA targets and is required for target release. Mol. Cell. Biol. 2009;29:6220–6231.[PubMed: 19797087]

Zernecke A., Schober A., Bot I., von Hundelshausen P., Liehn E.A., Möpps B., Mericskay M., Gierschik P., Biessen E.A., Weber C. SDF-1alpha/CXCR4 axis is instrumental in neointimal hyperplasia and recruitment of smooth muscle progenitor cells. Circ. Res. 2005;96:784–791.[PubMed: 15761195]

Zernecke A., Bidzhekov K., Noels H., Shagdarsuren E., Gan L., Denecke B., Hristov M., Käppel T., Jahantigh M.N., Lutgens E., Wang S., Olson E.N., Schober A., Weber C. Delivery of microRNA-126 by apoptotic bodies induces CXCL12-dependent vascular protection. Sci. Signal. 2009;2:ra81.[PubMed: 19996457]

Zhang Y., Liu D., Chen X., Li J., Li L., Bian Z., Sun F., Lu J., Yin Y., Cai X., Sun Q., Wang K., Ba Y., Wang Q., Wang D., Yang J., Liu P., Xu T., Yan Q., Zhang J., Zen K., Zhang C.Y. Secreted monocytic miR-150 enhances targeted endothelial cell migration. Mol. Cell. 2010;39:133–144.[PubMed: 20603081]

Zhu H., Fan G.C. Extracellular/circulating microRNAs and their potential role in cardiovascular disease. Am. J. Cardiovasc. Dis. 2011;1:138–149.[PubMed: 22059153]

Zimmet P., Alberti K.G., Shaw J. Global and societal implications of the diabetes epidemic. Nature. 2001;414:782–787.[PubMed: 11742409]

Zwaal R.F., Schroit A.J. Pathophysiologic implications of membrane phospholipid asymmetry in blood cells. Blood. 1997;89:1121–1132.[PubMed: 9028933]

Fig. 1

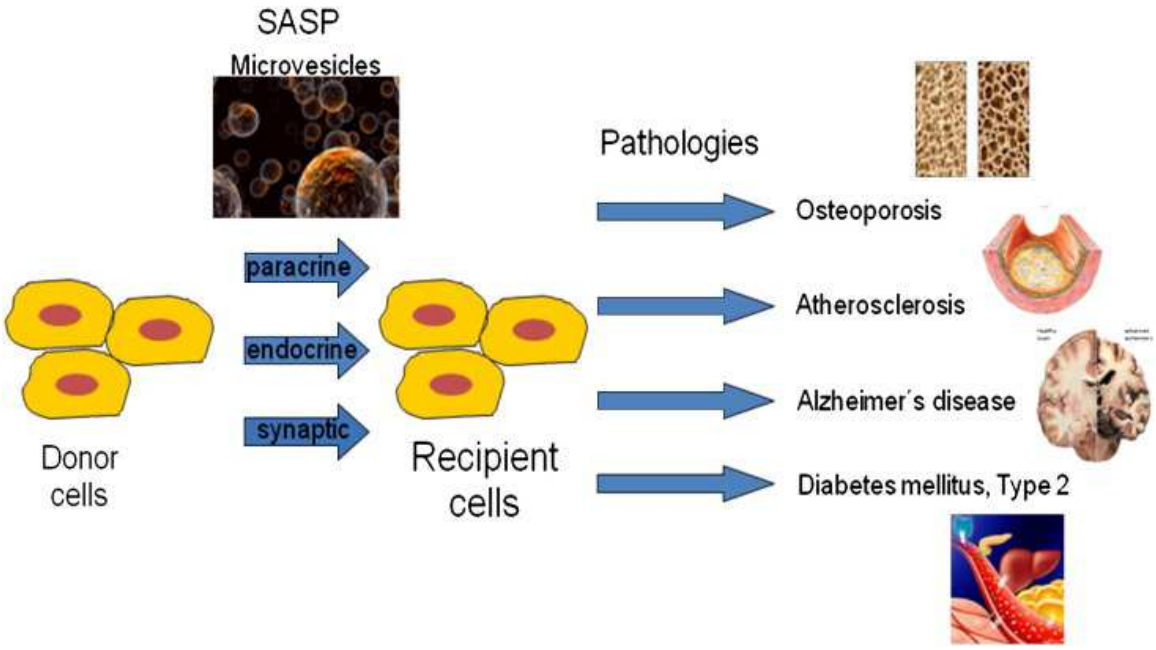

Senescent donor cells contribute to the senescence-associated secretory phenotype (SASP) by secreting not only soluble proteins but also microvesicles either in a paracrine, endocrine or synaptic manner. These vesicles are taken up by recipient cells and may cause or contribute to age related pathologies like osteoporosis, atherosclerosis, Alzheimer's disease or diabetes mellitus, type 2.

Table 1 Comparison of microvesicle types.

	Exosomes	Ectosomes	Apoptotic bodies
Size [nm]	30–100 nm	100–1000 nm	50–5000 nm
Floating density [g/ml]	1.10–1.21	N.K.	1.16–1.28
Sedimentation [g]	100,000–110,000	10,000–100,000	1500–100,000
Cargo	mRNA, miRNA, proteins	mRNA, miRNA, proteins	mRNA, miRNA,rRNA, DNA, proteins
Origin	Late endosomes	Plama membrane	Apoptotic cells
Specific marker	Tetraspanins(CD81, CD63) ESCRT member (Alix, TSG 101)	Integrins, selectins, metalloproteinases	Histones, DNA
Morphology	Cup shaped	Irregularly	Irregularly
Uptake of cargo	Specific	Specific	N.K.
Mode of release	Fusion of MVB with PM	PM blebbing by actomyosin contraction	PM blebbing by actomyosin contraction

The role of MicroRNAs in Cellular Senescence and Age-Related Conditions of Cartilage and Bone

Sylvia Weilner[1,2], Regina Grillari-Voglauer[1,2], Heinz Redl[3,4], Johannes Grillari[1,2,5], Thomas Nau[3,4,6]

[1] Dept. of Biotechnology, VIBT-BOKU, University of Natural Resources and Life Sciences Vienna, Austria

[2] Evercyte GmbH, Vienna, Austria

[3] Ludwig Boltzmann Institute for Experimental and Clinical Traumatology, Vienna, Austria

[4] The Austrian Cluster for Tissue Regeneration, Vienna, Austria

[5] Christian Doppler Laboratory for Biotechnology of Skin Aging

Correspondence to Thomas Nau or Johannes Grillari

[6] IMSART- Institute for Musculoskeletal Analysis Research and Therapy, Vienna, Austria

Correspondence to Thomas Nau or Johannes Grillari

Abstract

Objective: To review the current state of research on microRNAs in age-related diseases in cartilage and bone.

Methods: PubMed searches were conducted using separate terms to retrieve articles on i) the role of microRNAs on aging and tissue degeneration, ii) specific microRNAs that influence cellular and organisms senescence, iii) microRNAs in musculoskeletal age-related conditions, and iv) the diagnostic and therapeutic potential of microRNAs in musculoskeletal age-related conditions.

Results: A constantly increasing number of studies identify microRNAs associated with cellular aging and tissue degeneration. Specifically in regard to frailty, microRNAs have been found to influence the onset and course of age-related musculoskeletal conditions, such as osteoporosis, osteoarthritis and posttraumatic arthritis. Intracellular as well as extracellular microRNAs may be suitable to function as diagnostic biomarkers. Especially, extracellular microRNAs in vesicles may open the doors to novel therapeutic targets.

Conclusion: The available current research data suggest that microRNAs play an important role in orchestrating age-related processes and conditions of the musculoskeletal system. Further research may help to improve the understanding of the complexity of these processes on a cellular as well as extra-cellular level. The option to develop microRNA biomarkers and novel therapeutic agents for the degenerating diseases of bone and cartilage appears to be promising..

Introduction

Musculoskeletal tissue degeneration, in general, is thought to be an age-related process that may be aggravated or accelerated by injury or disease (Loeser, 2010). It has been well studied that the cellular and molecular processes during degeneration can be directly associated with those happening during aging. During the last 3 decades, research has shown that despite many environmental stimuli, genetic factors play an important role in the regulation of aging (Smith-Vikos and Slack, 2012). More recently, the role of microRNAs (miRNAs) as regulators of cellular and organism aging has been increasingly studied (Jung and Suh, 2012; Ukai et al., 2012; Yu et al., 2013). These short and non-coding RNAs regulate the translation of mRNA on a posttranscriptional level, and therefore widely influence the biological cell function . Currently, around 1400 different human miRNAs have been identified and reported in miRBase (http://www.mirbase.org). In terms of aging, a number of miRNAs has been shown to be up- or down regulated, thus they are considered to play a key role as regulators of the aging processes (Grillari and Grillari-Voglauer, 2010)(Weilner et al., 2012).

In this review article, we will first describe the present state of research of miRNAs regarding their function in the aging and tissue degeneration processes. We will then address studies that have focused on specific miRNAs that influence cellular and organism aging. Then we will discuss age-related diseases in cartilage and bone that are already being brought into connection with miRNAs. We will close by exploring the future role of miRNAs in the field of orthopaedic research.

MicroRNAs and cellular aging

Cellular aging

The phenomenon of irreversible cellular growth arrest of normal human cells after serial passaging *in vitro* is called cellular senescence and was first described by Leonard Hayflick and Paul Moorhead in 1961 (Hayflick and Moorhead, 1961). This cell cycle block can be caused by critically short telomeres, DNA damage, oncogenic signaling or cellular stress (Campisi and d'Adda di Fagagna, 2007). Senescent cells are not only characterized by a changed morphology and function but also by an altered intracellular protein expression as well as secretion profile compared to early passage cells (Campisi and d'Adda di Fagagna, 2007). It was long believed that cellular senescence is just an *in vitro* phenomenon, but in recent years an increasing number of papers were published showing not only that senescent cells accumulate with age *in vivo,* as for instance in the skin (Herbig et al., 2006; Jeyapalan et al., 2007), at sites of arteriosclerosis (Erusalimsky, 2009) or in the kidney (Koppelstaetter et al., 2008; Melk et al., 2004), but that they are also contributing to overall organism aging and age-related diseases. For example Baker et al. could demonstrate that the onset of age-related diseases could be delayed by removing $p16^{Ink4a}$ positive cells, a typical marker for cellular senescence, in mice (Baker et al., 2011). Furthermore the influence of senescent cells to organism aging was also shown by reactivating telomerase in mouse tissues that consequently “rejuvenate” (Bernardes de Jesus et al., 2012; Jaskelioff et al., 2011). Today, two pathways are known whose activation can lead to cellular senescence. Firstly, replicative senescence is triggered by exhausted replicative potential due to critical short telomeres (Campisi and d'Adda di Fagagna, 2007). Secondly, stress can induce premature senescence, triggered by cellular stressors like DNA damage or oncogenic signaling (Chen et al., 2008). Whatever the trigger for cellular senescence and thus cellular aging is, so far the two

executors of irreversible cell cycle arrest are either the p21 or the p16 dependent pathways (Campisi and d'Adda di Fagagna, 2007). Both pathways result in the activation of the retinoblastoma cell cycle inhibitory pathways, leading to cell cycle arrest, possibly followed by a permanent growth arrest and cellular senescence (Campisi and d'Adda di Fagagna, 2007).

Interestingly even in musculoskeletal tissue, like bone and cartilage, accumulation of senescent cells with age was observed. Mesenchymal stem cells (MSCs) are the source of bone matrix forming osteoblasts as well as of cartilage matrix forming chondroblasts. Since bone is continuously remodeled, a functionally adequate number of proliferating and differentiating stem cells for tissue regeneration is required. A number of studies reviewed by Kassem and Marie, examining the differences in the number of formed colonies by MSCs isolated from young and aged donors, led to no clear but rather contradictory results (Kassem and Marie, 2011). In summary, a strong decline in the number of MSCs can be observed in early adulthood as soon as skeletal growth is completed, but this reduction does not contribute to the frequently observed reduced bone matrix density in old age (Kassem and Marie, 2011). Although no conclusive reduction in the number of MSCs after the completion of skeletal growth has been observed so far a higher percentage of MSCs, exhibiting typical markers for senescence, such as β-galactosidase, was observed in cultures established from elderly donors, indicating that senescent MSCs accumulate with age *in vivo* and that they might thereby contribute to age related bone-loss (Stenderup et al., 2003) (Zhou et al., 2008). Supportingly a reduced replicative potential of human MSCs (Laschober et al., 2009; Stolzing et al., 2008) and osteoblasts (Kassem et al., 1997), isolated from elderly donors compared to young individuals has been reported.

Furthermore, increased protein levels of senescence inducing p53 and p21 were observed in aged MSCs (Zhou et al., 2008). Interestingly, p53 was shown to have an impact on osteogenesis of MSCs, since p53 knock down resulted in the initiation of osteogenic differentiation (Kim et al., 2012b). Taken together this studies show, that the share of cellular senescent MSCs increases with the population doubling *in vitro* as well as with the donors' age and that these observations go along with a reduced differentiation capacity.

Not only MSCs and osteoblasts were shown to enter cellular senescence. Chondrocytes of aged donors exhibited typical markers of senescence, such as reduced telomere length and enhanced β-galactosidase expression compared to young donors (Martin and Buckwalter, 2003). In addition, transfection of chondrocytes isolated from an elderly donor with the telomerase reverse transcriptase hTERT, resulted not only in elongated telomeres but enabled the transduced cells to undergo 275 more population doublings compared to normal cells, indicating that also chondrocytes are effected by replicative senescence (Martin and Buckwalter, 2003).

Another example for senescent cells and their contribution to the age associated degeneration of cartilage is provided by the group of Hoyland. They hypothesized that the reason for degenerated intervertebral discs might be senescent cells. When comparing cells isolated from non-degenerated and degenerated human tissue, reduced telomere length and replicative potential as well as increased $p16^{INK4A}$ levels and senescence associated β-galactosidase positive cells were detected in cell cultures isolated from degraded tissues. Even when cells isolated from two discs of the same individual were compared, differences in their mean telomere length could be observed, depending on the grade of tissue-degradation. (Le Maitre et al., 2007). Summarizing the data it is clear that cells known to be relevant for the

musculoskeletal tissue are also affected by cellular senescence and that they accumulate with age or in the case of musculoskeletal diseases.

MiRNAs are single stranded 22 – 24 nucleotide small non-protein coding RNAs, which have the ability to inhibit protein translation by recognizing and binding the 3´-untranslated region of specific target mRNAs (Fig. 1). In 1993, the first miRNA lin-4 was discovered in Caenorhabditis elegans (C. elegans) (Lee et al., 1993), and more than 10 years later, higher levels of lin-4 were demonstrated to have a positive effect on the nematodes life span (Boehm and Slack, 2005). MiRNAs do not only target one but up to several hundred mRNAs, resulting in the capability to repress the expression of components within one pathway, but also within related pathways. Thereby they rapidly control cellular processes like differentiation, proliferation, migration, autophagy, apoptosis and senescence (Bartel, 2004; Thum et al., 2008; Zhao and Srivastava, 2007), but they also effect processes of the entire organism, such as aging (Boehm and Slack, 2005). The importance of microRNAs in bone formation of adult organisms is emphasized by several studies showing that deletion of Dicer, a protein necessary for microRNA biogenesis, in either mature osteoblasts or in osteoclasts leads to an high bone mass phenotype in mice (Gaur et al., 2010; Mizoguchi et al., 2010; Sugatani and Hruska, 2009).

How do miRNAs and senescence interact?

Initially, different miRNA expression profiles in replicative senescence were shown for various cell types, such arterial and umbilical vein derived endothelial cells, replicated CD8(+) T cells, renal proximal tubular epithelial cells and skin fibroblasts(Hackl et al., 2010; Maes et al., 2008a; Rippe et al., 2012) , indicating that miRNAs might play an important role in orchestrating replicative senescence. Also in the case of human bone marrow derived mesenchymal stem an altered miRNA expression profile due to cellular senescence was observed. In particular an upregulation of miR-369-5p, miR-29c and let-7f was demonstrated upon replicative senescence (Wagner et al., 2008). However, whether the altered microRNA profile is a consequence of senescence or the altered microRNA profile triggers replicative senescence is still a matter of debate. Another prominent example for miRNAs being differentially regulated during senescence is miR-34a. MiR-34a is highly expressed in senescent fibroblasts (Tazawa et al., 2007), endothelial cells as well as in the heart and spleen of aged mice, suggesting a possible role of miR-34 in cardiovascular diseases (Ito et al., 2010). MiR-34a is known to target the class III histone deacetylase silent information regulator 1 (SIRT1) (Yamakuchi et al., 2008), and expression of miR-34a , which is going along with reduced SIRT1 levels, contributes to a positive p53 activating feedback loop leading to increased p21 levels thereby triggering senescence (Yamakuchi and Lowenstein, 2009). In regard to bone, bone formation and tumorigenesis in bone, miR-34a was observed to decrease in osteosarcoma cell lines (Li et al., 2013; Yan et al., 2012). Furthermore Yan et al. could demonstrate that overexpression of miR-34a inhibits the tumor growth and metastasis of osteosarcoma (Yan et al., 2012). This observation was confirmed by Li et al who demonstrated that miR-34a overexpressing tumor cells exhibit a reduced replicative potential indicating that this microRNA indeed impacts on the cell cycle progression (Liu et al., 2011).

However, whether the observed downregulation of miR-34a in osteosarcoma directly impairs bone formation, or if the enhanced formation is due to a prevention of senescence which would otherwise inhibit tumor formation, is still not clear (He et al., 2009).

MiRNAs are not only differentially regulated during replicative senescence, but also in stress induced premature senescence (Cufi et al., 2012; Li et al., 2009a; Li et al., 2012a). In regard to bone formation, first data on the miRNA expression profiles during senescence show changes in irradiation induced premature senescent osteoblasts as compared to early passage cells (Li et al., 2012b). Another study detected the miR-17-92 cluster, a group of microRNAs which were shown to be downregulated in low level irradiation induced senescent cells (Maes et al., 2008a; Maes et al., 2008b) but upregulated in osteosarcoma cell lines (Baumhoer et al., 2012), indicating that this family of miRNAs might also play a critical role in controlling cell cycle progression during bone formation.

Oxidative stress was shown to induce premature cellular senescence in various cell types (Brandl et al., 2011; Estrada et al., 2013; Feng et al., 2001; Sohal and Orr, 1998; Yudoh et al., 2005). Several studies could demonstrate that miRNAs play an important role in reactive oxygen species induced senescence (Bai et al., 2011; Cufi et al., 2012; Ito et al., 2010; Magenta et al., 2011; Menghini et al., 2009). Magenta et al. reported that miR-200c is upregulated upon H_2O_2-treatment in human endothelial cells, and that miR-200c overexpression alone causes growth arrest, apoptosis and cellular senescence (Magenta et al., 2011). Interestingly Li et al. reported in 2013, that miR-200b/c are usually downregulated in Osteosarcomas and that overexpression of those two microRNAs leads to a reduced proliferation potential indicating that this microRNAs indeed impact on the cell cycle progression of bone relevant cells (Li et al., 2013).

However, whether the altered microRNA profile is a consequence of stress induced senescence or of the afflicted DNA damage remains unclear.

What is the functional consequence of microRNAs in senescence?

Differential expression of miRNAs by cellular senescence in various cell types strongly suggests functional consequences of the differentially expressed miRNAs in the context of cellular aging, for which we present only some examples, predominantly of studies of bone derived tumor cells.

It was shown that miR-21 levels are upregulated in osteosarcoma cell lines, and that its overexpression correlates with enhanced cell invasion and migration of tumor cells by targeting and inhibiting the expression of reversion-inducing-cysteine-rich protein with kazal motifs (RECK), a protein which negatively regulates matrix metalloproteinase-9 (MMP-9) (Ziyan et al., 2011). It was also demonstrated that miR-21 is down regulated in bone marrow derived mesenchymal stem cells (BMSCs) of postmenopausal patients suffering from osteoporosis as well as in ovariectomized mice (Yang et al., 2013). Recombinant expression of miR-21 in murine BMSCs resulted not only in an enhanced osteoblastogenesis *in vitro*, but also in an increased bone formation *in vivo* (Yang et al., 2013).

Another prominent example for miRNAs to play an important role in the process of cellular senescence is miR-24. MiR-24 targets p16 mRNA and is downregulated in replicative senescent diploid fibroblasts (Lal et al., 2008) thereby promoting the p16 dependent senescence pathway. Interestingly, miR-24 was also demonstrated to have a key role in facilitating osteogenesis of MSCs (Goff et al., 2008). Therefore it is tempting to speculate that reduced miR-24 level contribute to the phenomenon of reduced proliferation potential, by facilitating p16 mediated senescence, as well as to decreased osteogenic differentiation potential of MSCs with age.

Not only p16, but also p21 as ultimate effector of senescence was shown to be regulated by miRNAs. Besides miRNAs, such as miR-663, the miR-17-92 cluster is a prominent example for the posttranscriptional repression of p21 via miRNAs (Yi et al., 2012). This cluster was not only reported in the context of cell cycle regulation, but to be deregulated in various cancer cell lines including osteosarcomas as well (Thayanithy et al., 2012).

MicroRNAs and age-related diseases in cartilage and bone

Several studies have revealed that miRNAs play a central role in age-related diseases, such as ***cardiovascular*** diseases, Alzheimer´s disease (AD), arthritis, dementia, cataract, osteoporosis, diabetes and cancer as reviewed by Schraml at el. (Schraml, 2012). Hereafter a few examples of deregulated miRNAs in patients suffering from age-related diseases regarding the bone or the cartilage are given.

Several studies have demonstrated the importance of miRNAs in cartilage development, maintenance and destruction (Karlsen et al., 2014; Song et al., 2013a; Song et al., 2013b; Sumiyoshi et al., 2010; Ukai et al., 2012; Vonk et al., 2014). MiRNA expression profiles were established, using chondrocytes isolated from patients with osteoarthritis and compared to healthy age matched controls. 7 differentially regulated miRNAs were found, among them hsa-miR-483-5p which was higher expressed in cells of osteoarthritic donors (Diaz-Prado et al., 2012). In contrast, hsa-miR-149*, hsa-miR-582-3p, hsa-miR-1227, hsa-miR-634, hsa-miR-576-5p and hsa-miR-641, were down-regulated in osteoarthritis (Diaz-Prado et al., 2012). Interestingly, these miRNAs were shown to influence pathways associated with cartilage function (Diaz-Prado et al., 2012). In this regard it was also shown that SIRT1 levels are deregulated in osteoarthritis chondrocytes. It is known that SIRT1

expression levels are tightly regulated by miRNAs and it was already demonstrated that SIRT1 levels change during the development of osteoarthritis (Diaz-Prado et al., 2012). One example of microRNAs having an influence on SIRT1 expression level is miR-34a. It was shown that miR-34a is upregulated in response to activated p53 and in turn inhibits the expression of SIRT1(Zhao et al., 2010). Interestingly elevated levels of miR-34a contribute to osteoarthritis since silencing of miR-34a in an osteoarthritis rat model resulted in reduced cartilage destruction (Abouheif et al., 2010). A positive effect on the preservation of cartilage in an osteoarthritis mouse model was observed due to miR-146a overexpression (Li et al., 2011). In other age-related diseases, such as osteoporosis or osteopenia, miRNAs were shown to have a high impact as well. Several miRNAs are known to influence the function of bone forming osteoblasts. For example miR-133a was not only shown to inhibit osteoblastogenesis by targeting Runx-2 but it also turned out as a potential biomarker since miR-133a levels are increased in patients suffering from osteoporosis as compared to healthy postmenopausal women (Li et al., 2008; Wang et al., 2012). Another promising candidate for a marker of osteoporosis is miR-214 whose expression negatively correlates with Alkaline phosphatase and Osteocalcin levels, two established bone formation marker (Wang et al., 2013). Furthermore overexpression of miR-138, which was shown to inhibit osteogenic differentiation of mesenchymal stem cells *in vitro*, was also demonstrated to cause an osteoporotic phenotype in mice (Eskildsen et al., 2011). MiR-182 suppresses osteogenesis of bone forming osteoblasts by knocking down its target Forkhead box O1 (FOXO1) (Kim et al., 2012a). On the other hand, some miRNAs are known to enhance the activity of bone resorbing osteoclasts. MiR-148a was shown to increase osteoclastogenesis in vitro by knocking down the expression of V-maf musculoaponeurotic fibrosarcoma oncogene homolog B (MAFB) (Cheng et al.,

2012). Supportingly the group of Luo could demonstrate that inhibiting miR-148a expression *in vivo* leads to impaired osteoclast development and increased bone mass in ovariectomized (OVX) and sham-operated control mice (Cheng et al., 2012). The influence of miRNAs on the development of osteoporosis was demonstrated by a study of Li et al.. MiR-2861 was shown to target histone deacetylase 5 (HDAC5), a protein facilitating Runx2 degradation (Li et al., 2009b). Silencing miR-2861 resulted in reduced osteogenesis in mice (Li et al., 2009b). Furthermore they also reported on a case of two young related individuals, who were suffering from primary osteoporosis due to mutations in miR-2861 (Li et al., 2009b).

Future role of MicroRNAs in musculoskeletal research

The high potential of miRNAs as diagnostic marker or biomarker has been mentioned on several occasions (Kosaka et al., 2010; Mitchell et al., 2008; Miyaki and Asahara, 2012; Pauley and Cha, 2011; Wittmann and Jack, 2010). As the majority of studies focused on the intracellular role of miRNAs, it was only recently, that they were detected in blood and other body fluids as well (Miyaki and Asahara, 2012). Mitchell et al. were the first to describe stable circulating miRNAs in cancer patients (Mitchell et al., 2008), which was consequently supported by findings in other studies (Kosaka et al., 2010; Wittmann and Jack, 2010) In terms of arthritis, Pauley et al. showed an increased expression of miR-146a in peripheral blood mononuclear cells from patients with rheumatoid arthritis (Pauley and Cha, 2011). Murata et al. described miRNAs in the synovial fluid of patients with rheumatoid as well as osteoarthritis. MiR-16, miR-146a, miR-155 and miR-223 in synovial fluid, all were higher in rheumatoid arthritis compared to osteoarthritis (Murata et al., 2010). MiRNAs as biomarker in synovial fluids seem to be a very exciting field for further research. Especially, the development of disease-specific profiling using synovial fluid as well

as peripheral blood could be promising. In terms of osteoarthritis and posttraumatic arthritis, the role of extracellular miRNAs in signaling that directly activates the arthritic process has been mentioned (Wittmann and Jack, 2011). Recently, we have reviewed that extracellular miRNAs are packed in secretory microparticles, such as exosomes, and so being transferable from tissue to tissue (Weilner et al., 2012). Miyaki and Asahara mentioned that extracellular miRNAs may play a similar role as cytokines, and could be considered as paracrine regulatory molecules for cell-cell or tissue-tissue communication (Miyaki and Asahara, 2012). They also pointed out that those mechanisms involving transport and functions of exosomes are not well understood yet and need to be explored further (Miyaki and Asahara, 2012). This may not only lead to new biomarkers, but may open novel therapeutic targets in osteoarthritis as well.

Wang et al. described miR-133a in human peripheral blood monocytes as potential biomarker of postmenopausal osteoporosis (Wang et al., 2012). MiR-133a was significantly upregulated in the low compared to the high bone mineral density group (Wang et al., 2012). They found three potential osteoclast related target genes, CXC11, CXCR3 and SLC39A1 which are known to play an important role in osteogenesis (Wang et al., 2012).

The use of miRNAs as therapeutic agent in joint diseases were demonstrated by Nagata et al.. They injected double-stranded miR-15a into arthritic joints of mice (Nagata et al., 2009) which was subsequently found in synovial cells, but not in chondrocytes (Nagata et al., 2009). MiR-15a lead to increased cell apoptosis by inhibiting the expression of B-cell CLL/lymphoma 2 (BCL-2), which is known to act as an inhibitor of apoptosis which is overexpressed in rheumatoid arthritis synovial fibroblasts (Nagata et al., 2009). Another possible therapeutic target might be represented by miR-210. Shoji et al. reported on the effect of intraarticular injection of

miRNA-210 on partially transected anterior cruciate ligaments in rats (Shoji et al., 2012). They observed healing of the ligament following miRNA-210 injection through enhancement of angiogenesis via upregulation of VEGF and FGF2 (Shoji et al., 2012)

Conclusions

MiRNAs play an important role in the aging process in general and in age-related diseases (Schraml, 2012). Due to the complexity of the spectrum of intracellular as well as extracellular miRNAs, the current understanding in this area is far from being complete. However, the number of reports addressing specific miRNAs and their role in tissue degeneration is constantly increasing. With regard to the age-related diseases of the musculoskeletal system, such as osteoporosis and osteoarthritis, promising studies have been undertaken that contribute to a better understanding of the underlying mechanisms of these conditions. The role of miRNAs as diagnostic biomarkers, tissue specific as well as in body fluids, has gained enormous research interest recently. Furthermore, it has been shown that miRNAs, locally and systemically, may represent future therapeutic agents.

Acknowledgements

Work in the lab of JG is supported by EU-FP7 “Frailomics”, Austrian Science Fund FWF - P24498-B20, CERIES, and the Christian Doppler Research association, the lab of RGV is supported by EU FP7 “Sybil”, Herzfelder’sche Familienstiftung and FWF I-510-B19.

Author Contributions

SW (1),(2): Conception, design and drafting of the article

RGV (2): Revising for important intellectual content

HR (2),(3): Revising for important intellectual content, final approval

JG (2),(3): Revising for important intellectual content, final approval

TN (1),(2),(3): Conception, design, drafting, revising and final approval

TN as the corresponding author also takes responsibility for the integrity of the work as a whole.

Competing Interest Statement:

JG and RGV are co-founder of Evercyte GmbH

References

Abouheif, M.M., Nakasa, T., Shibuya, H., Niimoto, T., Kongcharoensombat, W., and Ochi, M. (2010). Silencing microRNA-34a inhibits chondrocyte apoptosis in a rat osteoarthritis model in vitro. Rheumatology *49*, 2054-2060.

Bai, X.Y., Ma, Y., Ding, R., Fu, B., Shi, S., and Chen, X.M. (2011). miR-335 and miR-34a Promote renal senescence by suppressing mitochondrial antioxidative enzymes. Journal of the American Society of Nephrology : JASN *22*, 1252-1261.

Baker, D.J., Wijshake, T., Tchkonia, T., LeBrasseur, N.K., Childs, B.G., van de Sluis, B., Kirkland, J.L., and van Deursen, J.M. (2011). Clearance of p16Ink4a-positive senescent cells delays ageing-associated disorders. Nature *479*, 232-236.

Bartel, D.P. (2004). MicroRNAs: genomics, biogenesis, mechanism, and function. Cell *116*, 281-297.

Baumhoer, D., Zillmer, S., Unger, K., Rosemann, M., Atkinson, M.J., Irmler, M., Beckers, J., Siggelkow, H., von Luettichau, I., Jundt, G., *et al.* (2012). MicroRNA profiling with correlation to gene expression revealed the oncogenic miR-17-92 cluster to be up-regulated in osteosarcoma. Cancer genetics *205*, 212-219.

Bernardes de Jesus, B., Vera, E., Schneeberger, K., Tejera, A.M., Ayuso, E., Bosch, F., and Blasco, M.A. (2012). Telomerase gene therapy in adult and old mice delays aging and increases longevity without increasing cancer. EMBO molecular medicine *4*, 691-704.

Boehm, M., and Slack, F. (2005). A developmental timing microRNA and its target regulate life span in C. elegans. Science *310*, 1954-1957.

Brandl, A., Hartmann, A., Bechmann, V., Graf, B., Nerlich, M., and Angele, P. (2011). Oxidative stress induces senescence in chondrocytes. Journal of orthopaedic research : official publication of the Orthopaedic Research Society *29*, 1114-1120.

Campisi, J., and d'Adda di Fagagna, F. (2007). Cellular senescence: when bad things happen to good cells. Nature reviews Molecular cell biology *8*, 729-740.

Chen, J., Patschan, S., and Goligorsky, M.S. (2008). Stress-induced premature senescence of endothelial cells. Journal of nephrology *21*, 337-344.

Cheng, P., Chen, C., He, H.B., Hu, R., Zhou, H.D., Xie, H., Zhu, W., Dai, R.C., Wu, X.P., Liao, E.Y., *et al.* (2012). MiR-148a regulates osteoclastogenesis via targeting MAFB. Journal of bone and mineral research : the official journal of the American Society for Bone and Mineral Research.

Cufi, S., Vazquez-Martin, A., Oliveras-Ferraros, C., Quirantes, R., Segura-Carretero, A., Micol, V., Joven, J., Bosch-Barrera, J., Del Barco, S., Martin-Castillo, B.*, et al.* (2012). Metformin lowers the threshold for stress-induced senescence: a role for the microRNA-200 family and miR-205. Cell cycle *11*, 1235-1246.

Diaz-Prado, S., Cicione, C., Muinos-Lopez, E., Hermida-Gomez, T., Oreiro, N., Fernandez-Lopez, C., and Blanco, F.J. (2012). Characterization of microRNA expression profiles in normal and osteoarthritic human chondrocytes. BMC musculoskeletal disorders *13*, 144.

Erusalimsky, J.D. (2009). Vascular endothelial senescence: from mechanisms to pathophysiology. Journal of applied physiology *106*, 326-332.

Eskildsen, T., Taipaleenmaki, H., Stenvang, J., Abdallah, B.M., Ditzel, N., Nossent, A.Y., Bak, M., Kauppinen, S., and Kassem, M. (2011). MicroRNA-138 regulates osteogenic differentiation of human stromal (mesenchymal) stem cells in vivo. Proceedings of the National Academy of Sciences of the United States of America *108*, 6139-6144.

Estrada, J.C., Torres, Y., Benguria, A., Dopazo, A., Roche, E., Carrera-Quintanar, L., Perez, R.A., Enriquez, J.A., Torres, R., Ramirez, J.C.*, et al.* (2013). Human mesenchymal stem cell-replicative senescence and oxidative stress are closely linked to aneuploidy. Cell death & disease *4*, e691.

Feng, R., He, W., and Ochi, H. (2001). A new murine oxidative stress model associated with senescence. Mechanisms of ageing and development *122*, 547-559.

Gaur, T., Hussain, S., Mudhasani, R., Parulkar, I., Colby, J.L., Frederick, D., Kream, B.E., van Wijnen, A.J., Stein, J.L., Stein, G.S.*, et al.* (2010). Dicer inactivation in osteoprogenitor cells compromises fetal survival and bone formation, while excision in differentiated osteoblasts increases bone mass in the adult mouse. Developmental biology *340*, 10-21.

Goff, L.A., Boucher, S., Ricupero, C.L., Fenstermacher, S., Swerdel, M., Chase, L.G., Adams, C.C., Chesnut, J., Lakshmipathy, U., and Hart, R.P. (2008). Differentiating human multipotent mesenchymal stromal cells regulate microRNAs: prediction of microRNA regulation by PDGF during osteogenesis. Experimental hematology *36*, 1354-1369.

Grillari, J., and Grillari-Voglauer, R. (2010). Novel modulators of senescence, aging, and longevity: Small non-coding RNAs enter the stage. Experimental gerontology *45*, 302-311.

Hackl, M., Brunner, S., Fortschegger, K., Schreiner, C., Micutkova, L., Muck, C., Laschober, G.T., Lepperdinger, G., Sampson, N., Berger, P.*, et al.* (2010). miR-17, miR-19b, miR-20a, and miR-106a are down-regulated in human aging. Aging cell *9*, 291-296.

Hayflick, L., and Moorhead, P.S. (1961). The serial cultivation of human diploid cell strains. Experimental cell research *25*, 585-621.

He, C., Xiong, J., Xu, X., Lu, W., Liu, L., Xiao, D., and Wang, D. (2009). Functional elucidation of MiR-34 in osteosarcoma cells and primary tumor samples. Biochemical and biophysical research communications *388*, 35-40.

Herbig, U., Ferreira, M., Condel, L., Carey, D., and Sedivy, J.M. (2006). Cellular senescence in aging primates. Science *311*, 1257.

Ito, T., Yagi, S., and Yamakuchi, M. (2010). MicroRNA-34a regulation of endothelial senescence. Biochemical and biophysical research communications *398*, 735-740.

Jaskelioff, M., Muller, F.L., Paik, J.H., Thomas, E., Jiang, S., Adams, A.C., Sahin, E., Kost-Alimova, M., Protopopov, A., Cadinanos, J.*, et al.* (2011). Telomerase reactivation reverses tissue degeneration in aged telomerase-deficient mice. Nature *469*, 102-106.

Jeyapalan, J.C., Ferreira, M., Sedivy, J.M., and Herbig, U. (2007). Accumulation of senescent cells in mitotic tissue of aging primates. Mechanisms of ageing and development *128*, 36-44.

Jung, H.J., and Suh, Y. (2012). MicroRNA in Aging: From Discovery to Biology. Current genomics *13*, 548-557.

Karlsen, T.A., Jakobsen, R.B., Mikkelsen, T.S., and Brinchmann, J.E. (2014). microRNA-140 targets RALA and regulates chondrogenic differentiation of human mesenchymal stem cells by translational enhancement of SOX9 and ACAN. Stem cells and development *23*, 290-304.

Kassem, M., Ankersen, L., Eriksen, E.F., Clark, B.F., and Rattan, S.I. (1997). Demonstration of cellular aging and senescence in serially passaged long-term cultures of human trabecular osteoblasts. Osteoporosis international : a journal established as result of cooperation between the European Foundation for Osteoporosis and the National Osteoporosis Foundation of the USA *7*, 514-524.

Kassem, M., and Marie, P.J. (2011). Senescence-associated intrinsic mechanisms of osteoblast dysfunctions. Aging cell *10*, 191-197.

Kim, K.M., Park, S.J., Jung, S.H., Kim, E.J., Jogeswar, G., Ajita, J., Rhee, Y., Kim, C.H., and Lim, S.K. (2012a). miR-182 is a negative regulator of osteoblast proliferation,

differentiation, and skeletogenesis through targeting FoxO1. Journal of bone and mineral research : the official journal of the American Society for Bone and Mineral Research *27*, 1669-1679.

Kim, M., Kim, C., Choi, Y.S., Kim, M., Park, C., and Suh, Y. (2012b). Age-related alterations in mesenchymal stem cells related to shift in differentiation from osteogenic to adipogenic potential: implication to age-associated bone diseases and defects. Mechanisms of ageing and development *133*, 215-225.

Koppelstaetter, C., Schratzberger, G., Perco, P., Hofer, J., Mark, W., Ollinger, R., Oberbauer, R., Schwarz, C., Mitterbauer, C., Kainz, A.*, et al.* (2008). Markers of cellular senescence in zero hour biopsies predict outcome in renal transplantation. Aging cell *7*, 491-497.

Kosaka, N., Iguchi, H., and Ochiya, T. (2010). Circulating microRNA in body fluid: a new potential biomarker for cancer diagnosis and prognosis. Cancer science *101*, 2087-2092.

Lal, A., Kim, H.H., Abdelmohsen, K., Kuwano, Y., Pullmann, R., Jr., Srikantan, S., Subrahmanyam, R., Martindale, J.L., Yang, X., Ahmed, F.*, et al.* (2008). p16(INK4a) translation suppressed by miR-24. PloS one *3*, e1864.

Laschober, G.T., Brunauer, R., Jamnig, A., Fehrer, C., Greiderer, B., and Lepperdinger, G. (2009). Leptin receptor/CD295 is upregulated on primary human mesenchymal stem cells of advancing biological age and distinctly marks the subpopulation of dying cells. Experimental gerontology *44*, 57-62.

Le Maitre, C.L., Freemont, A.J., and Hoyland, J.A. (2007). Accelerated cellular senescence in degenerate intervertebral discs: a possible role in the pathogenesis of intervertebral disc degeneration. Arthritis research & therapy *9*, R45.

Lee, R.C., Feinbaum, R.L., and Ambros, V. (1993). The C. elegans heterochronic gene lin-4 encodes small RNAs with antisense complementarity to lin-14. Cell *75*, 843-854.

Li, G., Luna, C., Qiu, J., Epstein, D.L., and Gonzalez, P. (2009a). Alterations in microRNA expression in stress-induced cellular senescence. Mechanisms of ageing and development *130*, 731-741.

Li, H., Xie, H., Liu, W., Hu, R., Huang, B., Tan, Y.F., Xu, K., Sheng, Z.F., Zhou, H.D., Wu, X.P.*, et al.* (2009b). A novel microRNA targeting HDAC5 regulates osteoblast differentiation in mice and contributes to primary osteoporosis in humans. The Journal of clinical investigation *119*, 3666-3677.

Li, X., Gibson, G., Kim, J.S., Kroin, J., Xu, S., van Wijnen, A.J., and Im, H.J. (2011). MicroRNA-146a is linked to pain-related pathophysiology of osteoarthritis. Gene *480*, 34-41.

Li, X.H., Ha, C.T., Fu, D., and Xiao, M. (2012a). Micro-RNA30c negatively regulates REDD1 expression in human hematopoietic and osteoblast cells after gamma-irradiation. PloS one *7*, e48700.

Li, X.H., Ha, C.T., Fu, D., and Xiao, M. (2012b). REDD1 protects osteoblast cells from gamma radiation-induced premature senescence. PloS one *7*, e36604.

Li, Y., Zhang, J., Zhang, L., Si, M., Yin, H., and Li, J. (2013). Diallyl trisulfide inhibits proliferation, invasion and angiogenesis of osteosarcoma cells by switching on suppressor microRNAs and inactivating of Notch-1 signaling. Carcinogenesis *34*, 1601-1610.

Li, Z., Hassan, M.Q., Volinia, S., van Wijnen, A.J., Stein, J.L., Croce, C.M., Lian, J.B., and Stein, G.S. (2008). A microRNA signature for a BMP2-induced osteoblast lineage commitment program. Proceedings of the National Academy of Sciences of the United States of America *105*, 13906-13911.

Liu, C., Kelnar, K., Liu, B., Chen, X., Calhoun-Davis, T., Li, H., Patrawala, L., Yan, H., Jeter, C., Honorio, S.*, et al.* (2011). The microRNA miR-34a inhibits prostate cancer stem cells and metastasis by directly repressing CD44. Nature medicine *17*, 211-215.

Loeser, R.F. (2010). Age-related changes in the musculoskeletal system and the development of osteoarthritis. Clinics in geriatric medicine *26*, 371-386.

Maes, O.C., An, J., Sarojini, H., and Wang, E. (2008a). Murine microRNAs implicated in liver functions and aging process. Mechanisms of ageing and development *129*, 534-541.

Maes, O.C., An, J., Sarojini, H., Wu, H., and Wang, E. (2008b). Changes in MicroRNA expression patterns in human fibroblasts after low-LET radiation. Journal of cellular biochemistry *105*, 824-834.

Magenta, A., Cencioni, C., Fasanaro, P., Zaccagnini, G., Greco, S., Sarra-Ferraris, G., Antonini, A., Martelli, F., and Capogrossi, M.C. (2011). miR-200c is upregulated by oxidative stress and induces endothelial cell apoptosis and senescence via ZEB1 inhibition. Cell death and differentiation *18*, 1628-1639.

Martin, J.A., and Buckwalter, J.A. (2003). The role of chondrocyte senescence in the pathogenesis of osteoarthritis and in limiting cartilage repair. The Journal of bone and joint surgery American volume *85-A Suppl 2*, 106-110.

Melk, A., Schmidt, B.M., Takeuchi, O., Sawitzki, B., Rayner, D.C., and Halloran, P.F. (2004). Expression of p16INK4a and other cell cycle regulator and senescence associated genes in aging human kidney. Kidney international *65*, 510-520.

Menghini, R., Casagrande, V., Cardellini, M., Martelli, E., Terrinoni, A., Amati, F., Vasa-Nicotera, M., Ippoliti, A., Novelli, G., Melino, G.*, et al.* (2009). MicroRNA 217 modulates endothelial cell senescence via silent information regulator 1. Circulation *120*, 1524-1532.

Mitchell, P.S., Parkin, R.K., Kroh, E.M., Fritz, B.R., Wyman, S.K., Pogosova-Agadjanyan, E.L., Peterson, A., Noteboom, J., O'Briant, K.C., Allen, A.*, et al.* (2008). Circulating microRNAs as stable blood-based markers for cancer detection. Proceedings of the National Academy of Sciences of the United States of America *105*, 10513-10518.

Miyaki, S., and Asahara, H. (2012). Macro view of microRNA function in osteoarthritis. Nature reviews Rheumatology *8*, 543-552.

Mizoguchi, F., Izu, Y., Hayata, T., Hemmi, H., Nakashima, K., Nakamura, T., Kato, S., Miyasaka, N., Ezura, Y., and Noda, M. (2010). Osteoclast-specific Dicer gene deficiency suppresses osteoclastic bone resorption. Journal of cellular biochemistry *109*, 866-875.

Murata, K., Yoshitomi, H., Tanida, S., Ishikawa, M., Nishitani, K., Ito, H., and Nakamura, T. (2010). Plasma and synovial fluid microRNAs as potential biomarkers of rheumatoid arthritis and osteoarthritis. Arthritis research & therapy *12*, R86.

Nagata, Y., Nakasa, T., Mochizuki, Y., Ishikawa, M., Miyaki, S., Shibuya, H., Yamasaki, K., Adachi, N., Asahara, H., and Ochi, M. (2009). Induction of apoptosis in the synovium of mice with autoantibody-mediated arthritis by the intraarticular injection of double-stranded MicroRNA-15a. Arthritis and rheumatism *60*, 2677-2683.

Pauley, K.M., and Cha, S. (2011). miRNA-146a in rheumatoid arthritis: a new therapeutic strategy. Immunotherapy *3*, 829-831.

Rippe, C., Blimline, M., Magerko, K.A., Lawson, B.R., LaRocca, T.J., Donato, A.J., and Seals, D.R. (2012). MicroRNA changes in human arterial endothelial cells with senescence: relation to apoptosis, eNOS and inflammation. Experimental gerontology *47*, 45-51.

Schraml, E., Grillari, J. (2012). From cellular senescence to age-associated diseases: the miRNA connection. Longevity and healthspan *1*.

Shoji, T., Nakasa, T., Yamasaki, K., Kodama, A., Miyaki, S., Niimoto, T., Okuhara, A., Kamei, N., Adachi, N., and Ochi, M. (2012). The effect of intra-articular injection of

microRNA-210 on ligament healing in a rat model. The American journal of sports medicine *40*, 2470-2478.

Smith-Vikos, T., and Slack, F.J. (2012). MicroRNAs and their roles in aging. J Cell Sci *125*, 7-17.

Sohal, R.S., and Orr, W.C. (1998). Role of oxidative stress in senescence. Aging (Milano) *10*, 149-151.

Song, J., Kim, D., Chun, C.H., and Jin, E.J. (2013a). MicroRNA-9 regulates survival of chondroblasts and cartilage integrity by targeting protogenin. Cell communication and signaling : CCS *11*, 66.

Song, J., Lee, M., Kim, D., Han, J., Chun, C.H., and Jin, E.J. (2013b). MicroRNA-181b regulates articular chondrocytes differentiation and cartilage integrity. Biochemical and biophysical research communications *431*, 210-214.

Stenderup, K., Justesen, J., Clausen, C., and Kassem, M. (2003). Aging is associated with decreased maximal life span and accelerated senescence of bone marrow stromal cells. Bone *33*, 919-926.

Stolzing, A., Jones, E., McGonagle, D., and Scutt, A. (2008). Age-related changes in human bone marrow-derived mesenchymal stem cells: consequences for cell therapies. Mechanisms of ageing and development *129*, 163-173.

Sugatani, T., and Hruska, K.A. (2009). Impaired micro-RNA pathways diminish osteoclast differentiation and function. The Journal of biological chemistry *284*, 4667-4678.

Sumiyoshi, K., Kubota, S., Ohgawara, T., Kawata, K., Nishida, T., Shimo, T., Yamashiro, T., and Takigawa, M. (2010). Identification of miR-1 as a micro RNA that supports late-stage differentiation of growth cartilage cells. Biochemical and biophysical research communications *402*, 286-290.

Tazawa, H., Tsuchiya, N., Izumiya, M., and Nakagama, H. (2007). Tumor-suppressive miR-34a induces senescence-like growth arrest through modulation of the E2F pathway in human colon cancer cells. Proceedings of the National Academy of Sciences of the United States of America *104*, 15472-15477.

Thayanithy, V., Sarver, A.L., Kartha, R.V., Li, L., Angstadt, A.Y., Breen, M., Steer, C.J., Modiano, J.F., and Subramanian, S. (2012). Perturbation of 14q32 miRNAs-cMYC gene network in osteosarcoma. Bone *50*, 171-181.

Thum, T., Catalucci, D., and Bauersachs, J. (2008). MicroRNAs: novel regulators in cardiac development and disease. Cardiovascular research *79*, 562-570.

Ukai, T., Sato, M., Akutsu, H., Umezawa, A., and Mochida, J. (2012). MicroRNA-199a-3p, microRNA-193b, and microRNA-320c are correlated to aging and regulate human cartilage metabolism. Journal of orthopaedic research : official publication of the Orthopaedic Research Society *30*, 1915-1922.

Vonk, L.A., Kragten, A.H., Dhert, W.J., Saris, D.B., and Creemers, L.B. (2014). Overexpression of hsa-miR-148a promotes cartilage production and inhibits cartilage degradation by osteoarthritic chondrocytes. Osteoarthritis and cartilage / OARS, Osteoarthritis Research Society *22*, 145-153.

Wagner, W., Horn, P., Castoldi, M., Diehlmann, A., Bork, S., Saffrich, R., Benes, V., Blake, J., Pfister, S., Eckstein, V.*, et al.* (2008). Replicative senescence of mesenchymal stem cells: a continuous and organized process. PloS one *3*, e2213.

Wang, X., Guo, B., Li, Q., Peng, J., Yang, Z., Wang, A., Li, D., Hou, Z., Lv, K., Kan, G.*, et al.* (2013). miR-214 targets ATF4 to inhibit bone formation. Nature medicine *19*, 93-100.

Wang, Y., Li, L., Moore, B.T., Peng, X.H., Fang, X., Lappe, J.M., Recker, R.R., and Xiao, P. (2012). MiR-133a in human circulating monocytes: a potential biomarker associated with postmenopausal osteoporosis. PloS one *7*, e34641.

Weilner, S., Schraml, E., Redl, H., Grillari-Voglauer, R., and Grillari, J. (2012). Secretion of microvesicular miRNAs in cellular and organismal aging. Experimental gerontology.

Wittmann, J., and Jack, H.M. (2010). Serum microRNAs as powerful cancer biomarkers. Biochimica et biophysica acta *1806*, 200-207.

Wittmann, J., and Jack, H.M. (2011). microRNAs in rheumatoid arthritis: midget RNAs with a giant impact. Annals of the rheumatic diseases *70 Suppl 1*, i92-96.

Yamakuchi, M., Ferlito, M., and Lowenstein, C.J. (2008). miR-34a repression of SIRT1 regulates apoptosis. Proceedings of the National Academy of Sciences of the United States of America *105*, 13421-13426.

Yamakuchi, M., and Lowenstein, C.J. (2009). MiR-34, SIRT1 and p53: the feedback loop. Cell cycle *8*, 712-715.

Yan, K., Gao, J., Yang, T., Ma, Q., Qiu, X., Fan, Q., and Ma, B. (2012). MicroRNA-34a inhibits the proliferation and metastasis of osteosarcoma cells both in vitro and in vivo. PloS one *7*, e33778.

Yang, N., Wang, G., Hu, C., Shi, Y., Liao, L., Shi, S., Cai, Y., Cheng, S., Wang, X., Liu, Y.*, et al.* (2013). Tumor necrosis factor alpha suppresses the mesenchymal stem cell osteogenesis promoter miR-21 in estrogen deficiency-induced osteoporosis. Journal of

bone and mineral research : the official journal of the American Society for Bone and Mineral Research *28*, 559-573.

Yi, C., Wang, Q., Wang, L., Huang, Y., Li, L., Liu, L., Zhou, X., Xie, G., Kang, T., Wang, H.*, et al.* (2012). MiR-663, a microRNA targeting p21(WAF1/CIP1), promotes the proliferation and tumorigenesis of nasopharyngeal carcinoma. Oncogene *31*, 4421-4433.

Yu, K.R., Lee, S., Jung, J.W., Hong, I.S., Kim, H.S., Seo, Y., Shin, T.H., and Kang, K.S. (2013). MicroRNA-141-3p plays a role in human mesenchymal stem cell aging by directly targeting ZMPSTE24. Journal of cell science *126*, 5422-5431.

Yudoh, K., Nguyen v, T., Nakamura, H., Hongo-Masuko, K., Kato, T., and Nishioka, K. (2005). Potential involvement of oxidative stress in cartilage senescence and development of osteoarthritis: oxidative stress induces chondrocyte telomere instability and downregulation of chondrocyte function. Arthritis research & therapy *7*, R380-391.

Zhao, T., Li, J., and Chen, A.F. (2010). MicroRNA-34a induces endothelial progenitor cell senescence and impedes its angiogenesis via suppressing silent information regulator 1. American journal of physiology Endocrinology and metabolism *299*, E110-116.

Zhao, Y., and Srivastava, D. (2007). A developmental view of microRNA function. Trends in biochemical sciences *32*, 189-197.

Zhou, S., Greenberger, J.S., Epperly, M.W., Goff, J.P., Adler, C., Leboff, M.S., and Glowacki, J. (2008). Age-related intrinsic changes in human bone-marrow-derived mesenchymal stem cells and their differentiation to osteoblasts. Aging cell *7*, 335-343.

Ziyan, W., Shuhua, Y., Xiufang, W., and Xiaoyun, L. (2011). MicroRNA-21 is involved in osteosarcoma cell invasion and migration. Medical oncology *28*, 1469-1474.

Appendix F: Filed patents

Galectin-3

Compositions and methods for the treatment of bone disorders

The present invention relates to the therapy, prophylaxis and diagnosis of disorders that are associated with aberrant bone mineral density.

Metabolism and remodeling of the bone structure are the result of coordinated actions of bone-resorbing osteoclasts and bone-forming osteoblasts. While upon activation, osteoclasts resorb a portion of bone and finally undergo apoptosis, newly generated osteoblasts form bone at the site of resorption. Since development of osteoclasts is controlled by pre-osteoblastic cells, resorption and formation of bones are tightly coordinated.

An imbalance between osteoclast and osteoblast activities can result in skeletal abnormalities like osteoporosis (OP), which is characterized by decreased bone density and micro-architectural deterioration of bone tissue. The osteoporotic syndrome encompasses primary disorders such as postmenopausal or age-related OP, and secondary conditions that accompany disease states or medications. Low bone mineral density and low bone mass are the most important risk factor for osteoporosis.

Overall, the fact that the repair capacity of fractures is reduced and disorders like osteopenia or osteoporosis increase with age, implicates that the bone regeneration capacity is affected by the aging process.

Osteoporosis is estimated to affect 200 million women worldwide; in Europe, USA and Japan, osteoporosis affects an estimated 75 million people. Due to increased life expectancy, numbers are expected to increase.

Most of the currently available treatments aim at substantially increasing the bone density by using anti-resorptive strategies, i.e. they act by inhibiting bone resorption by osteoclasts. These therapies essentially include the use of bisphosphonates, estrogens, selective estrogen receptor modulators (SERMs), calcitonin and monoclonal antibodies such as denosumab, a monoclonal antibody against receptor activator of NFκB-ligand (RANKL), a factor made by osteoblasts which stimulates osteoclast development. These therapies have been shown to have limited efficacy. The first, and to date only, approved agent that stimulates new bone formation in the

treatment of osteoporosis in menopausal women is teriparatide, a portion of human parathyroid hormone, which is the primary regulator of calcium and phosphate metabolism in bone and kidney.

It has been an object of the invention to provide new agents and therapies for the treatment of bone disorders that result in new bone formation, thus reducing fracture at a higher rate than the available anti-resorptive therapies.

To solve the problem underlying the invention, the inventors focused on the process of osteogenesis.

Osteogenesis, i.e. the differentiation of mesenchymal stem cells into osteoblasts, is one of the basic mechanisms underlying the activities of osteoblasts, which are the key players in the formation of new bone.

In line with the finding that advanced age correlates with the incidence of reduced bone mineral density or bone mass disorders, it has been shown that the differentiation capacity of mesenchymal stem cells (MSCs) decreases with age, thereby contributing to slowed-down bone healing with age and to impaired bone remodeling leading to osteopenia or osteoporosis.

The experiments of the present invention focus on the role of circulating microvesicles (MVs) and their effect on the osteogenic differentiation capacity of mesenchymal stem cells (MSCs). While searching for systemic factors that are deregulated in old age and influence osteogenic differentiation capacity of mesenchymal stem cells (MSCs), it was surprisingly found that vesicular Galectin-3 is secreted by endothelial cells within CD63 negative and also CD63 positive MVs as well as in MVs isolated from human plasma of young people.

Galectin-3 (NG_017089.1 RefSeqGene, NR_003225.2, Isoform1: NM_002306.3, Isoform 1: Isoform 2: NP_002297.2, Isoform 2: NM_001177388.1, NP_001170859.1; protein and cDNA sequence: GenBank accession No.: AB006780.1) is a ubiquitously expressed lectin. It belongs to the family of galectins, a class of proteins exhibiting a conserved carbohydrate-recognition domain (CRD) which facilitates a beta-galactoside binding activity due to its NWGR amino acid sequence (Leffler *et al.*, 2004, *Glycoconjugate journal* 19, 433-440). In addition to the CRD, Galectin-3 has a collagen α-like and a short amino-terminal domain containing six predicted phosphorylation sites, whereof some are known to have also CRD-domain-independent functions. For example, phosphorylation of Serine 96 was shown to inhibit degradation of β-Catenin, an important mediator of Wnt-signalling (Song, S.*, et*

al, 2009, *Cancer Res* 69, 1343-1349). Depending on the state and type of the cells, Galectin-3 can be found intracellularly, in the extracellular matrix and the circulation. Recently, it has been shown that tyrosine phosphorylation by Calpain-4 is essential for Galectin-3 secretion (Menon *et al.,* 2011, Biochem Biophys Res Commun 410, 91-96). Galectin-3 has been shown to play a critical role in cellular processes such as pre-mRNA splicing, cell growth, cell cycle progression and apoptosis, as well as in systemic processes, inflammation, atherosclerosis, wound healing, prion infection and, most prominent, in tumour development and progression.

In the experiments of the present invention, it was tested if altered levels of Galectin-3, as observed in the plasma of young versus elderly individuals, might have an impact on the osteogenic differentiation capacity of mesenchymal stem cells.

It was confirmed that Galectin-3 levels are lower in elderly persons and that knock-down of Galectin-3 inhibits osteogenic differentiation of MSCs *in vitro*, while its overexpression before induction of osteogenesis accelerates the osteogenic differentiation process of MSCs even before Runx2 induces Galectin-3 expression during osteogenesis.

It can be concluded from the findings obtained in the experiments of the present invention that Galectin-3 will be useful in replacement therapies in patients with aberrant bone mineral density disorders, in particular in patients with reduced bone mass, e.g. osteoporotic patients, for restoring balanced osteogenesis.

In addition, it can be concluded that Galectin-3 levels in human plasma may serve as a biomarker indicating how permissive the systemic environment is to osteogenic differentiation.

In a first aspect, the present invention relates to a composition for the treatment and prophylaxis of disorders associated with aberrant bone mineral density or for accelerating bone healing, comprising, in a therapeutically effective amount, an agent that alters the level of Galectin-3 in mesenchymal stem cells, wherein said agent is selected from the group of

a) agents with the ability to increase the level of Galectin-3 in mesenchymal stem cells, selected from

i. Galectin-3 or fragments or variants or derivatives thereof, or

ii. nucleic acid molecules encoding Galectin-3 or fragments or variants thereof; or

iii. cells containing one or more nucleic acids molecule defined in ii.;

b) agents with the ability to decrease the level of Galectin-3 in mesenchymal stem cells, selected from
i. agents inhibiting Galectin-3 expression in mesenchymal stem cells or
ii. agents targeting the Serine 96 phosphorylation site of Galectin-3 protein, or
iii. dominant negative alleles of Galectin-3.

For the purpose of embodiment a), Galectin-3 may be any isoform of the protein. Alternatively to the naturally occuring Galectin-3 protein, or a nucleic acid molecule encoding it, a variant Galectin-3 polypeptide or a fragment or a nucleic acid molecule encoding such variant or fragment may be used. Variant Galectin-3 polypeptides having substantial sequence similarity to the Galectin-3 protein, such as 90%, 95% or 99% sequence identity to a corresponding portion of Galectin-3, the corresponding portion being any contiguous sequence of any length, such as 10, 20, 30, 40, 50 or more amino acids. In some embodiments, chemically similar amino acids may be substituted for amino acids in the Galectin-3 protein sequence (to provide conservative amino acid substitutions).
Furthermore, a Galectin-3 molecule modified by amino acids exchanges other than conservative substitutions may be useful, e.g. to enhance its activity. Optimization of the amino acid sequence may be achieved by methods known in the art, e.g. by site-directed mutagenesis.
In certain embodiments, the therapeutically active agent is a Galectin-3 derivative in which Galectin-3 is coupled to a chemical moiety that effects an increase of its half-life, activity or uptake in bone. By way of example, Galectin-3 derivatives may be obtained by conjugation to polyethylene glycol (Iversen et al., Theranostics. 2013, 3(3):201-9), or by N-glycosylation (Flintegaard *et al*., 2010, Endocrinology. Nov;151(11):5326-36). Alternatively, derivatization may be achieved by genetic modification that results in an N-terminal cyclic conformation (Cao *et al*., 2012, Diabetes Res Clin Pract. Jun; 96(3):362-70).
In certain therapeutic methods of the invention, Intralipid®, an FDA-approved fat emulsion, may be injected before admistering Galectin-3 to effect the protein's half-life (Liu *et al*., 2013, Biochim Biophys Acta. Jun; 1830(6):3447-53).
In a specific embodiment, the therapeutically active agent is a peptide containing the phosphorylation site Serine 96 of Galectin-3. Without wishing to be bound by theory -

since Galectin-3 phosphorylation may act as a scavenger of beta-Catenin, excess Galectin-3 may compete with -Catenin for phosphorylation, thereby protecting it from degradation so that it can exert its function in osteogenesis.

Galectin-3 variants, fragments or derivatives are useful within the scope of the present invention as long as their effect on differentiation of mesenchymal stem cells is equal to or greater than that of Galectin-3.

Preferably, a Galectin-3 peptide has a length of about 8 – 30 amino acids.

Galectin-3 variants or fragments may be routinely tested for usefulness in the present invention by transfecting MSCs or, as a model for MSCs, adipose-tissue derived stem cells (ASCs), with mammalian vector constructs containing the DNA sequence encoding the Galectin-3 protein or peptide of interest and determining its effect on osteogenic differentiation. MSCs and ASCs may be obtained by known methods, e.g. as described by Wolbank *et al.*, 2007 (Tissue Eng 13, 1173-1183) and Wolbank *et al*., 2009 (Tissue Eng Part A, 1843-1854).

The usefulness of Galectin-3 variants or derivatives may also be tested by incubating the test cells with such variant or derivative of interest. The effect may be quantified, e.g. as described in the Examples, by Alizarin staining to determine the cells' degree of calcification, and additionally be confirmed by qPCR of the early osteogenic marker alkaline phosphatase (ALP) and the late osteogenic markers osteonectin (ON) and osteocalcin (OC).

With respect to embodiment a), the term "Galectin-3" as used herein refers both to the naturally occurring protein and its therapeutically active variants/fragments/derivatives.

With respect to the present invention, the term "disorders associated with aberrant bone mineral density" ("bone mineral density disorders" or "bone density disorders" or "BMD disorders") refers both to conditions which are characterized, at least in part, by a decrease in bone mineral density (BMD), or bone mass respectively, that is associated with an aberrantly low level of Galectin-3, or, conversely, it refers to bone disorders associated with bone overgrowth and aberrantly high bone mineral density, in which bone formation and deposition exceed resorption.

For the purpose of the present invention, such disorders are due to an abnormal capacity of mesenchymal stem cells to differentiate into osteoblasts, such capacity including both the process of differentiation itself as well as its stimulation/activation.

A composition according to a) may be used to i) increase low bone density/low bone mass or to ii) accelerate bone healing, e.g. after fractures or iii) for the prevention of fractures in defined regions of the skeleton that are at high risk of fractures, e.g. the hip of a patient suffering from osteoporosis, iv) in dentistry/ periodontology when an increase of bone mass due to increased differentiation of mesenchymal stem cells is to be achieved.

In the case of i), Galectin-3 is the effective agent in a pharmaceutical composition to be administered systemically/parenterally, e.g. by subcutaneous bolus injection.

In certain embodiments, when administered systemically, in order to enrich Galectin-3 in osteogenic cells and to avoid tissue or organ-unspecific side effects, it may be linked to a bone-targeting molecule. Examples for bone-targeting molecules are, without limitation, bisphosphonates, lipids, or acidic oligopeptides, as described by Low and Kopecek, 2012 (Adv Drug Deliv Rev. 64(12): 1189–1204). Coupling Galectin-3 to bone-targeting molecules may be achieved according to methods known in the art. Examples of such methods are conjugation of Galecin-3 itself, or its delivery vehicle, e.g. liposomes, nanoparticles or microspheres, respectively, to bisphosphonates by a disulfide bridge (Doschak *et al*., 2009, Mol. Pharm. 6, 634-640) or to collagen-binding domains by fusing its cDNA to the N- or C-terminus of the protein (Ponnapakkam *et al*., 2011, Calcif. Tissue Int. 88 511–520). Alternatively, short peptides containing repetitive aspartate and/or glutamate sequences may be fused to the C- or N-terminus of the protein, such fusion constructs being obtainable by recombinant protein expression. Such constructs may additionally include a spacer such as the Fc region of human IgG to improve the targeting and/or to ensure the activity of the protein (Nishioka *et al*., 2006, Mol. Genet. Metab. 88 244–255).

Thus, in a further embodiment, the invention relates to Galectin-3, or a fragment or variant thereof, linked to a bone-targeting molecule.

According to yet another embodiment, Galectin-3 or a gene construct containing the Galectin-3 encoding DNA, is contained in a delivery vehicle. Examples of delivery vehicles for bone-targeting are cationic liposomes like dioleoyl trimethylammonium propane (DOTAP)-based cationic liposomes attached to six repetitive sequences of aspartate, serine, serine ((AspSerSer)(6)), as described by Zhang *et al., 2012 (Nat Med 18(2): 307-14)* for the delivery of siRNA to bone-forming surfaces.

In the case of ii) or iii), Galectin-3 is administered locally, either directly or as a component of a matrix (also known as “scaffold) or bolus or by implantation of Galectin-3 overexpressing cells.

A composition according to a) may be used, but its use is not limited to, ghosal hematodiaphyseal dysplasia syndrome (GHDD), osteoporosis, osteogenesis imperfecta osteopenia, Paget's disease, osteomyelitis, hypercalcemia, osteonecrosis, hyperparathyroidism, lytic bone metastases, periodontitis, and bone loss due to immobilization.

As defined in US 20130195863, and also used herein, the term "osteoporosis" includes any form of osteoporosis. For example, osteoporosis includes primary osteoporosis, post-menopausal and age-related osteoporosis, endocrine osteoporosis (including hyperthyroidism, hyperparathyroidism, Gushing's syndrome, and acromegaly), hereditary and congenital forms of osteoporosis (including osteogenesis imperfecta, homocystinuria, Menkes' syndrome, Riley-Day syndrome), and osteoporosis due to immobilization of extremities. The term also includes osteoporosis that is secondary to other disorders, including hemochromatosis, hyperprolactinemia, anorexia nervosa, thyrotoxicosis, diabetes mellitus, celiac disease, inflammatory bowel disease, primary biliary cirrhosis, rheumatoid arthritis, ankylosing spondylitis, multiple myeloma, lymphoproliferative diseases, and systemic mastocytosis. The term also includes osteoporosis secondary to surgery (e.g., gastrectomy) or to drug therapy, 20 including chemotherapy, endocrine therapy, anticonvulsant therapy, immuno-suppressive therapy, and anticoagulant therapy. The term also includes osteoporosis secondary to glucocorticosteroid treatment for certain diseases, including rheumatoid arthritis (RA), systemic lupus erythematosus (SLE), asthma, temporal arthritis, vasculitis, chronic obstructive pulmonary disease, polymyalgia rheumatica, polymyositis, and chronic interstitial lung disease. The term also includes osteoporosis secondary to glucocorticosteroid and/or immunomodulatory treatment to prevent organ rejection following organ transplant such as kidney, liver, lung, and heart transplants. The term also includes osteoporosis due to submission to microgravity, such as observed during space travel. The term also includes osteoporosis associated with malignant disease, such as breast cancer, prostate cancer.

A composition according to b) may be used for the therapy of disorders which aim at decreasing an aberrantly high bone density and bone overgrowth. Such disorders are

caused by bone formation and deposition that exceed resorption, potentially resulting in pathologically increased bone mass and strength. Examples are sclerosteosis, Simpson-Golabi-Behmel syndrome (SGBS), Van Buchem Disease

In order to determine whether a person is eligible for the treatment with a composition of the present invention, he or she may be first tested for BMD using approved physical methods. Examples are dual-energy X-ray absorptiometry (DXA or DEXA), quantitative computed tomography (QCT), qualitative ultrasound (QUS), single photon absorptiometry (SPA), dual photon absorptiometry (DPA), digital X-ray radiogrammetry (DXR) or single energy X-ray absorptiometry (SEXA). Such measurements rely on the measurement of bone density, which is considered to be an indicator also of bone mass. (Since the terms “bone density” and “bone mineral” density are often mostly interchangeably, they are also used, if not otherwise stated, synonymously for the purpose of the present invention).

The currently used relevant measure when screening for osteoporosis is the T-score, which is a comparison of a patient's BMD to that of a healthy thirty-year-old. The criteria of the World Health Organization are: the normal T-score is ≥ -1.0; osteopenia is defined by a T-score of -1.0 to -2.5; osteoporosis is defined by a T-score of ≤ -2.5.

In the context of the present invention, the term “aberrant BMD” designates, if the T-score is the relevant parameter, a BMD level outside the T-score range of -1,0 - +0,5. For the purpose of the present invention, this term also encompasses a level of BMD that is to be increased during bone healing, when the bone repair capacity after fractures is reduced.

Subsequently to the step of measuring BMD, the person’s Galectin-3 level in plasma is determined (either by a separate Galectin-3 test or by assessing Galectin-3 expression as a component of a diagnostic signature). If measuring BMD by a physical method, e.g. any of the methods mentioned above, is omitted, determining the Galectin-3 level is used as the only test for diagnosing a disorder correlating an aberrant BMD. In this case, the Galectin-3 level is the parameter for eligibility for a Galectin-3-based therapy. Eligibility for a Galectin-3-based therapy is given if the Galectin-3 plasma level deviates from a value of young, healthy individuals, by more than 15%. In addition, eligibility is given in case that the patient has one or more Galectin-3 mutations, or deficiencies in the response to Galectin-3, e.g. mutations in the down-stream signaling events induced by Galectin-3, or impaired binding of Galectin-3 to receptors, or impaired cellular uptake of Galectin-3. The therapeutically

effective amount of Galectin-3, i.e. the amount effective at dosages and for periods of time necessary to achieve the desired therapeutic result, i.e. the desired bone mineral density, may vary depending on factors such as the disease state, age, sex, and weight of the individual, and the ability of the therapeutic to elicit a desired response in the individual. Dosage regimens may be adjusted to provide the optimum therapeutic response.

Response to Galectin-3-based therapy may be determined by standard methods, i.e. by determining BMD as described above.

A "prophylactically effective amount" refers to an amount effective, at dosages and for periods of time necessary, to achieve the desired prophylactic result by increasing bone mineral density or preventing its decrease, thus preventing disorders like osteoporosis. A prophylactic dose may be used in subjects prior to or at an earlier stage of disease, and a prophylactically effective amount may be more or less than a therapeutically effective amount in some cases.

A composition of the invention containing the Galectin-3 protein, operably linked to a bone-targeting molecule, may be administered systemically, preferably parenterally, e.g. intravenously or subcutaneously, or locally, e.g. in the form of bone implants, prostheses or internal patches around bones.

As mentioned above, the Galectin-3 protein/peptide may also be packaged into lipid vesicles, or mixed with a polymer like polyethylenimine linked to a bone targeting 20 molecule.

In yet another embodiment, the Galectin-3 protein may be administered as a component of a so-called “protein activated matrix (PAM), i.e. a matrix impregnated with the protein of interest.

Matrices useful for drug delivery in bones, including controlled release composites, e.g. for delivering growth factors, are well known in the art and may be adapted for a therapeutic Galectin-3 protein. Examples are organic bone-derived matrices like demineralised bone matrix, autolyzed antigen-extracted allogenic bone; synthetic polymers like polylactic acid or polyglycolic acid homo-/heterodimer; natural polymers like collagen (types I and IV), non-collagenous proteins like fibrin and hydrogels. Example of inorganic matrices are natural bone mineral and thermoashed bone mineral, hydroxyapatite, tricalcium phosphate and other bioceramics, bioactive glass and coral (Kirker-Head, 2000, Adv Drug Deliv Rev 43: 65-92). Detailed reviews of composites as well as methods for incorparting the therapeutic agent into such

composites are provided by Lauzon *et al*., 2012 (Journal of Controlled Release 162, 502-520), and by Soundrapandian *et al*., 2009 (AAPS PharmSciTech. 10(4): 1158–1171).

Further examples of biomaterial matrices are described in US 20130195863. In yet another embodiment, to facilitate uptake of a Galectin-3 protein or peptide into the target cells, it may be operably linked to a CPP ("cell penetrating peptide"). Examples for CPPs, also known as protein transduction domains (PTDs), are transportan, pISl, Tat(48-60), pVEC, MAP and MTS, or the Oct4 transduction domain. A CPP-linked Galectin-3 may be obtained by recombinant production of the respective Galectin-3/CPP fusion protein/peptide.

For a formulation to be injected, the Galectin-3-containing composition contains components which are pharmaceutically acceptable. These may be in particular isotonic, sterile, saline solutions (monosodium or disodium phosphate, sodium, potassium, calcium or magnesium chloride and the like or mixtures of such salts), or dry, especially freeze-dried compositions which upon addition, depending on the case, of sterilized water or physiological saline, permit the constitution of injectable solutions. The pharmaceutical forms suitable for injectable use include sterile aqueous solutions or dispersions; formulations including sesame oil, peanut oil or aqueous propylene glycol; and sterile powders for the extemporaneous preparation of sterile injectable 20 solutions or dispersions.

In certain embodiments, the Galectin-3 therapeutic is a DNA molecule inserted in a vector that is administered according to methods for gene therapy known in the art. Vectors may be prepared from different type of viruses, including adenoviruses, adeno-associated viruses (AAV), herpes viruses (HSV), lentiviruses and retroviruses. When the Galectin-3 therapeutic is used in a gene therapy using a virus, an adenovirus vector is preferably used. As a useful adenovirus vector, a so-called "second generation adenovirus vector" (obtained from a first generation adenovirus vector lacking the E1/E3 domain by deleting the E2 or E4) or a third generation adenovirus vector in which all viral coding sequences are deleted. DNA replication and packaging of such so-called "gutless" (or helper-dependent) adenoviral vectors depend on a helper virus to provide viral gene products to support the vector. Adenoviral and other viral vectors and the requirements they must fulfill to be suitable for bone-directed gene therapy, are described by Fischer *et al*., 2011, Journal of Cranio-Maxillo-Facial Surgery 39, 54-64).

Alternatively, the Galectin-3 therapeutic may be administered in the form of a naked DNA or mRNA molecule.

In general, as for application of the protein, the dosage of the Galectin-3 nucleic acid molecule, i.e. when inserted in a gene therapy vector or applied as naked DNA or RNA, may depend to a large extent on the condition and size of the subject being treated as well as the therapeutic formulation, frequency of treatment and the route of administration. Regimens for continuing therapy, including dose, formulation, and frequency may be guided by the initial response and clinical judgment.

To improve uptake of DNA in gene therapeutical applications of Galectin-3, physical and chemical methods may be useful. Examples of physical methods are electroporation (using short pulses of high voltage to carry DNA across the cell membrane), the so-called “gene gun” (using DNA coated with gold particles loaded into a “gun” achieves penetration into the cells), sonoporation (using ultrasonic frequencies) magnetofection (in which DNA is complexed to a magnetic particles). Examples of chemical methods are lipoplexes and polyplexes as well as dendrimers.

According to certain embodiments, to achieve bone-directed expression of Galectin-3 in mesenchymal stem cells (osteoprogenitor cells), the vector construct may include an osteoprogenitor-specific promoter, as described for expression of BMP-2 20 (bone morphogenic protein 2) by Kumar *et al*., 2005, Biochimica et Biophysica Acta 1731, 95 – 103. Known osteoprogenitor-specific promoters are the Runx-2/cbfa1 (RUNX) promoter, the osteopontin (OPN) promoter, the collagen type 1a (COL) promoter and the osteocalcin (OCN) promoter. Since Galectin-3 expression is desirable during early stages of osteogenic differentiation (or activation of differentiation, respectively), the promoter cloned upstream of the Galectin-3 encoding DNA sequence is the COL or the RUNX promoter, preferably the RUNX promoter.

In embodiments of local administration, e.g. for accelerating bone healing after a fracture, the therapeutic Galectin-3 encoding nucleic acid molecule may be delivered to the site of interest by means of viral or non-viral vectors or as naked DNA or RNA. As reviewed by Pelled *et al.,* 2010 (Tissue Engineering: Part B, Volume 16, No.1, 13-20), localization of the therapeutic molecule within the fracture site may be assured either by physical placement at the target site or by gene release from a three-dimensional biomaterial implanted at or near the defect area. Useful physical placement methods include direct injection of the Galectin-3 protein, or the transgene respectively, into the fracture site. Preferably, in order for the DNA molecule to

penetrate cells *in situ*, it is delivered by a virus or forced into cells' nuclei by an electric pulse or ultrasonic wave. Preferably, an adenoviral vector is used, as described for expressing bone morphogenetic protein (BMP) Egermann *et al*., 2006 (Hum Gene Ther. May;17(5):507-17).

Alternatively to using a vector, *in vivo* electroporation or sonoporation may be used to deliver the therapeutic locally. Using these methods, the Galectin-3 encoding nucleic acid molecule is directly injected into a fracture and an electric pulse or ultrasonic wave is applied to the site either trans- or percutaneously.

In a further embodiment, mesenchymal stem cells derived from any source, including but not limited to bone marrow, adipose tissue, umbilical tissue, urine, or placenta, genetically engineered to overexpress Galectin-3, as described in the Examples, may be implanted at the defect site (Marie, 2011, Osteoporos Int 22:2023–2026).

In an alternative embodiment, localizing Galectin-3 at the site of interest, e.g. the fracture site, e.g. by transgene expression, is achieved by first binding Galectin-3 DNA/RNA to a delivery system (e.g. by adsorption, entrapment or immobilization, or by covalent binding; Luginbuehl *et al.*, 2004, Eur J Pharm Biopharm 58:197–208) and then implanting the gene-activated matrix (GAM) into the defect site, e.g. as described by Fang *et al*., 1996 (Proc Natl Acad Sci USA 93, 5753). To increase transfection efficiency, the DNA may be condensed by chemical vectors such as polyethyleneimine, liposomes or calcium-phosphate precipitates.

Useful matrices (GAMs, "gene-activated matrices") have been described above in the context with matrices for the delivery of the Galectin-3 protein.

Also when the therapeutically active agent, either in the form of a protein/peptide or in the form of a nucleic acid, is administered locally, either as such or incorporated in a matrix, it may advantageously be linked to a bone-targeting molecule. For the protein/peptide, this may be accomplished either by directly linking the protein/peptide to the bone-targeting molecule or by linking the delivery vehicle, e.g. a liposome, that contains the agent, with the bone-targeting molecule. In the case that a nucleic acid molecule is to be administered locally, incorporation of the bone-targeting molecule is achieved by linking it to the surface of the delivery vehicle. The same applies for a CPP. In certain embodiments, a Galectin-3 therapeutic of the invention, either containing Galectin-3 or the nucleic acid molecule encoding it, may be combined with one or more other therapeutic agents, e.g. teriparatide, denosumab, blosozumab, romosozumab, or one or more bone growth factors or the

respective encoding nucleic acid molecules, e.g. a BMP like BMP-2 and/or BMP-7, or RNAs, like e.g. RNAs antagonizing miR-31.

In a composition of the invention according to embodiment b) ii., the inhibitor of Galectin-3 expression may be selected from any *RNAi* (RNA interference) molecule including siRNAs, miRNAs, LNAs, phosphorothioate RNAs, antisense oligonucleotides, ribozymes and aptamers. According to embodiment b) ii., the inhibitor is an agent targeting the active site (Serine 96) of the Galectin-3 protein, e.g. a protein/peptide that competes with phosphorylation or prevents it.

According to embodiment b) iii., inhibition of Galectin-3 activity is achieved by overexpression of a dominant negative allele of Galectin-3. Dominant negative alleles of Galectin-3 may be selected upon testing truncation mutants of Galectin-3 that, upon overexpression in MSCs or during bone formation, inhibit or fail to accelerate osteogenic differentiation.

In this case, an inhibitor of Galectin-3, linked to a bone-targeting molecule, is the effective agent in a pharmaceutical composition to be administered systemically/parenterally/subcutaneously, or locally to the bone, either directly or in combination with one or more physical and chemical method to improve uptake, or as a component of a matrix (GAM, “gene activated matrix”) or bolus.

As for the Galectin-3 protein or peptide, uptake of a Galectin-3 inhibitor into the target cell may be facilitated by operably linking it to a CPP (“cell penetrating peptide”), as described e.g. in WO2008033285 . Examples for CPPs, also known as protein transduction domains (PTDs), are transportan, pISl, Tat(48-60), pVEC, MAP and MTS, or the Oct4 protein transduction domain.

In a further aspect, the present invention relates to methods and assays for diagnosing in a subject a disorder associated with aberrant bone mineral density, wherein the Galectin-3 level in mesenchymal stem cells of said subject is determined in a sample and a Galectin-3 level deviating from that of a healthy young individual (by ≥15%) is indicative for an aberrant bone mineral density. In preferred embodiments, the Galectin-3 protein level is determined by using an antibody binding specifically to Galectin-3. For the purpose of the present invention, neither the type of antibody nor the Galectin-3 epitope that it recognizes is critical. Preferably the antibody recognizes the full length of the Galectin-3 molecule,

In particularly preferred embodiments, Galectin-3 levels are determined using an ELISA assay.

The term “ELISA” refers to enzyme-linked immunosorbent assay (or EIA). Numerous ELISA methods and applications are known in the art and there are many ELISA test systems commercially available.

One example for an ELISA method is a “direct ELISA,” wherein the Galectin-3 antigen in a sample is detected. In one embodiment of the direct ELISA, a sample containing Galectin-3 is exposed to a solid (i.e., stationary or immobilized) support (e.g., a microtiter plate well). Galectin-3 within the sample becomes immobilized to the stationary phase, and is detected directly using an enzyme-conjugated antibody specific for Galectin-3.

In an alternative embodiment, an “indirect ELISA” is used. In one embodiment, Galectin-3 is immobilized to a solid support (e.g., a microtiter plate well) as in the direct ELISA, but is detected indirectly by first adding the anti-Galectin-3 antibody, followed by the addition of a detection antibody specific for the anti-Galectin-3 antibody, also known as “species-specific” antibodies (e.g., a goat anti-rabbit antibody), which are available from various manufacturers known to those in the art.

In other embodiments, a “sandwich ELISA” is used, where Galectin-3 (e.g. contained in a test sample) is immobilized on a solid support (e.g., a microtiter plate) via an antibody (i.e., a capture antibody) that is immobilized on the solid support and is able to bind to Galectin-3. Following the affixing of a suitable capture antibody to the immobilized phase, a sample is then added to the microtiter plate well, followed by washing. Galectin-3 present in the sample is bound to the capture antibody present on the support. In some embodiments, a sandwich ELISA is a “direct sandwich” ELISA, where the captured Galectin-3 antigen is detected directly by using an enzyme-conjugated antibody directed against the antigen. Alternatively, in other embodiments, a sandwich ELISA is an “indirect sandwich” ELISA, where the captured Galectin-3 antigen is detected indirectly by using an antibody directed against the antigen, which is then detected by another enzyme-conjugated antibody which binds the antigen-specific antibody, thus forming an antibody-antigen-antibody-antibody complex. Suitable reporter reagents are then added to detect the third antibody. Alternatively, in some embodiments, any number of additional antibodies are added as necessary, in order to detect the antigen-antibody complex. In some preferred embodiments, these additional antibodies are labeled or tagged, so as to permit their visualization and/or quantitation.

As used herein, the term “capture antibody” refers to an antibody that is used in a sandwich ELISA to bind (i.e., capture) Galectin-3 in a sample prior to its detection. For example, in some embodiments, a polyclonal antibody against Galectin-3 serves as a capture antibody when immobilized in a microtiter plate well. This capture antibody binds Galectin-3 present in a sample added to the well. In one embodiment of the present invention, biotinylated capture antibodies are used in conjunction with avidin-coated solid support. Another antibody (i.e., the detection antibody) is then used to bind and detect the antigen-antibody complex, in effect forming a “sandwich” comprised of antibody-antigen-antibody (i.e., a sandwich ELISA).

As capture antibody, any specific Galectin-3-binding antibody may be used, e.g. polyclonal serum, or monoclonal antibodies. Monoclonal anti-Galectin-3 antibodies are commercially available, e.g. from Pierce (A3A12, B2C10).

In the diagnostic method of the present invention, the sample is a preparation containing plasma-derived MVs. The sample may be obtained according to methods known in the art as described by Lehmann *et al.,* Cancer Res 68, 7864-7871 (2008), or using the method described in the Examples.

Alternatively, the Galectin-3 level may be determined directly in the plasma, i.e. without a preceding enrichment of MVs.

Brief description of the Figure:

Galectin-3 protein levels of microvesicles isolated from plasma of young and elderly donors

Examples

In the Examples, the following materials and methods were used:

a) Cell culture

i. Human umbilical vein endothelial cell (HUVEC)

Endothelial cells were isolated from human umbilical veins as described (Jaffe *et al.,* 1973, Clin Invest 52, 2745-2756; Chang, 2005, Mutat Res 576, 39-53 HUVECs were cultivated in gelatin-precoated flasks in EGM (Lonza) at 37°C in a humidified atmosphere with 5% CO_2. Cells were passaged once or twice a week at a split ratio of 1:2 to 1:6 according to the growth rate. HUVECs were cultivated to senescence

and stained for senescence- associated -galactosidase (SA--gal) activity as described by Chang, *et al*., 2005,Exp Cell Res 309, 121-136. For collection of supernatants, contact-inhibited (quiescent, PD19) and senescent (PD52 / 95% SA-β-gal positive) cells were allowed to secrete into HUVEC medium, depending on the experiment, for 48 hours.

ii. Human adipose-derived stem cells (ASCs) Subcutaneous adipose tissue was obtained during outpatient tumescence liposuction under local anestesia. ASCs were isolated as described (Wolbank *et al.,* 2007, Tissue Eng 13, 1173-1183; Wolbank *et al.,* 2009, Tissue Eng Part A 15, 1843-1854) and cultured in DMEM-low glucose/HAM´s F-12 supplemented with 4mM L-glutamine, 10% fetal calf serum (FCS, PAA) and 1ng/mL recombinant human basic fibroblast growth factor (rhFGF, R&D Systems) at 37°C, 5% CO_2 and 95% air humidity. Cells were passaged once or twice a week at a split ratio of 1:2 according to the growth rate. All differentiation protocols were carried out in 24 well cell culture plates. For osteogenic differentiation, ASCs were seeded at a density of $2x10_3$ cell per well. 72 hours after seeding cells were incubated with osteogenic differentiation medium (DMEM-low glucose, 10% FCS, 4 mM L-glutamine, 10 nM dexamethasone, 150 M ascorbate-2-phosphat, 10 mM -glycerolphosphate and 10 nM vitamine-D3) up to 4 weeks. For Alizarin staining of calcified structures, cells were fixed for 1 hour in 70% ethanol at -20°C. After brief rinsing, cells were stained for 20 minutes with 40 mM Alizarin Red solution (Sigma) and washed with PBS. For quantification, Alizarin was extracted for 30 minutes using 200 l 0.1M HCL/0.5% SDS solution.

b) Construction of Galectin-3 expression vector

Homo sapiens lectin, galactoside-binding, soluble, 3 (LGALS3 = Galectin-3), transcript variant 1 as transfection-ready DNA within the pCMV6-XL4 vector (SC118706), was purchased from Origin. The restriction enzyme site NotI upstream and downstream of the gene of interest was used to cut out the insert. The obtained insert was cloned into the NotI restriction site of pcDNA 3.1 hgro (+), a mammalian expression vector containing a CMV promoter and conferring Hygromycin B resistance.

c) Transfections

i) Human adipose-derived stem cells (ASCs)

ASCs were transfected using Neon® Transfection System (Life technologies). Cells were transfected according to the manufactures protocol. Briefly, $1x10^5$ ASCs resuspended in 10 µl buffer R, were mixed with 1µg of DNA or 10 pmol of siRNA and loaded into the Neon TM pipet tip. Subsequently cells were electroporated using the recommended parameters: Pulse voltage: 1400 V; pulse width: 10 ms; pulse number: 3. After electroporation, cells were directly transferred into a 6 well tissue culture vessel containing growth medium. ON-TARGETplus Non-targeting Pool (20 nmol) (D-001810-10-20, Dharmacon), ON-TARGETplus SMARTpool, Human LGALS3, (5 nmol) (L-010606-00-0005, Dharmacon).

ii) Human umbilical vein endothelial cells (HUVECs) HUVECs were transfected using Neon® Transfection System (Life technologies). Cells were transfected according to the manufactures protocol. Briefly; $5x10^5$ HUVECs resuspended in 100 µl buffer R were mixed with 5 µg of DNA and loaded into the Neon TM pipet tip. Subsequently, cells were electroporated using the recommended parameters: Pulse voltage: 1350 V; pulse width: 30 ms; pulse number: 1. After electroporation, cells were directly transferred into a gelatin precoated culture flask containing growth medium. pmaxGFP vector (Amaxa).

d) Assessment of apoptotic cell death

HUVECs were seeded in 12-well cell culture plates and were allowed to secrete into ASC or HUVEC medium for 48 hours. Thereafter, the cells were detached using 50 mM EDTA and stained with Annexin V- FITC and PI (Roche) according to the manufacturer´s instructions. Analysis of the percentage of apoptotic and necrotic/late-apoptotic cells were performed using a FACS-Calibur and the CellQuest software (Becton Dickinson).

e) Quantitative real-time PCR

Alizarin stainings were confirmed using different osteogenic differentiation marker genes. To this end, total ASCs RNA was isolated using Tri Reagent (Sigma) at different time points during osteogenesis. 7 days after differentiation start, the early osteogenic marker alkaline phosphate (ALP), 14 days after start of differentiation, the osteogenic marker osteonectin (ON) and 21 days after start of differentiation, the late osteogenic marker osteocalcin (OC) was measured Reverse transcription was performed using DyNAmo cDNA Synthesis Kit (Biozym) and qPCR was performed using the RotorGene2000 (Corbett).

Primer pair for quantifying ALP mRNA NM_000478.4 spans Exon 3 (319-438 nt) and 4 (439-554 nt).Primer pair for quantifying ON mRNA NM_003118
spans Exon 8 (789 -937 nt) and 9 (938-1086 nt). Primer pair for quantifying OC mRNA NM_001199662 spans Exon 3 (296-396 nt) and 4 (397-592 nt). Primer pair for quantifying GAPDH mRNA NM_002046.4 span Exon 8 (700 -1112 nt) and 9 (1113-1383 nt).

f) Microvesicle (MV) purification

MVs were purified by filtration and differential centrifugation as described by Lehmann *et al.,* Cancer Res 68, 7864-7871 (2008). In brief, cell culture supernatant was collected after a secretion period of 48 hours or plasma samples were thawed and diluted 1:2 in PBS. The conditioned medium or the diluted plasma sample was centrifuged at 500 g for 15 minutes to sediment cells, at 14.000 g for 15 minutes to eliminate cell debris and filtered through a 0.22 m filter. MVs were then sedimented by ultracentrifugation at 100.000 g for 60 minutes and the resultant pellet was washed with PBS. MV were used as fresh preparations for electron microscopy and differentiation experiments or conserved at -80°C for further analysis. For differentiation studies MV derived from $2x10_4$ HUVECs or 1 ml of human serum were resuspended in 50 l ASC growth medium and added per well ASCs.

g) Purification of CD63 positive exosomes

i. Preparation of immunoaffinity capture microbeads CD63 monoclonal antibody immunoaffinity capture microbeads (Dynabeads® M-270 Epoxy, Invitrogen) were

prepared with the aid of Dynabeads® Antibody Coupling Kit (Invitrogen) according to the manufacturer's protocol. Briefly, 5 mg of Dynabeads were washed with 1 ml of C1 solution. The supernatant was removed by placing the tube on a magnet whereby beads were able to collect at the tube wall. 50 µl of monoclonal CD63 antibody (ab8219 Abcam) were mixed with 200 µl of C1 solution. Washed beads were first mixed with prepared antibody solution and 250 µl of C2 solution were added afterwards. Beads were incubated at 37°C on a roller over night. The next day supernatant was removed by placing the tube on a magnet whereby beads were able to collect at the tube wall. Afterwards beads were washed with each 800 µl of HB, LB and finally SB buffer and stored at 4°C until use.

ii) Purification of CD63 positive exosomes by immunoaffinity capture microbeaded MVs were isolated as described above and subsequently incubated with CD63 antibody-coupled Dynabeads for 2 h at 4°C on a roller. Afterwards the tube was placed on a magnet allowing the beads to collect at the wall. Supernatant containing MV depleted of CD63 positive exosomes was decanted. CD63 positive MVs were eluted through incubation of beads with 140 µl of citric acid, pH=3. The tube was placed on a magnet allowing the beads to collect at the wall. Supernatant containing CD63 positive MVs was decanted and immediately mixed with 50 µl of 1M NaOH for neutralization. CD63 positive MVs were conserved at -80°C for further analysis.

h) Electron microscopy

Purified MVs were left to settle on nickel coverslips (200 mesh, hexagonal, Pioloform-coated Athene copper grids). After fixation with 4% paraformaldehyde, MVs were stained with 2% uranyl acetate for 30 seconds, coverslips were left to dry and visualized using a transmission electron microscopy (TEM), Philips model CM 12 electron microscope (Philips, Eindhoven, NL).

For electron microscopy in-situ hybridization (EM-ISH), MV pellets were permeabilized with 0.1% Triton-X for 5 minutes at room temperature. After washing with PBS, MVs were incubated for at least 4 hours with hybridization buffer as described 98. For each sample 1 pM of the LNA DIG-labeled single stranded probe (Exiqon, Denmark) was denaturated in denaturizing hybridization buffer (containing 50% formamide, 5x SSC, 5x Denhardt´s solution, 0.1% Tween, 0.25% CHAPS, 200g

ml-1 yeast RNA, 500g ml-1 salmon sperm DNA) by incubation at 80°C for 5 minutes. Probes were placed on ice quickly. MVs were mixed with the probe and 5 hybridized at 50°C over night. After hybridization, samples were washed stringently with 0.2 x SSC at 60°C for 1 hour. Thereafter, MV were incubated with Anti-DIG antibody (Roche) for 30 minutes and an additional hour with the second 5nm gold particle-labeled antibody (Sigma). After washing with PBS, MVs were embedded in Epon, approximately 80 nm sections on average, were cut using an Ultramicrotom (Ultracut, Reichelt) and then analyzed using transmission electron microscopy (TEM), Philips model CM 12 electron microscope (Philips, Eindhoven, NL).

i) Western blot

Total proteins and proteins from MVs were extracted and separated on polyacrylamide gels, before transfer to a PVDF membrane (BioRad). The membrane was blocked in 3% skimmed milk, incubated with the CD63 antibody (sc-15363 Santa Cruz), Galectin-3 antibody [A3A12] (ab2785 Abcam) or GAPDH antibody [FL-33] (sc-25778 Santa Cruz), followed by incubation with the corresponding secondary antibody Alexa Fluor 680-conjugated anti-rabbit IgG (Molecular Probes) or Alexa Fluor 800-conjugated anti-mouse IgG (Molecular Probes). Signal intensities were analyzed by using the Odyssey infrared image system (LiCor).

j) Statistics

Data were statistically analyzed using Student´s t test, one-way ANOVA and one-way ANOVA followed by the Dunn´s method as indicated. Analyses were performed with SigmaPlot 10.0 (SigmaPlot, Germany). The tests were two-sided with type 1 error probability of 0.05. Data are presented as mean values ± SEM.

Example 1 Microvesicles isolated from plasma from elderly donors reduce osteogenic differentiation capacity of ASCs. In order to test whether osteogenic differentiation capacity of MSCs is influenced by *ex vivo* plasma-derived MVs and by the donors age, MVs smaller than 200 nm in diameter were isolated from donors younger than 25 or older than 55 years by different centrifugation steps. Electron microscopy was performed to confirm size and shape.

MSCs derived from adipose tissue were used as model system. ASCs were characterized in detail. In particular, the differentiation capacity towards the osteogenic and adipogenic lineage, the immunomodulatory properties as well as expression of typical and atypical surface markers were examined by phytohemagglutinin activation assay and flow cytometric analysis for the presence or absence of the surface markers CD14, CD34, CD45, CD73, CD90, HLA ABC, HLA DR and CD105.

Subsequently, ASCs were seeded one day before exposing them to plasma derived MVs for 72 hours. After 3 days osteogenic differentiation was induced as described (*Wolbank et al.*, 2009,Tissue Eng Part A 15, 1843-1854). It could be shown that differentiation capacity was reduced to 30 % when cells were co-incubated with MVs isolated from the plasma of healthy elderly donors compared to ASCs exposed to MVs of young donors as quantified by Alizarin Red staining.

Example 2 Microvesicular Galectin-3 is elevated in healthy young donors

Since proteins have been reported to be packaged into MVs, the known microvesicular repertoire of proteins, as published by Mathivanan, S. & Simpson, R.J. ExoCarta: Proteomics 9, 4997-5000 (2009) was compared with a list of proteins known to be involved in the Wnt-siganling pathway, an important pathway for the induction of osteogenic differentiation. Galectin-3 resulted as the most prominent member.

MVs from plasma of healthy young (20-25 years) and healthy elderly female donors (older than 55 years) were isolated and Galectin-3 protein levels were analyzed by Western blot. While no large differences in Galectin-3 levels in plasma of young donors were observed, reduced levels could be seen in the group of women older than 55 years (Figure: healthy elderly female donors (E); young healthy controls (Y).

In order to exclude the possibility that Galectin-3 is not a component of MVs but co-sediments in protein aggregates due to ultracentrifugation, the pellet obtained by ultracentrifugation was used to purify CD63 positive MVs by an immuno-affinity capture assay, since CD63 is an established microvesicular marker. Successful separation of the CD63-containing fraction was confirmed by Western blot when CD63 positive MV fraction was loaded against CD63 negative MV fraction. Thus, it was confirmed that Galectin-3 is a component of *ex-vivo* plasma derived CD63 positive MVs.

Example 3 Impact of Galectin-3 level on osteogenic differentiation capacity

Since proteins are transferred to recipient cells by microvesicles, it was tested if altered levels of Galectin-3 in ASCs have an impact on osteogenic differentiation. Osteogenic differentiation was induced 3 days after transient transfection of ASCs with a plasmid overexpressing Galectin-3. Elevated Galectin-3 levels were confirmed using Western blot. It was found that Galectin-3 alone was sufficient to significantly increase osteogenic differentiation (~3 fold), as quantitated by Alizarin staining as well as by qPCR of the early osteogenic marker ALP and the late osteogenic markers osteonectin (ON) and osteocalcin (OC). In agreement with this, osteogenic differentiation was decreased when ASCs were transfected with siRNA against Galectin-3. Knock-down of Galectin-3 was confirmed by Western blotting; it resulted in ~30 % lower osteogenesis as quantitated by Alizarin staining and confirmed by qPCR of ALP, ON and OC.

Example 4 Galectin-3 acts upstream of Runx-2 in increasing osteogenic differentiation capacity

Galectin-3 was already known to be expressed in the late stage of osteoblast 20 maturation and that its expression is induced by the transcription factor Runx-2, a master regulator of ostogenic differentiation. In contrast to the work published before, it could be shown here that Galectin-3 acts upstream of Runx-2: Galectin-3 overexpressing ASCs, which were induced to undergo osteogenic differentiation, show elevated ALP m-RNA level as measured by qPCR and enhanced ALP enzymatic activity on day 7 while Runx-2 expr

ession is not induced until day 12 as analyzed by qPCR. These observations suggest a surprising and unexpected mechanism, namely that Galectin-3 induces a positive feed forward loop, since its enhanced expression accelerates osteogenic differentiation and in association also Runx-2 expression, which in turn results in Galectin-3 expression.

Example 5 Endothelial cells are a possible source of Galectin-3 containing plasma derived microvesicles. Since endothelial cells line the vasculature and secrete a large variety of factors to the circulation, it was examined whether they also secrete Galectin-3. Therefore MVs were isolated from the supernatant of human umbilical vein endothelial cells (HUVECs) after a 48 h secretion period by differential

centrifugation. Electron microscopy confirmed the isolation of membrane vesicles smaller than 120 nm in diameter and positive for CD63, which is an established microvesicular marker. In addition, the presence of CD63 positive MVs in conditioned medium was confirmed by Western blot. Subsequently, Western blot of CD63 positive MVs isolated from the cell culture supernatant revealed that Galectin-3 is indeed a component of CD63 positive MVs derived from endothelial cells.

Example 6 Endothelial microvesicles deliver genetic information to adipose-derived mesenchymal stem cells

In order to test whether endothelial MVs have the ability to interact with and transfer their cargo to MSCs, transiently transfected GFP-expressing HUVECs were prepared. 24 hours after transfection, HUVECS were washed twice and medium was changed in order to ensure the removal of remaining vector constructs in the supernatant. After a secretion period of 48 hours, MVs were isolated from cell culture supernatant of transfected or untransfected HUVECs.

Subsequently, ASCs were exposed to MVs for 3 days. Compared to MVs of untransfected cells, MVs isolated from GFP-transfected cells contained GFP mRNA as shown by qPCR and ASCs exposed to GFP-MVs showed GFP signals in a punctuate pattern within the cytoplasm compared to ASCs exposed to MVs of untransfected HUVECs, which showed no fluorescent signal No transfer of GFP was observed in the negative control. The obtained results indicate that a genetic transfer between endothelial derived MVs and ASCs is indeed possible.

Example 7 Microvesicles of senescent endothelial cells fail to induce osteogenic differentiation capacity . Since senescent endothelial cells were shown to accumulate with age *in vivo*, it was tested whether MVs of senescent cells effect the differentiation capacity of ASCs differently when compared to MVs of early passage cells. After a secretion period of 48 hours, MVs smaller than 200 nm in diameter were isolated from cell culture supernatant of HUVECs at an early population doubling level, at quiescence as well as from HUVECs at replicative senescence. HUVECS were passaged to 52 population doublings before irreversible growth arrest and morphological changes were observed. Replicative senescence of HUVECs was additionally confirmed by beta-galactosidase staining. During the secretion period, no differences in the number of apoptotic cells between the early population doubling

and the replicative senescent culture was observed, thereby excluding that an observed effect might result from a larger share of apoptotic cells within the senescent cell culture.

Subsequently, ASCs were seeded 24 hours before exposing them to MVs isolated from cell culture supernatant of senescent or early passage quiescent HUVECs, and induced to undergo osteogenesis after a period of 72 hours. Osteogenic differentiation of ASCs incubated with MVs derived from replicative senescent cells was reduced to 50%, as quantified by Alizarin staining and by reduced ALP mRNA expression levels.

Example 8 Vesicular Galectin-3 influences osteogenic differentiation capacity

In order to test if elevated microvesicular Galectin-3 levels indeed contribute to an enhanced osteoblastogenesis, HUVECs were transfected with Galectin-3 or the corresponding empty vector control. 24 hours after transfection, HUVECS were washed twice and medium was changed in order to ensure the removal of remaining vector constructs in the supernatant. After a secretion period of 48 hours, MVs were isolated from cell culture supernatant of transfected or untransfected HUVCEs.

Overexpression of Galectin-3 was confirmed by Western blot. Subsequently, MVs of HUVECS transfected with Galectin-3 or with empty control vector were isolated and co-incubated with ASCs for 72 hours before osteogenic differentiation was induced. Exposure of MVs isolated from Galectin-3 overexpressing HUVECs to ASCs caused a doubling of calcium depositions as quantified by Alizarin Red staining, indicating that vesicular Galectin-3 level indeed impact on the osteogenic differentiation capacity of ASCs.

Claims

1. A composition for the treatment and prophylaxis of disorders associated with aberrant bone mineral density or for accelerating bone healing, comprising, in a therapeutically effective amount, an agent that alters the level of Galectin-3 in mesenchymal stem cells, wherein said agent is selected from the group of

a) agents with the ability to increase the level of Galectin-3 in mesenchymal stem cells, selected from

i. Galectin-3 or fragments or variants or derivatives thereof, or

ii. nucleic acid molecules encoding Galectin-3 or fragments or variants thereof; or

iii. cells containing one or more nucleic acid molecules defined in ii.;

b) agents with the ability to decrease the level of Galectin-3 in mesenchymal stem cells, selected from

i. agents inhibiting Galectin-3 expression in mesenchymal stem cells, or

ii. agents targeting the Serine 96 phosphorylation site of Galectin-3 protein, or

iii. dominant negative alleles of Galectin-3.

2. The composition of claim 1, wherein Galectin-3, or a fragment or variant thereof, is linked to a bone-targeting molecule.

3. The composition of claim 1, wherein Galectin-3, or a fragment or variant thereof, is contained in a delivery vehicle that is linked to a bone-targeting molecule.

4. The composition of claim 2 or 3, wherein said bone-targeting molecule is selected from the group of bisphosphonates, collagen-binding domains, lipids or acidic oligopeptides.

5. The composition of claim 3, wherein said delivery vehicle is selected from liposomes, nanoparticles or microspheres.

6. The composition of any one of claims 1 to 5 for the prophylaxis and treatment of disorders associated with a reduced bone mineral density.

7. The composition of any one of claims 1 to 5 for or prophylaxis of osteopenia or osteoporosis.

8. The composition of any one of claims 1 to 5 for local administration to accelerate bone healing, wherein said agent is incorporated in a matrix.

9. The composition of claim 8, wherein said matrix is a demineralised bone matrix, an autolyzed antigen-extracted allogenic bone matrix, a polylactic acid or polyglycolic acid homo- or heterodimer, a collagen matrix, fibrin or a hydrogel.

10. The composition of claim 1, wherein said agent a) ii. is naked DNA or RNA.

11. The composition of claim 1, wherein said agent a) ii. is a DNA molecule inserted in a vector.

12. The composition of claim 1, wherein said agent a) iii. is a mesenchymal stem cell genetically engineered to overexpress Galectin-3.

13. Galectin-3, or a fragment or variant thereof, linked to a bone-targeting molecule.

14. The use of Galectin-3, or a fragment or variant thereof, for the treatment or prophylaxis of disorders associated with decreased bone mineral density.

15. The use according to claim 14, wherein said disorder is osteopenia or osteoporosis.

16. A method for the treatment of disorders associated with decreased bone mineral density, said method comprising administering a composition, containing, as the active agent, an agent with the ability to increase the level of Galectin-3 in mesenchymal stem cells, wherein said agent is selected from

i. Galectin-3 or fragments or variants or derivatives thereof, or

ii. nucleic acid molecules encoding Galectin-3 or fragments or variants thereof; or

iii. cells containing one or more nucleic acid molecules defined in ii.

17. A method for the treatment of disorders associated with increased bone mineral density, said method comprising administering a composition, containing, as the active agent, an agent with the ability to decrease the level of Galectin-3 in mesenchymal stem cells, wherein said agent is selected from

i. inhibitors of Galectin-3 expression in mesenchymal stem cells, or

ii. agents targeting the Serine 96 phosphorylation site of Galectin-3 protein, or

iii. dominant negative alleles of Galectin-3.

18. The method of claim 17, wherein said disorder is osteopetrosis.

19. A method of diagnosing in a subject a disorder associated with an aberrant bone mineral density, comprising determining said subject's Galectin-3 level

a) in microvesicles purified from plasma, or

b) directly in plasma.

20. The method of claim 19, wherein the Galectin-3 level is determined by an enzyme-linked immunosorbent assay (ELISA).

21. The method of claim 19 or 20, wherein a reduced Galectin-3 level is indicative of osteopenia or osteoporosis.

22. An assay to determine the Galectin-3 level for use in a method for the diagnosis of disorders associated with a decreased bone mineral density.

Abstract

The invention relates to compositions and methods for the treatment, prophylaxis and diagnosis of disorders associated with aberrant bone mineral density. More particularly, the invention relates to increasing Galectin-3 levels in mesenchymal stem cells to increase osteogenesis. Compositions comprising Galectin-3 or nucleic acids encoding Galectin-3 may be administered systemically or locally and are useful for the treatment of diseases like osteoporosis and for accelerating bone healing. The

invention also relates to methods for diagnosing bone diseases, wherein the level of Galectin-3 is measured.

Appendix G: Submitted manuscripts

Secreted microvesicular miR-31 inhibits osteogenic differentiation of mesenchymal stem cells

Elisabeth Schraml[1, *], Sylvia Weilner[1,3,11 *], Matthias Wieser[1,2], Paul Messner[4], Karl Schneider[1,3], Klemens Wassermann[1,3], Lucia Micutkova[5], Klaus Fortschegger[6], Andrea B. Maier[7], Rudi Westendorp[8], Heinrich Resch[10], Susanne Wolbank[3,9], Heinz Redl[3,9], Pidder Jansen-Dürr[5], Peter Pietschmann[10], Regina Grillari-Voglauer[1,2,11] and Johannes Grillari[1,11,#]

* Equally contributed to this study

[1] Department of Biotechnology, BOKU - University of Natural Resources and Life Sciences Vienna, Muthgasse 18, 1190 Vienna, Austria

[2] ACIB Muthgasse 18, 1190 Vienna

[3] Ludwig Boltzmann Institute for Experimental and Clinical Traumatology, AUVA Research Center, Donaueschingenstrasse 13, A-1200 Vienna, Austria

[4] Department of NanoBiotechnology, Vienna Institute of BioTechnology, University of Natural Resources and Life Sciences Vienna, Austria

[5] Institute of Biomedical Aging Research, Austrian Academy of Sciences, Austria

[6] Children's Cancer Research Institute (CCRI), St. Anna Kinderkrebsforschung, Vienna, Austria

[7] VU University Medical Center, Department of Internal Medicine, Section of Gerontology and Geriatrics, Amsterdam, the Netherlands

[8]Department of Gerontology and Geriatrics, Leiden University Medical Center, Leiden, the Netherlands

[9] Austrian Cluster for Tissue Regeneration, Austria

[10] Department of Pathophysiology and Allergy Research, Center of Pathophysiology, Infectiology and Immunology, Medical University of Vienna, Vienna, Austria

[11] Evercyte GmbH, Muthgasse 18, 1190 Vienna, Austria

#Johannes Grillari, Institute of Applied Microbiology, University of Natural Resources and Applied Life Sciences, Vienna, Muthgasse 18, 1190 Vienna
Tel: +43 1 36006 6230, FAX +43 1 3697615
Email: johannes.grillari@boku.ac.at

HIGHLIGHTS:

►Microvesicles impact on osteogenic differentiation of adipose tissue derived mesenchymal stem cells ►MiR-31 is present in high levels in microvesicles of replicative senescent endothelial cells and of elderly donors ►MiR-31 inhibits osteogenic differentiation by knocking-down its target FZD3 ►FZD3 is robustly induced early during osteogenic differentiation ►MiR-31 might be a plasma-based biomarker for age/age-associated diseases

Summary

Damage to cells and tissues is one of the driving forces of aging and age-related diseases. To counteract this functional decline, various repair systems are in place. Especially the property of adult stem cells to self-renew and differentiate is essential for homeostasis and regeneration of tissues and organs. However, not only their functionality declines with age[1], but also the systemic environment of the elderly negatively impacts on them, either by circulating factors that inhibit stem cell functions, or by the absence of factors that would be needed to support it[2,3]. However, such factors, sources and molecular mechanisms involved are not well understood yet. Consequently gaining insights into the aging systemic environment and its impact on stem cell regulation might be a key for the successful application of cell based therapies for the elderly.

Here we found miR-31 to be such a factor, present at elevated levels in the plasma of elderly and of osteoporosis patients. As a potential source of its secretion, we identified senescent endothelial cells, which are known to increase during aging *in vivo*[4]. We demonstrate that endothelial miR-31 is secreted within microvesicles and taken up by mesenchymal stem cells where it inhibits osteogenic differentiation.

Therefore, we suggest that microvesicular miR-31 in the plasma of elderly might play a role in the pathogenesis of age related impaired bone formation and that miR-31 might be a valuable plasma-based biomarker for aging and for a systemic environment that does not favor cell based therapies whenever osteogenesis is a limiting factor.

Introduction

Various repair systems at the tissue level are at work that counteract the functional decline driving and accompanying the organismal aging process, such as adult stem cells[5]. However, also stem cell functionality declines with age, due to both intrinsic and extrinsic factors[5]. Specifically, extrinsic factors circulating in the blood do influence stem cell behavior in aging of organisms[6]. Since senescent human cells are known to have an altered secretory behavior termed senescence-associated secretory phenotype (SASP), such extrinsic factors that inhibit tissue repair and regeneration might be provided by senescent cells. Indeed, the importance of senescence *in vivo* was demonstrated recently, as removal of senescent cells postpones the onset of age-associated diseases[7], similar to the anti-aging effects obtained by re-elongation of eroded telomeres[8].

Specifically, endothelial cells (ECs) line the blood vessels and senescent ECs are known to accumulate in the vessel wall [4,9], suggesting that senescent endothelial cells may secrete specific factors impacting on the systemic environment during aging. Unlike SASP of human fibroblasts[10], very little data are yet available on the endothelial SASP (eSASP).

Results

To address the possibility that components of the eSASP would influence mesenchymal stem cell (MSC) function, adipose derived MSCs (ASCs) were exposed to conditioned media derived from senescent or quiescent early passage human umbilical vein endothelial cells (HUVECs) for 3 days before inducing osteogenic differentiation. Alizarin Red S staining for Ca^{2+} deposition was performed 21 days after induction. ASCs were isolated from different donors, showed typical morphology (Fig. S1A) and stained positive for adult mesenchymal as well as negative for typical hematopoietic stem cell marker (Fig. S1B). Senescent endothelial cells were growth arrested, showed a large flattened morphology and stained positive for SA-β-gal activity (Fig. S1C) as published earlier [11]. No significant increase in apoptosis was observed during the 48h period of secretion under all experimental conditions (Fig. 1A) thereby excluding effects mediated by apoptotic vesicles. Senescent endothelial cell supernatants decreased the osteogenic differentiation of ASCs (Fig. 1B) compared to ASCs exposed to conditioned medium

of early passage HUVECs as visualized by staining for Ca^{2+} deposition using Alizarin Red S staining.

Recently microvesicles (MVs) were discovered to be secreted *in vitro* by various cell types but also to be present in body fluids such as blood as reviewed by Mathivanan and coworkers[12]. They serve as vehicles for RNA and proteins and enable a protected and targeted transport from the donor to the recipient cell, thereby representing a new type of cell-cell communication[12]. We isolated the fraction containing microvesicles below 220 nm in size by differential centrifugation[13], hereinafter referred to as total MV fraction, from cell culture supernatant of quiescent, early passage HUVECs and of replicatively senescent HUVECs in order to narrow down the fraction of supernatant containing the osteogenesis inhibitory activity. Electron microscopy confirmed the isolation of membrane vesicles, which were smaller than 100 nm in size (Fig. 1C), and reacted positive for CD63 staining (Fig. 1D), a transmembrane protein and established microvesicular marker[14]. In addition, the presence of CD63 positive MVs in the total MV fraction isolated from conditioned medium was confirmed by Western blot (Fig. S1B)

ASCs were then exposed to total MV fraction isolated from conditioned media of senescent or early passage derived HUVECs for 3 days before osteogenesis was induced (Fig 1E). Indeed, osteogenic differentiation of ASCs incubated with MVs of senescent cells was significantly decreased, as shown by a reduction of calcium deposition (Fig 1F, G) and by decreased expression of the osteogenic marker gene alkaline phosphatase (ALP) (Fig. 1H) compared to ASCs exposed to MVs secreted by quiescent early passage endothelial cells.

In order to confirm that the osteogenesis inhibitory activity of the total MV fraction indeed resides in the MVs and not in protein aggregates that might co-sediment, we depleted the pellet fraction after ultracentrifugation from CD63 positive MVs by immuno-affinity capture (Fig. 1I) using anti-CD63 antibody coupled beads, hereinafter referred to as $CD63^-$ fraction. Successful separation of the CD63 containing fraction was confirmed by Western blot when total MV fraction was compared to CD63 negative fraction (Fig. 1J) as well as by comparing the eluted $CD63^+$ fraction against $CD63^-$ fraction (Fig. 1K). In order to control, if depletion of the $CD63^+$ microvesicles also rescues the inhibitory effect of the MVs isolated from senescent HUVECs, ASCs were exposed to the total MV fraction, or the $CD63^-$ fraction, as outlined in Fig. 1I.

Subsequently osteogenic differentiation was induced and quantified by changes in ALP mRNA as marker. Indeed, the inhibitory activity of the senescent cell derived total MV fraction was depleted with the depletion of CD63 positive microvesicles (Fig 1L) indicating that the inhibitory activity is mediated by senescent HUVECs derived CD63 positive MVs.

Since miRNAs have been reported to be packaged into MVs[15], we analyzed the expression of age-related miRNA species[16] in MVs derived from early quiescent versus senescent cells and focused on miR-31 since it is upregulated intracellulary in senescent HUVECs[16] and since it recently turned out to be a master regulator of osteogenesis by targeting Runx2[17], Osterix[18] and SATB2[19] . We confirmed that miR-31 is upregulated in HUVECs during both replicative (Fig. 2A) and stress-induced senescence (Fig. S2C, D), as well as in senescent human liver endothelial cells (Fig. S2A) and human retinal microvascular endothelial cells (Fig. S2B) compared to corresponding quiescent early passage cells. In addition, miR-31 expression was increased in conditioned medium (Fig. 2B) and in MVs (Fig. 2C) derived from replicatively (Fig. 2B-C) as well as from stress induced (Fig. S2E) senescent HUVECs compared to quiescent, early passage cells. In particular, microvesicular miR-31 was found to be enriched in the total MV fraction (~4 fold) (Fig. 2D) compared to the $CD63^-$ fraction isolated from senescent endothelial cells, suggesting that the majority of endothelially secreted miR-31 is secreted within CD63 positive MVs. Its localization within MVs was additionally confirmed by electron microscopy of in situ hybridized samples (Fig. 2E). In order to test, if miR-31 alone is sufficient to inhibit osteogenic differentiation of ASCs, we then proceeded to transiently transfect ASCs with miR-31 mimicks. Transfection success was confirmed by qPCR (Fig. S3A). Indeed, miR-31 alone was sufficient to significantly inhibit osteogenic differentiation by ~50% as visualized and quantitated by Alizarin Red S staining (Fig. 3A, B), as well as by decreased expression of osteocalcin (OC) mRNA (Fig. 3C). This is supported by our findings that miR-31 overexpression in both C3Ht101/2 and C2C12 cells, representing two established mouse model systems of osteogenic differentiation[20], resulted in an anti-osteogenic effect as well (Fig. S3C and S3D).

MiR-31 regulates FZD3, a Wnt5A receptor, in the context of breast cancer invasiveness[21], and we observed that FZD3 mRNA was also downregulated upon miR-31 transfection in ASCs (Fig. 3D). In order to test whether FZD3 has a crucial

role in osteogenesis we compared FZD3 mRNA levels of differentiated versus undifferentiated ASCs and found that FZD3 mRNA is upregulated during osteogenesis 4 days after induction compared to non-differentiating ASCs (Fig. 3E). To address the question, if depletion of FZD3 mRNA would be sufficient to inhibit osteogenesis, FZD3 gene expression was silenced by specific siRNA (Fig. S3B), which led to a significant inhibition of osteogenesis compared to non targeting siRNA transfected cells (Fig. 3F).

In order to test whether endothelial derived MVs are able to interact with and to release their content into ASCs and thus transfer microRNAs from endothelial cells to ASCs, HUVECs were transfected with cel-miR39, a *Caenorhabditis elegans* miRNA with no homologue in humans[22]. MVs isolated from transfected HUVECs were added to ASCs and indeed, intracellular cel-miR39 levels of ASCs increased with exposure time (Fig. 3G) and microvesicular dose (Fig. 3H).

To see, if miR-31 might be transferred to ASCs as recipient cells via MVs as well, we exposed ASCs to senescent or early passage cell derived MVs. Indeed, exposure to senescent cell derived microvesicles resulted in a 3-fold increase of miR-31 levels in ASCs (Fig. 3I) compared to ASCs exposed to quiescent early passage HUVECs, accompanied by a decrease in FZD3 mRNA (Fig 3J).

To test, if microvesicularly transferred miR-31 is crucial to confer the inhibitory effect of senescent HUVECs derived MVs on osteogenic differentiation, we pre-transfected ASCs using anti-miR-31 or a non targeting anti-miRNA as control, 24h before exposing them to the total MV fraction isolated from conditioned medium of senescent HUVECs. Transfection success of antimiR-31 was confirmed (Fig S3E). Anti-miR31 transfection indeed rescued the inhibition of osteogenic differentiation, mediated by MVs of senescent HUVECs, as quantified by Alizarin Red S staining (Fig. 3K) and qPCR of OC mRNA (Fig. 3L). Moreover, antimiR-31 transfection of ASCs also rescued the decrease of FZD3 mRNA levels upon treatment of ASCs with MVs (Fig. 3M). In order to exclude the possibility that the observed restored osteogenic differentiation capacity results from the antimiR-31 transfection we transfected ASCs with antimiR-31 or a non targeting anti-miRNA as control without exposing them to MVs. AntimiR-31 transfection of ASCs alone had no significant influence on osteogenic differentiation capacity as shown by Alizarin Red S staining (Fig. 3K), and on OC (Fig. 3L) und FZD3 (Fig. 3M) mRNA level.

Since senescent cells accumulate with age *in vivo*, and since endothelial cells line the vasculature, we were curious to see whether miR-31 might also be secreted to the circulation. We did not observe large differences in miR-31 levels in plasma of young donors. However, we did observe large variations and a subpopulation with significantly increased miR-31 plasma levels in the group of women older than 50 years (Fig. 4A).

We reasoned that if high miR-31 is related to decreased bone formation we might expect upregulated plasma miR-31 levels also in osteoporotic patients. Indeed, miR-31 levels in plasma derived from male osteoporosis patients was significantly increased compared to healthy age matched controls (Fig. 4B).

Based on these results, we addressed the question if microvesicles isolated from elderly individuals with high miR-31 levels in the plasma would also inhibit osteogenesis. Therefore, we isolated MVs from human blood plasma and performed electron microscopy to confirm size and shape (Fig. 4C). Indeed, total MV fraction derived from elderly donors failed to induce osteogenic differentiation compared to MVs isolated from plasma of young individuals (Fig. 4D and E). In order test, if the inhibitory activity of the total MV fraction isolated from elderly donors again resides in the CD63 positive MVs, we depleted them from the total MV fraction by affinity purification. Coincubation of ASCs with the $CD63^-$ fraction of an elderly donor resulted in an enhanced osteogenic differentiation capacity compared to ASCs exposed to the total MV fraction as confirmed by quantification of Ca^{2+} depositions (Fig 4F) and qPCR of ALP mRNA (Fig 4G) indicating that the inhibitory activity again resided in the CD63 positive MV fraction.

Finally, we confirmed that even in the case of ex-vivo derived MVs of elderly donors miR-31 is a crucial, osteogenesis impacting microvesicular factor, since antimiR-31 transfection of ASCs prior to total MV fraction exposure rescued the inhibitory effect of plasma derived MVs as quantified by Alizarin Red S staining (Fig. 4H), ALP (Fig. 4I) as well as OC (Fig. 4J) mRNA levels. In addition FZD3 mRNA levels were restored (Fig. 4K).

Discussion

Here, we set out to identify factors that contribute to the negative effect of the aged systemic environment on the functionality of adult stem cells[23]. With regard to bone and its regeneration capacity mesenchymal stem cells give rise to bone forming osteoblasts but there is evidence that their osteogenic differentiation capacity decreases with age[24,25]. Therefore we focused on extracellular factors impacting on osteogenic differentiation capacity of ASCs. Besides well-known factors like the growth hormone or estrogen whose level decline with age and contribute to impaired bone formation hardly any other circulating factors are known in this context [26,27]. We hypothesized that such factors might be provided by microvesicles (MVs) that are known to be contained in most body fluids [12]. Recently circulating MVs were not only shown to stabilize and protect their cargo efficiently from degradation but also to contribute to a directed and highly specific cell-cell communication [12,28].

As potential source of factors impacting on stem cell fate we focused on the microvesicular secretome of endothelial cells (ECs) for several reasons: (i) ECs line the vasculature and are thereby able to secret factors into the circulation. (ii) Senescent ECs which were shown to exhibit an altered intracellular expression profile compared to early passage quiescent cells *in vitro* were also observed *in vivo* [9,29,30]. (iii) MSCs are in close proximity to ECs within the bone [31,32]. In such microvesicles derived from senescent ECs, we found that miR-31 is enriched within secreted CD63 positive MVs of replicatively and stress induced senescent ECs and that miR-31 transferred via microvesicles is conferring the osteogenesis inhibiting activity of senescent cell derived microvesicles. These findings demonstrate that not only the transcription of miRNAs[16] but also their secretion changes when cells enter senescence. That this *in vitro* observation might also be relevant *in vivo* is supported by many publications which report on alterations in the level and composition of circulating miRNAs associated with various health problems such as tumors or age-associated diseases [33-36]. But how many microvesicles in the circulation might derive from the endothelium? Current estimates suggest that up to 8% of circulating microvesicles are derived from ECs in young mice [15] and humans [37]. However, the amount of microvesicles released by ECs might be larger than initially expected due to sampling artifacts. In addition, the number of microvesicles secreted by senescent cells [38],which might be caused by p53 activation [39] is higher than from early passage cells. This would also suggest that in elderly organisms the relative amount of

microvesicles derived from senescent ECs might be even higher. Due to these data indicating the *in vivo* relevance of circulating microvesicles, we tested if miR-31 high plasma levels are also found in elderly individuals. Indeed, miR-31 turned out to be upregulated in elderly donors as well as in patients suffering from osteoporosis. Furthermore our data show that vesicular miR-31 is contributing to the osteogenesis inhibiting property of microvesicles isolated from plasma of elderly donors.

The observation of this study that antimiR-31 transfection of ASCs alone had no effect on osteogenesis, explainable by the observation that ASCs exhibited relatively low intracellular miR-31 levels, but that transfection of ASCs exposed to MVs had a positive effect on osteoblastogenesis emphasizes once more the importance of the stem cell environment.

MiR-31 turned out as a master regulator of osteogenesis recently. Specifically, its inhibition by antimiR-31 in bone marrow stromal stem cells seeded onto a scaffold in a critical-sized calvarial defect in rats leads to more new bone formation compared to non-targeting control transfected cells [40]. This effect might be mediated by de-repression of its already known osteogenesis relevant targets Runx2 [17], Osterix [18] and SATB2 [19], to which we here add FZD3 mRNA, a validated target of miR-31 in the field of breast cancer metastasis [21] and a member of the non-canonical Wnt signaling pathway [41]. Since FZD3 is robustly upregulated 4 days after induction of osteogenic differentiation, it might well turn out as a novel early marker of osteogenesis, as it was also found to increase during osteogenesis by other studies [42].

Taken together these data support our hypothesis that decreased osteogenesis *in vivo* might be caused by secreted and circulating microvesicles high in miR-31. Their uptake into MSCs might then lead to impaired osteoblastogenesis which in turn might shift the delicate balance between bone forming osteoblasts and bone resorbing osteoclasts to the osteoclast resulting in reduced bone mineral density and bone quality (Fig. 4L).

Finally, we show for the first time that microvesicles from senescent cells contribute to an aged systemic environment that fails to support tissue regeneration. Thus miR-31 might represent a biomarker and therapeutic target for conditions/diseases whenever osteoblast differentiation is a limiting factor. Finally, we also suggest that understanding and controlling the systemic environment might turn out to be a key

factor for the success of stem cell based medicine, especially in regard to age associated diseases.

Experimental procedures

Cell culture

Human umbilical vein endothelial cell (HUVEC)

Endothelial cells were isolated from human umbilical veins as described [13,49] HUVECs were cultivated in gelatin precoated flasks in M199 with Earle's salts supplemented with 4 mM glutamine, 15% fetal calf serum (FCS) and 10% endothelial cell growth supplement (ECGS) containing 170 U/ml heparin at 37°C in a humidified atmosphere with 5% CO_2. Cells were passaged once or twice a week at a split ratio of 1:2 to 1:4 according to the growth rate. HUVECs were cultivated to senescence and stained for senescence associated β-galactosidase (SA-β-gal) activity as described previously [13]. For collection of supernatants, contact inhibited (quiescent, PD19) and senescent (PD53 / 95% SA-β-gal positive) cells were allowed to secrete into ASC or HUVEC medium, depending on the experiment, for 48 hours.

Human adipose-derived stem cells (ASCs)

Subcutaneous adipose tissue was obtained during outpatient tumescence liposuction under local anesthesia with patient consent. ASCs were isolated as described before [18,50] and cultured in DMEM-low glucose/HAM´s F-12 supplemented with 4mM Lglutamine,10% fetal calf serum (FCS, PAA) and 1ng/mL recombinant human basic fibroblast growth factor (rhFGF, R&D Systems) at 37°C, 5% CO_2 and 95% air humidity. Cells were passaged once or twice a week at a split ratio of 1:2 according to the growth rate.

C2C12 and C3Ht101/2

The mouse skeletal osteo/myoblast cell line (C2C12) obtained from ATCC were cultured in Dulbecco's Modified Eagle's Medium (DMEM) high glucose,supplemented with 5% heat inactivated fetal calf serum (FCS) and 2 mmol/L Lglutamine at 37°C in a humidified atmosphere with 5% CO2.

Mouse embryonic fibroblast cells C3Ht10 1/2 obtained from ATCC were cultured in DMEM/Ham´s F-12 containing 10% FCS at 37°C in a humidified atmosphere with 5%

CO_2.

Induction of osteogenic differentiation in ASCs

All differentiation protocols were carried out in 24 well cell culture plates. For osteogenic differentiation ASCs were seeded at a density of $2x10_3$ cell per well. 72 hours after seeding cells were incubated with osteogenic differentiation medium (DMEM-low glucose, 10% FCS, 4mM L-glutamine, 10nM dexamethasone, 150µM ascorbate-2-phosphat, 10mM β-glycerolphosphate and 10nM vitamine-D3) up to 4 weeks.

Osteocalcin specific reporter gene assay

The influence of miRNA-31 transfection on osteogenic differentiation was analyzed using the C2C12 and C3Ht10 1/2 cell line in conjunction with an osteocalcin specific reporter gene assay [26]. C2C12 and C3Ht10 1/2 cells are capable of differentiating to the osteogenic lineage upon treatment with recombinant BMPs, which is observable by the induction of alkaline phosphatase, osteocalcin and other osteoblast specific genes. The cells, seeded in a T175, were first transfected with 99 µg of the osteocalcin reporter system and after 24 h reverse transfected with 30 nM miRNA-31, antimiR-31 or scrambled miRNA control #2 as control using Ambions siPORT™ *Neo*FX™. Osteogenic differentiation was induced using 100ng/ml or 300ng/ml recombinant BMP2 (InductOS, Pfizer), controls were not induced with growth factor. Osteocalcin reporter activity was assessed after 6 days of differentiation by determining Metridia luciferase activity in the cell culture supernatants using Clontech Ready-To-Glow Secreted Luciferase System Kit. On day 12 Alizarin Red S staining was performed to further analyze the degree of differentiation as described subsequently.

Alizarin Red S Staining

For Alizarin Red S staining of calcified structures, cells were fixed for 1 hour in 70% ethanol at -20°C. After brief rinsing, cells were stained for 20 minutes with 40mM Alizarin Red S solution (Sigma) and washed with PBS. For quantification Alizarin Red S was extracted for 30 minutes using 200µl 0.1M HCL/0.5% SDS solution. The extracted dye was measured at 425nm.

Transfections

ASCs were transfected using siPORT™ *Neo*FX™ transfection reagent (Applied Biosystems). Cells were transfected with 10nM precursor hsa-miR-31, antimiR-31 or scrambled miRNA control #2 (Ambion) according to the manufacturer's protocol. Three days after transfection, differentiation was started as described before. 100 nM FZD3 siRNA (Dharmacon, L-005502-00-0005) and siRNA control were transfected with Dharmafect 1 (Dharmafect) according to manufactures protocol.

Assessment of apoptotic cell death

HUVECs were seeded in 12-well cell culture plates and were allowed to secrete into ASC or HUVEC medium for 48 hours. Thereafter, the cells were detached using 50mM EDTA and stained with Annexin V- FITC and PI (Roche) according to the manufacturer´s instructions. Analysis of the percentage of apoptotic and necrotic/late-apoptotic cells were performed using a FACS-Calibur and the CellQuest software (Becton Dickinson).

Induction of stress induced premature senescence

SIPS was induced by tBHP treatment of HUVECs on 5 consecutive days for one hour each by adding tBHP to a final concentration of 35 µM, 50 µM or 75 µM in the medium. Permanent growth arrest was induced by 75 µM tBHP as assessed by microscopic follow up for 14 days. Supernatants were collected, centrifuged at 1900g, 4°C and used freshly for MV preparation or stored at -80°C. Supernatant volumes were normalized to the number of HUVECs at the time of supernatant harvest. Cell culture medium incubated for 48 hours at 37°C was used as additional control.

Quantitative real-time PCR

Alizarin Red S stainings were confirmed using different osteogenic differentiation marker genes. Therefore total ASCs RNA was isolated using Trizol (Invitrogen) at different time points before and during osteogenesis. 7 days after differentiation start the early osteogenic marker alkaline phosphatase (ALP) was used, 21 days after differentiation start the late osteogenic marker osteocalcin (OC) was used. Reverse transcription was performed using DyNAmo cDNA Synthesis Kit (Biozym) and qPCR was performed using the RotorGene2000 (Corbett).

For miRNA analysis specific TaqMan assays (Applied Biosystems) were used according to manufactures protocol.

For isolation of RNA from blood samples, 250-500µl serum was used to isolate total RNA using Trizol LS reagent (Invitrogen). To allow for normalization of sample to sample variation in RNA isolation, 25fmol synthetic C-elegans miRNAs cel-miR-39 were added before isolation. Serum samples (12 healthy old donors and 17 healthy young donors) were obtained from R. Westendorp, Department of Gerontology & Geriatrics C2-R, Leiden University Medical Center, The Netherlands or C. Gabriel, Blutzentrale, Linz. Osteoporotic serum samples were obtained from Heinrich Resch, Department of Medicine 2, St. Vincent Hospital, Austria. Institutional ethics committees approved the study, and written, informed consent has been obtained from each subject.

Microvesicle (MV) purification

MV were purified by filtration and differential centrifugation as described previously [44]. In brief, supernatants were collected after incubation of 48 hours. Conditioned media were centrifuged at 500g for 15 minutes to sediment cells and at 14.000g for 15 minutes to eliminate cell debris and filtered through a 0.22µm filter. MVs were then sedimented by ultracentrifugation at 100.000g for 60 minutes and the resultant pellet was washed with PBS. MV were used as fresh preparations for electron microscopy or conserved at -80°C for further analysis. For differentiation studies MV derived from $2x10^4$ HUVECs or 1 ml of human serum were resuspended in 50µl PBS and added per well ASCs.

Depletion of CD63 positive microvesicles

Preparation of Immunoaffinity Capture Microbeads

CD63 monoclonal antibody immunoaffinity capture microbeads (Dynabeads® M-270 Epoxy, Invitrogen) were prepared using Dynabeads® Antibody Coupling Kit (Invitrogen) according to the manufacturer's protocol. Briefly 5 mg of Dynabeads were washed with 1 ml of C1 solution. The supernatant was removed by magnetic sedimentation of the beads and 50µl of monoclonal CD63 antibody (ab8219 Abcam) were mixed with 200 µl of C1 solution. Washed beads were first mixed with prepared antibody solution and 250µl of C2 solution were added afterwards. Beads were incubated at 37°C on a roller overnight.

The next day supernatant was removed by placing the tube on a magnet whereby beads were able to collect at the tube wall. Afterwards beads were washed with each 800µl of HB, LB and finally SB buffer and stored at 4°C until use.

Purification of CD63 positive microvesicles by immunoaffinity capture microbeads

Isolated MVs were incubated with CD63 antibody coupled Dynabeads for 2 h at 4°C on a roller. Afterwards the tube was placed on a magnet allowing the beads to collect at the wall. Supernatant containing MV depleted of CD63 positive MVs was decanted. MV depleted of CD63 positive MVs derived from $2x10^4$ HUVECs or 1 ml of human serum were resuspended in 50µl PBS and added per well ASCs.

CD63 positive MVs were eluted through incubation of beads with 140 µl of citric acid pH=3. The tube was placed on a magnet allowing the beads to collect at the wall. Supernatant containing CD63 positive MVs was decanted and immediately mixed with 50 µl of 1M NaOH for neutralization. CD63 positive MVs derived from $2x10^4$ HUVECs or 1 ml of human serum were resuspended in 50µl PBS and added per well ASCs.

Electron microscopy

Purified MVs were left to absorb on coated nickel grids (200 mesh, hexagonal, Pioloform-coated Athene nickel grids). After fixation with 4% paraformaldehyde MVs were stained with 2% uranyl acetate for 30 seconds, the grids were left to dry and the absorbed material was visualized using transmission electron microscopy (TEM), (Philips model CM 12 electron microscope, Philips, Eindhoven, NL).

For electron microscopy *in-situ* hybridization (EM-ISH) MV pellets were permeabilized with 0.1% Triton-X for 5 minutes at room temperature. After washing with PBS MVs were incubated for at least 4 hours with hybridization buffer as described previously [51]. For each sample 1pM of the LNA DIG-labelled single stranded probe (Exiqon, Denmark) was denaturated in denaturizing hybridization buffer (containing 50% formamide, 5x SSC, 5x Denhardt´s solution, 0.1% Tween, 0.25% CHAPS, 200µg ml^{-1} yeast RNA, 500µg ml^{-1} salmon sperm DNA) by incubation at 80°C for 5 minutes. Probes were placed on ice quickly. MV were mixed with the probe and hybridized at 50°C over night. After hybridization samples were washed stringently with 0.2 x SSC at 60°C for 1 hour. Subsequently, MVs were incubated with Anti-DIG antibody (Roche) for 30 minutes and an additional hour with the second 5nm gold particle labelled antibody (Sigma). After washing with PBS MV

were embedded in Epon, and 80 nm, on average, sections were cut using an ultramicrotom (Ultracut, Reichert) and then analyzed by transmission electron microscopy (TEM, Philips model CM 12 electron microscope ,Philips, Eindhoven, NL).

Western Blot

Total proteins and proteins from microvesicles as well as the fraction depleted of CD63 positive MVs were extracted and separated on polyacrylamide gels containing trihalo compounds , before transfer to a PVDF membrane (Roth, Germany). The membrane was blocked in 3% skimmed milk, incubated with the CD63 antibody (sc-15363 Santa Cruz). Alexa Fluor 680-conjugated anti-rabbit IgG (Molecular Probes) or peroxidase-coupled secondary antibody was used as secondary antibodies. Signal intensities were analyzed by using the Odyssey infrared image system (LiCor) or subjected to enhanced chemiluminescence using ECL Western Blotting Substrate (Pierce) on a Chemidoc (Biorad) respectively.

Osteoporosis Patients

14 men with idiopathic osteoporosis and a mean age ~53 years were studied. Osteoporosis was defined by the presence of low trauma fractures at vertebral or peripheral sites and/or by dual energy X rax absorptiometry (T-scores less than -2.5). In all subjects secondary causes of osteoporosis (such as glucocorticoid treatment, alcohol abuse or thyrotoxicosis) had been excluded by an appropriate clinical and laboratory evaluation.

Statistics

Data were statistically analyzed using Student´s *t* test, one-way ANOVA and one-way ANOVA followed by the Dunn´s method as indicated. Analyses were performed with SigmaPlot 10.0 (SigmaPlot, Germany). The tests were two-sided with type 1 error probability of 0.05. Data are presented as mean values ± SEM. Samples were not blinded systematically but repetitions of experiments were performed by different operators and methods having unbiased read-outs were.

Acknowledgements

We are grateful to Astrid Gillich, Andreas Gruber, Barbara Gepp and Florian Weiss for excellent technical assistance, Georg Feichtinger for providing the Osteocalcin reporter and Tim Hardman for proofreading of the manuscript.

This work has been supported by FWF Project P24498, the GEN-AU Project 820982 „Non-coding RNAs", FP7 project FRAILOMIC, as well as grants by the Herzfelder'sche Familienstiftung. The financial support by the Austrian Federal Ministry of Economy, Family and Youth and the National Foundation for Research, Technology and Development is gratefully acknowledged as well as financial support by Chanel Research and Technology.

Conflict of interest:

JG and RGV are co-founders of Evercyte GmbH, Vienna, Austria. A patent application describing miR-31 as a marker and therapeutic target in deranged bone metabolism has been filed.

Author contribution

Elisabeth Schraml: planning and performing experiments, writing
Sylvia Weilner: planning and performing experiments, writing
Matthias Wieser: planning of experiments
Paul Messner: planning and performing electron microscopy
Karl Schneider: performing experiments
Klemens Wassermann: performing experiments
Lucia Micutcova: providing ideas and reagents
Klaus Fortschegger: planning and performing experiments
Andrea B. Maier: planning and providing of serum samples
Rudi Westendorp: planning and providing of serum samples
Heinrich Resch: planning and providing of serum samples
Susanne Wolbank: planning and providing of mesenchymal stem cells
Heinz Redl: planning and providing of mesenchymal stem cells
Pidder Jansen-Dürr: planning and discussion
Peter Pietschmann: planning and providing of mesenchymal stem cells
Regina Grillari-Voglauer: planning and writing
Johannes Grillari: planning and writing

Figure Legends

Figure 1: CD63 positive Microvesicles (MVs) of senescent HUVECs reduce osteogenic differentiation capacity of ASCs

(A) Apoptotic cell death of early quiescent passage (PD21) or replicative senescent (PD49) HUVECs 48 hours after secretion into ASC or HUVEC medium was measured using Annexin V-FITC and PI staining (N=3) (B) Representative example of Alizarin Red S staining for Ca^{2+} deposition of ASCs exposed to conditioned media of early quiescent passage (Y), senescent (S) or unconditioned medium (C) as well as without switching to differentiation medium (undiff). Treated cells were induced to differentiate into the osteogenic lineage. Differentiation was visualized using Alizarin Red S staining for Ca^{2+} deposition at day 21 of differentiation. Representative pictures of 3 independent experiments are shown. (C) MVs were isolated from conditioned medium of HUVECs, prepared for EM imaging and stained by uranyl acetate. The EM image shows representative MV membrane vesicles of ~ 50 to 100 nm in diameter. (D) CD63 as marker of MVs was immunogold-labelled with anti-CD63 antibody (5 nm gold particles, see arrows) and visualized by electron microscopy. The dotted lines accentuate the border of selected MVs adsorbed to the coated Ni-grid after weak staining with uranyl acetate. (E) Time scheme of experimental design. ASCs were exposed to microvesicles from early quiescent passage (13 PD) or senescent (53PD) cells and unconditioned control medium for 3 days, then medium was changed to differentiation medium and Alizarin Red S staining for Ca^{2+} deposits was performed after 21 days. In addition quantitative qPCR for the osteogenic marker mRNA alkaline phosphatase (ALP) was performed after 7 days. (F-H) ASCs were preincubated in the presence of MVs derived from early quiescent passage (Y),senescent (S) cells or in the absence of exogenously added MVs (C) for 3 days before osteogenic differentiation was induced as well as without switching to differentiation medium (undiff). MVs were isolated freshly for each experiment from different HUVEC cell lines. (F) Representative images of Alizarin Red S stained ASCs of 3 independent differentiations after 21 days are shown. (G) Ca^{2+} deposition was quantitated using Alizarin Red S staining and spectrophotometric analysis at 425 nm. (H) Quantitative qPCR for ALP mRNA at day 7 after induction of differentiation relative to GAPDH was performed. Error bars indicate the standard deviations of 3 independent measurements. (I) Scheme of experimental design. After 48h of secretion, conditioned supernatant (SN) was

collected from senescent cells and centrifuged for 15 minutes at 500g. Next the supernatant was centrifuged at 14000 g für 15 minutes in order to remove all cell debris. The remaining supernatant was filtered through a 220nm filter before it was centrifuged for 1h at 100 000g. Subsequently the supernatant was discarded while the obtained MV containing pellet, referred to as total MV fraction (tMV), was resuspended in 2ml PBS. 1ml was loaded for 2h at 4°C on anti CD63 antibody coupled magnetic beads, while the remaining 1ml was stored at 4°C. After 2h of incubation tMV as well as the supernatant of the immune isolated fraction containing no CD63 positive vesicles, referred to as $CD63^-$ fraction ($CD63^-$), were centrifuged for 1h at 100 000g. Finally, the pellets of the tMV and of the $CD63^-$ fraction were resuspended in PBS and added to ASCs. (J) Western blot analysis of HUVEC cell lysate, the tMV fraction and the $CD63^-$ fraction using anti CD63 antibody. (K) Western blot analysis of the $CD63^-$ fraction as well as of eluted CD63 positive MVs ($CD63^+$) using anti CD63 antibody as well as an image of the corresponding gel before blotting showing proteins stained with trihalo compounds as a loading control. (L) Decreased osteogenic differentiation potential of ASCs exposed to isolated total MV fraction (tMV) of senescent endothelial cells compared to ASCs treated with CD63 negative fraction ($CD63^-$) as quantified by the early osteogenic differentiation marker ALP mRNA 7 days after induction of osteogenesis relative to GAPDH using qPCR.
ns: not significant, *: $p<0.05$, **: $p<0.01$, ***: $p<0.001$ in comparison to control. Data are presented as mean values ± SM and were statistically analyzed using Student´s *t* test.

Figure 2: MiR-31 is enriched in CD63 positive microvesicles of senescent endothelial cells

(A) MiR-31 expression is upregulated in senescent (S) versus early quiescent passage (Y) HUVECs (N=3) as analyzed by qPCR and normalized to the snRNA U6 as internal control. (B) Similarly, miR-31 was detected at high levels after RNA isolation from supernatants (SN) (N=3) and (C) from MVs of senescent (S) versus early quiescent (Y) passage HUVECs (N=3) as analyzed by qPCR and normalized to the secreting cell number and spiked in cel-miR39 as internal control. (D) Significantly increased miR-31 levels in total MV fraction (tMV) of senescent endothelial cells compared to the fraction which is depleted of CD63 positive MVs ($CD63^-$) as analyzed by qPCR and normalized to cel-miR39 as internal control (E)

Localization of miR-31 within MVs by electron microscopy in situ hybridization (EM-ISH). Arrowhead indicates immunogold labelled anti-DIG antibody after hybridizing a DIG labelled antimiR-31 probe to permeabilized MVs.

***: $p<0.001$ in comparison to control. Data of this figure are presented as mean values ± SM and were statistically analyzed using Student´s *t* test.

Figure 3: Vesicular MiR-31 reduces osteogenesis by knocking down FZD3 mRNA

(A-C) ASCs were transfected with miR-31 or a non-targeting miRNA control (miRC) as negative control 3 days before induction of osteogenic differentiation. As control, ASCs were not exposed to differentiation inducing medium (undiff). (A) Representative images of Alizarin Red S stained ASCs at day 21 of differentiation of 3 independent experiments are shown. (B) Osteogenic differentiation was quantitated by spectrophotometrical analysis of Alizarin Red S staining for Ca^{2+} deposition (n=3). (C) qPCR for the osteogenic marker osteocalcin (OC) at day 21 of differentiation normalized to GAPDH confirms inhibition of osteogenic differentiation after miR-31 transfection. (D) ASCs were transiently transfected with miR-31, non-targeting control (miRC) and non-transfected (untransf.) 3 days before induction of osteogenesis. 4 days later, FZD3 mRNA was quantified by qPCR and normalized to GAPDH. MiR-31 transfection of ASCs results in downregulated, FDZ3 mRNA compared to non-targeting control transfected cells. (E) FDZ3 mRNA is upregulated 4 days after osteogenic differentiation start as analyzed by qPCR relative to GAPDH. (F) Knockdown of FDZ3 by siRNAs (siFZD3) in ASCs inhibits osteogenic differentiation compared to non-targeting control transfected (siC) or untransfected (untransf.) cells as quantified by spectrophotometric analysis of Ca^{2+} deposition using Alizarin Red S staining at day 21 of differentiation. (G) Intracellular cel-miR39 levels of ASCs that were exposed to MVs isolated from cel-miR39 transfected HUVECs for 1, 12, 24 or 72 hours were quantified by qPCR relative to snRNA U6. (H) Intracellular cel-miR39 levels of ASCs that were exposed for 72 hours to MVs isolated from the indicated number of cel-miR39 transfected HUVECs or from non-targeting control (miRC) transfected HUVECs were quantified by qPCR relative to snRNA U6. Intracellular levels of miR-31 (I) and FZD3 mRNA (J) in ASCs after treatment with MVs for 72 hours derived from early quiescent passage (Y), senescent (S) HUVECs or control medium (C), were quantified by qPCR relative to snRNA U6 (I) or GAPDH (J) . (K-M) ASCs were transfected with antimiR-31 or a non-targeting miRNA control (antimiRC).

Either no or MVs of senescent HUVECs were added 24 hours post transfection. (K) Alizarin Red S stained calcium depositions were quantified by measuring the optical density at 425nm at day 21 of differentiation, (L) OC mRNA levels normalized to GAPDH were measured 21 days and (M) FZD3 levels relative to GAPDH 4 days after induction of osteogenic differentiaton by qPCR.
Error bars derived from 3 independent experiments. ND: non-differentiated.
ns: not significant, **: $p<0.01$, ***: $p<0.001$ in comparison to control. Data are presented as mean values ± SM and were statistically analyzed using Student´s *t* test.

Figure 4: Effects of plasma MVs derived from young and elderly donors on ASCs. (A) Upregulation of miR-31 levels relative to cel-miR39 as spike in control in plasma samples derived from healthy, female elderly donors (n=17) compared to young healthy controls (n=12). RNA was always isolated from the same volume of plasma (B) miR-31 levels relative to cel-miR39 as spike in control in plasma derived from male osteoporosis patients (n=14) were significantly increased compared to healthy age matched controls (n=11). RNA was always isolated from the same volume of plasma. (C) Microvesicles isolated from human plasma as analyzed by electron microscopy showing typical morphology. (D-E) ASCs were exposed to MVs derived from healthy donors younger than 25 (Y) and elderly donors of above 55 years (E) for 3 days before inducing osteogenesis. As controls, no MVs were added (C) as well as no differentiation was induced (undiff). (D) Representative images of Alizarin Red S stained 3 independent differentiations 21 days after induction of osteogenic differentiation are shown. (E) ASCs of 2 different donors were treated with MVs derived from young and elderly donors. Osteogenic differentiation was analyzed by quantitation of Alizarin Red S staining for Ca^{2+} deposition. Results derived from 3 independent replicates of each donor are shown. (F-G) ASCs showed a decreased osteogenic differentiation potential after treatment with the total MV fraction (tMV) isolated from an elderly miR-31 high donor compared to ASCs exposed to the CD63 negative fraction ($CD63^-$) as (F) quantified by Alizarin Red S staining for Ca^{2+} deposition at day 21 of differentiation and (G) shown on the basis of ALP mRNA normalized to GAPDH at day 71 of differentiation. (H-J) ASCs were transfected with antimiR-31 or a non-targeting miRNA control (antimiRC), 24h before total plasma MV fraction from an elderly miR-31 high donor was added. (H) Osteogenic differentiation

was analyzed by quantitation of Alizarin Red S staining for Ca^{2+} deposition at day 21 of differentiation. (I) ALP, (J) OC and (K) FZD3 mRNA levels normalized to GAPDH were measured 7, 21 or 4 days after differentiation start using qPCR, showing the rescue of osteogenic differentiation capacity despite MV coincubation due to antimiR-31 transfection. (L) Overview of our working hypothesis: Exosomes/MVs/Supernatant derived from senescent endothelial cells affect differentiation potential of ASCs via miRNA-31 delivery by knocking down its target FZD3 mRNA. Thereby, the "senescent" environment hampers tissue regeneration by inhibiting the induction of osteogenesis. Therefore, the systemic environment of the elderly might favour loss of bone mass and inhibit bone healing.

*: $p<0.05$, **: $p<0.01$, ***: $p<0.001$ in comparison to control. Data are presented as mean values ± SM and were statistically analyzed using Wilcoxon signed rank test in Fig. 4.B and Student´s *t* test for figures 4E-K.

Figure S1:

(A) Representative microscope image of ASCs showing a typical morphology. (B) Representative flow cytometric analysis of two donors used in this study, ASC57 and ASC60, show expression of ASC specific (ASC*) and mesenchymal stem cell surface markers and did not show hematopoietic stem cells surface marker. (C) Early quiescent passage (PD13) and senescent (PD53) endothelial cells that were used for isolating MVs from conditioned medium were stained for senescence associated β-galactosidase activity, representative images are shown. (D) Western blot analysis of MVs protein lysate detected with antiCD63 antibody.

Figure S2:

MiR-31 is upregulated intracellularly in senescent (S) versus early quiescent passage (Y) (A) human liver endothelial cells (ECs) (S = senescent; Y = early quiescent passage; N=3) and (B) human retinal microvascular endothelial cells (hReEC) (S = senescent; Y = early quiescent passage; N=3) as analyzed by qPCR and normalized to the snRNA U6 as internal control.

(C) SIPS treatment of endothelial cells results in growth arrest at 75 µM tBHP**.** HUVECs were pulsed with the indicated concentration of tBHP. Growth was monitored by cell counting. Representative figures until day 5 of treatment indicating growth arrest at the highest dose are shown. MVs were isolated from tBHP pulsed

endothelial cells after 14 days, when no additional cell proliferation was observed in the cells treated with 75 µM tBHP. In contrast, after exposure to 35 µM tBHP the cells completely recovered and resumed growth (N=3). MiR-31 is also induced by tBHP treatment of HUVECs (D) endogenously and (E) accumulates in MVs derived from treated versus replicative senescent or untreated HUVECs. Error bars indicate the standard deviations of 3 independent measurements.
*: $p<0.05$, **: $p<0.01$, ***: $p<0.001$. Data are presented as mean values ± SM

Figure S3:

(A) ASCs were transfected with miR-31, non-targeting miRNA control (miRC) or MOCK transfected (untransf.). Taqman based qPCR showing increased intracellular miR-31 levels relative to snRNA U6 24 h and 48 h after transient transfection compared to non targeting miRNA control or MOCK transfected cells. , . (B) Confirmation of FZD3 knockdown relative to GAPDH of siFZD3 transfected cells compared to non-targeting miRNA control (miRC) transfected ASCs 24 hours after transfection using qPCR. (C, D) Confirmation that miR-31 is a general regulator of osteogenesis. (C) C3Ht101/2 and (D) C2C12, two mouse mesenchymal mulitpotent cell lines were induced to undergo osteogenic differentiation upon addition of bone morphogenic protein 2 (BMP2), which was inhibited by transient transfection of miR-31 compared to non-targeting miRNA control (miRC) and MOCK transfected (untransf.) cells measured by Osteocalcin reporter activity. (N=4). (E) Taqman based qPCR showing downregulated intracellular miR-31 levels relative to snRNA U6 24 h after transient antimiR-31 transfection compared to non-targeting miRNA control (antimiRC) transfected cells.).
ns: not significant, *: $p<0.05$, **: $p<0.01$, ***: $p<0.001$. Data are presented as mean values ± SM

References

1. Rando, T. Stem cells, ageing and the quest for immortality. *Nature* **441**, 1080-1086 (2006).
2. Conboy, I.*, et al.* Rejuvenation of aged progenitor cells by exposure to a young systemic environment. *Nature* **433**, 760-764 (2005).
3. Matsumoto, Y.*, et al.* Reduced number and function of endothelial progenitor cells in patients with aortic valve stenosis: a novel concept for valvular endothelial cell repair. *Eur Heart J* **30**, 346-355 (2009).
4. Erusalimsky, J.D. Vascular endothelial senescence: from mechanisms to pathophysiology. *Journal of applied physiology* **106**, 326-332 (2009).
5. Liu, L. & Rando, T.A. Manifestations and mechanisms of stem cell aging. *The Journal of cell biology* **193**, 257-266 (2011).
6. Conboy, I.M.*, et al.* Rejuvenation of aged progenitor cells by exposure to a young systemic environment. *Nature* **433**, 760-764 (2005).
7. Baker, D.J.*, et al.* Clearance of p16Ink4a-positive senescent cells delays ageing-associated disorders. *Nature* **479**, 232-236 (2011).
8. Jaskelioff, M.*, et al.* Telomerase reactivation reverses tissue degeneration in aged telomerase-deficient mice. *Nature* **469**, 102-106 (2011).
9. Minamino, T. & Komuro, I. Vascular cell senescence: contribution to atherosclerosis. *Circulation research* **100**, 15-26 (2007).
10. Coppé, J.P.*, et al.* Senescence-associated secretory phenotypes reveal cell-nonautonomous functions of oncogenic RAS and the p53 tumor suppressor. *PLoS Biol* **6**, 2853-2868 (2008).
11. Chang, M.W.*, et al.* Comparison of early passage, senescent and hTERT immortalized endothelial cells. *Experimental cell research* **309**, 121-136 (2005).
12. Mathivanan, S., Ji, H. & Simpson, R.J. Exosomes: extracellular organelles important in intercellular communication. *Journal of proteomics* **73**, 1907-1920 (2010).
13. Deregibus, M.C.*, et al.* Endothelial progenitor cell derived microvesicles activate an angiogenic program in endothelial cells by a horizontal transfer of mRNA. *Blood* **110**, 2440-2448 (2007).
14. Valadi, H.*, et al.* Exosome-mediated transfer of mRNAs and microRNAs is a novel mechanism of genetic exchange between cells. *Nat Cell Biol* **9**, 654-659 (2007).
15. Hunter, M.P.*, et al.* Detection of microRNA expression in human peripheral blood microvesicles. *PloS one* **3**, e3694 (2008).
16. Hackl, M.*, et al.* miR-17, miR-19b, miR-20a, and miR-106a are down-regulated in human aging. *Aging Cell* **9**, 291-296 (2010).
17. Deng, Y.*, et al.* Effects of a miR-31, Runx2, and Satb2 Regulatory Loop on the Osteogenic Differentiation of Bone Mesenchymal Stem Cells. *Stem cells and development* (2013).
18. Baglio, S.R., Devescovi, V., Granchi, D. & Baldini, N. MicroRNA expression profiling of human bone marrow mesenchymal stem cells during osteogenic differentiation reveals Osterix regulation by miR-31. *Gene* (2013).
19. Deng, Y.*, et al.* The role of miR-31-modified adipose tissue-derived stem cells in repairing rat critical-sized calvarial defects. *Biomaterials* **34**, 6717-6728 (2013).

20. Feichtinger, G.A., *et al.* Enhanced reporter gene assay for the detection of osteogenic differentiation. *Tissue engineering. Part C, Methods* **17**, 401-410 (2011).
21. Valastyan, S., *et al.* A pleiotropically acting microRNA, miR-31, inhibits breast cancer metastasis. *Cell* **137**, 1032-1046 (2009).
22. Hergenreider, E., *et al.* Atheroprotective communication between endothelial cells and smooth muscle cells through miRNAs. *Nat Cell Biol* **14**, 249-256 (2012).
23. Rando, T.A. Stem cells, ageing and the quest for immortality. *Nature* **441**, 1080-1086 (2006).
24. Zhu, H., *et al.* Regulation of autophagy by a beclin 1-targeted microRNA, miR-30a, in cancer cells. *Autophagy* **5**, 816-823 (2009).
25. Roholl, P.J., Blauw, E., Zurcher, C., Dormans, J.A. & Theuns, H.M. Evidence for a diminished maturation of preosteoblasts into osteoblasts during aging in rats: an ultrastructural analysis. *J Bone Miner Res* **9**, 355-366 (1994).
26. Worley, R.J. Age, estrogen, and bone density. *Clinical obstetrics and gynecology* **24**, 203-218 (1981).
27. Frindik, J.P., Kemp, S.F. & Sy, J.P. Effects of recombinant human growth hormone on height and skeletal maturation in growth hormone-deficient children with and without severe pretreatment bone age delay. *Hormone research* **51**, 15-19 (1999).
28. Ekstrom, K., *et al.* Characterization of mRNA and microRNA in human mast cell-derived exosomes and their transfer to other mast cells and blood CD34 progenitor cells. *Journal of extracellular vesicles* **1**(2012).
29. Erusalimsky, J.D. Vascular endothelial senescence: from mechanisms to pathophysiology. *J Appl Physiol (1985)* **106**, 326-332 (2009).
30. Erusalimsky, J.D. & Kurz, D.J. Endothelial cell senescence. *Handbook of experimental pharmacology*, 213-248 (2006).
31. Crisan, M., *et al.* A perivascular origin for mesenchymal stem cells in multiple human organs. *Cell stem cell* **3**, 301-313 (2008).
32. Shi, S. & Gronthos, S. Perivascular niche of postnatal mesenchymal stem cells in human bone marrow and dental pulp. *Journal of bone and mineral research : the official journal of the American Society for Bone and Mineral Research* **18**, 696-704 (2003).
33. Chen, X., *et al.* Characterization of microRNAs in serum: a novel class of biomarkers for diagnosis of cancer and other diseases. *Cell research* **18**, 997-1006 (2008).
34. Noren Hooten, N., *et al.* Age-related changes in microRNA levels in serum. *Aging* **5**, 725-740 (2013).
35. Weilner, S., Schraml, E., Redl, H., Grillari-Voglauer, R. & Grillari, J. Secretion of microvesicular miRNAs in cellular and organismal aging. *Experimental gerontology* (2012).
36. Olivieri, F., Rippo, M.R., Procopio, A.D. & Fazioli, F. Circulating inflamma-miRs in aging and age-related diseases. *Frontiers in genetics* **4**, 121 (2013).
37. Diehl, P., *et al.* Microparticles: major transport vehicles for distinct microRNAs in circulation. *Cardiovascular research* **93**, 633-644 (2012).
38. Lehmann, B.D., *et al.* Senescence-associated exosome release from human prostate cancer cells. *Cancer research* **68**, 7864-7871 (2008).

39. Yu, X., Harris, S.L. & Levine, A.J. The regulation of exosome secretion: a novel function of the p53 protein. *Cancer research* **66**, 4795-4801 (2006).
40. Deng, Y.*, et al.* Repair of critical-sized bone defects with anti-miR-31-expressing bone marrow stromal stem cells and poly(glycerol sebacate) scaffolds. *European cells & materials* **27**, 13-24; discussion 24-15 (2014).
41. Lee, E.H.*, et al.* Disruption of the non-canonical WNT pathway in lung squamous cell carcinoma. *Clinical medicine. Oncology* **2008**, 169-179 (2008).
42. Chakravorty, N.*, et al.* Pro-osteogenic topographical cues promote early activation of osteoprogenitor differentiation via enhanced TGFbeta, Wnt, and Notch signaling. *Clinical oral implants research* **25**, 475-486 (2014).

Figure 1

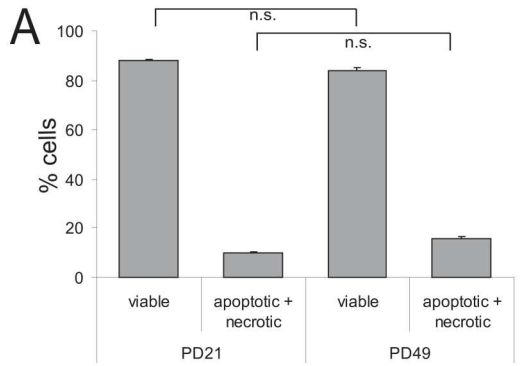

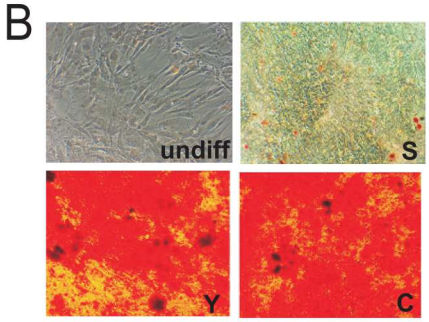

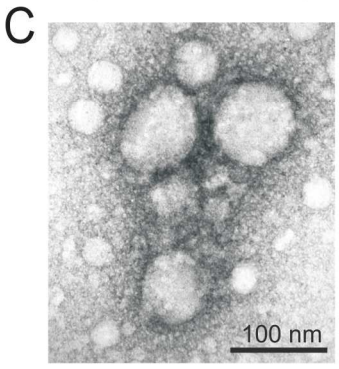

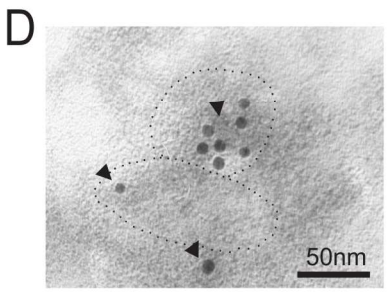

Figure 1

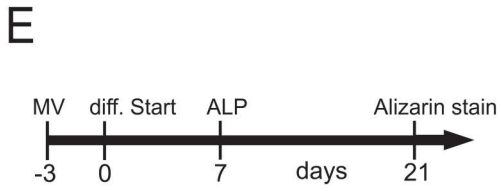

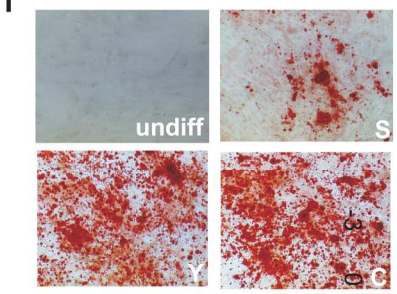

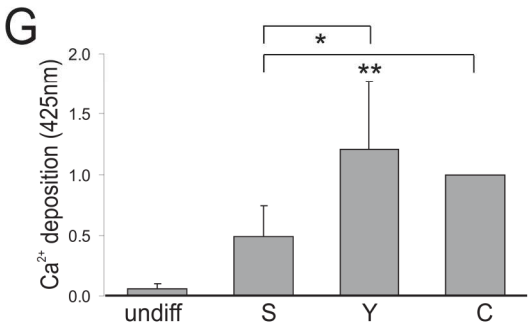

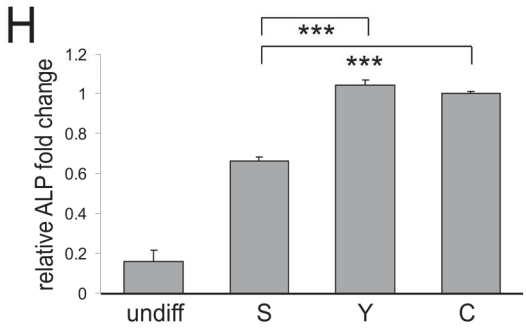

Figure 1

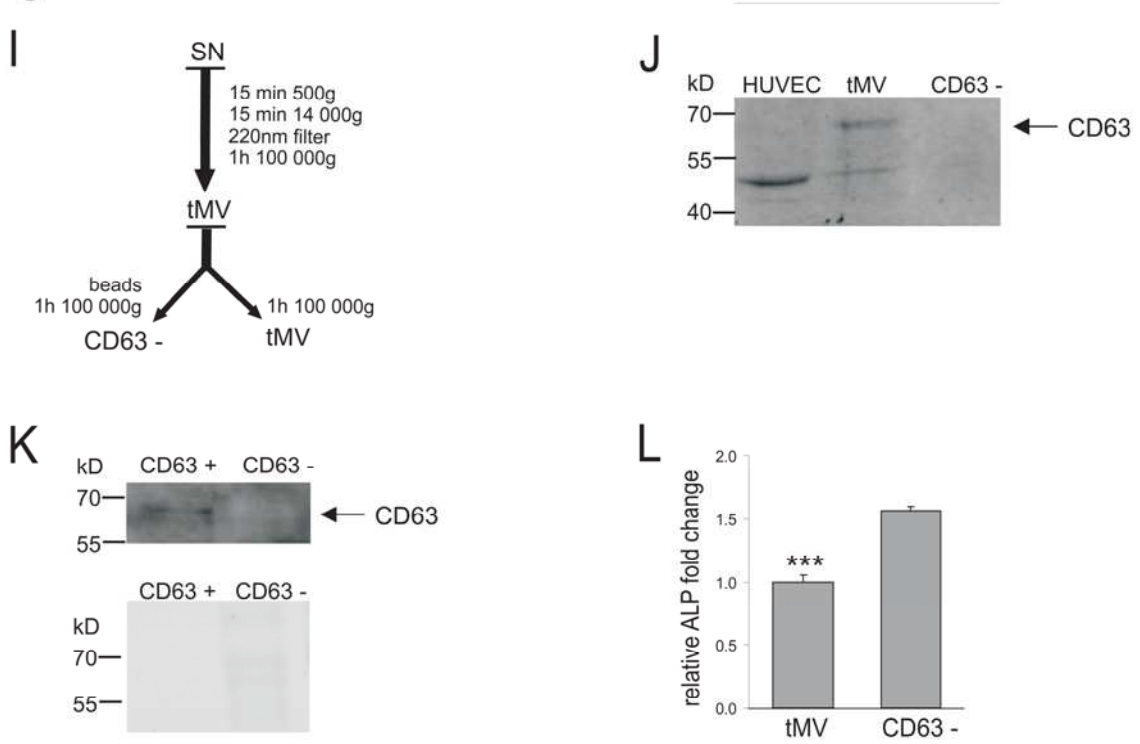

Figure 2

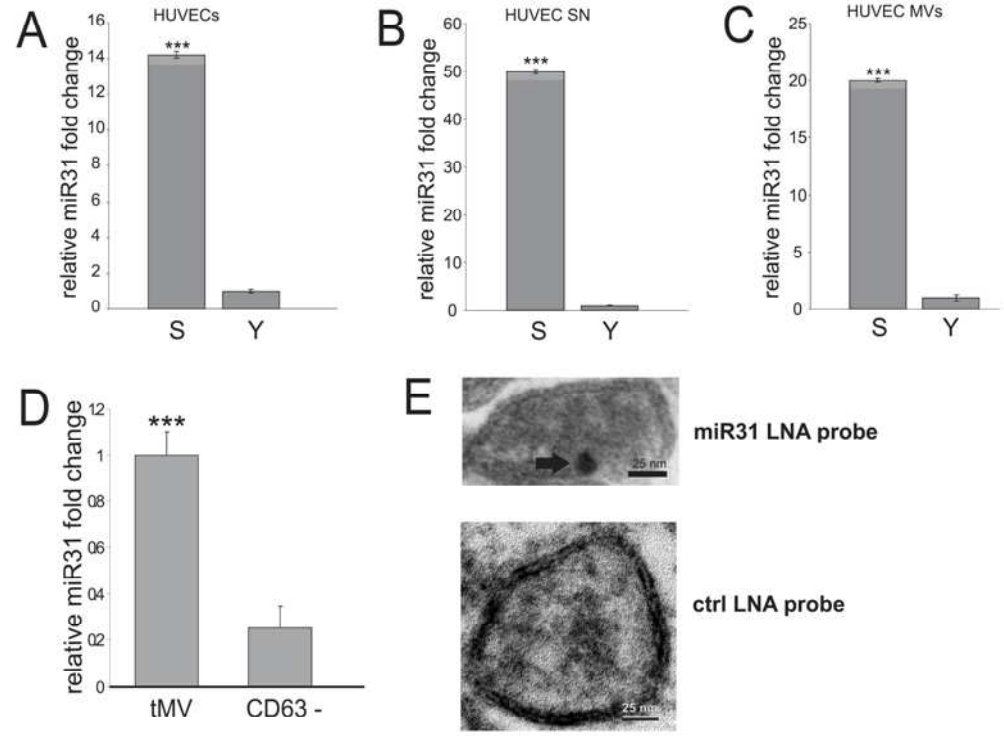

Figure 3

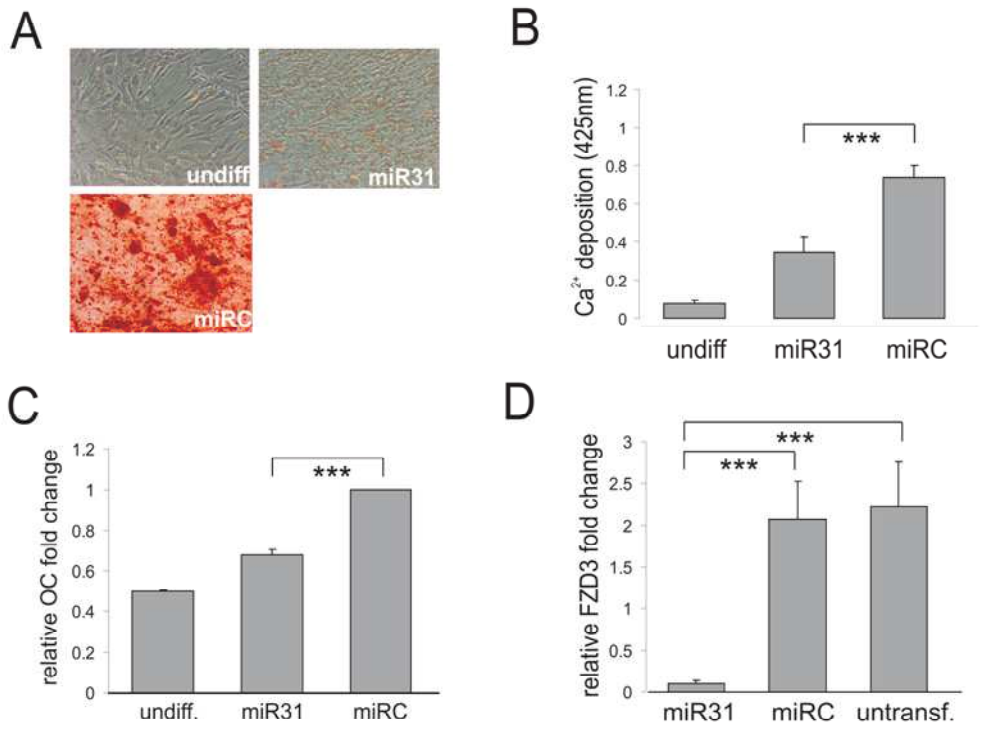

Figure 3

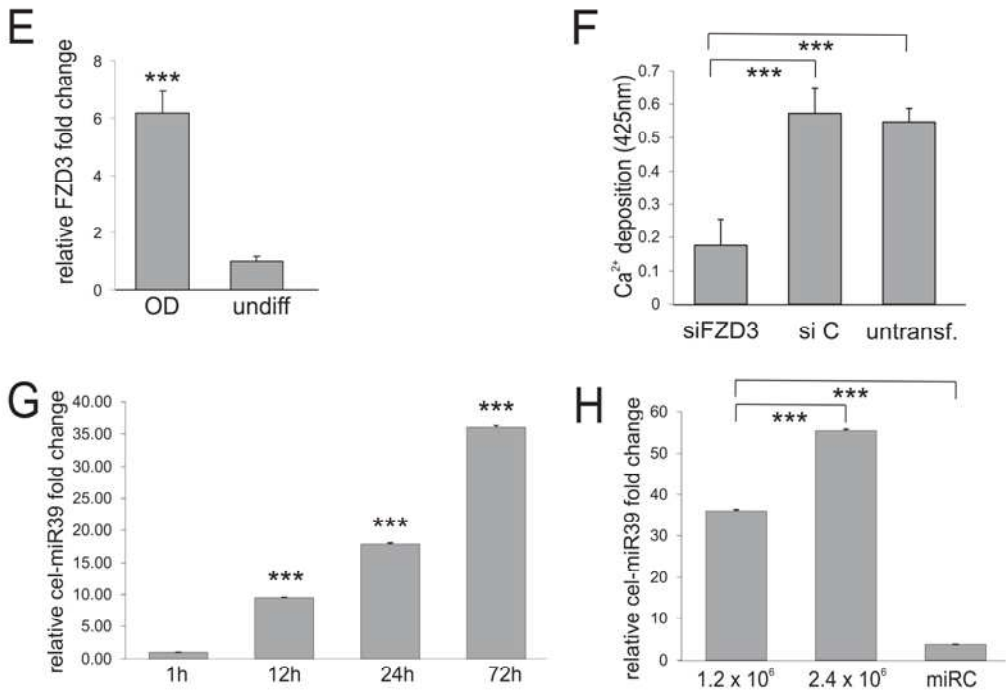

Figure 3

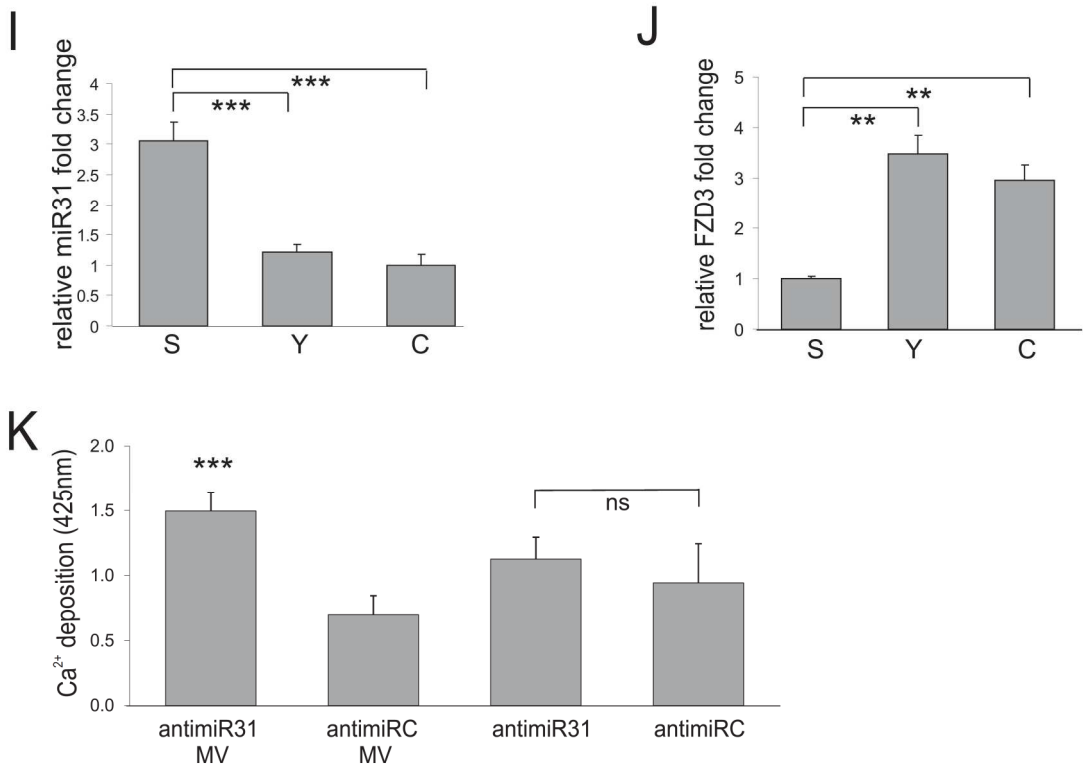

Figure 3

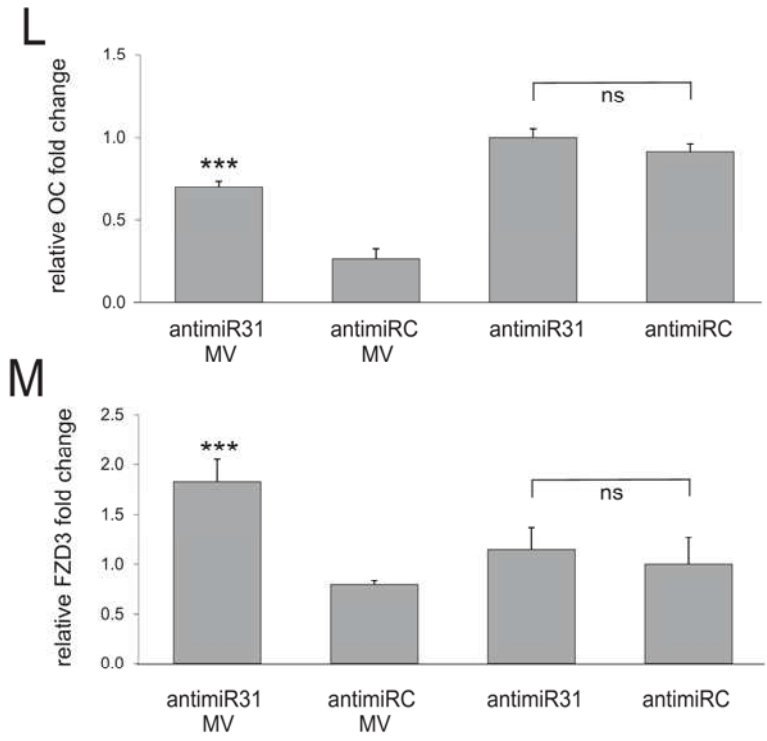

Figure 4

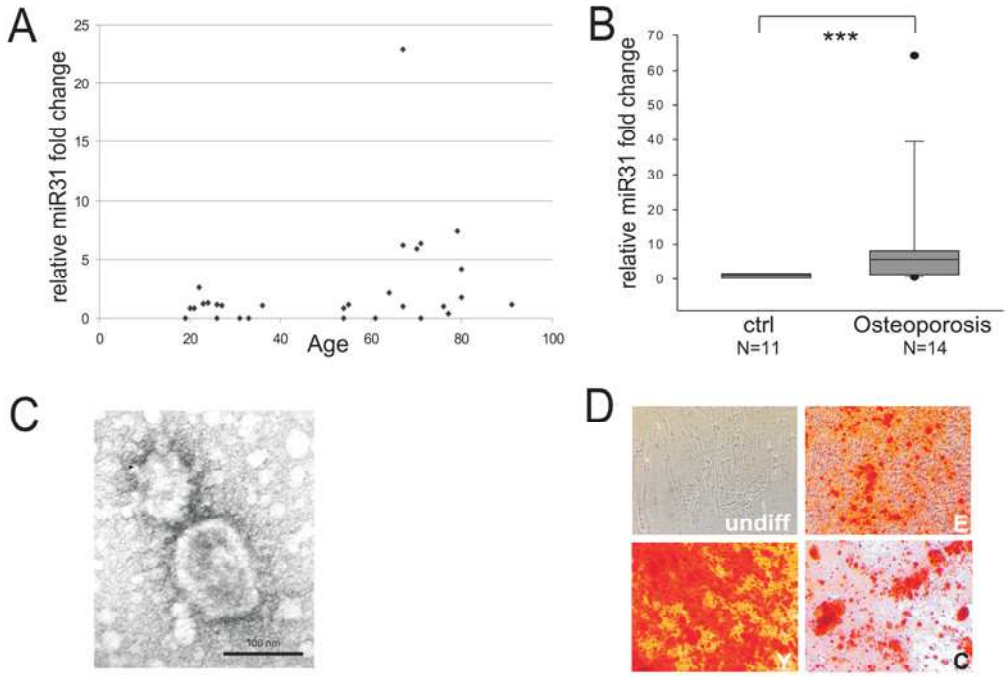

Figure 4

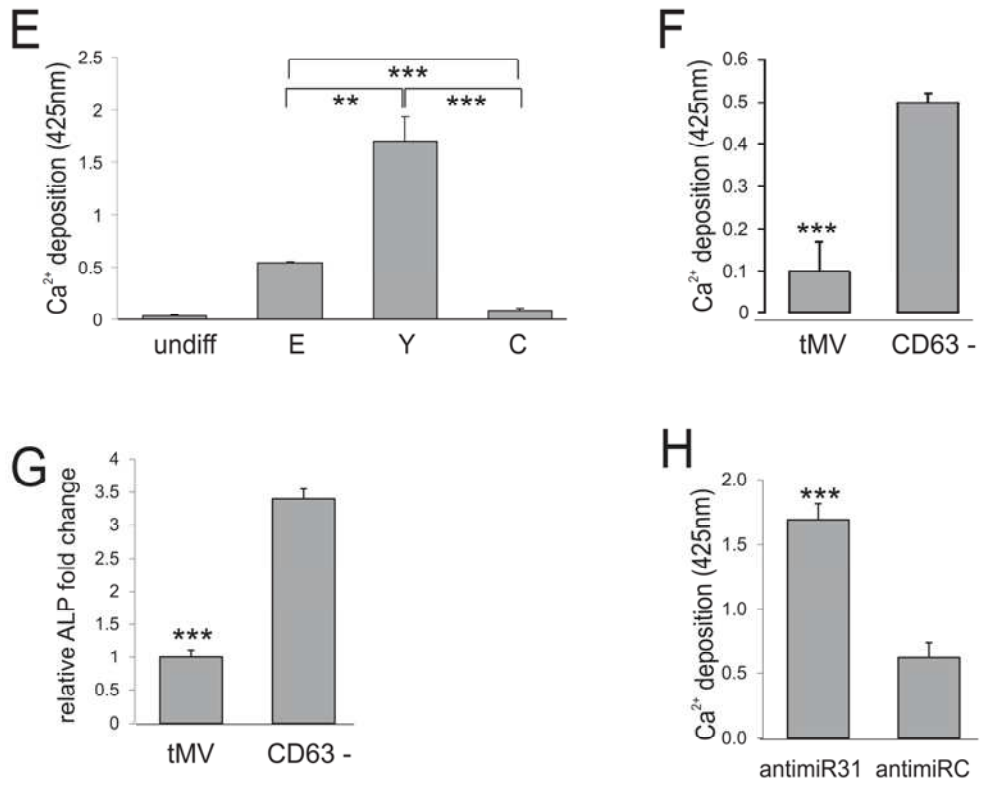

Figure 4

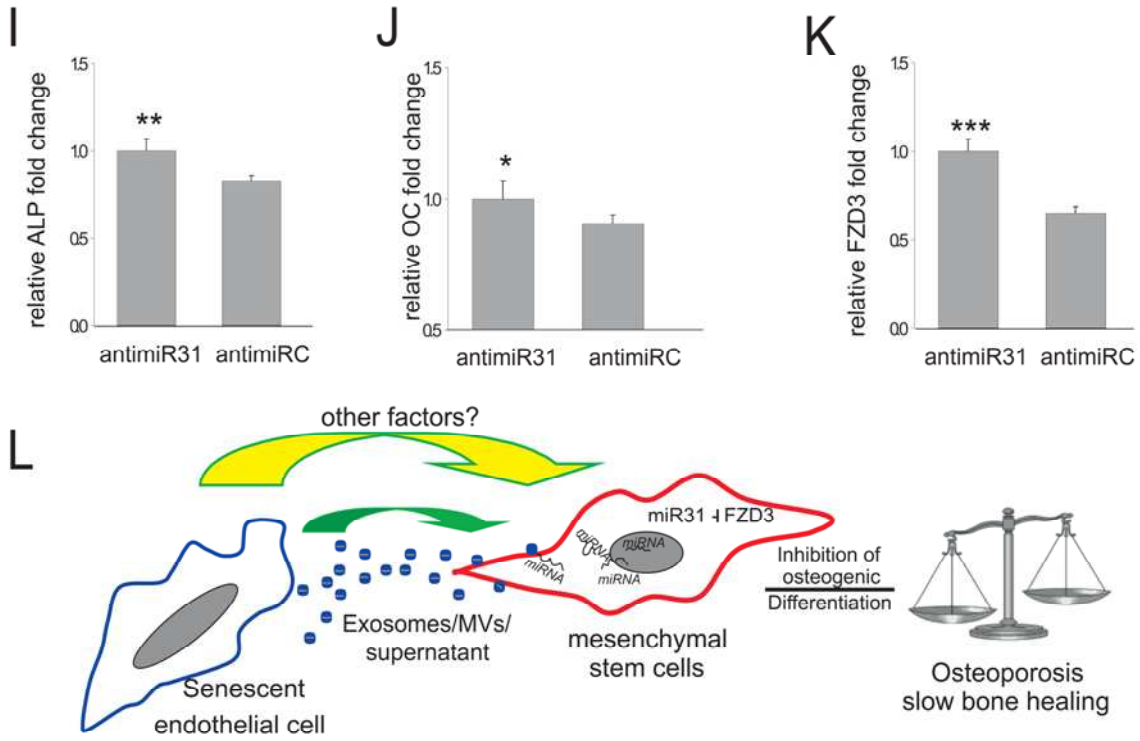

Figure S1

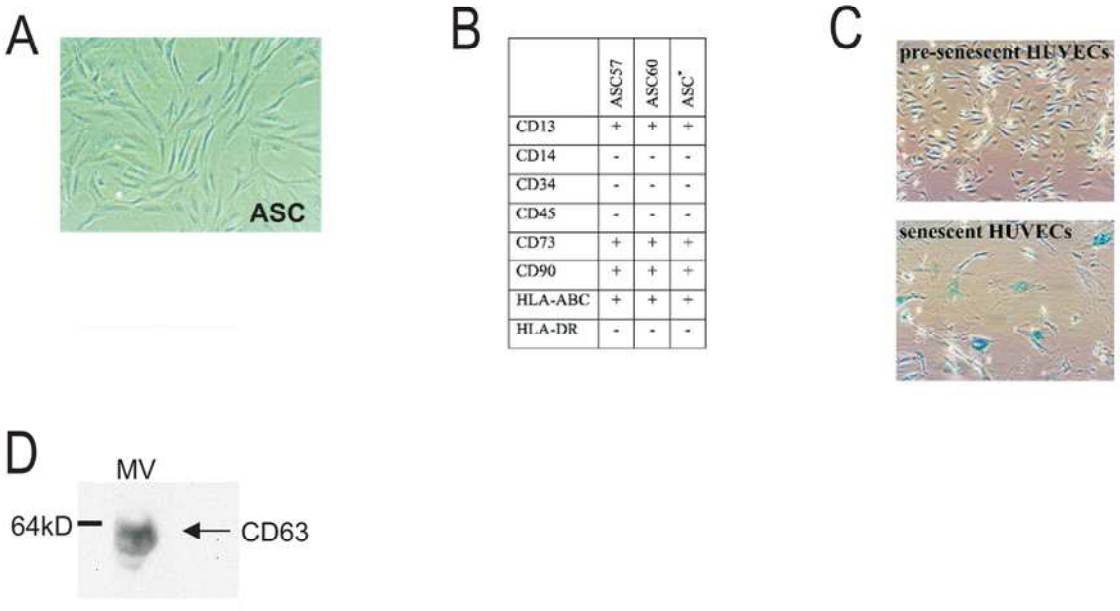

Figure S2

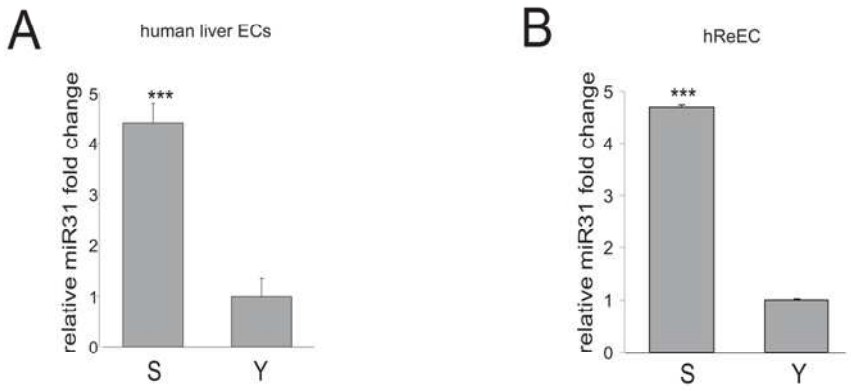

Figure S2

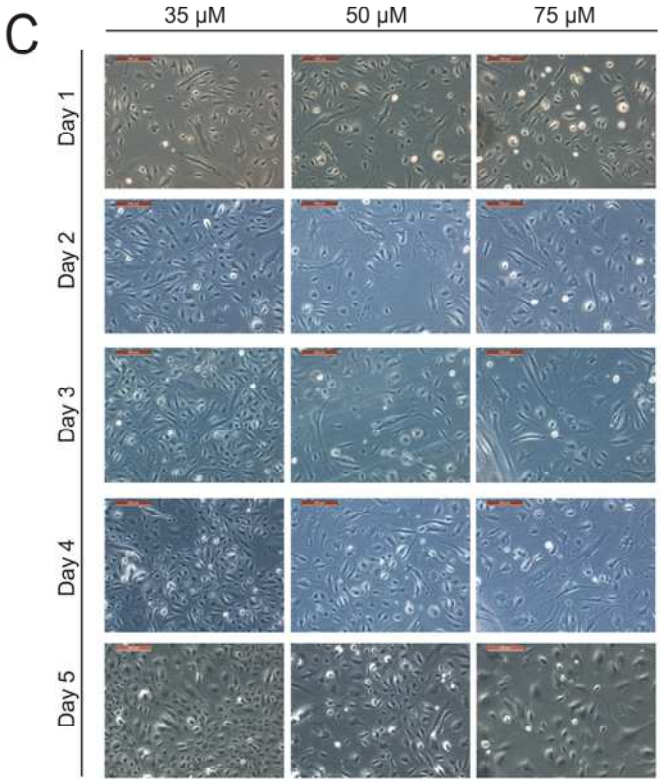

Figure S2

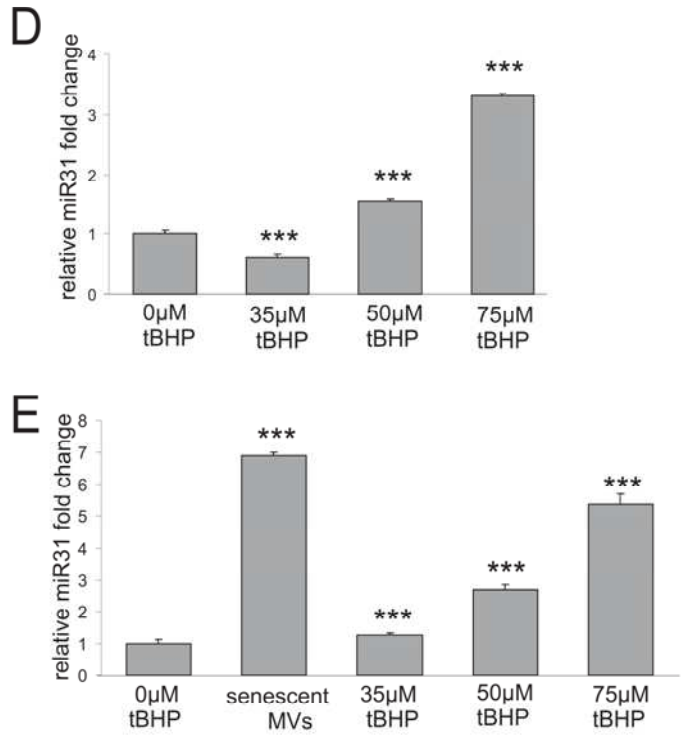

Figure S3

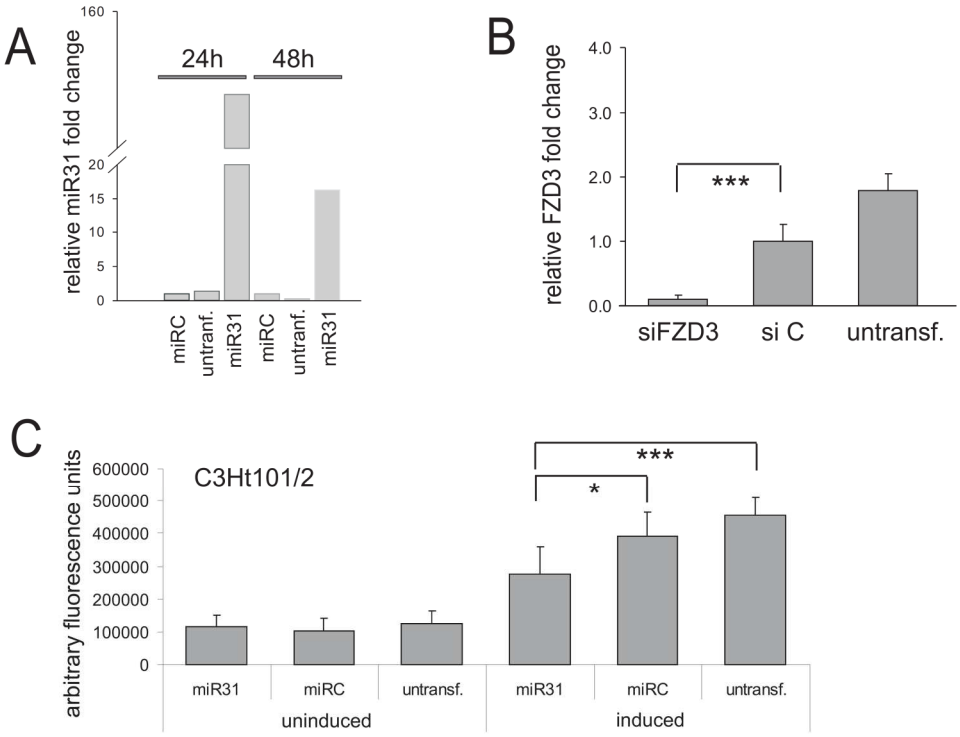

Figure S3

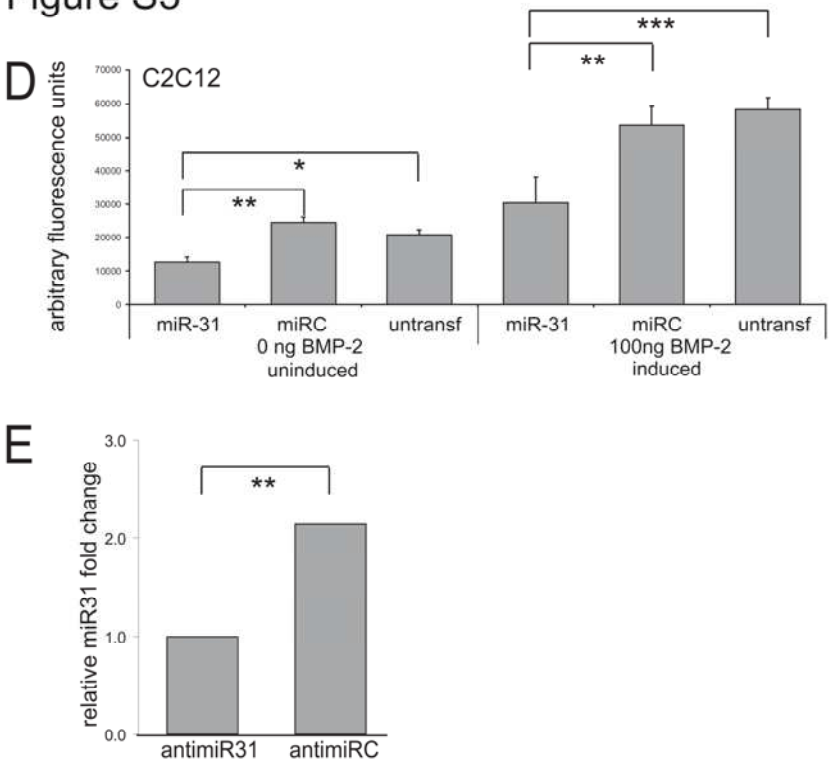
D
C2C12
arbitrary fluorescence units
70000
60000
50000
40000
30000
20000
10000
0
*
**
***
miR-31
miRC
0 ng BMP-2
uninduced
untransf
miR-31
miRC
100ng BMP-2
induced
untransf

E
relative miR31 fold change
3.0
2.0
1.0
0.0
**
antimiR31
antimiRC

First steps towards skin reconstruction for patients with epidermolysis bullosawith the use of autologous urine-derived mesenchymal stem cells

Rita Reynoso[1]*, Verena Wally[2]*, Markus Schosserer[1,5], Bogdan Jug[1], Sylvia Weilner[3,5], Ivana Buric[1], Johannes Grillari[1,3,4,5], Johann W. Bauer[2], Regina Grillari-Voglauer[1,3,5]

[1] Department of Biotechnology, BOKU - University of Natural Resources and Life Sciences Vienna, Muthgasse 18, A-1190 Vienna, Austria

[2] Division of Experimental Dermatology and EB House Austria, Department of Dermatology, Paracelsus Medical University Salzburg, Muellner Hauptstraße 48, A-5020 Salzburg, Austria

[3] Evercyte GmbH, Muthgasse 18, A-1190 Vienna, Austria

[4] Christian Doppler-Laboratory on Biotechnology of Skin Aging

[5] Austrian Cluster for Tissue Regeneration, Vienna, Austria

* Those authors contributed equally

Correspondence to
Regina Grillari-Voglauer
Department of Biotechnology
BOKU - University of Natural Resources and Life Sciences Vienna
Muthgasse 18, A-1190 Vienna, Austria.
regina.grillari@boku.ac.at
or
Johann Bauer
Division of Experimental Dermatology, EB House Austria
Muellner Hauptstrasse 48, A-5020 Salzburg, Austria
Jo.Bauer@salk.at

Abstract

Regenerative medicine is strictly dependent on stem cells as a source for a high diversity of somatic cells. However, the isolation of such from individuals suffering from severe genetic skin blistering disease like epidermolysis bullosa (EB) is often associated with further organ damage.

We provide here an optimized protocol for the reproducible isolation of mesenchymal stem cells from urine, even from small volumes as obtained from patients with EB. Furthermore, we describe a basic characterization of those urine-derived stem cells (USCs) from healthy donors, as well as from patients with EB, and demonstrate their potential to differentiate into chondrocytes and osteoblasts, as well as their immune-modulatory properties.

Thus, USCs provide a novel and non-invasive source of stem cells, which might be applied for gene-therapeutic approaches to improve the quality of life of patients with EB in the future.

Introduction

Epidermolysis bullosa (EB) is a devastating disease of the skin and mucous membranes, caused by mutations in either one of 17 genes encoding structural proteins required for skin integrity. Patients suffer from extensive blistering upon minor mechanical impact due to the reduced connectivity of the skin layers. In severe subtypes of EB, the continuous wounding of the skin causes a constant need for repair, which leads to the depletion of epidermal stem cells and thus to multiple chronic wounds (Fine et al. 2008).

Currently, *ex vivo* gene therapy is the most promising therapeutic approach concerning safety and technical realization. In 2006, Mavilio et al. described the transplantation of an *in-vitro* engineered skin graft of 50 cm^2 onto the backside of a leg of a patient with EB (Mavilio et al. 2006). Therefore, epidermal stem cells were isolated from patient skin biopsies, retrovirally transduced with a wildtype copy of the defective laminin ß3 (LAMB3) cDNA in a MFG vector, and expanded *in vitro*. Clinically, the patient showed no more blistering in the area of the transplanted skin until 6.5 years after the transplantation, proving the long-term stability and safety of this approach (De Rosa et al. 2013). However, the recovery of pertinent epidermal

stem cells, which usually requires multiple skin biopsies, is an extremely displeasing and painful demand especially for patients with EB. Thus, other sources for the non-invasive recovery of stem cells, such as urine, are required.

Zhang and co-workers recently described the isolation of mesenchymal-like stem cells from urine. These multi-potent cells are termed urine-derived stem cells (USCs) and were shown to have the potential to differentiate towards osteocytes, chondrocytes, adipocytes, myocytes and endothelial cells (Bharadwaj et al. 2011; Guan et al. 2014; Bharadwaj et al. 2013; Lang et al. 2013; Liu, Wang, et al. 2013; Wu et al. 2011; Zhang et al. 2008; Liu, Pareta, et al. 2013). These mesenchymal lineages, such as fibroblasts, could be used for the treatment of patients suffering from dystrophic EB. Furthermore, recent reports suggest that mesenchymal stem cells can also be trans-differentiated into epidermal cells (Chavez-Munoz et al. 2013; Păunescu et al. 2007), which might be beneficial for the treatment of the other subtypes. Thus, the isolation of USCs from urine might provide a non-invasive route for the painless recovery of stem cells from patients with EB.

We show here that by using an optimized protocol USCs could be reproducibly isolated from small volumes of urine from healthy donors, as well as from patients with EB. Recovered USCs were positive for various marker genes and could be differentiated into osteocytes and chondrocytes. Furthermore USCs showed similar immunomodulatory properties as MSCs.

Materials and methods

Isolation of USCs from urine

Mid- and last-stream urine from healthy donors was collected into sterile recipes, transferred to 50 ml tubes and centrifuged for 5 min at 500 x g. Thereafter, the supernatant was discarded and cells were washed twice with PBS. The remaining pellet was re-suspended in culture medium and seeded into one well of a 24-well plate for male donors or a 6-well plate for female donors.

Culture plates (Nunc) were either used without coating or coated with Collagen (Sigma Aldrich). Four different formulations of culture medium were used:

I- Primary urine cells culture medium (pUSCs, according to the method described by Zhang et al. (Bharadwaj et al. 2011), 50% Keratinocyte-SFM (Gibco), 33.75% DMEM (PAA), 11.25% Hams F12, 5% Fetal calf serum (FCS, PAA), 5 ng/ml Epidermal growth factor (Sigma Aldrich), 50 ng/ml Bovine pituitary extract (Sigma Aldrich), 30 ng/ml Cholera toxin (Sigma Aldrich), 0.4 µg/ml Hydrocortisone (Sigma Aldrich), 5 ng/ml Insulin (Sigma Aldrich), 1.8 x 10^{-4} M Adenine (Sigma Aldrich), 5 µg/ml Holo-Transferrin (VWR), 2 nM Triiodo-L-thyronine (Life Technologies))

II- MesenCult® MSC Basal Medium supplemented with MesenCult™ Mesenchymal Stem Cell Stimulatory Supplement (Stem Cell

III- MesenPRO RS™ supplemented with MesenPRO RS™ Growth Supplement (Gibco)

IV- EGM™-2 Bulletkit (Lonza).

All formulations were additionally supplemented with 100 U/ml penicillin and 100 µg/ml streptomycin (Sigma).

Urine pH was measured and samples were also evaluated for the presence of glucose, leucocytes, nitrites, proteins and blood using Combur Test HC (Cobas) (Belik et al. 2008).

The local ethic commissions either approved this study (Vienna) or declared that no formal approval is required, as long as no clinical trials are conducted (Salzburg). All the donors gave informed consent before providing urine samples. Thus, the study was performed in accordance with the Declaration of Helsinki.

Immunophenotypic characterization of USCs

After 3 or 4 passages, USCs and adipose derived stem cells (ASCs) as control, were seeded into 8 well chamber slides (µ-Slide, IBIDI-Treat surface, IBIDI) without coating. Next day, cells were rinsed with PBS and fixed with 3.6% formaldehyde in PBS for 10 min at room temperature.

After two consecutive washes with PBS, the cells were stained for 1 h at room temperature with antibodies against CD14 (from mouse, ab7800, Abcam), CD34 (from mouse, FITC-labeled, 555821, BD Pharmingen), CD44 (from mouse, SAB4700184, Sigma Aldrich), CD73 (from mouse, FITC-labeled, 561254, BD Pharmingen), CD90 (from mouse, PE-labeled, 555596, BD Pharmingen), CD105 (from mouse, FITC-labeled, 561443, BD Pharmingen), CD117 (from mouse, FITC-labeled, 561443, BD Pharmingen), CD133 (from rabbit, ab19898, Abcam), Vimentin (from mouse, FITC-labeled, 562338, BD Pharmingen), and Collagen I (from rabbit, ab292, Abcam). For antibodies without dye-conjugate, samples were washed three times and incubated with Dyelight488 or Dyelight549-conjugated secondary antibodies against mouse or rabbit (Jackson Immunoresearch) for one hour. Finally, the wells were washed twice with PBS, stained with Hoechst 33258 for 5 min, washed once with PBS and analyzed by fluorescence microscopy on a Leica DMI-6000 microscope equipped with filter sets for DAPI, GFP and RFP.

Cell differentiation

For osteogenic differentiation, 3000 cells were seeded into one well of a 24-well plate without coating containing 1 ml DMEM low glucose (PAA) supplemented with 10% FCS, 10 nM dexamethasone (Sigma), 150 µM ascorbate 2-phosphate (Sigma), 10 nM vitamin D3 (Sigma) and 10 mM L-glycerophosphate (Sigma). The plates (Nunc) were kept in a humidified incubator (37ºC and 5% CO_2) and the culture medium was changed twice a week for 28 days.

For healthy donors, the medium was aspirated after this time and the cells were washed three times with PBS. Then, cells were fixed in ice-cold 70% ethanol for 1 h at -20°C and washed three times with distillated water. The cells were incubated with 40 mM Alizarin Red solution (Sigma) at room temperature for 10 min and washed until all remaining traces of dye were removed. Representative pictures were acquired on a Leica DMI microscope equipped with a color-camera.

Cells differentiated from patients with EB were equilibrated in an alkaline-phosphatase (AP)-buffer (0.1 M Tris-HCl pH 9.5, 0.1 M NaCl, 0.05 M $MgCl_2$) for 10 minutes. Then, cells were

incubated in 2% NBT/BCIP (Sigma) in AP-buffer for 75 minutes and representative microscope pictures were acquired.

For chondrogenic differentiation, 3000 cells were seeded in 24-well plates (Nunc) without coating containing 2 ml DMEM/Ham's F12 supplemented with 10% FCS, 6 µg/ml insulin (Sigma), 0.2 mM ascorbic acid-2P (Fluka) and 10 ng/ml TGF-β1 (R&D). The plates (Nunc) were kept in a humidified incubator (37ºC and 5% CO_2) and the culture medium was changed twice a week for 28 days.

After this period, the medium was aspirated and the cells were washed three times with PBS. Then, the cells were incubated with 3.6% formaldehyde in PBS for 1 h, washed three times with distillated water and incubated with 1% Alcian blue 8GX staining solution (Sigma) at room temperature for 30 min. The cells were washed until all traces of remaining dye were removed and representative microscope pictures were acquired.

Cell differentiations were confirmed by analyzing relative expression levels of different marker genes. Primer sequences are given in Table 1. Therefore, cells were harvested by trypsinization and total RNA was isolated using QIAzol Lysis Reagent (Qiagen), according to the manufacture's protocol. RNA pellets were dried and re-suspended in 50 µl RNase-free water. RNA was quantified using a NanoDrop Spectrophotometer (Thermo Scientific) and 100 ng of total RNA were reverse transcribed using Dynamo cDNA synthesis kit (Finnzymes). For quantification of osteocalcin mRNA, qPCR was performed on a Rotorgene Q (Qiagen) using SensiMix Plus SYBR-Green Mix. Expression values were normalized to GAPDH and are indicated as fold changes relative to control.

The relative abundance of Collagen X, Aggrecan and GAPDH mRNAs were evaluated by semi-quantitive real-time PCR (SQRT-PCR). After reverse transcription as above, PCR products were

generated using GoTAQ Polymerase (Promega) and separated on a 2% agarose gel in 1x TBE buffer. The number of cycles was adjusted so that saturation was not reached.

Target	Primer sense	Primer antisense
GAPDH[1,2]	GCCAACGTGTCAGTGGTGGA	CACCACCCTGTTGCTGTAGCC
Osteocalcin[1]	ATCAAAGAGGAGGGGAACCTA	AGGAAGTAGGGTGCCATAACA
Osteocalcin[2]	GTGCAGAGTCCAGCAAAGGT	TCAGCCAACTCGTCACAGTC
Collagen X[1]	CCCTTTTTGCTGCTAGTATCC	CTGTTGTCCAGGTTTTCCTGGCA
Aggrecan[2]	ACAGCTGGGGACATTAGTGG	GTGGAATGCAGAGGTGGTTT

[1]Primer used for USCs from healthy donors

[2]Primer used for USCs from patients with EB.

Evaluation of immunomodulatory properties

The isolation of peripheral blood mononuclear cells (PBMCs) from whole blood and subsequent lymphocyte separation by plate adherence were performed as described previously (Reynoso et al. 2012). Two different concentrations of USCs (4×10^5 or 2×10^5) were seeded and allowed to attach in individual wells of 6 well-plates (Nunc). Then the medium was replaced with 4×10^5 lymphocytes in RPMI medium supplemented with 10% FCS and 4 mM glutamine. For the activation of lymphocytes 2.4 µg/ml phytohemagglutinin (PHA, Sigma) were used. After 48 h, proliferation of lymphocytes was determined by bromodeoxyuridine (BrdU) incorporation as described previously (Wieser et al. 2008). Briefly, 10 µM BrdU were added to the culture medium and lymphocytes were harvested after 24 h. Fixation and permeabilization were followed by staining with anti-BrdU primary antibody (BD Biosciences) and goat-anti-mouse DyLight 488 conjugate secondary antibody (Pierce). Finally, BrdU incorporation was analyzed by flow cytometry (FACSDiva, BD Biosciences).

Statistical analysis

All the experiments were performed in biological triplicates at least. Correlations were studied using the Pearson test. Association between urine volume and the presence of colonies was

determined by Chi-Square test. The differences in gene expression, as well as in the number of colonies depending on collagen coating were analyzed by Student's t-test. The statistical significance of cell culture characteristics depending on culture medium and lymphocytes proliferation were assessed by one-way ANOVA followed by Bonferroni multiple-comparison post-hoc test. All statistical tests were performed in SPSS (IBM). p-values ≤ 0.05 were considered significant.

Results

Characteristics of donors and urine

Urine provides a source for mesenchymal-like stem cells, also termed USCs (Bharadwaj et al. 2011), which we envision to be applicable for the treatment of patients with EB in the future. In order to establish a robust isolation protocol of USCs in our lab, we obtained in total 112 urine samples from 21 different healthy donors. The pH of the urine varied from 5.3 to 7.6 and only one sample was positive for nitrites, being all of them negative for the presence of glucose, leucocytes, proteins and blood. The volume of urine varied from 50 to 495 ml and there was no correlation between any of these parameters and the presence or quantity of colonies of USCs ($p = 0.484$ and $p = 0.58$, respectively) (Table 1). This result indicates that the volume of urine do not influence the success rate of USCs isolation and even from small volumes of urine, as usually provided by patients with EB,USCs can be isolated.

Establishment of a reproducible USCs isolation protocol from healthy donors

In order to isolate USCs, urine was centrifuged and cells were seeded either in 24-well plates for male donors or 6-well plates for female donors. Urine samples showed a variable content of squamous cells, being in general more abundant in female samples (FIG. 1A). Cell colonies appeared most frequently between 3 and 8 days after isolation. Eventually, samples from specific donors showed the first colony after 2-3 weeks.

In the following we define successful isolation of USCs, when at least one colony was obtained. As shown in Table 1, the success rate of isolations from male donors was higher than from female donors (70% vs. 42%). However, we observed that by isolating multiple samples from the same donor within two weeks (2-3 samples per day, 3 times per week), at least two successful isolations from each donor could be obtained.

Morphology of freshly isolated USCs-enriched cells from urine

Urine derived cells exhibited morphologies ranging from more epithelial to more elongated-fibroblastoid, independent of the donor. This indicates that a mixed population of different cell types was present immediately after isolation. Representative pictures of primary colonies are shown in FIG 1B. However, after three passages the cell morphology became homogeneously elongated-fibroblastoid. This cell population homogeneous in morphology is henceforth referred to as USCs and was used for all upcoming experiments. It is unclear, however, if the epithelial cells are lost over passaging due to the media enriching for fibroblastoid cells. The isolated cells reached confluence at around 12 days (FIG. 1C). In general the replicative life span ranged from 4.5 to 12 population doublings, after which cells stopped growing and displayed typical senescent morphology (FIG. 1D).

Optimization of culture conditions

In order to optimize the culture conditions for USCs, we tested different media formulations. Consequently, urine samples were obtained from four donors and the cells were cultivated either in MesenCult, MesenPRO, EGM-2 or pUSCs medium. We did not see major differences in cell morphology depending on the culture medium used (FIG. 2A). Cells from only one out of five samples showed cell proliferation in EGM-2 and also in this case cells stopped growing after passage 3. Interestingly, when either MesenCult or MesenPRO medium was used some colonies appeared already as soon as 3 days after isolation. Nevertheless, we did not find significant differences between the four media formulations regarding the necessary timeframe for colony formation. The number of colonies and the time needed to passage the cells for the first time did not differ significantly either (Table 2). Cells cultivated in MesenPRO or MesenCult stopped cell division after passage 1 in some cases, while in pUSCs medium they grew for longer periods of time and reached significantly higher population doublings (PDs) compared to MesenCult ($p = 0.013$) or MesenPRO ($p = 0.006$) (Table 2).

In addition, we tested whether the pre-coating of culture dishes with collagen improved the efficiency of isolation and culture of USCs. Surprisingly, the number of colonies was significantly higher when the plates were not coated ($p = 0.026$) (FIG. 2B)

In summary these results indicate that USCs can be cultivated in different media formulations, but pUSCs medium without collagen coating of culture dishes is most efficient for expanding the cells.

USCs express typical markers for mesenchymal stem cells (MSCs)

In order to test if the urine-derived cells are indeed enriched for USCs, the expression of MSC surface markers including CD73, CD90 and CD105 [6], as well as a lack of hematopoietic surface markers was analyzed by indirect immunofluorescence. Adipose derived mesenchymal stem cells (ASCs) served as positive control. Indeed, the surface marker profile of USCs resembled closely that of ASCs, as both were positive for the mesenchymal stem cells markers CD44, CD73, CD90, CD105, Vimentin and Collagen I, and negative for the hematopoietic markers CD14, CD34, CD117 and CD133 (FIG. 3).

These results are consistent with previous findings and corroborate that USCs closely resemble MSCs.

USCs have the potential to differentiate into osteogenic and chondrogenic lineages

In order to further confirm that our USCs are functionally similar to MSCs and previously published USCs, we studied their potential to differentiate into osteoblasts and chondrocytes. Therefore, USCs were exposed to osteogenic induction medium for 4 weeks. At the end of this time period the cells aggregated and formed calcium precipitates, which were confirmed by alizarin red staining (FIG. 4A). On transcriptional level, osteocalcin mRNA expression showed a significant 2-fold increase in induced cells when they were compared to the control ($p = 0.05$) (FIG. 4B).

When USCs were cultivated with chondrogenic induction medium over a period of 28 days, cells formed aggregates as expected during differentiation, and stained positive for proteoglycans using Alcian blue (FIG. 4C). At mRNA level, differentiated USCs exhibited detectable levels of Collagen X in contrast to the non-differentiated control cells (FIG. 4D).

These results demonstrate that USCs are indeed able to differentiate toward the osteogenic and chondrogenic lineages.

USCs have immunomodulatory properties

Finally, we wanted to test if USCs also display the typical immunosuppressive activity towards lymphocytes. Therefore, USCs were co-cultured with lymphocytes and after PHA stimulation the proliferation levels of lymphocytes were analyzed by measuring BrdU incorporation. Indeed, USCs inhibited the formation of cell clusters typically found after *in vitro* activation of lymphocytes (Hamann et al. 1986) (FIG. 5A). Similarly, lymphocyte proliferation was significantly reduced by 50% ($p = 0.02$) by co-culturing with USCs at a lymphocytes:USCs ratio of 1:1 (FIG. 5B).

These observations strongly suggest that USCs have all the characteristics of MSCs, including surface marker profile, differentiation potential as well as immunomodulatory properties.

USCs from patients with EB

After the optimization of USCs isolation and cultivation, as well as the characterization of USCs from healthy donors, we tested if our protocol was also applicable to samples from patients with epidermolysis bullosa in another laboratory (FIG. 6A). In total, 33 urine samples were obtained from 25 donors, suffering from different types of EB (dystrophic EB, junctional EB, EB simplex) (Table 3). In contrast to urine samples from healthy volunteers, the average volume from patients with EB was only 58.3 ml, probably due to the fact that in some patients the urinary tract is also affected from blistering and scarring, rendering urination painful. Interestingly, the mean

number of colonies was with 1.6 colonies per patient only slightly lower than the mean number of healthy volunteers (1.9). The number of samples showing cell proliferation was similar between both groups (60% patients with EB, 58% healthy volunteers) (Table 3).

Also EB-patient derived USCs differentiated into chondrogenic and osteogenic lineages, as could be shown by positive alzian blue (chondrogenic lineages) or NBT/BCIP (osteogenic lineages) staining and morphologic characteristics of the respective lineages. SQRT-PCR revealed the expression of lineage-specific genes compared to undifferentiated controls (FIG. 6B).

These data confirm that our optimized protocol is also applicable to the reproducible isolation of functional USCs from urine of patients with EB.

Discussion

We describe here the isolation and characterization of cells from human urine termed USCs, which display similar markers, differentiation potential and immunomodulatory properties as adipose tissue derived mesenchymal stem cells (ASCs).

In contrast to the isolation of bulk urine cells and their reprogramming to induced pluripotent stem cells (iPSCs) recently described by us (Zhou et al. 2011; Zhou et al. 2012), the direct isolation of USCs and their subsequent (trans-)differentiation in various cell lineages offers the advantage that transfection steps or the transduction with putatively oncogenic viruses can be completely omitted. However, since USCs have only a narrow differentiation potential compared to iPSCs, their usage for the generation of certain tissues, especially those originating from the ecto- and endoderm, is limited.

We and others already showed that USCs can be differentiated into the main mesenchymal lineages, such as chondrocytes and osteoblasts. Already fibroblasts could be beneficial for the treatment of patients suffering from dystrophic EB. However, recent reports demonstrate that ASCs, MSCs derived from adipose tissue, can also be trans-differentiated into keratinocyte-like cells just by co-incubation with conditioned medium or cultured keratinocytes. Furthermore,

those cells were able to form a stratified structure similar to human skin on top of a decellularized dermal matrix (Chavez-Munoz et al. 2013). Paunescu et al. demonstrated the differentiation of bone-marrow derived mesenchymal stem cells into keratinocytes by incubation with a mixture of different growth factors (Păunescu et al. 2007).

We therefore hypothesize that also USCs have the potential to trans-differentiate into keratinocyte-like cells, which could later be used for the engineering of transplantable skin-grafts as therapeutic approach for patients with EB. The isolation of functional USCs from patients with EB, as shown here, is the first important step in this process.

Next, a reproducible protocol for the generation of therapeutically relevant amounts of keratinocytes from USCs is required, which might be hindered by their limited number, proliferation and differentiation potential. However, we are convinced to circumvent this problem by generating purer USCs-populations by FACS or other enrichment strategies in the future. Furthermore, the limited number of cells can be certainly compensated by processing multiple samples, since USCs can be easily and inexpensively isolated, and which is more important, without causing any discomfort to the patients.

Summarized, the work presented here suggests a promising novel non-invasive route for obtaining stem cells from patients with EB, which might be used for therapeutic approaches after resolving the last open technical issues. Importantly, the retrieval of USCs might also be beneficial for the treatment of autoimmune disorders {Farini, 2014 #145} and other diseases, where taking biopsies is painful.

Acknowledgments

This work was supported by the Austrian Science Fund (FWF, project I510) and FP7 project Frailomic.

The authors want to thank Maximilian Bönisch for technical support.

Author Disclosure Statement

Regina Grillari-Voglauer is co-founder and CTO of Evercyte GmbH. Johannes Grillari is co-founder and CSO of Evercyte GmbH.

Authors contribution

RR. planned and performed experiments, analyzed data and wrote the manuscript.

VW. planned and performed experiments and collaborated with the preparation and correction of the manuscript.

MS. performed experiments, analyzed data and wrote the manuscript.

BJ. performed experiments and analyzed data.

SW. planned and performed experiments.

IB. performed experiments.

JG. planned experiments, interpreted the data and corrected the manuscript.

JWB. planned experiments and corrected the manuscript.

RGV. planned experiments, interpreted the data, supervised the project, and wrote the manuscript.

References

1. Belik R, W Follmann, GH Degen, PH Roos, M Blaszkewicz, HJ Knopf and K Golka (2008). Improvements in culturing exfoliated urothelial cells in vitro from human urine. J Toxicol Environ Health A 71: 923–929.

2. Bharadwaj S, G Liu, Y Shi, C Markert, K-E Andersson, A Atala and Y Zhang (2011). Characterization of urine-derived stem cells obtained from upper urinary tract for use in cell-based urological tissue engineering. Tissue Eng Part A 17: 2123–2132.

3. Bharadwaj S, G Liu, Y Shi, R Wu, B Yang, T He, Y Fan, X Lu, X Zhou, H Liu, A Atala, J Rohozinski and Y Zhang (2013). Multipotential differentiation of human urine-derived stem cells: potential for therapeutic applications in urology. Stem Cells 31: 1840–1856.

4. Chavez-Munoz C, KT Nguyen, W Xu, S-J Hong, T a Mustoe and RD Galiano (2013). Transdifferentiation of adipose-derived stem cells into keratinocyte-like cells: engineering a stratified epidermis. PLoS One 8: e80587.

5. Fine J-D, RAJ Eady, EA Bauer, JW Bauer, L Bruckner-Tuderman, A Heagerty, H Hintner, A Hovnanian, MF Jonkman, I Leigh, JA McGrath, JE Mellerio, DF Murrell, H Shimizu, J Uitto, A Vahlquist, D Woodley and G Zambruno (2008). The classification of inherited epidermolysis bullosa (EB): Report of the Third International Consensus Meeting on Diagnosis and Classification of EB. J Am Acad Dermatol 58: 931–950.

6. Guan J, X Niu, F Gong, B Hu, S Guo, Y Lou, C Zhang, Z Deng and Y Wang (2014). Biological characteristics of human Urine derived Stem Cells: potential for cell-based therapy in neurology. Tissue Eng Part A.

7. Hamann A, D Jablonski-Westrich and HG Thiele (1986). Contact interaction between lymphocytes is a general event following activation and is mediated by LFA-1. Eur J Immunol 16: 847–850.

8. Lang R, G Liu, Y Shi, S Bharadwaj, X Leng, X Zhou, H Liu, A Atala and Y Zhang (2013). Self-renewal and differentiation capacity of urine-derived stem cells after urine preservation for 24 hours. PLoS One 8: e53980.

9. Liu G, RA Pareta, R Wu, Y Shi, X Zhou, H Liu, C Deng, X Sun, A Atala, EC Opara and Y Zhang (2013). Skeletal myogenic differentiation of urine-derived stem cells and angiogenesis using microbeads loaded with growth factors. Biomaterials 34: 1311–1326.

10. Liu G, X Wang, X Sun, C Deng, A Atala and Y Zhang (2013). The effect of urine-derived stem cells expressing VEGF loaded in collagen hydrogels on myogenesis and innervation following after subcutaneous implantation in nude mice. Biomaterials 34: 8617–8629.

11. Mavilio F, G Pellegrini, S Ferrari, F Di Nunzio, E Di Iorio, A Recchia, G Maruggi, G Ferrari, E Provasi, C Bonini, S Capurro, A Conti, C Magnoni, A Giannetti and M De Luca (2006).

Correction of junctional epidermolysis bullosa by transplantation of genetically modified epidermal stem cells. Nat Med 12: 1397–1402.

12. Păunescu V, E Deak, D Herman, IR Siska, G Tănasie, C Bunu, S Anghel, C a Tatu, TI Oprea, R Henschler, B Rüster, R Bistrian and E Seifried (2007). In vitro differentiation of human mesenchymal stem cells to epithelial lineage. J Cell Mol Med 11: 502–508.

13. Reynoso R, M Wieser, D Ojeda, M Bönisch, H Kühnel, F Bolcic, H Quendler, J Grillari, R Grillari-Voglauer and J Quarleri (2012). HIV-1 induces telomerase activity in monocyte-derived macrophages, possibly safeguarding one of its reservoirs. J Virol 86: 10327–10337.

14. De Rosa L, S Carulli, F Cocchiarella, D Quaglino, E Enzo, E Franchini, A Giannetti, G De Santis, A Recchia, G Pellegrini and M De Luca (2013). Long-Term Stability and Safety of Transgenic Cultured Epidermal Stem Cells in Gene Therapy of Junctional Epidermolysis Bullosa. Stem Cell Reports 2: 1–8.

15. Wieser M, G Stadler, P Jennings, B Streubel, W Pfaller, P Ambros, C Riedl, H Katinger, J Grillari, R Grillari-voglauer, P Ambros, C Riedl, H Katinger and J Grillari (2008). hTERT alone immortalizes epithelial cells of renal proximal tubules without changing their functional characteristics. Am J Physiol Ren Physiol 4: 1365–1375.

16. Wu S, Z Wang, S Bharadwaj, SJ Hodges, A Atala and Y Zhang (2011). Implantation of autologous urine derived stem cells expressing vascular endothelial growth factor for potential use in genitourinary reconstruction. J Urol 186: 640–647.

17. Zhang Y, E McNeill, H Tian, S Soker, K-E Andersson, JJ Yoo and A Atala (2008). Urine derived cells are a potential source for urological tissue reconstruction. J Urol 180: 2226–2233.

18. Zhou T, C Benda, S Dunzinger, Y Huang, JC Ho, J Yang, Y Wang, Y Zhang, Q Zhuang, Y Li, X Bao, H-F Tse, J Grillari, R Grillari-Voglauer, D Pei and MA Esteban (2012). Generation of human induced pluripotent stem cells from urine samples. Nat Protoc 7: 2080–2089.

19. Zhou T, C Benda, S Duzinger, Y Huang, X Li, Y Li, X Guo, G Cao, S Chen, L Hao, Y-C Chan, K-M Ng, JC Ho, M Wieser, J Wu, H Redl, H-F Tse, J Grillari, R Grillari-Voglauer, D Pei

and M a Esteban (2011). Generation of induced pluripotent stem cells from urine. J Am Soc Nephrol 22: 1221–1228.

Figures:

FIG. 1. Morphology of USCs. **A,** Immediately after seeding (d0), urine samples show different contents of squamous cells, ranging from only few cells to complete coverage of the surface (from left to right panel). Representative pictures of four different donors are shown. **B,** Approximately 3 days (d3) after seeding, the formation of colonies could be observed. The variability in size and morphology between donors, as well as between two samples from the same donor are shown. **C,** Approximately 10 days (d10) after seeding, the cells reached confluence. Even within two different samples from the same donor, differences in cell morphology could be observed at his stage. **D,** After 10 PDs on average USCs stopped proliferation and showed the typical senescent morphology. Samples from two different donors are depicted. d:day

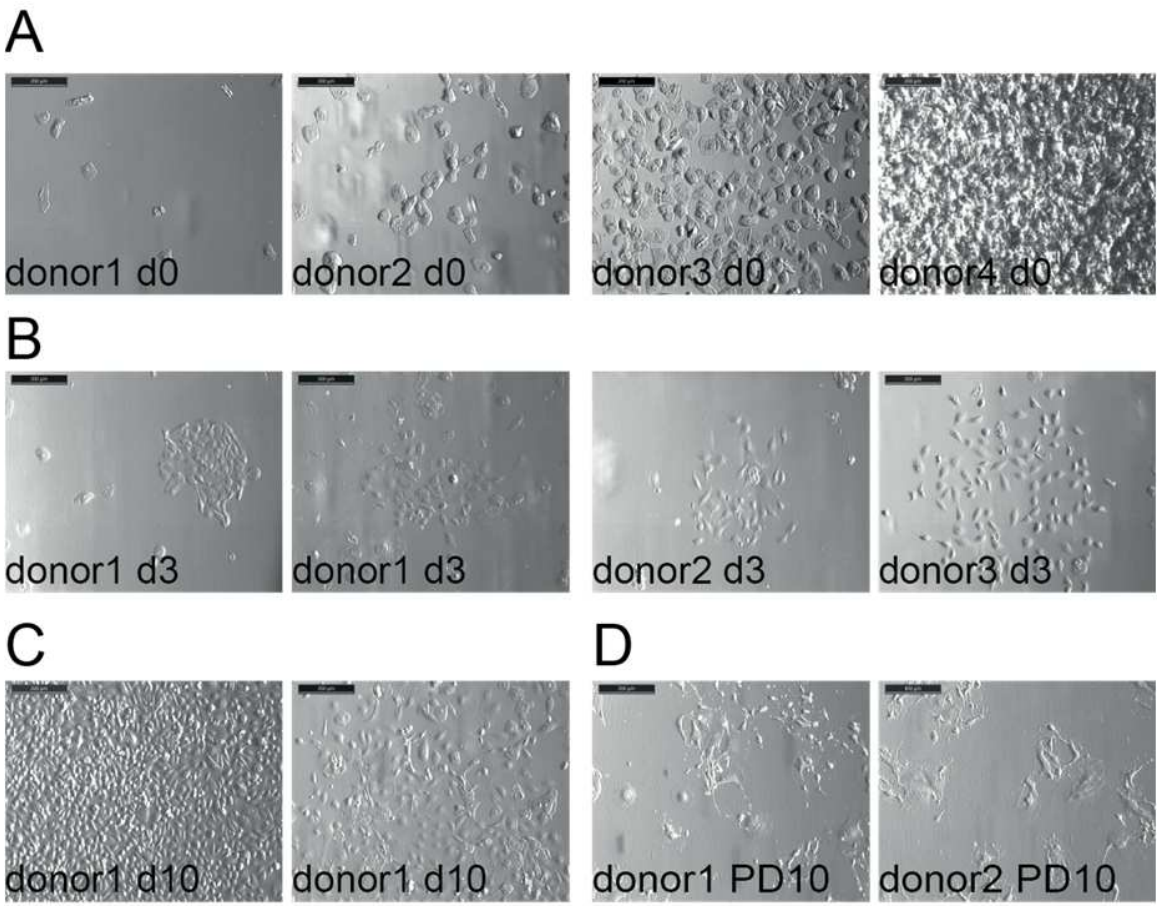

FIG. 2. Media optimization for the isolation and cultivation of USCs. **A,** Comparison of the effect of different medium formulations on the isolation and growth characteristics of USCs. The values represent the mean of at least biological triplicates, except EGM-2. Only one sample showed proliferation in EGM-2. Error bars represent the standard deviation. **B,** Representative images of cells on day 6-7 after isolation of one donor. **C,** Collagen-coating reduces significantly the efficiency of USCs-isolation ($p = 0.026$). Error bars indicate the standard deviation of biological triplicates.

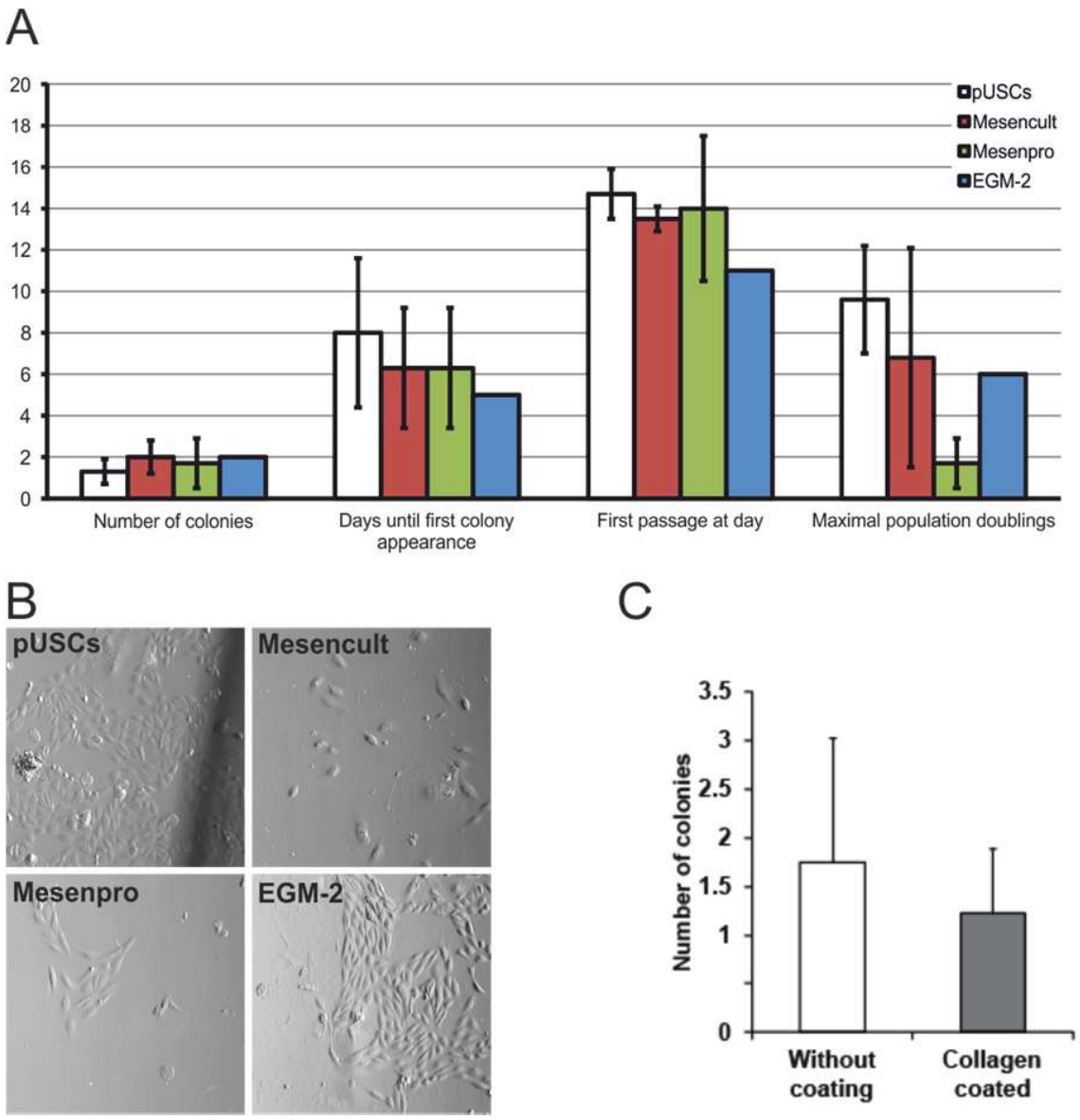

FIG. 3. USCs surface marker expression patterns resemble those of ASCs. Representative immunofluorescence images of USCs and ASCs as control are shown. USCs, as well as ASCs, stained positive for the typical MSC markers CD44, CD73, CD90 and CD105, and negative for the hematopoietic markers CD14, CD34, CD117 and CD133. Additionally, the mesenchymal markers Vimentin and Collagen I stained positive both in USCs and ASCs.

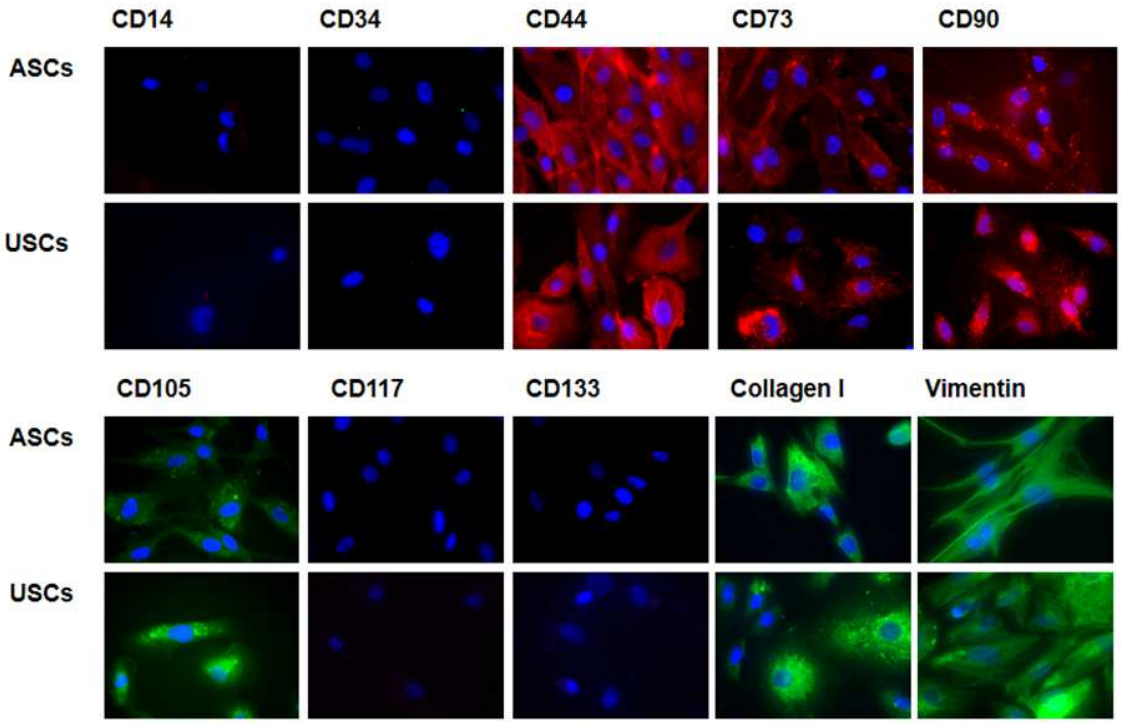

FIG. 4. USCs have the potential to differentiate towards osteocytes and chondrocytes. **A,** Osteogenic differentiation: After 28 days of culture in the induction medium, USCs stained positive for Alizarin red in contrast to the un-induced control. Representative images are shown. **B,** mRNA expression of Osteocalcin relative to GAPDH was analyzed by qPCR. Induced cells showed a significant increase compared to the un-induced control ($p = 0.05$). Error bars indicate the standard deviation from three biological replicates (three different donors). Con.: control, Ind.: induced. **C,** Chondrogenic differentiation: Representative pictures showing morphological changes and alcian blue positive staining of USCs after 28 days of induction, compared to an un-induced control, are depicted. **D,** The chondrogenic marker Collagen X (Coll. X) could only be detected in induced cultures by semi-quantitive PCR. GAPDH was used as loading control. Numbers represent different donors, I: induced, C: control, L: 100 bp ladder.

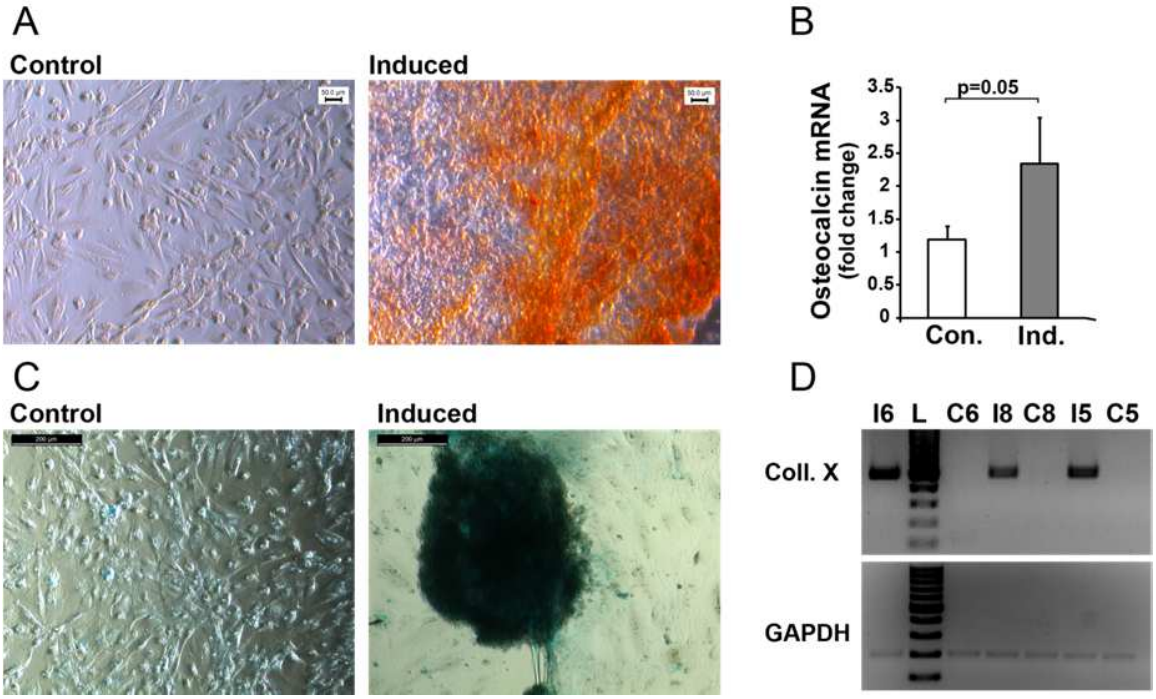

FIG. 5. **USCs display immunomodulatory properties. A**,The presence of USCs inhibited the typical cluster formation of lymphocytes after their activation by PHA. Representative pictures of lymphocytes alone (1:0) and lymphocytes and USCs at a 1:1 ratio are shown. **B**, USCs reduced PHA- activated lymphocyte proliferation in a dose-dependent manner. Error bars indicate the standard deviation of biological triplicates.

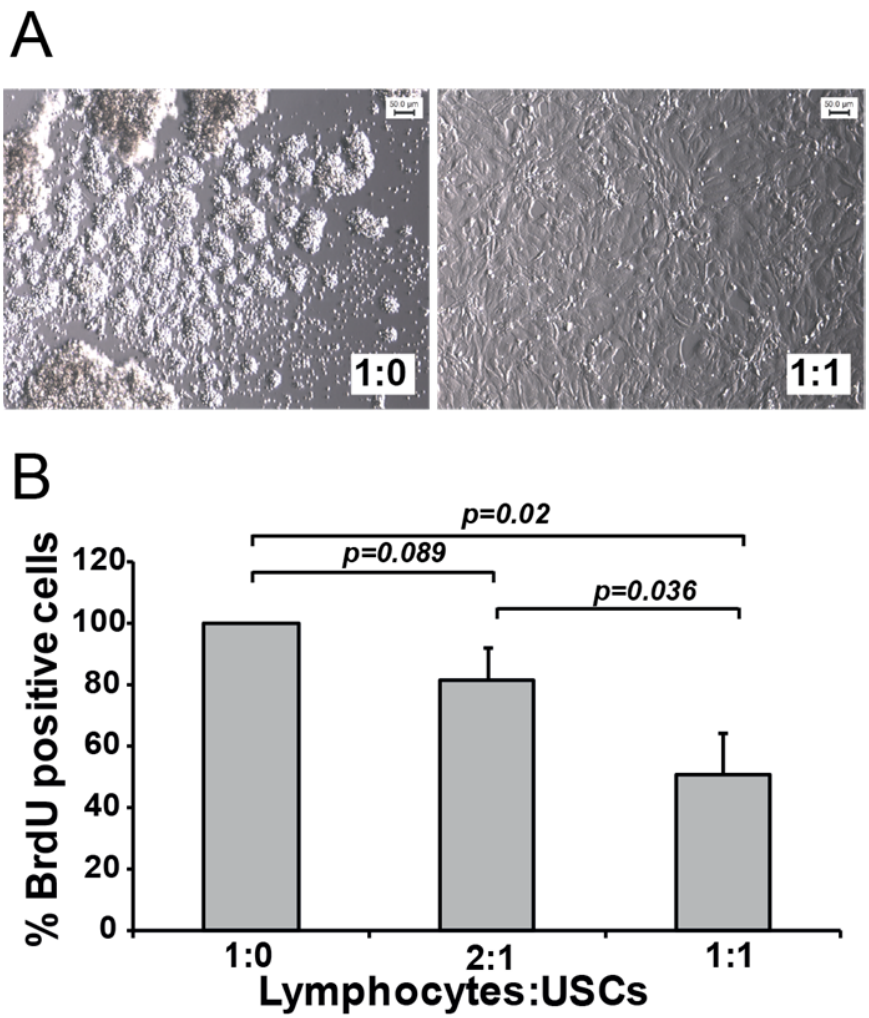

FIG. 6. Isolation and differentiation of USCs from patients with EB. **A,** Representative colonies of USCs isolated from patients with EB are shown. **B,** Chondrogenic differentiation: Representative pictures showing morphological changes and alcian blue positive staining of USCs after 18 days of induction, compared to an un-induced control, are depicted (left). The chondrogenic marker Aggrecan could only be detected in induced cultures by semi-quantitive PCR. GAPDH was used as loading control. I: induced, C: control (right). **C,** Osteogenic differentiation: After 15 days of culture in the induction medium, EB-USCs stained positive for NBT/BCIP in contrast to the un-induced control. Representative images are shown (left). mRNA expression of Osteocalcin (Osteoc.) was analyzed by semi-quantitive PCR. Induced cells showed a significant increase compared to the un-induced control. GAPDH was used as loading control. C: control, I: induced (right).

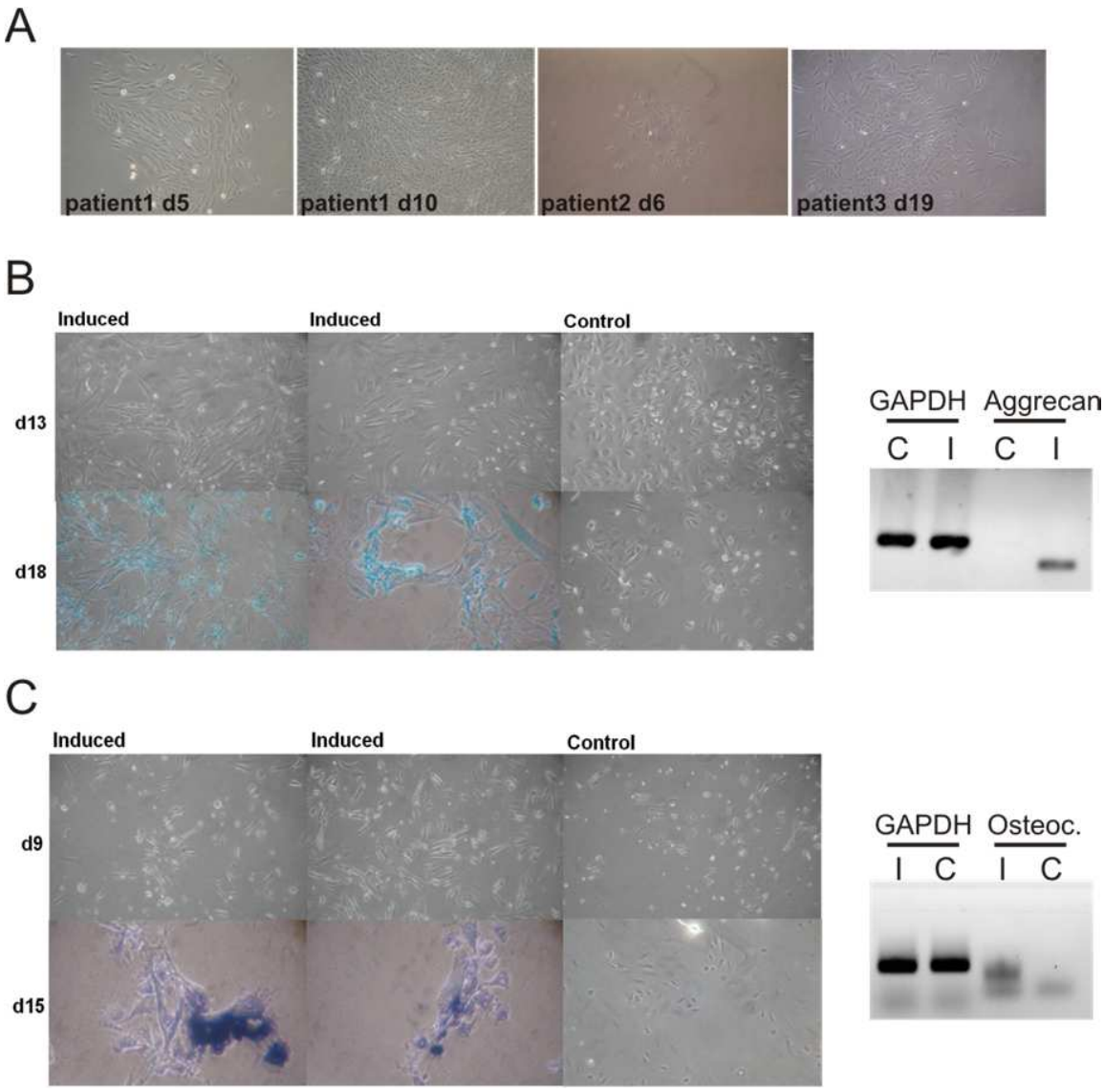

Tables:

TAB. 1. Donor characteristics and isolation success of USCs from healthy donors.

	Donors	Samples	Samples with cell proliferation (%)	Colonies formed* (± SD)	Urine volume in ml (± SD)
Total	21	127	59	2.1 ±1.4	202 ±77
Male	14	75	70	2.3 ±1.6	200 ±82
Female	7	52	42	1.6 ±0.8	203 ±72

*only successful isolations were considered

TAB. 2. Comparison of the effect of different medium formulations on USCs. The values represent the mean and standard deviation of at least biological triplicates, unless indicated otherwise.

	Colonies	Days until first colony appearance	First passage at day	Maximal population doublings
pUSCs	1.3 ±0.6	8.0 ±3.6	14.7 ±1.2	9.6 ±2.6
Mesencult	2.0 ±0.8	6.3 ±2.9	13.5 ±0.6	6.8 ±5.3
Mesenpro	1.7 ±1.2	6.3 ±2.9	14.0 ±3.5	1.7 ±1.2
EGM-2	2.0*	5.0*	11.0*	6.0*

*only one sample showed cell proliferation in EGM-2.

TAB. 3. **Donor characteristics and isolation success of USCs from patients with EB.** DEB: dystrophic EB, JEB: junctional EB, EBS: EB simplex.

	Donors	Samples	Samples with cell proliferation (%)	Colonies formed*	Urine volume in ml (± SD)
Total	25	33	61	1.6	58
DEB	14	19	47	1.3	58
JEB	2	2	50	1.5	67.5
EBS	5	7	71	1.3	46
Unknown	4	5	100	2.2	61

*only successful isolations were considered

Appendix H: Manuscripts in preparation

MiR-10a, miR-10b, miR-22, miR-133b and miR-328 are differentially regulated in serum from patients with osteoporotic fractures

Draft Author List:

Sylvia Weilner[1,2], Verena Keider[1,2], Susanna Skalicky[2], Michael Wagner[1], Heinz Redl[3], Peter Dovjak[4], Peter Pietschmann[5], Regina Grillari[1,2], Johannes Grillari[1,2,6,*], Matthias Hackl[1,7]

Affiliations

1 Department of Biotechnology, BOKU – University of Natural Resources and Life Sciences Vienna, Muthgasse 18, A-1190 Vienna, Austria

[2] Evercyte GmbH, Muthgasse 18, A-1190 Vienna, Austria

[3] LBI Wien

[4] LKH Gmunden

[5] AKH Wien

[6] CD Labor Chanel

[7] TAmiRNA GmbH, Muthgasse 11, A-1190 Vienna, Austria

Keywords: Osteoporosis, microRNA, fracture, plasma, biomarker, miR-10a, miR-10b, miR-133b

* Correspondance to
Johannes Grillari
Department of Biotechnology
BOKU – University of Natural Resources and Life Sciences Vienna
Muthgasse 18, A-1190 Vienna, Austria
johannes.grillari@boku.ac.at
Tel.: +43 1 47654 6230

Abstract

Osteoporosis is characterized by a systemic reduction in bone mass leading to increased bone fragility and an increased risk of bone fracture. Several guidelines have

been introduced to assist the early assessment of fracture risk as well as treatment response, which include several non-invasive imaging techniques, as well as the analysis of clinical parameters and biochemical markers of bone turnover. Recently, microRNAs have been identified to be secreted into the bloodstream from cells belonging to various tissues, thus, possibly indicating pathological processes occurring in different body parts. Proof that microRNAs play an important role in the control of bone homeostasis between anabolism and catabolism has already been given. However, it is not known whether the balance of both processes is also reflected in the levels of circulating microRNAs.

In this study we profiled the levels of 175 microRNAs in serum samples obtained from 7 patients with osteoporotic fractures at the femoral neck, and 7 age-matched control samples. Exploratory data analysis on the basis of all detected miRNAs did not result in a clear clustering of both groups. However, differential expression analysis identified 5 miRNAs with significantly (FDR adj. $p < 0.05$) altered serum levels in response to fracture (miR-10a, miR-10b, miR-22, miR-133b, miR-328). Functional screening of miRNA activity during osteogenic differentiation showed that miR-10a and miR-10b significantly repress osteogenic differentiation of fat-derived mesenchymal stem cells.

Overall, these data provide first proof that microRNA levels in peripheral blood change in post-traumatic patients suffering from osteoporosis. Future studies will show, whether this knowledge can be used to improve current diagnostic methodologies to predict fracture risk and treatment response in osteoporosis patients.

Introduction

Osteoporotic fractures are caused by an increase in bone fragility, which can occur due to low bone mass and microarchitectural changes in bone tissue. Such fractures are the critical hard outcome of osteoporosis, which affects more than 75 million people in the United States, Europe and Japan(Kanis et al. 2013). With a lifetime risk of 30% - 40% to be affected by vertebral or non-vertebral fractures in developed countries, osteoporosis has an incidence rate similar to that of coronary heart disease. Furthermore, with the exception of forearm fractures, osteoporotic fractures are associated with increased mortality. Most fractures cause acute pain and lead to patient hospitalization, immobilization and often slow recovery.

Assessment of fracture risk is one of the most important aspects of diagnosing osteoporosis. Therefore, analysis of bone mass by measuring bone mineral density (BMD) is currently the only clinical parameter of the skeleton that is routinely analyzed in clinical practice and part of the WHO FRAX questionnaire(Kanis et al. 2013). However, the assessment of T-Scores does not necessarily improve fracture risk prediction in combination with established clinical scores of fracture risk(Rubin et al. 2013), due to lacking correlation with bone strength and bone metabolism(Cefalu 2004). In order to estimate the rate of bone formation, bone resorption and eventually bone quality and therapeutic treatment response, several molecular bone turnover markers (BTM) have been identified(Vasikaran et al. 2011). Of these, serum procollagen type I N propeptide (s-PINP) and serum C-terminal telopeptide of type I collagen (s-CTX) have been recommended by The International Osteoporosis Foundation (IOF) and the International Federation of Clinical Chemistry and laboratory Medicine (IFCC) as reference BTMs(Vasikaran et al. 2011). Both markers are derived from collagen metabolism, either from cathepsin K mediated collagen hydrolysis (s-CTX) or as collagen building blocks produced by osteoblasts. Nevertheless, specificity and sensitivity of these markers have to be further validated.

Other markers of bone metabolism might be derived from the signaling pathways that play a major role in bone formation and resorption, such as WNT, BMP-2 or RANKL. Recently, increased attention has been attributed to the importance of microRNAs (miRNAs), small non-coding RNAs that regulate gene expression(Bartel 2009), in the

control of bone metabolism(Dong et al. 2012; Zhao et al. 2013). Several miRNAs were shown to silence osteogenic inhibitors during stem cell differentiation into osteocytes(Trompeter et al. 2013), to regulate BMP2 mediated osteoblast proliferation and differentiation(Li et al. 2008), or orchestrate the activity of WNT-signalling(Kapinas et al. 2009). Therefore, the potential of miRNAs as therapeutic agents accelerating bone regeneration or as diagnostic targets for evaluating bone metabolism and fracture risk has recently been acknowledged(van Wijnen et al. 2013). A non-invasive approach to fracture risk assessment could therefore be presented by the analysis of blood-circulating miRNAs, which have started to become extensively analyzed in the context of disease, especially cancer and cardiovascular disease, or non-pathological processes such as ageing(Weilner et al. 2013). In order to provide a first proof-of-principle, that osteoporosis and especially osteoporotic fractures lead to changes in patterns of blood-circulating miRNAs, we set out to profile 175 miRNAs in 14 serum samples, 7 of which were derived from patients suffering from fractures at the femoral neck and 7 control samples that were matched according to several clinical parameters such as age. Our results indicate significant difference in the levels of 5 miRNAs, 4 of which have been previously reported to be involved in osteoblast differentiation or activity.

Material and Methods

Study Population

Ethical approval was granted by the upper Austrian ethics committee for the collection of serum samples from 14 subjects by centrifugation at room temperature at 2000xg for 15 minutes after incubation at room temperature for 30 minutes. Subjects were classified into two groups (n=7) based on prior occurrence of osteoporotic femoral fractures (Figure 1a). Of the analyzed characteristics such as age, body mass index (BMI), sampling interval after surgery, BMD T-Score, Vitamin D and PTH, only BMI showed significant differences.

RNA Isolation from Serum

Serum samples were frozen at -80°C for long term storage. Upon RNA isolation, serum was thawed at 37°C, centrifuged and 200 µl serum were homogenized in 750 µl Qiazol

containing 35 fmol synthetic cel-miR-39-3p spike-in control. RNA isolation was performed using chloroform and the miRNeasy isolation kit (Qiagen, Germany) for RNA precipitation and purification with the following deviations from the standard protocol: 200 µl plasma were homogenized in 750 µl Qiazol. Exactly 500 µl aqueous phase were taken, 1 µl Glycogen (Ambion, TX) were added to a final concentration of 50 µg/ml and precipitated with 750 µl 100% Ethanol. Columns were washed three times with RPE buffer and plasma-RNA was eluted once in 30 µl nuclease-free water and stored at -80°C. Quantitation of cel-miR-39-3p was performed in quadruplicates on a Qiagen Rotorgene using the respective Taqman microRNA Assay Kit and Mastermix (Applied Biosystems).

microRNA qPCR profiling

Screening of miRNA expression was performed by Exiqon Inc. in Denmark using 384-well serum/plasma focus panels, which cover 175 distinct human miRNAs that have been repeatedly found to circulate in serum or plasma. First, 4 µl of isolated RNA were reverse transcribed in 20 µl reactions using the miRCURY LNA Universal RT reaction kit. UniSp3 and UniSp6 are synthetic controls that were added at this step and subsequently analyzed to detect presence of enzyme inhibitors. RT-reactions were diluted 50-fold prior to qPCR analysis and each miRNA was assayed once per sample in a 10 µl reaction using the Roche LC 480 Real-Time PCR System (Roche, Germany).

qPCR data analysis

Melting curve analysis was performed and miRNA PCR reactions with more than one peak were excluded from the analysis. Amplification efficiencies were calculated using algorithms similar to the linreg software package. Efficiencies ranged between 1.8 and 2.1 for most miRNAs. Individual reactions that gave efficiencies < 1.6 were excluded from the dataset. Background levels for each miRNA were generated by assaying a “no template” cDNA synthesis control on a full serum/plasma focus panel plate. The majority of miRNA assays did not yield any signal and background Cp was set to 42. We required every miRNA assay to exhibit signals > 5 Cps lower than the background value to be included in the analysis. Normalization of Cp-values was performed based on the average Cp of the miRNA assays detected across all 14 samples (124 assays). Normfinder software was used to confirm that the stability of the average Cp was higher

than the stability of any individual miRNA assay in the data set. The following equation was used for normalization: normalized Cp (dCp) = average Cp (124 assays) – assay Cp (sample). This results in a delta Cp (dCp) value, which is a relative log_2-transformed measure for expression where higher values indicate a higher concentration and lower dCp values indicate lower concentration in plasma.

Statistical data analysis

Hierarchical clustering and heatmap production was performed in R using the "heatmap.2" function of the gplot package. Euclidean distance was taken as distance metric, and clusters were generated using complete linkage. Principal component analysis was performed in R using the prcomp function. Differential miRNA expression analysis was performed by calculating p-values in Excel 2010 using the two-sided TTEST formula and assumed equal distribution. P-value adjustment for multiple testing was performed using Benjamini-Hochberg FDR calculation.

MicroRNA transfection in fat-derived mesenchymal stem cells

See chapter Material and Methods

Results

Sample characteristics and selection

In this study we set out to analyze the levels of blood-circulating miRNAs from patients with osteoporotic fractures, in order to enhance our understanding of potential risk factors that contribute to the occurrence of type I osteoporosis. Therefore, we obtained samples from 14 female individuals, of which 7 had suffered from fractures at the femoral neck (median age 70y, 66.5 - 71) and had undergone surgery. Based on the age distribution of these individuals, 7 age-matched control samples were chosen with equivalent normal distribution of age (median age 70y, 68 – 75). Further clinical parameters of all 14 donors are included in Figure 1a. Besides age, also Vitamin D3 or parathyroid hormone levels were found to be equal between both groups (Fig 1b). However, body mass index (BMI) was higher in the control group compared to the fracture group.

Sample and RNA quality were controlled at several stages during the analysis process. Cel-miR-39-3p was spiked prior to RNA isolation and analyzed by qPCR to ensure consistent RNA isolation (Fig 2a). In addition two synthetic spike-in controls, UniSp3 and UniSp6, were added to the isolated RNA in order to test for the presence of enzyme inhibitors (Fig 2b). The uniform Cp values obtained for all spike-ins confirmed successful RNA isolation, reverse transcription and qPCR. Based on a recent study by Blondal et al., the degree of contamination with erythrocyte RNA was assessed by computing the dCp between miR-23a-3p and miR-451a-5p, which is known to be highly transcribed in erythrocytes (ref). The results indicated relatively high levels (> 6) for five samples (Fig 2c). Consequently we identified miRNAs that could originate from hemolysis by correlating the expression levels to miR-451a-5p levels (Supp. Fig. 1) using Pearson correlation. In total 10 miRNAs, with a PCC > 0.9 (including miR-451a) were identified and removed from the data set. Thus, a total of 165 miRNAs remained in the data-set, which were further normalized to the average Cp-value in each sample, which was identified as the most robust reference using Normfinder (ref). The resulting delta Cp (dCp) values can be regarded as $\log_2$ transformed relative expression value and were used for explorative and statistical data analysis.

Explorative data analysis does not clearly discriminate fracture from control samples

We performed principal component on the basis of 149 miRNAs, which were called present in at least 12 out of 14 plasma samples using R/Bioconductor. The first three independent principal components accounted for a total variance of 61.1% but could not clearly separate the analyzed samples into distinct clusters (Fig 3a). Consequently, hierarchical clustering on the basis of 124 miRNA, which were called present across all 14 samples was performed (Fig 3b). While this analysis resulted in two distinct clusters containing 5 and 9 samples, respectively, both clusters consisted of samples from patients with fractures and respective controls. Thus, based on this dataset, no discrimination of samples derived from patients with osteoporotic femoral neck fractures from the age-matched control samples could be achieved on the basis of circulating miRNA levels.

Statistical data analysis identifies 5 miRNAs deregulated upon femoral neck fractures

In the next step, differential expression analysis was performed to identify circulating miRNAs that are deregulated in serum upon the occurrence of femoral fractures in women. Therefore, dCp values from each group were analyzed by Students T-Test followed by Benjamini-Hochberg p-value correction for multiple testing (q-value). All 165 miRNAs were ranked according to their q-value and a FDR-threshold of 0.05 was imposed (Tab 1, Fig 4a). In total, 5 miRNAs fulfilled this criterion (Fig 4b), of which 3 miRNAs were up-regulated in plasma from fracture patients (miR-10a, miR-10b, miR-22) and 2 were down-regulated (miR-133b, miR-328)

Bioinformatic target gene prediction

An estimation of the biological function of these 5 miRNAs was performed using the DIANA miRPath target gene prediction tool in order to predict the union of potential miRNA targets and to analyze target enrichment in KEGG pathways. Using two distinct prediction algorithms (microT v 4.0 and Targetscan 5.0) the KEGG pathways with significantly enriched targets were identified (p-value < 0.05) for both predictions (Table 2). Out of 29 pathways that were identified, five were common to both prediction algorithms, of which Wnt signaling pathway (including the canonical and Wnt/Ca^{2+} pathway) was ranked second according to the average p-value (Table 2).

Functional characterization of microRNAs

microRNAs that were found up-regulated in fracture patients (miR-10a, miR-10b, miR-22) were selected for overexpression in fat-derived mesenchymal stem cells prior to osteogenic differentiation, while down-regulated miRNAs (miR-328) were inhibited using antagomiR inhibitors. Although down-regulated in fractures miR-133b was overexpressed as well, since it was previously that miR-133a/b are muscle specific with no expression in stem cells(E. J. Lee et al. 2008; Zaharieva et al. 2013). Two days after transfection, miRNA overexpression or knockdown was confirmed by qPCR (Fig 5a). At day 4 after transfection osteogenic differentiation was induced and Alkaline Phosphatase (ALP) activity and calcification were chosen as read outs for osteogenic differentiation at day 7 and day 21, respectively. Analysis of both markers clearly indicates that overexpression of miR-10a/b results in significant repression of osteogenic differentiation. Overexpression of miR-22 did not show any effect, while down-regulation of miR-328 reduced ALP activity and slightly decreased calcification (Fig. 5b/c).

Discussion

Several studies have shown that specific miRNA signatures in the blood stream can be representative for the absence or presence of pathological conditions, or even the stage of a certain disease. In this study we set out to compare the levels of secreted miRNAs from 7 patients suffering from osteoporotic fractures to 7 control samples with similar distribution of age and additional clinical parameters except BMI. Our analysis identified 5 out of 175 miRNAs as differentially expressed after correction for multiple testing. Among these, miR-10a/b and miR-22 were up-regulated in patients suffering from femoral neck fractures, while miR-133b and miR-328 were found to be down-regulated.

miRNA-10a and miR-22 were recently described to aid osteogenic differentiation by silencing the expression of osteoblast inhibitors such as cyclin dependant kinase 6 (CDK6) or histone deacetylase 4 (HDAC4)(Trompeter et al. 2013). Therefore, increasing concentrations of these miRNAs in serum of fracture patients might indicate higher osteoblast activity and differentiation due to regeneration of fracture. The down-regulation of miR-133b in serum of fracture patients supports this assumption, since it is known from in vitro experiments that a decrease in miR-133b is during BMP-2 induced osteoblast differentiation of C2C12 progenitor cells allows an increase in the expression of its target gene Runx-2, a transcription factor that is crucial to osteoblast differentiation(Li et al. 2008).

In addition, bioinformatics target prediction listed WNT-signaling as one of five cellular pathways that were identified as significantly enriched using two independent target prediction algorithms. Canonical WNT-signaling is known to play an important role in the signaling cascade that mediates bone metabolism, because it enhances osteoblast proliferation and mineralization through the stabilization of β-catenin(Marcellini et al. 2012). The β-catenin inhibiting binding-protein CTNNBIP1 was found present among the targets predicted for miR-10a/b(Trompeter et al. 2013), and down-regulation of CTNNBIP1 could enhance β-catenin accumulation in the nucleus and therefore the expression of factors supporting osteogenic differentiation.

The fact that the levels of miRNAs, which have previously been identified as regulators of osteogenic differentiation, are found to be altered in patients suffering from osteoporotic fractures at the femoral neck indicates that homeostasis of bone metabolism can be detected by the non-invasive analysis of circulating miRNAs. This

knowledge is extremely valuable, since it justifies further studies that aim to analyze miRNA levels at an earlier stage during osteoporosis, before fractures have occurred. These population based prospective studies will give insights into whether specific miRNAs signatures can be helpful in improving current strategies for patient stratification according to their fracture risk.

Figures and Tables

a

Patient ID	Gender	Fracture	Age	Date of surgery	Date of sampling	Sampling Interval (days)	BMI	DEXA T-Score	Hydroxy-vitamin D (µg/L)	PTH (ng/L)
15.	female	femoral neck	62	25.08.2010	03.09.2010	9	17.30	n/a	9.9	20
155.	female	femoral neck	64	17.03.2011	29.03.2011	12	27.89	n/a	10.1	59
400.	female	femoral neck	82	05.12.2011	15.12.2011	10	23.14	-0.30	21.9	39
25.	female	femoral neck	72	24.08.2010	10.09.2010	17	19.49	n/a	14.1	44
279.	female	femoral neck	71	20.08.2011	30.08.2011	10	25.46	-2.50	24.3	32
83.	female	femoral neck	87	03.12.2010	10.12.2010	7	25.10	-0.40	6.2	137
49.	female	femoral neck	69	01.10.2010	15.10.2010	14	25.04	n/a	18.5	-
152.	female	control	78	-	-	-	28.0	-1.40	21.7	40
326.	female	control	70	-	-	-	32.3	1.10	26.8	33
333.	female	control	67	-	-	-	31.6	2.30	13.2	37
336.	female	control	69	-	-	-	27.3	-1.00	9.9	65
365.	female	control	80	-	-	-	28.0	3.00	43.8	33
79.	female	control	72	-	-	-	24.5	-1.60	11.9	48
93.	female	control	61	-	-	-	35.5	-1.10	13.1	41

b

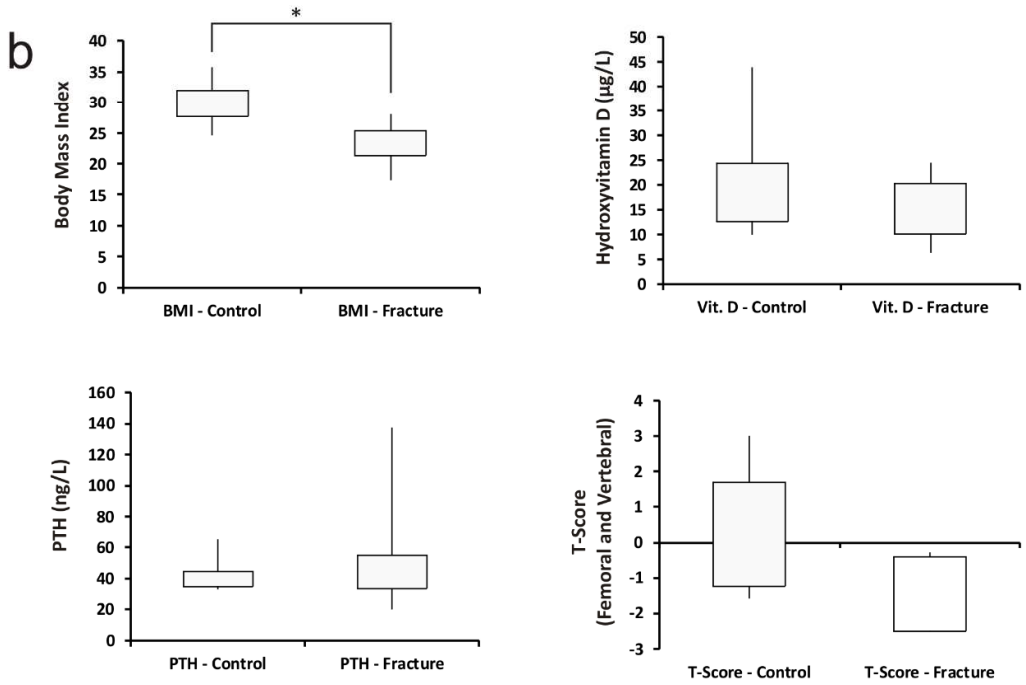

Figure 1: Overview of clinical parameters: a) Table with patient specific data for age, surgery and blood sampling date, body mass index (BMI), bone mineral density measured as T-Score at the femor and vertebral spine, Hydroxyvitamin-D and parathyroid hormone (PTH) levels. b) Boxplot illustration of selected parameters. * Student´s T-Test $p < 0.05$

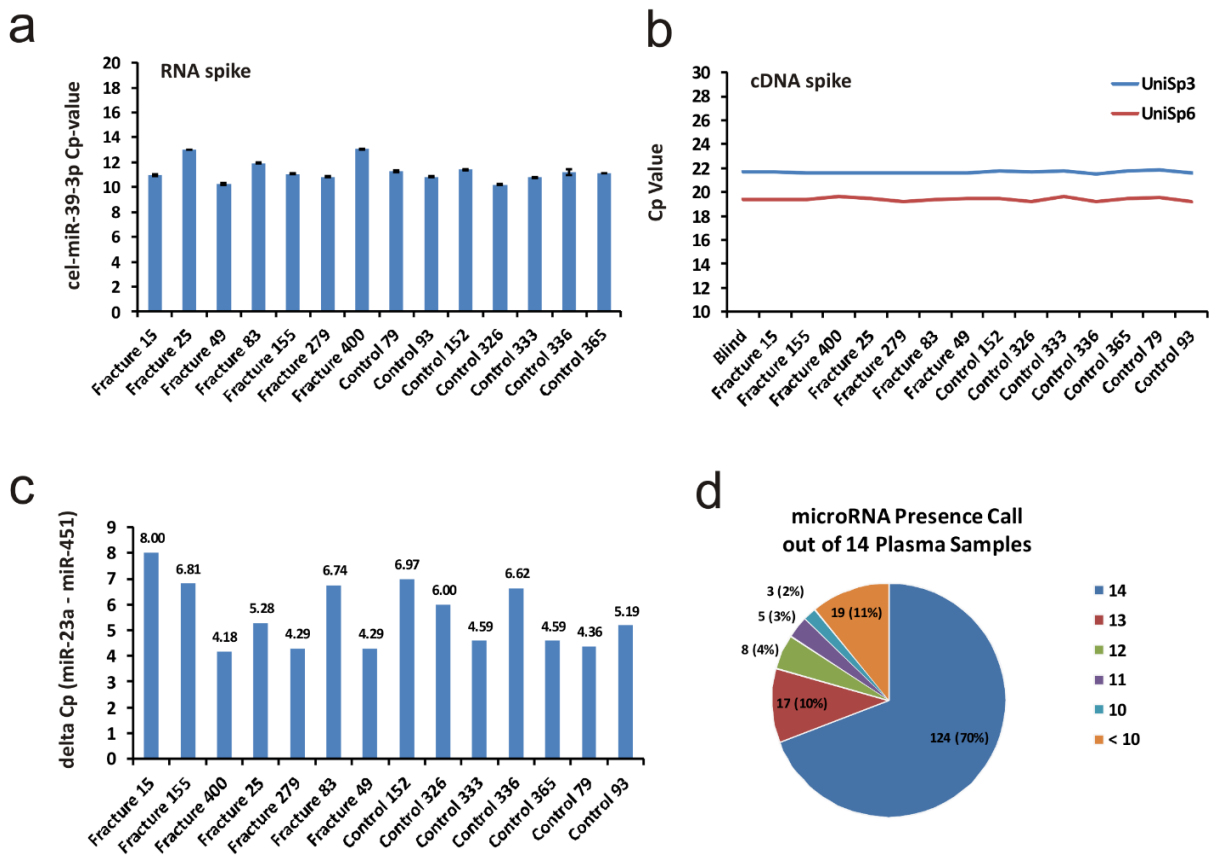

Figure 2: Quality attributes of qPCR plasma profiling: a,b) Synthetic RNA oligonucleotides were added to the organic solvent prior to RNA isolation (cel-miR-39-3p) and to isolated RNA prior to cDNA synthesis (UniSp3 and 6) and analyzed by qPCR to detect presence of enzyme inhibitors. RAW Cp-values for RNA spike-ins cel-miR-39-3p, UniSp3 and UniSp6 are given for all 14 samples. c) Contamination of plasma RNA with erythrocyte RNA was detected by analyzing miR-451a levels relative to miR-23a (delta Cp values, dCp). dCp values below 5 indicate low risk of contamination, while dCp values > 7 indicate high risk of contamination. d) Analysis of microRNA presence calls by qPCR across 14 plasma samples.

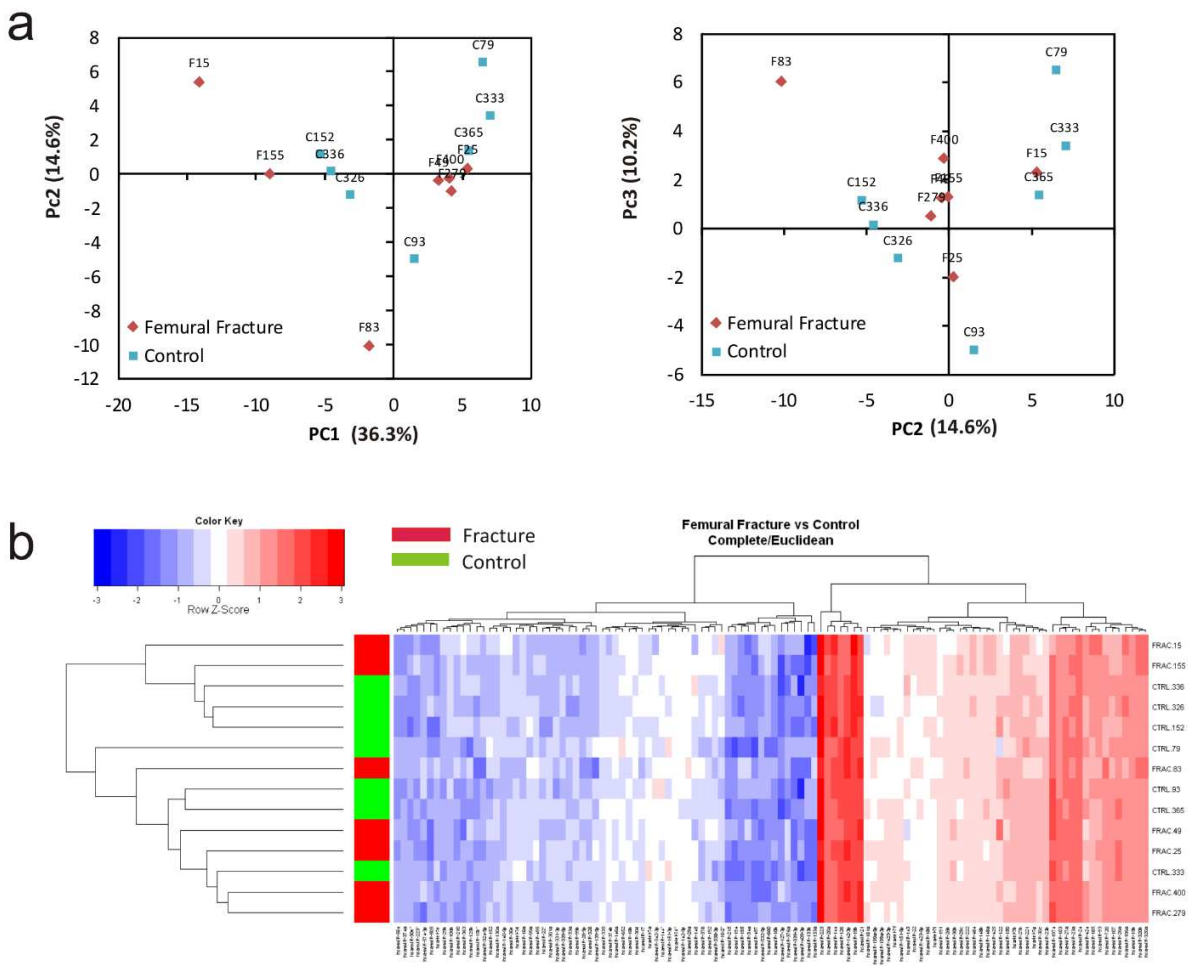

Figure 3: Exploratory analysis of circulating microRNA levels: a) Principal component analysis was performed on microRNAs with present calls in 12 or more clinical samples, and which did not respond to the level of erythrocyte contamination (degree of haemolysis). h) Hierarchical cluster analysis was performed using Euclidean square distance as distance metric and complete cluster linkage.

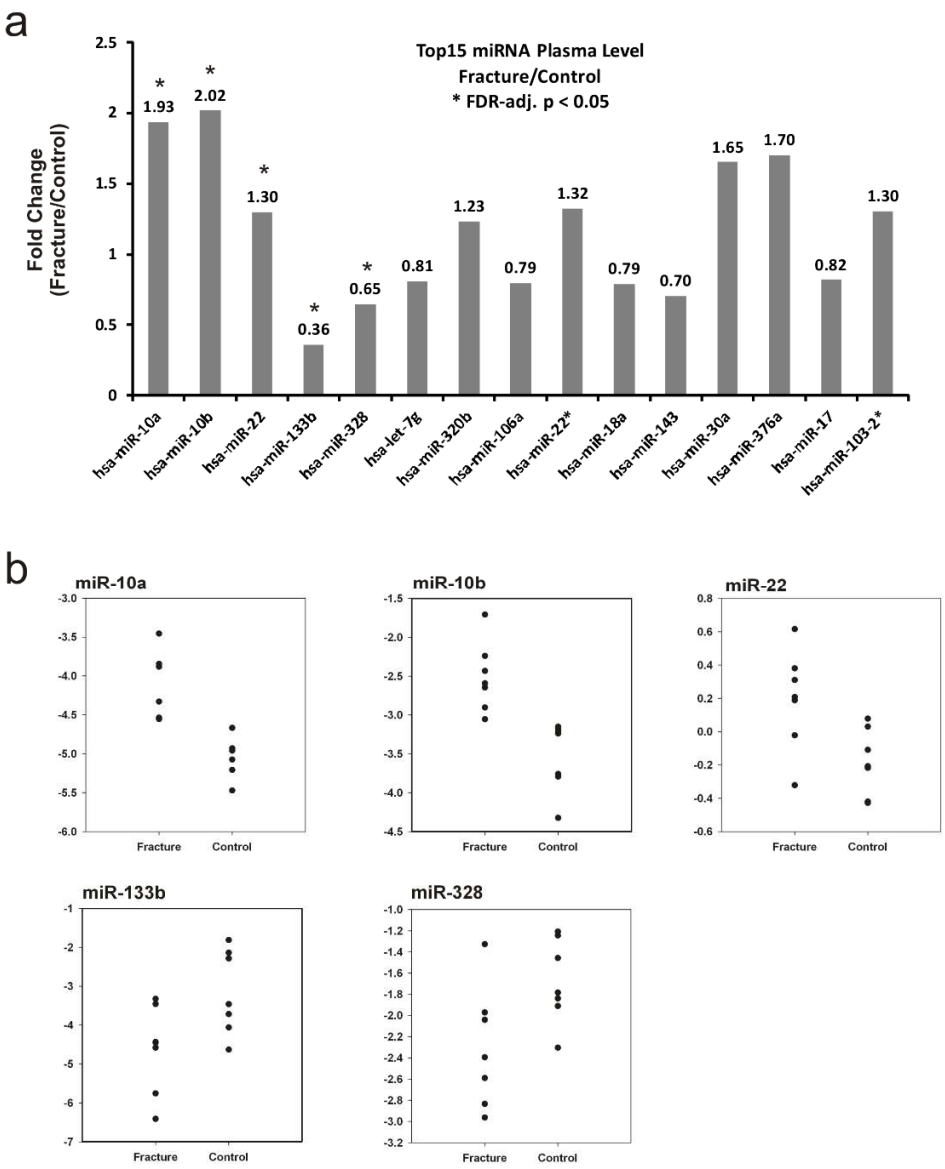

Figure 4: Statistical analysis of differential microRNA expression in plasma derived from patients with fractures and respective controls: a) Fold changes were calculated for the top 15 microRNAs sorted by false-discovery rate adjusted p-values. Fold changes are given for miRNAs in plasma from patients with fracture compared to control. * indicate miRNAs with FDR-adjusted p-values < 0.05. b) Dot plots showing individual normalized log2 transformed expression (dCp values) for 5 simiRNAs in patients with (n=7) or without fracture (n=7).

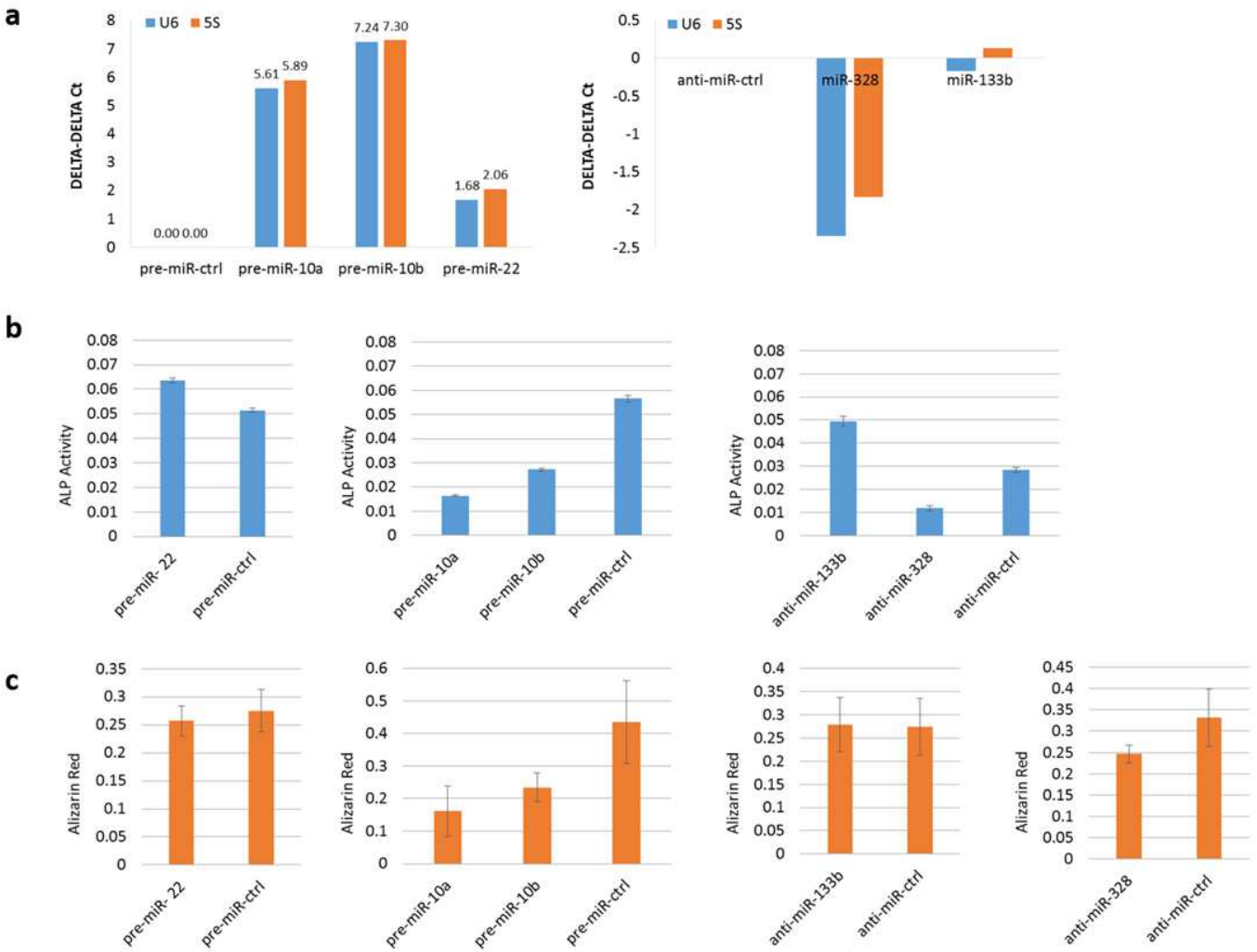

Figure 5: microRNA transfection and osteogenic differentiation: a) qPCR confirmation of microRNA overexpression and knockdown. b) Alkaline Phosphatase (ALP) activity at day 7 post differentiation (average +/- S.D. n=X). c) Alizarin Red incorporation at differentiation endpoint (average +/- S.D. n=X).

Table 1: Plasma microRNA levels, Top 15 sorted by FDR-adjusted p-value

Rank	miRNA	Count*	Fracture Avg	Fracture SD	Control Avg	Control SD	D vs H ddCp**	ddCp SD	D vs H FC	FC SD	T-TEST p-value	FDR BH q-value
1	hsa-miR-10a	12	-4.10	0.40	-5.05	0.25	0.95	0.65	1.93	0.90	0.001	0.002
2	hsa-miR-10b	14	-2.51	0.41	-3.52	0.41	1.01	0.83	2.02	1.24	0.001	0.023
3	hsa-miR-22	14	0.19	0.28	-0.18	0.18	0.38	0.46	1.30	0.65	0.017	0.034
4	hsa-miR-133b	14	-4.63	1.04	-3.16	1.00	-1.47	2.04	0.36	3.04	0.028	0.041
5	hsa-miR-328	14	-2.30	0.53	-1.68	0.37	-0.62	0.89	0.65	1.26	0.034	0.048
6	hsa-let-7g	14	1.25	0.27	1.55	0.19	-0.31	0.46	0.81	0.66	0.041	0.077
7	hsa-miR-320b	14	3.03	0.34	2.73	0.14	0.30	0.48	1.23	0.62	0.07	0.09
8	hsa-miR-106a	14	2.54	0.37	2.88	0.21	-0.33	0.58	0.79	0.79	0.08	0.09
9	hsa-miR-22*	14	-1.84	0.25	-2.24	0.46	0.40	0.72	1.32	1.18	0.09	0.10
10	hsa-miR-18a	14	-1.67	0.25	-1.32	0.39	-0.34	0.63	0.79	1.02	0.09	0.11
11	hsa-miR-143	14	-0.18	0.49	0.33	0.50	-0.51	0.99	0.70	1.49	0.10	0.12
12	hsa-miR-30a	13	-3.81	0.54	-4.54	0.79	0.72	1.33	1.65	2.12	0.11	0.12
13	hsa-miR-376a	14	-2.44	0.70	-3.21	0.86	0.77	1.56	1.70	2.42	0.12	0.13
14	hsa-miR-17	14	-1.20	0.31	-0.91	0.28	-0.29	0.59	0.82	0.88	0.12	0.14
15	hsa-miR-103-2*	12	-4.53	0.29	-4.91	0.40	0.38	0.69	1.30	1.09	0.13	0.16

* present calls out of 14 samples
** = $\log_2$ fold change

Table 2: KEGG pathway and target enrichment of miR-10a/b, miR-22, miR-133b and miR-328

KEGG	microT v4	Targetscan 5.0	Avg p-value	Overlapping predicted targets
Adherens junction	x	x	2.79E-07	EGFR, EP300, FGFR1, IGF1R, INSR, MAP3K7, MLLT4, PTPRF, SNAI1, SSX2IP, TGFBR1, WASF1, YES1
Wnt signaling pathway	x	x	8.06E-04	BTRC, CTBP2, CTNNBIP1, EP300, FBXW11, FRAT2, MAP3K7, NFAT5, PPP2CA, PPP2CB, TBL1X, WNT4
Regulation of actin cytoskeleton	x	x	2.53E-03	ARPC5, CRK, DIAPH2, EGFR, FGF1, FGFR1, IQGAP2, ITGA10, ITGA5, ITGB8, MSN, MYH9, PAK6, PFN2, PIK3CA, PIP4K2B, PIP5K3, SLC9A1, TIAM1, WASF1
Chronic myeloid leukemia	x	x	4.33E-03	AKT3, PIK3CA
ErbB signaling pathway	x	x	1.96E-02	AKT3, CBL, CDKN1A, CRK, EGFR, ERBB3, ERBB4, MAP2K4, PAK6, PIK3CA

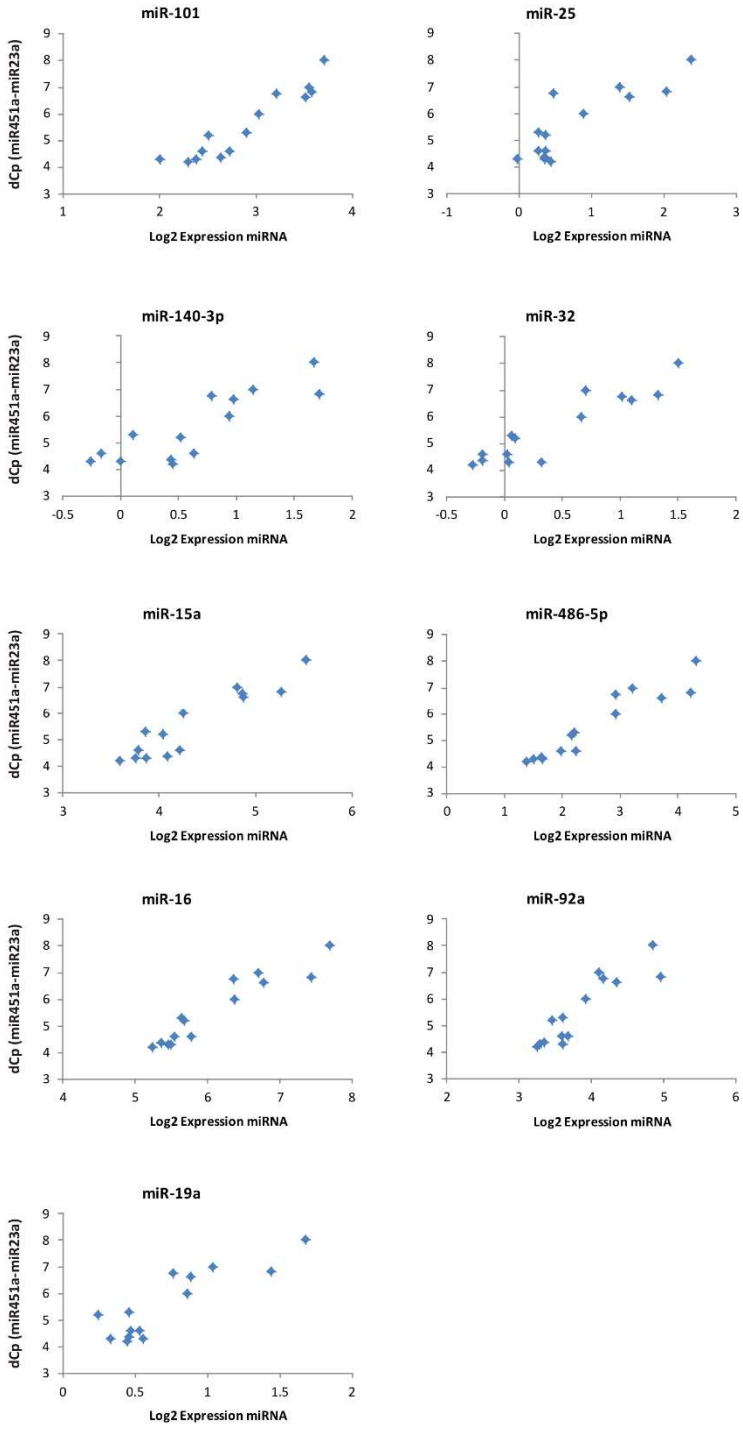

Supporting Figure 1: microRNAs with high correlation to miR-451a indicating presence of erythrocyte RNA: Scatterplots showing the correlation of microRNA plasma levels and the haemolysis score, calculated as miR-451a – miR-23a. Pearson correlation coefficients are: hsa-miR-101, 0.94; hsa-miR-140-3p, 0.85; hsa-miR-15a, 0.93; hsa-miR-16, 0.94; hsa-miR-19a, 0.87; hsa-miR-25, 0.86; hsa-miR-32, 0.92; hsa-miR-486-5p, 0.94; hsa-miR-92a, 0.90;

References

1. Kanis, J. A. *et al.* European guidance for the diagnosis and management of osteoporosis in postmenopausal women. *Osteoporos. Int. J. Establ. Result Coop. Eur. Found. Osteoporos. Natl. Osteoporos. Found. USA* **24,** 23–57 (2013).

2. Rubin, K. H. *et al.* Comparison of different screening tools (FRAX®, OST, ORAI, OSIRIS, SCORE and age alone) to identify women with increased risk of fracture. A population-based prospective study. *Bone* **56,** 16–22 (2013).

3. Cefalu, C. A. Is bone mineral density predictive of fracture risk reduction? *Curr. Med. Res. Opin.* **20,** 341–349 (2004).

4. Vasikaran, S. *et al.* Markers of bone turnover for the prediction of fracture risk and monitoring of osteoporosis treatment: a need for international reference standards. *Osteoporos. Int. J. Establ. Result Coop. Eur. Found. Osteoporos. Natl. Osteoporos. Found. USA* **22,** 391–420 (2011).

5. Bartel, D. P. MicroRNAs: target recognition and regulatory functions. *Cell* **136,** 215–233 (2009).

6. Dong, S., Yang, B., Guo, H. & Kang, F. MicroRNAs regulate osteogenesis and chondrogenesis. *Biochem. Biophys. Res. Commun.* **418,** 587–591 (2012).

7. Zhao, X. *et al.* MicroRNAs regulate bone metabolism. *J. Bone Miner. Metab.* (2013). doi:10.1007/s00774-013-0537-7

8. Trompeter, H.-I. *et al.* MicroRNAs miR-26a, miR-26b, and miR-29b accelerate osteogenic differentiation of unrestricted somatic stem cells from human cord blood. *BMC Genomics* **14,** 111 (2013).

9. Li, Z. *et al.* A microRNA signature for a BMP2-induced osteoblast lineage commitment program. *Proc. Natl. Acad. Sci. U. S. A.* **105,** 13906–13911 (2008).

10. Kapinas, K., Kessler, C. B. & Delany, A. M. miR-29 suppression of osteonectin in osteoblasts: regulation during differentiation and by canonical Wnt signaling. *J. Cell. Biochem.* **108,** 216–224 (2009).

11. Van Wijnen, A. J. *et al.* MicroRNA functions in osteogenesis and dysfunctions in osteoporosis. *Curr. Osteoporos. Rep.* **11,** 72–82 (2013).

12. Weilner, S., Schraml, E., Redl, H., Grillari-Voglauer, R. & Grillari, J. Secretion of microvesicular miRNAs in cellular and organismal aging. *Exp. Gerontol.* **48,** 626–633 (2013).

13. Lee, E. J. *et al.* Systematic evaluation of microRNA processing patterns in tissues, cell lines, and tumors. *RNA N. Y. N* **14,** 35–42 (2008).

14. Zaharieva, I. T. *et al.* Dystromirs as serum biomarkers for monitoring the disease severity in duchenne muscular dystrophy. *PloS One* **8,** e80263 (2013).

15. Marcellini, S., Henriquez, J. P. & Bertin, A. Control of osteogenesis by the canonical Wnt and BMP pathways in vivo: cooperation and antagonism between the canonical Wnt and BMP pathways as cells differentiate from osteochondroprogenitors to osteoblasts and osteocytes. *BioEssays News Rev. Mol. Cell. Dev. Biol.* **34,** 953–962 (2012).

Curriculum vitae

Dipl. Ing. Sylvia Weilner

Hauptstraße 2
E-mail: Sylvia.weilner@boku.ac.at
3464 Perzendorf

PERSONAL DATA:

Date of birth:	18.08.1983
Place of birth:	Tulln
Citizenship:	Austria
Marital status:	Unmarried

EDUCATION:

Since 2011	PhD thesis: *The role of extracellular vesicles in osteogenesis* University of Natural Resources and Applied Life Sciences, Vienna Department of Biotechnology, Institute of Applied Microbiology Supervisor: Dr. Johannes Grillari, Associate Professor
2008 – 2011	Study of Biotechnology (with distinction) University of Natural Resources and Applied Life Sciences, Vienna. Master thesis: *Fanconi Anemia, telomeres and cellular senescence*. Department of Biotechnology, Institute of Applied Microbiology Supervisior: Dr. Johannes Grillari, Associate Professor
2002 – 2008	Study of Food Science and Biotechnology University of Natural Resources and Applied Life Sciences, Vienna. Bachelor thesis: *Use of canola and palm oil instead of fuel oil* Department of Material Sciences and Process Engineering

	Supervisior: Dr. Herbert Braun, Ao.Univ.Prof.
2001 – 2002	Study of Technical Physics, University of Technology, Vienna , Austria (not finished)
1993 – 2001	Bundesrealgymnasium with emphasis on natural sciences, Stockerau, Austria

AFFILIATIONS / QUALIFICATIONS:

Member of the International society for extracellular vesicles (ISEV)
Member of the European calcified tissue society (ECTS)
Member of the Austrian Association of Molecular Life Sciences and Biotechnology (ÖGMBT)
Member of the Österrischer Verband für Strahlenschutz (ÖVS)
Deputy commander of the radiation protection group of the district Korneuburg
Deputy commander of the volunteer fire brigade Perzendorf

COMPUTER SKILLS:

Microsoft Office (Word, Excel, Access, PowerPoint)
CorelDraw
SigmaPlot
SPSS
GraphPad

LANGUAGES:

German (mother tongue)
English (excellent)
Russian (fundamentals)

PRIZES:

Prize for high quality oral presentation, ISEV 2014, Rotterdam, The Netherlands, 2014
Leistungsstipendium BOKU, Vienna, Austria, 2013
Posterprize Wissenschaftliche Herbsttagung der Österreichische Gesellschaft für Knochen und Mineralstoffwechsel 2013, Vienna, Austria, 2013
Leistungsstipendium BOKU, Vienna, Austria, 2010

WORKING EXPERIENCES:

Since 01.2013	GrillariI Labs/ Evercyte Type of work: senior scientist
08.2012 – 12.2013	University of Natural Resources and Applied Life Sciences, Department of Biotechnology Type of work: scientific collaborator
01.2011 – 07.2012	GrillariI Labs/ Trauma Care Consult Type of work: scientific collaborator
2008 – 11.2010	University of Natural Resources and Applied Life Sciences, Department of Forest- and Soil Sciences, Prüflabor für Umweltradioaktivität und Strahlenschutz Type of work: Quality assurance representative – establishment, improvement and control of quality management system, organization of internal audits.
2005 – 11.2010	University of Natural Resources and Applied Life Sciences, Department of Forest- and Soil Sciences, Low-Level Counting (LLC)-Labor Arsenal Type of work: Physical-chemical technician - wet lab experiments, writing of reports.
2004-2006	University of Natural Resources and Applied Life Sciences,

Department of Integrative Biology and Biodiversity Research:
Type of work: Statistic tutor - correction of written exams.

LIST OF PUBLICATIONS:

S. Weilner, E. Schraml. H. Redl, R. Voglauer-Grillari, J. Grillari: Secretion of microvesicular miRNAs in cellular and organismal aging. Exp. Gerontol. 48(7):626-33 (2013)

S. Schraml, **S. Weilner**, K. Wassermann, M. Wieser, P. Messner, A.B. Maier, H. Redl, P. Pietschmann, R. Grillari-Voglauer, J. Grillari: MicroRNA-31-a novel therapeutic target for bone regeneration and osteoporosis. J TISSUE ENG REGEN M.; 6: 31-31, (2012)

F.J. Maringer, V. Gruber, M. Hrachowitz, A. Baumgartner, **S. Weilner**, C. Seidel: Long-term monitoring of the danube river- sampling techniques, radionuclide metrology and radioöcological assessment. Appl. Radiat., 67, 894-900; ISSN 0969-8043, (2009)

TALKS AND POSTER PRESENTATIONS:

Talk: European Calcified Tissue Society Congress PhD Training (27. – 30.06.2014) “Age dependent influence of extracellular vesicles on osteogenic differentiation” (Oxford, United Kingdom)

Poster: PhD symposium of the Young Scientist Association (YSA) of the Medical University of Vienna (11-12.06.2014) “Age-dependent influence of plasma derived extracellular vesicles on osteogenic differentiation capacity of mesenchymal stem cells” (Vienna, Austria)

Poster: European Calcified Tissue Society Congress (17. – 20.05.2014) “Levels of circulating vesicular microRNA-31 increase with age as well as in the case of osteoporosis and inhibit osteogenic differentiation of mesenchymal stem cells” (Prague, Czech Republic)

Poster: World Congress on Osteoporosis, Osteoarthritis and Musculoskeletal Diseases (02. – 05.04.2014) “Age-dependent loss of microvesicular Galectin-3 and its consequences on bone formation *in vitro* and *in vivo*” (Sevilla, Spain)

Talk: ISEV 2014 – International society for extracellular vesicles (30.04 – 03.05.2014) “Circulating vesicular microRNA-31 levels as marker for impaired osteogenesis” (Rotterdam, the Netherlands)

Talk: ISEV 2014 – International society for extracellular vesicles (30.04 – 03.05.2014) “Age-dependent loss of microvesicular Galectin-3 and its consequences on bone formation *in vitro* and *in vivo*” (Rotterdam, the Netherlands)

Poster: World Congress on Osteoporosis, Osteoarthritis and Musculoskeletal Diseases (02. – 05.04.2014) “Levels of circulating vesicular microRNA-31 increase with age as well as in the case of osteoporosis and inhibit osteogenic differentiation of mesenchymal stem cells” (Sevilla, Spain)

Poster: World Congress on Osteoporosis, Osteoarthritis and Musculoskeletal Diseases (02. – 05.04.2014) “Age-dependent loss of microvesicular Galectin-3 and its consequences on bone formation *in vitro* and *in vivo*” (Sevilla, Spain)

Talk: PACT Foundation Symposium (03.04.2014) “MiR31 in Bone Regeneration” (Vienna, Austria)

Poster: **S. Weilner**, E. Schraml, V. Keider, H. Redl, P. Pietschmann, R. Grillari-Voglauer, J. Grillari
Wissenschaftliche Herbsttagung der Österreichische Gesellschaft für Knochen und Mineralstoffwechsel 2013 (16.11.2013) “Galectin 3 is a component of circulating microvesicles and boosts osteogenic differentiation of mesenchymal stem cells“ (Vienna, Austria)

Talk: ISEV 2013 – International society for extracellular vesicles (17. – 20.04.2013) “Levels of circulating vesicular microRNA-31 increase with age and inhibit osteogenic differentiation capacity of mesenchymal stem cells” (Boston, USA)

Poster: **S. Weilner**, E. Schraml, V. Keider, F. Weiß, H. Redl, R. Grillari, J. Grillari
ISEV 2013 – International society for extracellular vesicles (17. – 20.04.2013) “Galectin 3 boosts osteogenic differentiation” (Boston, USA)

Talk: Exosomes and Microvesicles 2012 (29.09. – 02.10.2012) “CD63-positive extracelluar vesicles secreted by senescent endothelial cells or isolated from plasma of elderly reduce osteogenic differentiation capacity of adult mesenchymal stem cells (MSCs) via microRNA-31” (Orlando, USA)

Talk: Genau-Meeting 2012 (28. – 29.03.2012) „MiR-31 is secreted by senescent endothelial cells and inhibits osteogenesis of mesenchymal stem cells” (Innsbruck, Austria)

Poster: **S. Weilner**, E. Schraml, K. Wassermann, K. Schneider, H. Redl, J. Grillari
3rd TERMIS world congress 2012 – Tissue Engineering and Regenerative Medicine (05. – 08.09.2012) “Exosomes secreted by senescent endothelial cells or isolated from plasma of elderly reduce osteogenic differentiation capacity of mesenchymal stem cells (MSCs) via microRNA-31 delivery” (Vienna, Austria)

Poster: K. Wassermann, E. Schraml, **S. Weilner**, H. Redl, J. Grillari
Tissue Remodeling in Ageing and Disease - Emerging Insights into a Complex Pathology (27. – 28.03.2012) “MicroRNA-31 as novel biomarker of aging? Secretetion by senescent endothelial cells and inhibition of osteogenicdifferentiation of mesenchymal stem cells”

Poster: F.J. Maringer, V. Gruber, M. Hrachowitz, C. Seidel, **S. Weilner**: Radioecology of the Danube: From environmental monitoring to radiation protection assessment. Proc. IRPA Regional Congress for Central and Eastern Europe Brasov, Romania, 24 – 28 September, (2007)

RESEARCH REPORT AND EXPERT´S REPTORT:

F.J. Maringer, C. Seidel, A. Baumgartner, **S. Weilner**, F. Rechberger: Überwachung der Radioaktivität im österreichsichen Abschnitt der Donau 2008 - 2010. Bundesministerium für Land- und Forstwirtschaft, Umwelt und Wasserwirtschaft, 75, (2010)

F.J. Maringer, **S. Weilner**, A. Baumgartner, V. Gruber, F. Rechberger, C. Seidel: Strahlenexposition durch Radionuklide im Trinkwasser - Anwendung und Evaluation von Dosismodellen zur Ermittlung der Exposition durch Radionuklide im Trinkwasser. Bundesministerium für Gesundheit und Frauen, 62, (2010)

F.J. Maringer, C. Seidel, **S. Weilner**, V. Gruber, A. Baumgartner : Überwachung der Donauradioaktivität 2007 - 2009. Bundesministerium für Land- und Forstwirtschaft, Umwelt und Wasserwirtschaft, 85 , (2009)

C. Seidel, F.J. Maringer, A. Baumgartner, V. Gruber, J. Idinger, **S. Weilner**: Radioökologische Untersuchung Oberösterreichs unter Anwendung des Bioindikators Fichtennadeln. Im Auftrag des Landes OÖ, Direktion Umwelt und Wasserwirtschaft, Abteilung Umweltschutz/Strahlenschutz, 95, (2009)

F.J. Maringer, A. Baumgartner, V. Gruber, C. Seidel, **S. Weilner**, Y. Nabyvanets, V. Kanyevets, G. Laptyev : Joint Danube Survey 2 - Final Scientific Report - Radioactivity. ICPDR - International Commission for the Protection of the Danube River, Vienna International Center, pp 203-208, (2008)

F.J. Maringer, **S. Weilner,** V. Gruber, A. Baumgartner : Überwachung der Donauradioaktivität zur radiologischen Beweissicherung im Zuge der großräumigen Überwachung der Umwelt im Zeitraum 2004 bis 2008. Bundesministerium für Land- und Forstwirtschaft, Umwelt und Wasserwirtschaft, 44 , (2008)

V. Gruber, F.J. Maringer, A. Baumgartner, **S. Weilner**: Trinkwasserradiometrie Oberösterreich 2004-2006. Teilprojekt Bevölkerungsexposition. Amt der oberösterreichischen Landesregierung, 102 , (2006)

F.J. Maringer , M. Hrachowitz, V. Gruber, **S. Weilner**: AQUATERRA - Integrated modelling of the river-sediment-soil-groundwater system; advanced tools for the management of catchment areas and river basins in the context of global change: Analysis results of isotopes characterization sediments . European Commission FP 6 (Proj No 505428, GOCE), 21, (2005)

MASTER AND BACHELOR STUDENT

Melanie Winter: Since 02.2014, *Molecular mechanism of Galectin-3 influence on osteogenic differentiation*
Anja Miscevic: Since 02.2014, *MicroRNAs in osteoporosis and bone formation*
Verena Keider: 06.2012 – 02.2013, *Galectin 3 in oste*ogen*ic differentiation*
Michael Wagner: 04.2012 – 11.2012, *Exosomes in osteogenic differentiation*
Florian Weiss: 11.2011 – 05.2012, *MicroRNA-31 in osteogenic differentiation*